Evaluation of sodium iodide symporter (*hNIS*) mediated targeted radioiodine therapy in breast cancer by non-invasive imaging

By

Sushmita Chatterjee

TATA MEMORIAL CENTRE

A thesis submitted to the Board of Studies in Life Sciences
In partial fulfilment of the requirements for the Degree of

DOCTOR OF PHILOSOPHY
of
HOMI BHABHA NATIONAL INSTITUTE

February, 2015

HomiBhabha National Institute

Recommendations of the Viva Voce Board

As members of the Viva Voce Board, we recommend that the dissertation prepared by Mrs. Sushmita Chatterjee titled 'Evaluation of sodium iodide symporter (hNIS) mediated targeted radioiodine therapy in breast cancer by non-invasive imaging' be accepted as fulfilling the requirements for the degree of Doctor of Philosophy.

Chairperson: Dr. Rajiv Sarin _____ Date: 2.2.16

Convener: Dr. Abhijit De _____ Date: 2-2-16.

Member 1: Dr. S.V. Chiplunkar _____ Date: 2.2.16

Member 2: Dr. Sudeep Gupta _____ Date: 2.2.16

Member 3: Dr. Prasanna Venkatraman _____ Date: 2-2-16

External Examiner: Dr. G.K. Rath _____ Date: 2/2/16

The final approval and acceptance of this dissertation is contingent upon the candidate's submission of the final copies of the dissertation to HBNI.

I hereby certify that I have read this dissertation prepared under my direction and recommend that it may be accepted as fulfilling the dissertation requirement.

Date: 2/2/16

Place: Kharghar, Navi Mumbai.

Guide: Dr. Abhijit De

STATEMENT BY AUTHOR

This dissertation has been submitted in partial fulfilment of requirements for an advanced degree at Homi Bhabha National Institute (HBNI) and is deposited in the Library to be made available to borrowers under rules of the HBNI.

Brief quotations from this dissertation are allowable without special permission, provided that accurate acknowledgement of source is made. Requests for permission for extended quotation from or reproduction of this manuscript in whole or in part may be granted by the Competent Authority of HBNI when in his or her judgment the proposed use of the material is in the interests of scholarship. In all other instances, however, permission must be obtained from the author.

S Chatterjee

Sushmita Chatterjee

Navi Mumbai,

February 2016

DECLARATION

I, hereby declare that the investigation presented in the thesis has been carried out by me. The work is original and has not been submitted earlier as a whole or in part for a degree / diploma at this or any other Institution / University.

Navi Mumbai,
February 2016

Sushmita Chatterjee

Evaluation of sodium iodide symporter (*hNIS*) mediated targeted radioiodine therapy in breast cancer by non-invasive imaging

By

Sushmita Chatterjee

TATA MEMORIAL CENTRE

A thesis submitted to the Board of Studies in Life Sciences
In partial fulfilment of the requirements for the Degree of

DOCTOR OF PHILOSOPHY
of
HOMI BHABHA NATIONAL INSTITUTE

August, 2015

STATEMENT BY AUTHOR

This dissertation has been submitted in partial fulfilment of requirements for an advanced degree at Homi Bhabha National Institute (HBNI) and is deposited in the Library to be made available to borrowers under rules of the HBNI.

Brief quotations from this dissertation are allowable without special permission, provided that accurate acknowledgement of source is made. Requests for permission for extended quotation from or reproduction of this manuscript in whole or in part may be granted by the Competent Authority of HBNI when in his or her judgment the proposed use of the material is in the interests of scholarship. In all other instances, however, permission must be obtained from the author.

Navi Mumbai, **Sushmita Chatterjee**

August 2015

DECLARATION

I, hereby declare that the investigation presented in the thesis has been carried out by me. The work is original and has not been submitted earlier as a whole or in part for a degree / diploma at this or any other Institution / University.

Navi Mumbai,
August 2015

Sushmita Chatterjee

List of Publications

Published:

Chatterjee S., Malhotra R, Varghese F, et al. Quantitative immunohistochemical analysis reveals association between sodium iodide symporter and estrogen receptor expression in breast cancer. *PloS one.* 2013;8(1):e54055.

Chatterjee S., Thaker N., De A. Combined 2-Deoxy Glucose and metformin improves therapeutic efficacy of sodium iodide symporter mediated targeted radioiodine therapy in breast cancer cells. ***Breast cancer: targets and therapy (Dove Med Press). 2015;7:251-265***

Other Publications:

Chatterjee S., De A. Applications of lentiviral vectors in molecular imaging. *Frontiers in Bioscience (Landmark Ed).* 2014;19:835-853.

Shete H., **Chatterjee S.**, De A., Patravale V. Long chain lipid based tamoxifen NLC. Part II: pharmacokinetic, biodistribution and *in vitro* anticancer efficacy studies. *International journal of pharmaceutics.* Sep 15 2013;454(1):584-592.

Chatterjee S., Rao V. L. Papineni : Focus on a recent molecular imaging workshop in India. *Translational Cancer Research*, Vol.2 No. 5, Feb 2013

Conferences attended:

Evaluation of Human Sodium Iodide Symporter Gene Expression in Indian breast cancer Subtypes: **Sushmita Chatterjee**, Frency Varghese, Renu Malhotra, Asawari Patil, Sudeep Gupta and Abhijit De. IACR Annual Meeting, ACTREC, 2012.

Combined 2-Deoxy Glucose and Metformin improves therapeutic efficacy of radioiodine treatment in sodium iodide symporter expressing breast cancer cells: **Sushmita Chatterjee,** Asawari Patil, Vani Parmar, Sudeep Gupta and Abhijit De. WIN Symposium, Paris, France 2014.

Understanding the regulatory network of sodium iodide symporter protein glycosylation for improved gene targeted radioiodine therapy : **Sushmita Chatterjee**, Madhura Kelkar, Shruti B. Menon, Rajiv Kalraiya and Abhijit De. AICBC, CDRI Lucknow 2014.

ACKNOWLEDGEMENT

It feels good to reach the destination, but its journey that matters at the end. I, therefore take the opportunity to thank everyone whose contributions made it a worthwhile and undelible journey.

Firstly I would like to sincerely thank my mentor, Dr. Abhijit De for his constant encouragement and valuable suggessions throughout the project tenure. It would not have been possible to develop my scientific skills and explore the ideas without his training and the independence he provides at work . His contribution and teaching towards writing manuscripts and thesis has been of great help.

I sincerely thank Director and Deputy Director of ACTREC for providing such an excellent infrastructure and instruementation facilities at ACTREC. I would also like to give special thanks to my doctoral committee members Dr. Rajiv Sarin, Dr. S.C. Chiplunkar, Dr. Sudeep Gupta and Dr. Prasanna Venkatraman for their time to time invaluable suggessions towards progress and right direction for compilation of the project. I would like to give special thanks to Dr. Pritha Ray not only for her valuable suggessions but also for providing me her lab facilities and material whenever it was required.

I am grateful to Dr. Asawari Patil for always taking time out of her busy schedule for providing the tissues and scoring the IHC samples. I am also thankful to biorepository facility and Mr. Madan for providing fresh tissue sample. I would also like to thank Dr. Pradnya Kowtal for providing with her own thyroid tissue sample block.

I also thank Mr. Dandekar for his prompt help during any problems with the instruments.. A sincere thanks to Mr. Chawan for helping and teaching me handling of patient tissues for RNA extraction. I thank Sadhana Kannan for her assistance with statistical analysis. I am grateful to the staff of microscopy, genomic and FACS facility for their support. I specially thank Mrs. Tanuja and Mrs. Vaishali for their innumerable assistance in capturing the microscopic images. I also thank the staff of animal house, scope cell, steno pool, library, administration, accounts and IT department.

I wish to thank Dr. M.G.R. Rajan and Dr. Savita Kulkarni from Radiation Medical Center, TMH, Parel for providing the facility to perform radioactivity related experiments.

I am thankful to ACTREC for fellowship which helped my survival in an expensive city like Mumbai. I am also thankful to HBNI and ACTREC for providing financial assistance to present my work in an international platform at "WIN Symposium", Paris, France.

I thank my awesome labmates Madhura, Amir, Shalini, Maitreyi, Renu, Shruti, Aakansha and Abhishek for making it a comfortable and absolutely enjoyable experience in lab. Healthy scientific discussions with Madhura had always been helpful. I am thankful to Amir for teaching me many softwares including Adobe photoshop and Graphpad software, helping with the proof reading of my presentations and always been there in my good and bad times. I thank the juniors Shalini, Maitreyi and Arijit for making the lab atmosphere more lively and healthy. I also thank project trainees who worked under my guidance Manjari, Nirmal and Shruti for their sincere contribution towards the project. I thank past trainees of lab Ishan, Puja, Akshi, Jennifer, Dippal and many others who had always made it a great experience in lab. I also thank Ray lab members for their help and support.

PhD braught wonderful bunch of people tn my life in form of my batchmates Tanmoy, Puja, Rupa, Madhura, Snehal, Rubina, Shafqat, Srikanta, Kedar and Bhanu,. My special thanks to Tanmoy for always been there and listening to me patiently whether its meaningful or not and helping me with every aspect of life unconditionally. I also thank my great friends in ACTREC Abira, Monica, Kaushal and Piyush for always been there to relieve me and cheering me up during stresfull times. Moments shared with them will be remembered for life long. I also thank my extended family which is in form my roommates in hostel Rubina, Ratika, Puja and Rupa who made my life completely joyful and stressfree outside my home. I am grateful to my seniors Gaurav, Paulami, Ajit Chande and Ajit Sharma for their constant suggessions and help in various aspects. Its important to have a life outside lab for a balanced mind and soul. I therefore wish to specially thank my dance teachers Mr. Sidney and Mrs. Candy for providing food for my soul in form of teaching dance during weekends after a busy, hectic week in lab.

Last but not the least I am thankful to my parents and in laws for their endless support, understanding and patience throughout my Ph.D. I am highly obliged to them for bearing my absence from many important occasions and never complaining for the same. This journey would not have been completed without the enormous love, support, care, patience and encouragement of my husband, Mr. Varun Sharma. Thank you

Sushmita Chatterjee

Table of Contents

Synopsis……1

List of Figures……16

List of Tables……18

Abbreviations……19

Chapter 1

1 Introduction and Review of Literature 20

1.1 Breast Cancer: 21

1.2 Risk factors: 22

1.3 Diagnosis: 23

1.4 Breast cancer Stages 24

1.5 Histological grade 24

1.6 Histology of normal breast 25

1.7 Histopatholgy of breast cancer 26

1.8 Breast cancer biomarkers 27

1.9 Metastasis 28

1.10 Disease management 29

1.10. 1 Surgery 29

1.10. 2 Radiotherapy 30

1.10. 3 Chemotherapy 30

1.10. 4 Targeted therapy 31

1.11 Sodium Iodide Symporter (NIS) 32

1.11. 1 Historical perspective of NIS 33

1.11. 2 Iodide organification in thyroid 34

1.11. 3 Molecular characteristics of NIS 35

1.11. 4 NIS expression in extra thyroidal tissues 37

1.11. 5 NIS expression in thyroid malignancy 38

1.11. 6 Clinical application of NIS in thyroid cancer 39

1.11. 7 NIS expression in breast cancer 39

1.11. 8 NIS as a therapeutic gene 40

1.11. 9 NIS as a reporter gene 42

1.12 Molecular imaging 43

1.12. 1 Radionuclide imaging 44

1.12. 2 Optical imaging 45
1.12. 3 Cerenkov bioluminescence imaging 47
1.13 Rationale of the study 48
1.14 Aims & Objectives 50

Chapter 2

2 Evaluation of NIS expression in primary breast tumour tissues and it's correlation with various prognostic markers of breast cancer 51
2.1 Introduction 52
2.2 Materials and Methods 55
2.2. 1 Study population 55
2.2. 2 Immunohistochemitry 56
2.2. 3 Pathological scoring 57
2.2. 4 Digital image analysis 57
2.2. 5 Immunofluorescence 58
2.2. 6 Quantitative real time PCR 58
2.2. 7 Statistical analysis 59
2.3 Results 59
2.3. 1 NIS protein expression in primary breast tumour tissue 59
2.3. 2 Comparison of digital image analysis with pathological scoring 63
2.3. 3 Localization of NIS in breast cancer tissue 65
2.3. 4 NIS transcript levels in primary breast tumour tissue 66
2.3. 5 NIS protein expression with respect to prognostic markers 68
2.3. 6 NIS transcript levels with respect to prognostic markers 70
2.3. 7 Correlation of NIS expression at RNA and protein level in breast cancer 71
2.3. 8 NIS expression in breast fibroadenoma 73
2.4 Discussion 74

Chapter 3

3 Understanding of NIS expression in breast cancer patients with primary and metastatic tumour…….. 79
3.1 Introduction 80
3.2 Methods 82
3.2. 1 Study population 82
3.2. 2 Statistical analysis 83
3.3 Results 83
3.3. 1 NIS expression in breast cancer lymph node metastatic tissue 83
3.3. 2 NIS expression in metastatic lymph node tissue as compared to primary BC tissue 86

3.4 Discussion 88

Chapter 4

4 Development of a NIS over-expressing breast cancer cell model & Evaluation of radioiodide mediated therapeutic effect in the model by molecular imaging techniques 91

4.1 Introduction 92

4.2 Methods 95

4.2. 1 Plasmids used 95

4.2. 2 Preparation of NIS over-expression plasmid 96

4.2. 3 Cells and culture conditions 98

4.2. 4 Preparation of NIS expressing breast cancer cell line 98

4.2. 5 Luciferase assay 98

4.2. 6 Immunofluorescence for NIS and γH2A.X foci assay 99

4.2. 7 Iodide uptake assay 99

4.2. 8 Iodide efflux assay 99

4.2. 9 Real time PCR 100

4.2. 10 Western blotting 100

4.2. 11 Glycosylation PCR array 101

4.2. 12 Clonogenic assay 102

4.2. 13 Cell cycle analysis and apoptosis assay 102

4.2. 14 Tumour xenografts and ^{131}I therapy 102

4.2. 15 *In vivo* bioluminescence imaging 103

4.2. 16 Cerenkov luminescence imaging 103

4.2. 17 Statistics 104

4.3 Results 104

4.3. 1 Preparation of NIS over-expressing MCF-7 cells 104

4.3. 2 Glycosylation gene expression profile of the cells expressing NIS in membrane versus cytoplasm 108

4.3. 3 Characterization of the experimental model with correlated expression of the therapeutic and reporter gene 112

4.3. 4 Therapeutic efficacy of radioiodide in NIS over-expressing MCF-7 cells 115

4.3. 5 Development of ZR-75-1 NIS over-expressing cells 116

4.3. 6 Evaluation of radioiodide mediated therapeutic effect in NIS expressing tumour cell model by molecular imaging techniques 119

4.4 Discussion 124

Chapter 5

5 Effect of 2-DG and metformin as radiosensitizers for increased radioiodine mediated DNA damage in NIS expressing breast cancer cells 129

5.1 Introduction 130
5.2 Materials and Methods 132
5.2. 1 MTT assay 132
5.2. 2 ATP measurement 132
5.2. 3 Statistics 132
5.3 Results 133
5.3. 1 Effect of 2-DG and metformin combination on tumor cell ablation upon Cobalt60 radiation treatment 133
5.3. 2 Effect of radiosensitizers on different prospects of irradiated cells 135
5.3. 3 Effect of 2-DG and metformin combination on treatment efficacy of radioiodine (^{131}I) in NIS expressing cells 137
5.3. 4 Effect of radiosensitizers in combination with radioiodine (^{131}I) on foci formation 138
5.3. 5 Toxicity effect of radiosensitizers in combination with ^{131}I on plain MCF-7 cells with cytoplasmic NIS localization 140
5.4 Discussion 141
Summary 145
Bibliography 150
Appendix:Materials & Methods 167

Synopsis

1. Name of the Student: SUSHMITA CHATTERJEE

2. Name of the Constituent Institution: Tata Memorial Centre**,** Advanced Centre for Treatment Research and Education in Cancer

3. Enrolment No. : LIFE09200904014

4. Title of the Thesis: Evaluation of sodium iodide symporter (hNIS) mediated targeted radioiodine therapy in breast cancer by non-invasive imaging.

5. Board of study: Life Science

Introduction:

Human sodium iodide symporter (NIS) is a transmembrane glycoprotein that aids in active transport of Na^+ and I^- inside the thyroid follicular cells. Energy used for the uptake of Na^+ and I^- is obtained from the Na^+-K^+ ATPase pump. Other than the presence of NIS in thyroid gland, its expression is also evident in some of the extra thyroidal tissues including salivary gland, gastric mucosa, lactating mammary gland and ovary. As NIS can mediate intracellular delivery of radioiodide, it is of great interest as a therapeutic tool in thyroidal as well as non-thyroidal cancer. Ability of this molecule to uptake iodine has been used for more than over 70 years in diagnosis and treatment of thyroid malignancies.

In the year 2000, Tazebay *et al.* reported that NIS molecule is expressed in above 80% of breast cancer (BC) cases as opposed to its absence in normal, non-lactating breast tissue[1]. Following this study there were several reports suggesting NIS transcript or protein over expression in BC[2-8]. Translational medicine based studies have also been carried out for testing the efficacy of NIS based therapy and diagnosis in malignant primary as well as metastatic BC settings[2,4,9]. However the variation in NIS expression level across the various BC subtypes was unknown.

In addition to analysis of NIS expression in BC patient samples, few groups have over expressed NIS under ubiquitous or mammary tissue specific promoters and evaluated its efficacy for diagnosis as well as therapeutics in BC cells[10-12].

Rationale: As mentioned in the introduction various groups suggest high NIS expression in BC but its subtype specific expression is not known at present. Ryan *et al*. in 2013 reported NIS expression at the transcript level from 75 BC patient samples including all major subtypes and observed significantly high NIS expression in ER, PR-ve, HER2 +ve

subtypes[13]. However the status of NIS at protein level was not reported. As an ion transporter, the NIS protein expression as well as localization is important, therefore immunohistochemistry (IHC) for NIS in BC subtypes may provide important information relevant for addressing functional use of NIS based therapy to the clinic.

In the experimental models developed for evaluation of NIS based ^{131}I therapy in BC cancer, all the previous studies suggest regression of tumour with ^{131}I *in vivo,* however within 10 days of post-treatment tumour recurs[12]. Thus although ^{131}I alone results in tumour growth inhibition, but tumour recurrence suggests further improvement is required in radioiodine therapy of NIS expressing BC cells. A strategy that can be used but still unexplored is addition of radio sensitizers to enhance ^{131}I mediated damage to NIS expressing cells. Exploring the combination of radio sensitizers with radioiodine may show improved therapeutic efficacy in NIS expressing BC cells.

Aims & Objectives: Based on the above rationale following are the objectives of the thesis:

1. Understanding of NIS expression in breast cancer patients

2. Understanding the efficacy of NIS based radioiodine therapy in an experimental model using engineered cells

Results :

Objective 1. Understanding of NIS expression in breast cancer patients

1.1 Evaluation of NIS expression in primary breast tumour tissues and it's correlation with various prognostic markers of breast cancer:

In order to understand NIS expression level in BC we performed immunohistochemistry (IHC) in 181 primary breast tumour FFPE tissue (formalin fixed paraffin embedded)

samples including all major BC subtypes. The number and average age of samples in each subtype is as mentioned in the following table:

	ER+ve, PR+ve, HER2-ve	ER+ve, PR+ve, HER2-ve	ER-ve, PR-ve, HER2+ve	ER-ve, PR-ve, HER2-ve
Sample#	55	26	41	59
Mean age (years)	49	51	50	49

As appeared in DAB (3, 3' Diaminobenzidine) stained IHC staining, the NIS staining was mainly diffused cytoplasmic type, however in very limited numbers of tissue samples (n=4) membrane NIS expression was observed using the same protocol and antibody. Tumour adjacent normal breast tissues were stained negative and membrane specific staining was observed in salivary gland tissue used as positive control. A thyroid papillary carcinoma tissue was also used as positive control, which showed diffused cytoplasmic pattern for NIS staining. Of the total number of samples analyzed, 78% BC cases were positively stained for NIS. Receptor subtype specific classification showed that 90% samples of ER, PR+ve, HER2-ve and 92% of ER, PR +ve, HER2+ve subtype are positive for NIS expression whereas only 74% HER2 enriched (ER, PR –ve, HER2 +ve) and 60% of TNBC (ER, PR –ve, HER2 -ve) samples are positive for NIS expression. Further, NIS staining intensity comparison was done keeping one thyroid papillary carcinoma tissue sample as a positive reference. Subtype specific intensity analysis of tumour tissue samples showed equivalent or lesser staining intensity as compared to the thyroid carcinoma reference used and therefore are categorized as 3+, 2+, 1+ and negative (0) scores by pathological as well as digital IHC analysis methods. We observed significant difference among the subtypes in terms of NIS expression. Next we compared NIS expression on the basis of ER status in patient samples and observed that frequency of

samples showing positive NIS expression is significantly high in ER+ve samples ($p<0.0001$). Classification on the basis of HER2, chemotherapy and menopausal status did not show any significant difference in frequency of samples showing NIS expression. Further to compare NIS expression between the age groups, we divided the patient samples into 2 groups i.e. age group above 50 and below 50 years. We observe increased frequency of patients showing positive NIS staining in the age group below 50 as compared to in the age group above 50 ($p=0.0283$), indicating significant differences in the age groups. We also evaluated NIS expression in 20 fibroadenoma breast tissues and all the tissues showed positive NIS expression.

Since, previous reports so far poorly depicts if NIS expression at the transcript and protein level correlates or not, we have thoroughly analyzed the NIS transcript by real time PCR in 59 primary breast tumour tissue samples. The samples in each subtype included 20 ER, PR+ve, HER2-ve, 15 ER, PR+ve, HER2+ve, 12 ER, PR-ve, HER2+ve and 12 ER, PR-ve, HER2-ve subtypes. We performed Q RT PCR using TaqMan probe and GAPDH was used as an endogenous control for normalization. We used RNA from normal breast tissue for relative assessment in malignant breast tissue and employed $2^{-\Delta\Delta ct}$ method to calculate the NIS expression in breast tumour tissue as compared to normal breast tissue. We observed significant upregulation of NIS expression in the breast tumour tissue as compared to normal breast tissue. When compared among the subtypes, we observed significantly high NIS expression in ER, PR+ve, HER2-ve subtype as compared to ER, PR-ve, HER2-ve subtype ($p=0.0435$). However no significant difference was observed among the other subtypes. Further, we classified the data on the basis of ER status and observed significantly high NIS expression in ER+ve samples as compared to ER-ve samples ($p=0.0194$), which is concordant with our IHC data. Our data indicates close association of NIS expression with ER positivity. Further classification on the basis

of age, HER2 and menopause status did not show any significant difference in NIS mRNA expression among the groups. Further to investigate the correlation of NIS expression at the transcript and translational level, we procured 20 samples simultaneously fixed in formalin (for IHC) as well as RNase later (for real time PCR) and evaluated NIS protein and mRNA expression level respectively. Except for 2 samples, all other samples showed correlated expression of NIS mRNA and protein (R^2=0.696). However for different scoring intensity of NIS at IHC, the difference in NIS expression at RNA level was not significant. Our data for the first time indicates variation in NIS expression at the transcript as well as translational level with respect to such prognostic factors, however the samples used in the study is only from Indian population and whether it holds true to the BC patients from other geographical locations is a matter of investigation.

1.2. Understanding of NIS expression in BC patients with primary vs. metastatic tumour:

Since NIS expression pattern has not been compared between primary tumour and its metastatic counterpart in previous studies, we performed immunohistochemistry in 45 paired (45 primary and 45 lymph node metastatic tumours from the same patients) paraffin embedded BC tissue samples. Overall total number of samples in each subtype includes 18 ER, PR+ve, HER2-ve, 5 ER, PR+ve, HER2+ve, 13 ER, PR-ve, HER2+ve and 9 TNBC (Triple negative BC) subtype. Among the metastatic cases only 1 (2%) sample showed 3+ score, 30 (67%) samples showed 2+ score and 11 (24%) samples showed 1+ score for NIS expression. NIS expression in metastatic tumour tissue samples was compared with their respective primary tumour tissue samples. The results suggest that in 78% of the metastatic tumour tissue samples NIS intensity was either equal or higher than their respective primary tumour tissue samples, indicating scope of NIS mediated

radioiodine therapy in the metastasized tissue as well. Renier *et al.* reported previously high NIS expression in the BC brain metastatic tissue[2], however comparative study including all subtypes is lacking in literature and our report indicates distinct differences in NIS expression among metastatic tumour of BC subtypes. Any significant difference was not observed in relation to age, HER2 receptor and menopausal status.

Objective 2. Understanding the efficacy of NIS based radioiodine therapy in an experimental model using engineered cells

2.1. <u>Development of a NIS over-expressing MCF-7 and ZR-75-1 cell model:</u>

Extending the study in an experimental model, an attB integrase based plasmid vector system was made incorporating human NIS as first cistron and a fusion reporter gene (TurboFP-Fluc2) as second cistron linked by EMCV-IRES (Encephalomyocarditis Virus-Internal Ribosomal Entry Site) DNA sequence under the chicken beta actin promoter and this vector system was used for construction of MCF-7 and ZR-75-1 stable cells. Stable cell lines generated were characterized for the expression of NIS as well as luciferase/fluorescence reporter proteins. By performing stringent screening of clonal population, we obtained MCF-7 cell clones which express NIS predominantly either at the cell membrane or in the cytoplasm with different intensity levels; however for ZR-75-1 all the clones showed predominant cytoplasmic over-expression of NIS. The expression of NIS was also verified at transcript as well as for functioning in terms of inward iodine pumping ability which was found to be well correlated with NIS protein expression levels. An increase in iodine uptake was evident in MCF-7 stable cell clone expressing NIS at membrane when compared with the plain MCF-7 or MCF-7 stable cells expressing NIS in cytoplasm. Since NIS is a glycosylated protein, the defect in its membrane targeting is probably due to incomplete glycosylation. To further characterize the difference at the molecular level in the established MCF-7 clonal cell population with

cytoplasmic or membrane NIS expression, we performed glycosylation RT profiler PCR array and checked the expression levels of 84 gene signatures involved in the process of glycosylation. The array data suggests distinct up- or down-regulation of specific subsets of glycosylation enzymes in the two established cell populations. Specifically, the expression level of mannosidases, sialidases, mannosyltranferases and sialyltransferases were found significantly high in NIS membrane clones than the cytoplasmic clones.

In case of cytoplasmic NIS expressing clones, iodine uptake was equivalent to that of plain MCF-7 cells, which indicates that for functional implication, NIS protein must be located at the cell membrane. In order to show specificity of NIS for iodine uptake we used potassium perchlorate ($KClO_4$) which specifically blocks NIS. Incubation of NIS expressing MCF-7 stable cells with potassium perchlorate showed complete inhibition of iodine uptake. Since the time window for iodine retention inside the cells plays a crucial role for cellular damage, we also evaluated the time for release of iodine from the stable cells. In order to do so iodine efflux assay was performed at different time points. We observed that 90% of iodine is released in initial 20 minutes, possibly indicating lack of iodine trapping (organification) method in BC cell.

2.2. Evaluation of radioiodine mediated therapeutic effect in NIS expressing tumour cell model by molecular imaging techniques:

Once the NIS expressing cells were characterized, we evaluated the effect of ^{131}I therapy on viability of NIS expressing MCF-7 (clone 22) and ZR-75-1 (clone 1) cells by clonogenic and apoptotic assay. We observed complete cell death with 100µCi ^{131}I where as with 50µCi ^{131}I 40% cell death in MCF-7 and 85% cell death in ZR-75-1 NIS expressing clones was observed.

Further in order to understand distribution of ^{131}I in the animal model we performed Cerenkov luminescence imaging (CLI). In brief, Cerenkov radiation generates when

charged particles travel through an optically transparent, insulating material with a velocity that exceeds the speed of light. The visible light generated is called Cerenkov luminescence which can be captured by ultrasensitive CCD optical imaging system. As a process of standardization different doses of ^{131}I was added in 96 black well plate and CLI was performed using IVIS *in vivo* imaging system. We observed dose dependent increase in the signal intensity, which can be blocked by placing a black paper to cover the wells. Further, CLI after intra peritoneal injection of ^{131}I showed signal in the thyroid and tumour of ZR-75 xenografted nude mice suggesting possibility of using CLI in *in vivo* mice xenograft model.

For *in vivo* evaluation of therapeutic potential of NIS, $6x10^6$ NIS over-expressing ZR-75-1 cells (clone 1) were implanted for subcutaneous tumour growth in 8 nude mice and when the tumour volume reached to a measurable size, we initiated ^{131}I therapy. Before starting ^{131}I therapy thyroid of the control as well as treated group mice were blocked with T4 and methimazole for 7 days and the thyroid blocking was continued further throughout the experiment. Tumour bearing mice were randomized into 2 groups, control and ^{131}I treated. Based on the previous literature reports we treated tumour bearing mice with weekly dose of 1mCi ^{131}I for 3 weeks. Further CLI imaging after 24 hrs of 1mCi ^{131}I injection (intra peritoneal) showed tumour specific accumulation where as thyroid was significantly blocked (no signal observed). To monitor the efficacy of radioiodine therapy bioluminescence imaging was performed and quantification of the luminescence signal showed that in the control group there was continuous increase in the signal intensity over 3 weeks. However in the treated group luminescence signal intensity was decreased after 2 weeks of therapy and it reduced further after 3 weeks, indicating tumour regression by radioiodine treatment.

2.3. Effect of 2-DG and metformin as a radio sensitizer for increased radioiodine mediated damage in NIS expressing cells :

As therapeutic potential of NIS in BC is often found limited due to low iodine uptake and/or fast efflux rate of iodine due to lack of appropriate iodine organification system, to further enhance NIS mediated ^{131}I therapeutic efficacy, the scope of radio sensitizers as a combination strategy is explored. Radiosensitization using either metformin or 2-DG (2-Deoxy-D-glucose) in various cancer cell has been reported previously. In the present study combination of two radio sensitizer drugs were used to enhance NIS mediated radioiodine therapy. Two BC cell lines, MCF-7 and MDA MB231 were tested to optimize minimal drug doses required for radiosensitization in combination with cobalt 60 radiation. A combination of 2/4mM metformin and 20mM 2-DG with 2Gy Cobalt60 radiation showed significant radiosensitization effect ($p=0.0002$) in MCF-7 cells. In cells treated with the combination therapy increased DNA damage is indicated by γH2A.X foci formation. In addition to MCF-7 cells, effect of radio sensitizers on Cobalt60 radiotherapy in MDA MB231 cells was also evaluated. In MDA MB231 cells combination of 4mM metformin and 5mM 2-DG dose with 2 Gy radiation showed significant decrease in cell survival as compared to 2 Gy radiation alone ($p=0.0020$, CI=95%). In NIS over-expressing MCF-7 BC cells effect of optimized drug concentrations was evaluated and we observed significant radiosensitization ($p=0.0019$) on combining the drugs with 50μCi ^{131}I. Apoptosis data corroborated with the result of clonogenic assay showing significant increase in apoptotic population upon dual drug mediated radiosensitization. We also observed lowered ATP content post 2-DG and metformin treatment. Since our patient sample data suggests cytoplasmic loacalization of NIS in majority of patient samples, we also evaluated the effect of radio sensitizer's combination with ^{131}I in plain MCF-7 cell. Our data shows that 50uCi ^{131}I results in 30%

cell death which increases to 60% on addition of 2-DG and metformin. Thus our results provide novel information and open up the possibility of using radio sensitizers for enhanced radioiodine treatment efficacy in BC cells over-expressing NIS protein.

Conclusion:

Detailed analysis of the patient samples in the present work suggests upregulated expression of NIS in majority of the BC tissues in Indian population. Our results from real time as well as IHC show positive correlation of NIS with ER receptor positivity. Further, evaluating NIS protein expression in 45 paired samples of lymph node metastatic and primary breast tumours, good correlation was established, indicating NIS expression status remains unaltered.

In the experimental settings, we engineered mammalian expression vector for correlated expression of human NIS and luciferase reporter and established NIS over-expressing MCF-7 and ZR-75-1 cell clones. Thorough molecular and functional characterization of two distinct MCF-7 clonal populations with distinct pattern of NIS localization was carried out during this study. We observe distinct differences in their glycosylation enzyme expression profile, suggesting important role of glycosylation in correct membrane targeting of NIS protein. Further, cell culture survival assay upon ^{131}I treatment suggests significant loss in viability with radioiodine therapy that can be further enhanced by the use of 2 radio sensitizers namely, 2-DG and metformin. The encouraging radiosensitization effect observed may aid in targeted radioiodine therapy in BC cells with NIS expression.

References:

1. Tazebay UH, Wapnir IL, Levy O, et al. The mammary gland iodide transporter is expressed during lactation and in BC. *Nature medicine.* Aug 2000;6(8):871-878.

2. Renier C, Vogel H, Offor O, Yao C, Wapnir I. BC brain metastases express the sodium iodide symporter. *Journal of neuro-oncology.* Feb 2010;96(3):331-336.

3. Upadhyay G, Singh R, Agarwal G, et al. Functional expression of sodium iodide symporter (NIS) in human BC tissue. *BC research and treatment.* Jan 2003;77(2):157-165.

4. Wapnir IL, Goris M, Yudd A, et al. The Na+/I- symporter mediates iodide uptake in BC metastases and can be selectively down-regulated in the thyroid. *Clinical cancer research : an official journal of the American Association for Cancer Research.* Jul 1 2004;10(13):4294-4302.

5. Wapnir IL, van de Rijn M, Nowels K, et al. Immunohistochemical profile of the sodium/iodide symporter in thyroid, breast, and other carcinomas using high density tissue microarrays and conventional sections. *The Journal of clinical endocrinology and metabolism.* Apr 2003;88(4):1880-1888.

6. Renier C, Yao C, Goris M, et al. Endogenous NIS expression in triple-negative BCs. *Annals of surgical oncology.* Apr 2009;16(4):962-968.

7. Ryan J, Curran CE, Hennessy E, et al. The sodium iodide symporter (NIS) and potential regulators in normal, benign and malignant human breast tissue. *PloS one.* 2011;6(1):e16023.

8. Tandon A. Sodium iodide symporter, estrogen receptor, and progesterone receptor expression in carcinoma breast- An immunohistochemical analysis *Indian journal of pathology and microbiology.* 2011;54(4):745-751.

9. Moon DH, Lee SJ, Park KY, et al. Correlation between 99mTc-pertechnetate uptakes and expressions of human sodium iodide symporter gene in breast tumour tissues. *Nuclear medicine and biology.* Oct 2001;28(7):829-834.

10. Renier C, Vogel H, Offor O, Yao C, Wapnir I. BC brain metastases express the sodium iodide symporter. *Journal of neuro-oncology.* Feb 2010;96(3):331-336.

11. Gholami S, Chen CH, Lou E, et al. Vaccinia virus GLV-1h153 in combination with 131I shows increased efficiency in treating triple-negative BC. *FASEB journal : official publication of the Federation of American Societies for Experimental Biology.* Feb 2014;28(2):676-682.

12. Trujillo MA, Oneal MJ, Davydova J, Bergert E, Yamamoto M, Morris JC, 3rd. Construction of an MUC-1 promoter driven, conditionally replicating adenovirus that expresses the sodium iodide symporter for gene therapy of BC. *BC research : BCR.* 2009;11(4):R53.

13. Montiel-Equihua CA, Martin-Duque P, de la Vieja A, et al. Targeting sodium/iodide symporter gene expression for estrogen-regulated imaging and therapy in BC. *Cancer gene therapy.* Jul 2008;15(7):465-473.

14. Ryan J, Curran CE, Hennessy E, et al. The Sodium Iodide Symporter (NIS) and Potential Regulators in Normal, Benign and Malignant Human Breast Tissue. *PloS one.* Jan 2011;6(1).

Publications in peer-reviewed journal:

Published:

Chatterjee S., Malhotra R, Varghese F, et al. Quantitative immunohistochemical analysis reveals association between sodium iodide symporter and estrogen receptor expression in breast cancer. *PloS one.* 2013;8(1):e54055.

Accepted:

Chatterjee S., Thaker N., De A. Combined 2-Deoxy Glucose and metformin improves therapeutic efficacy of sodium iodide symporter mediated targeted radioiodine therapy in breast cancer cells. *Breast Cancer: targets and therapy, Dovepress (in press)*

Communicated:

Other Publications:

Chatterjee S., De A. Applications of lentiviral vectors in molecular imaging. *Frontiers Bioscience (Landmark Ed).* 2014;19:835-853.

Shete H., **Chatterjee S.**, De A., Patravale V. Long chain lipid based tamoxifen NLC. Part II: pharmacokinetic, biodistribution and *in vitro* anticancer efficacy studies. *International journal of pharmaceutics.* Sep 15 2013;454(1):584-592.

Chatterjee S., Rao V. L. Papineni : Focus on a recent molecular imaging workshop in India. *Translational Cancer Research*, Vol.2 No. 5, Feb 2013

Conferences attended:

Evaluation of Human Sodium Iodide Symporter Gene Expression in Indian breast cancer Subtypes: **Sushmita Chatterjee**, Frency Varghese, Renu Malhotra, Asawari Patil, Sudeep Gupta and Abhijit De. IACR Annual Meeting, ACTREC, 2012.

Combined 2-Deoxy Glucose and Metformin improves therapeutic efficacy of radioiodine treatment in sodium iodide symporter expressing breast cancer cells: **Sushmita Chatterjee,** Asawari Patil, Vani Parmar, Sudeep Gupta and Abhijit De. WIN Symposium, Paris, France 2014.

Understanding the regulatory network of sodium iodide symporter protein glycosylation for improved gene targeted radio-iodine therapy : **Sushmita Chatterjee**, Madhura Kelkar, Shruti B. Menon, Rajiv Kalraiya and Abhijit De. All India Cell Biology Annual Meeting, CDRI Lucknow 2014.

Signature of Student: S Chatterjee

Date: 29.06.2015

Doctoral Committee:

S. No.	Name	Designation	Signature	Date
1.	Dr. Rajiv Sarin	Chairman		29.6.15
2.	Dr. Abhijit De	Guide/ Convener		29-06-15
3.	Dr. S.V. Chiplunkar	Member		6.7.15
4.	Dr. Sudeep Gupta	Member		30/6/15
5.	Dr. Prasanna Venkatraman	Member		

Forwarded Through:

Dr. S.V. Chiplunkar
Director, ACTREC

Chairperson,
Academic & training Program, ACTREC

Prof. K. Sharma
Director, Academics

T.M.C.
PROF. K. S. SHARMA
DIRECTOR (ACADEMICS)
TATA MEMORIAL CENTRE,
PAREL, MUMBAI

List of Figures

Figure 1.1 *Epidemiology of BC*[24] 22
Figure 1.2 *Breast cancer stages*[29] 24
Figure 1.3 *Structure of the mammary gland. Terminal ductal–lobular unit (TDLU), composed of ductal cells, is the unit thought to be the origin of most BC. Lobule is made up of two primary types of cells in normal ducts: outer contractile myoepithelial and inner columnar luminal cells*[35]*.* 26
Figure 1.4 *The image showing presence of NIS at basolateral membrane of a thyrocyte. NIS uptakes* Na^+ *and* I^- *in 2:1 ratio. The energy for this transport is obtained from* Na^+/K^+ *ATPase pump*[73]*.* 33
Figure 1.5 *Ilustration of a thyroid follicular cell showing iodide transport by NIS. The transported iodide is further organified in multiple steps with the aid of pendrin and thyroid peroxidise (TPO) molecule*[83]*.* 35
Figure 1.6 *The schematic representing proposed model of NIS with 13 trans membrane helices*[83]**.** 36
Figure 1.7 *The schematic showing principle of Cerenkov luminescence imaging.* 47
Figure 2.1 *Images of NIS staining pattern in major subtypes of BC.* 61
Figure 2.2 *NIS expression in primary breast tumour tissue.* 62
Figure 2.3 *Chart representing IHC scoring intensity in various BC subtypes. It is to be noted that a major number of samples in ER, PR+ve, HER2-ve subtype show 2+ score for NIS where as in TNBC a major number of samples show negative NIS expression.* 63
Figure 2.4 *Images captured using higher magnification can assign correct scoring by reducing the averaging effect contributed from the stomal areas.* 64
Figure 2.5 *Immunofluorescence staining reveals NIS and HER2 receptor overlaps at the tumour cell membrane in few cases. Human patient tissue samples stained with NIS and HER2 specific antibody followed by detection with Alexafluor488 (green) and Dylight633 (red) labelled secondary antibodies respectively.* 66
Figure 2.6 *Intensity of NIS expression at transcript level in different subtypes of BC. Data is represented as fold change as compared to normal breast. NIS expression level is significantly high in ER,PR+ve, HER2-ve group as compared to TNBC group* 68
Figure 2.7 *NIS expression in association with ER expression and age group* 69
Figure 2.8 *Association of NIS with HER2 and menopausal status* 70
Figure 2.9 *Association of NIS transcript levels with various prognostic factors of BC* 71
Figure 2.10 *BC tissue samples with their respective transcript and protein level of NIS expression showing correlated NIS expression* (R^2*=0.6964)* 73
Figure 2.11 *NIS expression in fibroadenoma of breast and its comparison with BC* 74
Figure 3.1 *Representative immunohistochemistry images for NIS in primary breast tissue and their respective lymph node metastatic tissue showing variation in subcellular localization.* 84
Figure 3.2 *Intensity of NIS expression in lymph node metastatic tissues. Any significant difference was not observed among various subtypes on the basis of NIS expression.* 85
Figure 3.3 *NIS expression in lymph node metastatic tissue with respect to* 86
Figure 3.4 *IHC images of representative primary breast tumour tissues and their respective lymph node metastatic tissues.* 87
Figure 3.5 *Comparison of NIS expression variation between primary and lymph node metastatic tumour tissue in various BC subtypes. The graph suggests that majority of the samples show equal or higher expression in lymph node metastatic tissue as in their respective primary tumour*

tissue and a very small subset of population shows lower NIS expression in the lymph node than their primary counterpart. 88
Figure 4.1 *Vector map of the plasmid backbones used in the study* 95
Figure 4.2 *Cloning strategy for construction of pcDNA3.1+ attB-CAG-NIS-IRES-Turbofp. Fluc2.* ..97
Figure 4.3 *Schematic of the workflow for glycosylation PCR array* 101
Figure 4.4 *Validation of the vector construct developed to evaluate expression of various genes* 105
Figure 4.5 *Endogenous NIS expression in a panel of BC cell lines showing weak cytoplasmic staining. Scale bar represents 20µm.* 106
Figure 4.6 *Screening of MCF-7 cells transfected with the bicistronic vector for co-expression of the therapeutic and a reporter gene.* 107
Figure 4.7 *Maintenance of the NIS and reporter gene expression over various passages* 108
Figure 4.8 *Role of glycosylation in differential localization of NIS* 109
Figure 4.9 *Clustering analysis of the glycosylation PCR array data by MEV software showing 2 distinct clusters of MCF-7 clones based on the expression of genes involved in the process of glycosylation.* 111
Figure 4.10 *Graphs depicting the levels of glycosylation genes in membrane vs. cytoplsmic NIS expressing clones.* 111
Figure 4.11 *Development of the experimental MCF-7 BC model with correlated expression of the therapeutic and reporter gene.* 113
Figure 4.12 *Radioactive iodide (^{125}I) uptake assay in MCF-7 NIS expressing clones .* 114
Figure 4.13 *Evaluation of in vitro therapeutic efficacy of radioiodide (^{131}I) in MCF-7 membrane NIS over-expressing clone (clone 22) .* 116
Figure 4.14 *Development of NIS expressing ZR-75-1-1 BC cells.* 117
Figure 4.15 *^{131}I toxicity assay in ZR-75-1 clone1 cells .* 118
Figure 4.16 *Cerenkov luminescence imaging with ^{131}I* 119
Figure 4.17 *In vivo Cerenkov luminescence imaging with ^{131}I in ZR-75-1 tumour bearing mice. Mice were imaged after 24 and 72 hours of 1mCi ^{131}I injection.* 121
Figure 4.18 *In vivo BLI with ^{131}I in ZR-75-1 NIS over-expressing tumour bearing mice to evaluate therapeutic efficacy of radioiodide. The mice in the treated group (n=3) were injected with 1mCi of ^{131}I for 3 weeks. BLI was performed weekly prior to the therapy.* 123
Figure 5.1 *Cytotoxic effect of 2-DG and metformin* 133
Figure 5.2 *Effect of 2-DG, metformin and their combination with Cobalt60 radiation on MCF-7 and MDA MB231 cells.* 134
Figure 5.3 *Effect of cobalt 60 radiation in combination with radio sensitizers on DNA damage of MCF-7 cells* 136
Figure 5.4 *Cell cycle status at different time points of treatment of MCF-7 cell. Data showing elongation of S phase in combination therapy after 48 hours of treatment. However, S phase elongation is not maintained till 48 hours when cells are treated with radiation alone.* 137
Figure 5.5 *Effect of 2-DG, metformin and their combination with ^{131}I treatment on MCF-7-NIS cell survival and apoptosis.* 138
Figure 5.6 *Effect of ^{131}I in combination with radio sensitizers on DNA damage of MCF-7 NIS expressing cells .* 139
Figure 5.7 *Effect of 2-DG, metformin and their combination with ^{131}I treatment on survival of plain MCF-7 cells.* 140

List of Tables

Table 1.1	Criteria for grading a BC tissue sample	**25**
Table 1.2	List of major chemotherapeutic agents used in BC treatment	**31**
Table 2.1	Characteristics of patient cohort from which primary breast tumour tissue samples was procured to evaluate NIS expression by immunohistochemistry.	**60**
Table 2.2	Table showing comparison of digital analysis and pathological scoring	**64**
Table 2.3	Characteristics of the patient cohort for which tumour tissue was procured to evaluate NIS expression at the transcript level.	**67**
Table 2.4	Table representing RQ scores for NIS with their respective IHC score	**72**
Table 3.1	Characteristics of patient cohort from which primary as well as lymph node meastatic breast tumour tissue was procured to evaluate NIS expression by immunohistochemistry	**83**
Table 4.1	Characteristics of the cell lines used in the study	**98**

Abbreviations

2-deoxy glucose (2-DG), 132
3, 3'-diaminobenzidine tetrahydrochloride (DAB), 55
Aromatase inhibitors (AIs), 80
Bioluminescence imaging (BLI), 44
Bovine serum albumin (BSA), 55
Breast cancer (BC), 20
Cell surface associated mucin (MUC-1), 92
Cerenkov luminescence imaging (CLI), 47
Circulating tumour cells (CTCs), 27
Cystic fibrosis transmembrane conductance regulator (CFTR), 33
DAPI (4',6-diamidino-2-phenylindole)., 98
Ductal carcinoma in situ (DCIS), 28
Electronic Medical Record (EMR), 55
Epidermal growth factor receptor (EGFR),, 31
ERE (Estrogen Response Element), 37
Estrogen receptor (ER), 26
Estrogen responsive element (ERE), 37
Fine needle aspiration (FNA), 22
Formalin fixed paraffin embedded (FFPE), 58
Glyceraldehydes 3-phosphate dehydrogenase (GAPDH), 58
Horse raddish peroxidise (HRP), 55
Human epidermal growth factor receptor (HER2), 26
Immunohistochemistry (IHC), 38
Infiltrating ductal carcinoma (IDC), 81
Insulin-like growth factor (IGF), 31
Intelligence quotient (IQ), 32
Magnetic Resonance Imaging (MRI), 22
Measles virus (MV), 41
Molecular imaging (MI), 42
National Surgical Adjuvant Breast and Bowel Project (NSABP), 28
Overall survival (OS), 28
Positron emission tomography (PET), 38
Progesterone receptor (PR), 26
Prostate specific antigen (PSA), 40
Real time polymerase chain reaction (RT-PCR), 39
Region of interest (ROI), 102
Retinoic Acid Receptor (RAR), 76
Rous Sarcoma virus (RSV), 92
Single photon emission computed tomography (SPECT), 42
Terminal ductal lobular unit (TDLU), 24
Thyroglubulin (Tg), 33
Thyroid stimulating hormone (TSH), 33
Trans retinoic acid, 75
Tris borate saline-tween20 (TBST), 55
Urokinase type plasminogen activator (uPA1), 28

Introduction and Review of Literature

1.1 Breast Cancer:

Breast cancer (BC) is the most frequent cancer among women and 2nd most frequent cancer worldwide, with more than 1.7 million cases diagnosed in 2012 according to GLOBOCAN 2012. It is the most commonly diagnosed cancer among females (**Figure 1.1A**) in 140 of 184 countries and accounts for nearly 1 in 3 cancers diagnosed in women in USA[14,15]. In India too, BC is the most common cancer among females in urban areas [16]. With rate of BC incidence increasing by 0.5-2% per annum, BC has now exceeded the number of cervix cancer incidence. BC is the fifth most common cause of cancer deaths among all cancers, whereas it is the most common cause of cancer deaths among women in less developed countries, including India. In developed countries, it is the 2nd most common cause of cancer deaths among females after lung cancer (**Figure 1.1B**). Worldwide, BC lead to 5,22,000 deaths in the year 2012. Compared to 2008, GLOBOCAN 2012 statistics suggest a 20% increase in BC incidence and 14% increase in mortality worldwide. In addition to this, the frequency of young females diagnosed with BC is very high. Around 6.6% of BC cases are reported in women below 40 years of age, while the incidence is 2.5% and 0.65% in women below 35 and 30 years of age, respectively[17,18]. In Asian countries the incidence of BC in females peaks at the age of 40s [19] where as in European countries and USA it peaks at the age of 60s. More than 80% of Indian BC patients are less than 60 years of age. The proportion of Indian BC patients under the age of 35 varies between 11% at Tata Memorial Hospital, Mumbai [20] to 26% at SGPGIMS, Lucknow[19] . BC at young age tend to exhibit large size tumour, higher number of metastatic lymph nodes, poorer tumour grade, aggressive tumour subtypes, earlier and more frequent loco regional recurrences, and poor survival [21,22]. Thus, there is a need to prioritize BC screening and control.

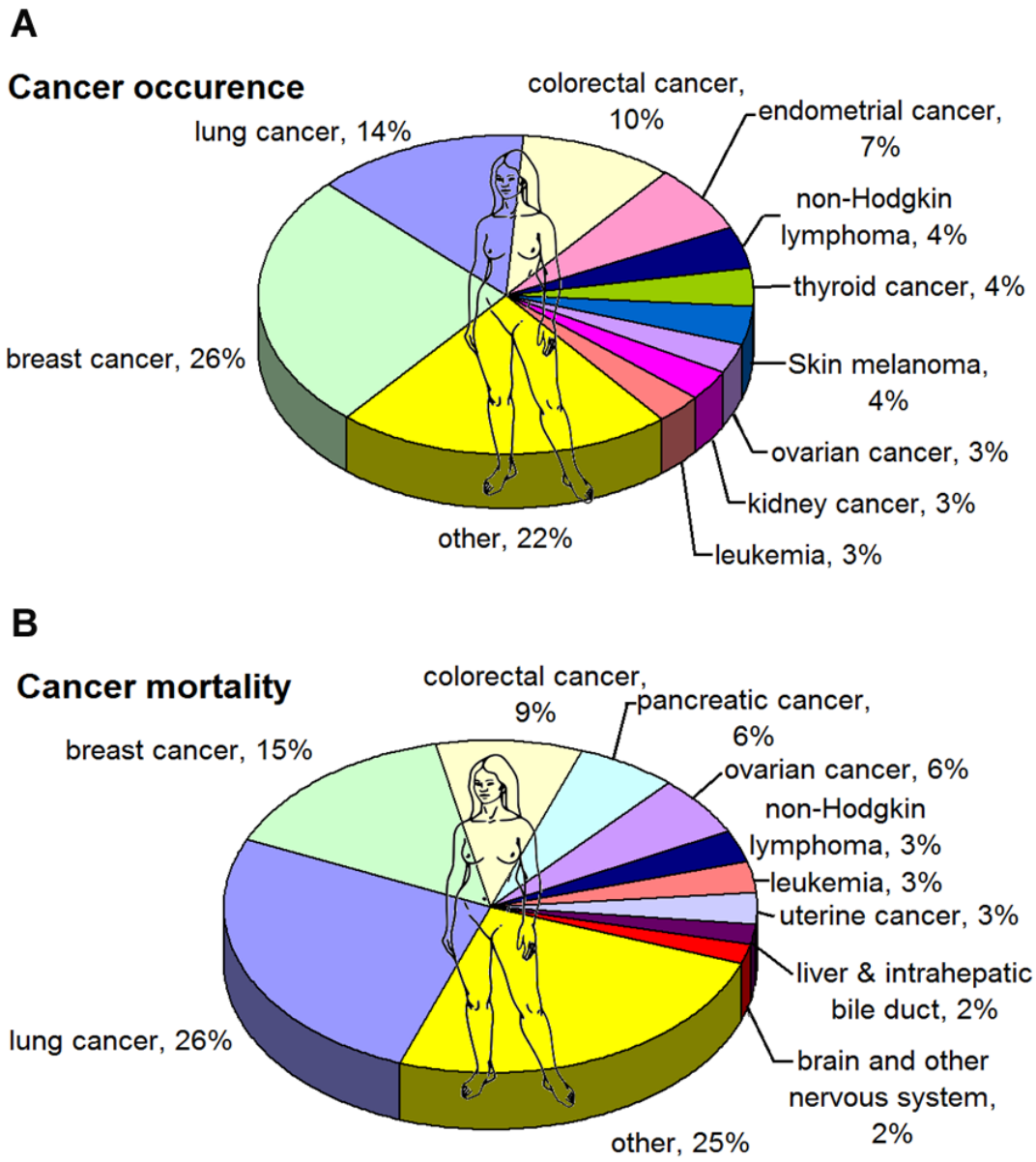

Figure 1.1 *Epidemiology of BC*[23] ***A.*** *BC occurrence in women in developed countries* ***B.*** *BC mortality in women in developed countries.*

1.2 Risk factors:

Incidence of BC depends on several risk factors which include modifiable as well as non-modifiable factors. Modifiable risk factors include late age at first child birth, use of oral contraceptives and hormone replacement therapy, postmenopausal obesity, cigarette smoking and alcohol consumption. Non-modifiable risk factors include sex, increasing

age, family history of breast or ovarian cancer, germ line mutation in a high-risk BC susceptibility gene, benign breast disease with atypical hyperplasia, early age at menarche, late age at menopause, dense mammary tissue etc.[24-26]. Many of these factors affect the level of reproductive hormone in females, thereby increasing the risk of BC incidence. Post menopausal women with higher level of endogenous hormones (estrogen and testosterone) are at increased risk of BC compared to women with lower hormonal levels[27]. Women with family history of BC, especially first degree relative are at higher risk of developing BC. BC incidence resulting from inherited mutations is 5-10%. High breast tissue density (amount of mammary and connective tissue relative to fatty tissue) is a strong and independent risk factor for BC development.

1.3 Diagnosis:

Since cancer is curable if detected early, diagnosis plays a very important role. BC diagnosis includes physical breast examination, imaging tests, analysis of nipple discharge and biopsies of suspicious areas.

Imaging tests create image of the body using X-rays, magnetic field, sound waves or radioactive tracer. Mammography involves irradiation of breast with X-rays. Ultrasound can be used to distinguish between cysts and solid masses as well as benign and malignant tumours. However, its use instead of mammography for screening purpose is not recommended. In case of nipple discharge some of the fluid is collected and is examined under the microscope for presence of cancer cell. However, absence of cancer cell from nipple discharge does not confirm absence of BC. Biopsy is the ultimate test to find if cancer is present. Different types of biopsies include fine needle aspiration (FNA) biopsy, core biopsy, vacuum assisted breast biopsy, excisional and incisional surgical biopsy.

1.4 Breast cancer stages:

Stage describes state of cancer progression in body. Determination of stage is based on tumour size, invasiveness, lymph node involvement and metastatic status (**Figure 1.2)**. Determining the stage of BC is important as it helps in understanding the prognosis and determines possible treatment strategies for the BC patient. BC stage is usually expressed as a number on the scale of 0 to IV, with stage 0 referring to the non-invasive cancer and stage IV describing invasive cancer that has been spread to different organs of the body.

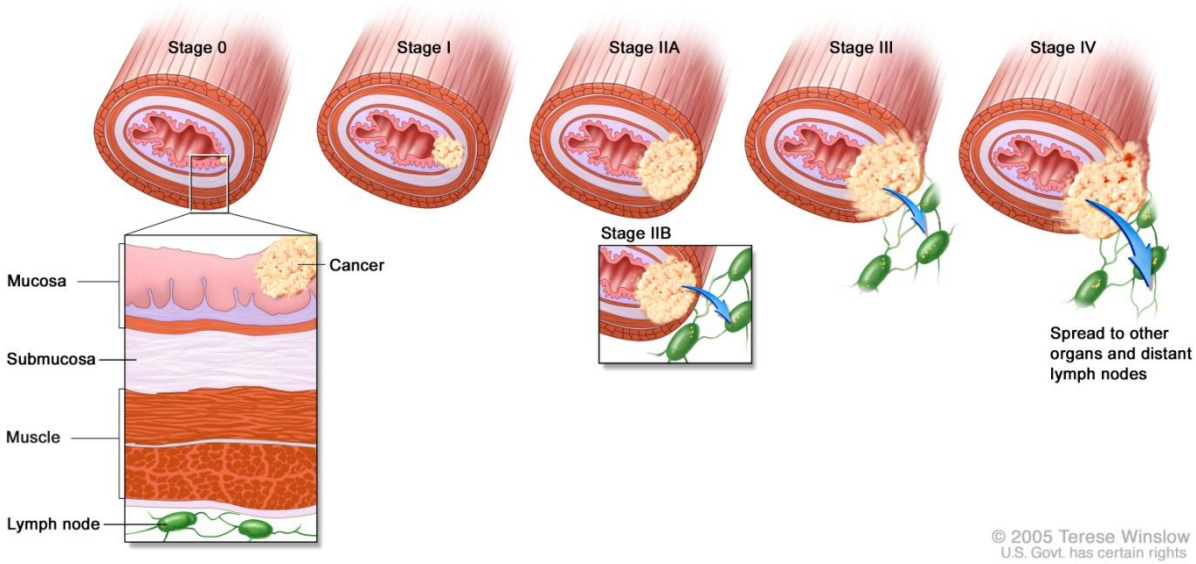

Figure 1.2 *Breast cancer stages*[28]

1.5 Histological grade:

Histological grading plays a very important role for treatment of BC. Many reports suggest its close association with survival [29]. Grading is determined based on 3 characteristics of the cells which include tubule formation, nuclear pleomorphism and mitotic counts (**Table 1.1**). Determination of tumour grade is based on Scarf Boom Richardson grading system which was modified by Elston and Ellis[30,31]. All the three

mentioned characters of the cells are scored on the scale of 1-3. The score of the three characters are then added and the score obtained is determined for grading on the scale of 3-9.

Low grade tumours are known to have more favourable prognosis than high grade - poorly differentiated tumours[32,33]. High grade tumours are also known to show negative hormone receptor status where as the case is opposite with low grade tumours.

Table 1.1 *Criteria for grading a BC tissue sample*

Feature	Score
Tubule and gland formation	
Majority of tumour (>75%)	1
Moderate degree (10-75%)	2
Little or none (<10%)	3
Nuclear pleomorphism	
Small, regular uniform cells	1
Moderate increase in size and variability	2
Marked variation	3
Mitotic counts	
Dependent on microscopic field area	1-3

1.6 Histology of normal breast:

The functional unit of the mammary gland is a tubular and glandular element embedded in the fibro-fatty tissue of the breast. The secretory part of the gland is terminal ductal lobular unit (TDLU), which is connected to an excretory part i.e. the large ductal system (**Figure 1.3**). Mammary secretions occur in lobule, which is made up of alveolar glands encompassed by specialized stroma. Lobular gland is surrounded by a single layer of

cuboidal cells known as luminal epithelial cells, which is supported by underlying loosely connected myoepithelial cells. Secretions from lobules are collected via small terminal ductules that discharge into large ductal system (major lacticiferous duct) and is excreted at nipple via a secretory pore forming the lacticiferous duct orifice.

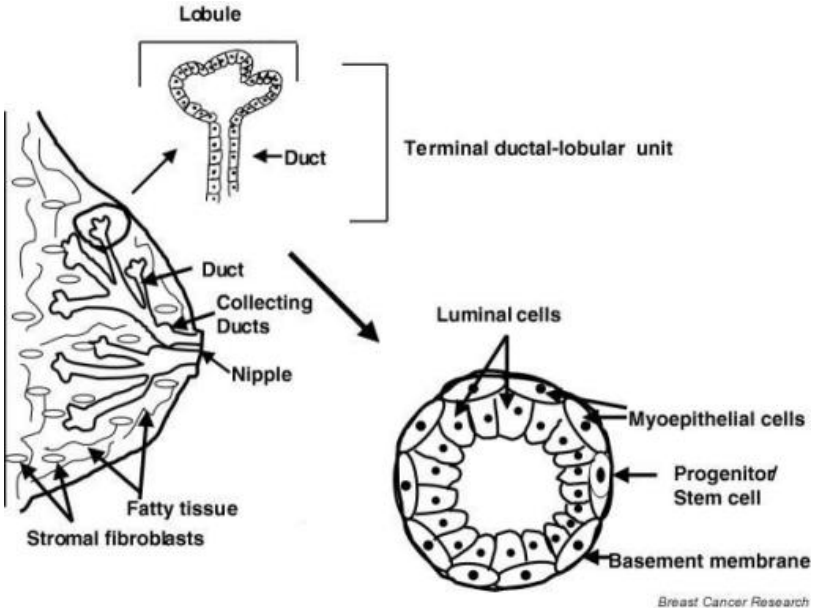

Figure 1.3 *Structure of the mammary gland. Terminal ductal–lobular unit (TDLU), composed of ductal cells, is the unit thought to be the origin of most BC. Lobule is made up of two primary types of cells in normal ducts: outer contractile myoepithelial and inner columnar luminal cells*[34].

1.7 Histopatholgy of breast cancer:

Histological type refers to the growth pattern of tumour. Pathologists identify specific morphological and cytological patterns in BCs that are closely associated with outcome of the disease. Histologically BC is divided largely into two groups: carcinomas and sarcomas. Carcinomas arise from breast epithelial cells where as sarcomas arise from stromal cells of the mammary gland. However sarcomas account for less than 1% of primary breast tumours. Breast carcinomas can be divided into in situ or invasive

carcinomas. Among all the BCs, invasive ductal carcinoma accounts for 80% cases and invasive lobular carcinoma accounts for 10-15% cases. Other BC histologic types are special types that include colloid (mucinous), medullary, micropapillary and tubular subtypes.

1.8 Breast cancer biomarkers:

Estrogen receptor (ER), progesterone receptor (PR) and Human epidermal growth factor receptor (HER2) are important prognostic factors for BC. These factors regulate proliferation and differentiation of mammary cells. ER/PR positivity is observed in 2/3rd of BCs. It is reported that BC patients with ER/PR positivity have less risk of mortality as compared to patients with ER/PR negative breast tumours[35,36].

Various studies suggest that steroid receptor status is closely associated with the disease outcome when follow-up time is short, but the association is considerably weaker in long time follow-up studies[37]. The hormone receptor status is also important for predicting response to endocrine therapy. 80% patients with ER/PR positive status responds to endocrine therapy where as less than 10% patients with ER/PR negative status show response to hormonal therapy.

Another important biomarker is a member of tyrosine kinase receptor family, namely, HER2. In a normal mammary epithelial cell, HER2 controls division, growth and repair of the cell. However in around 25% of BC cases, HER2 gene is amplified resulting in uncontrolled growth and division of these cancer cells[38,39]. HER2 positive tumours are known to have worse prognosis than HER2 negative tumours[38,40]. HER2 positive patients are generally treated with the 1st line therapy of trastuzumab, a monoclonal antibody that binds to extracellular domain of HER2 receptor. However, only 50% patients with advanced disease are known to respond to trastuzumab therapy[41].

In addition to these biomarkers which are routinely used in clinic today, there are constant research efforts to investigate the molecular signatures for classification of BC and to predict treatment response. Through expression analysis of a large number of genes, it is possible to find set of multiple genes that correlate well with a specific biological behaviour of tumour. Based on molecular classification BC is classified into four subgroups- luminal, basal-like, HER2 enriched and normal gland like[42]. With advancement in gene expression analysis technologies the number of molecular categories has expanded[43]. Recently BC has been classified into 10 molecular subtypes based on copy number variants, single nucleotide polymorphism and acquired gene copy number aberrations[44].

1.9 Metastasis:

As in majority of the cancers, metastasis to distant site is the main cause of BC related deaths [45]. Patients detected with BC are at risk of developing metastasis for their entire life span. The common site for BC metastasis is bone, brain, lung and liver.

The common risk factors for metastasis are presence of tumour in lymph node, larger tumour size, loss of histopathological differentiation and vessel invasion in patients with negative tumour in axillary lymph node[46,47]. Due to vast heterogeneity of the disease, it is difficult to predict the prognostic markers and risk factors for development of metastasis. Among various markers, HER2 has a value as a prognostic marker[48]. Owing to its vital role in metastasis prediction and treatment prognosis, testing HER2 expression status is a standard of practice in clinics at present. Another potential prognostic marker is presence of disseminated tumour cells, known as circulatory tumour cells and several reports suggest association of circulating tumour cells (CTCs) with metastasis and disease outcome [49]. However, few reports contradict the use of CTC detection for disease prognosis[50] . Thus, further studies are required to establish clinical importance of CTCs.

Few other markers with prognostic value include presence of BC cell in bone marrow, expression of urokinase type plasminogen activator (uPA1) and matrix metalloproteinases (MMPs)[51,52].

1.10 Disease management:

Currently BC therapy is based on individual patient's clinical examination. Planning of treatment is made by a multidisciplinary team involving an oncologist, pathologist, radiologist, radiation oncologist and onco-surgeon. Tumour grade plays an important role in diagnosis and management of BC because of its independent prognostic value. In addition to grade, histological classification by expert pathologists is considered for treatment decision. With the advancements in genomic analysis tools, scope of personalized therapy has been explored in past decade. This has given rise to an array of drugs. At present BC management involves the following strategies:

1.10. 1 Surgery:

Radical mastectomy was developed by Dr. William Halsted in the late 1800 and it led to significant improvement in the overall survival (OS) of BC patients[53]. For a century, radical mastectomy was the main therapy for BC. Over the years, it became evident that all of the BC patients do not require radical mastectomy. The procedure was finally replaced by modified radical mastectomy and eventually by breast conserving surgery, owing primarily to the efforts of various clinical trials from National Surgical Adjuvant Breast and Bowel Project (NSABP) and Milan group. Radiation became the preferred method for loco regional treatment in suitable BC patients. At present, breast conservation surgery is the main line of treatment for majority of patients along with adjuvant therapy of whole body radiation. Adjuvant therapy with radiation is known to decrease the risk of local recurrence in all subtypes of ductal carcinoma in situ (DCIS). Outcome of surgery combined with adjuvant therapy is comparable to mastectomy.

1.10. 2 Radiotherapy:

Radiotherapy is effective as adjuvant as well as palliative BC treatment. Reports suggest that adjuvant radiotherapy results in decreased risk of first recurrence in all risk groups and improves overall survival[54]. Although there has been advancement in BC radiotherapy, the molecular basis of radiosensitivity, and biomarkers/ gene signatures to detect the possible responders is not yet known. Further research in this field is required to identify non responders, where radiotherapy will result in toxicity.

Although the beneficial effects of radiation are well known in BC, it is sometimes associated with morbidity and mortality. Recognition and reduction of radiation associated toxicity is critical for oncologist. Specific radiation related toxicities are cardiac toxicity, secondary malignancies, radiation pneumonitis and lymphedema. However with the advancements in 3D planning and improved radiation dose distributions, radiation associated side effects have been reduced.

Radiation therapy thus plays an important role in multimodality therapy of BC patients, allowing breast conservation, improved locoregional control and overall survival.

1.10. 3 Chemotherapy:

Search for cytotoxic agents to treat cancer began with German scientist Paul Ehrlich in 1900's and by 1960s, many of the combinations of cytotoxic agents had been tested[55]. Doxorubicin was considered as most effective drug against BC as early as 1970s[56]. Combination therapy of anthracyclines with cyclophosphamide was the standard therapy for a long time[57]. Further development of taxanes was a breakthrough in the systemic treatment of BC[58]. Following the development of taxanes, other cytotoxic drugs were developed including vinorelbine, vinca alkaloids, gemcitabine, capecitabine, ixabepilone and eribulin[59-62]. Clinical trials of combination and sequential therapy led to the development of third-generation adjuvant chemotherapy. Major progress in BC therapy

was achieved by development of adjuvant chemotherapy. At present, available chemotherapeutic drugs for the treatment of BC can be classified into alkylating agents, anthracyclines, plant alkaloids and topoisomerase inhibitors (**Table 1.2**).

In past few years, much advancement has been made in the treatment of metastatic BC as well[63]. The chemotherapeutic drugs that are used for the treatment of BC metastasis include anthracyclines, taxanes and 5-fluorouracils. Epothilones and ixabepilone are new cytotoxic drugs that showed better therapeutic effects in metastatic BC patients[64]. Despite steady progress in the treatment with systemic agents, most BCs develop resistance to these drugs.

Table 1.2 *List of major chemotherapeutic agents used in BC treatment*

Types of Chemotherapeutic Agent	Examples
Alkylating agents	Cisplatin, Carboplatin, Cyclophosphamide
Anthracyclines	Doxorubicin, Epirubicin, Idarubicin
Plant alkaloids	Paclitaxel, Vinorelbine, Vindesine
Topoisomerase inhibitors	Irinotecan, Etoposide, Teniposide

1.10. 4 Targeted therapy:

Improved understanding of carcinogenesis mechanisms and altered molecular events in BC has led to the identification of novel molecular targets and development of targeted therapies. Targeting the molecules that are involved in the process of growth, survival, metastasis, angiogenesis and invasion of carcinoma cell is critical for effective therapy of cancer. In past few decades, many monoclonal antibodies and molecular inhibitors have been developed to target molecules involved in growth and progression of cancer cells. Clinical trials have demonstrated that several of these agents significantly improve the survival and outcome of the BC patients. The first and to date most successful targeted

BC therapy is the competitive inhibitor for ER, tamoxifen[65]. Adjuvant therapy with tamoxifen is known to reduce disease recurrence and annual BC death rate by 1/3[rd66].

Followed by this, trastuzumab was developed, which is a monoclonal antibody against HER2 receptor[67]. Trastuzumab targets the extracellular domain of the HER2 protein. In 1998, after the demonstration of significant survival benefit, trastuzumab was approved by the US Food and Drug Administration as first-line treatment in combination with paclitaxel for women with metastatic HER2/neu-positive BC. Several other targeted agents currently under evaluation in preclinical and clinical trials include inhibitors of epidermal growth factor receptor (EGFR), dual EGFR and HER2 inhibitors, VEGF/VEGFR inhibitors, and agents that interfere with crucial signaling pathways such as PI3K/AKT/mTOR and RAS/MEK/ERK; agents against other tyrosine kinases such as Src, insulin-like growth factor (IGF)/IGF-receptor (IGFR); agents that promote apoptosis such as Poly ADP ribose polymerase inhibitors; agents that target invasion and metastasis such as matrix metalloproteinase inhibitors and others[68]. One of the target proteins also under active research investigation for BC therapy is the sodium iodide symporter.

1.11 Sodium iodide symporter (NIS)

NIS is a plasma membrane glycosylated protein with 13 transmembrane helices. It mediates active transport of iodide inside the thyroid follicular cells. NIS couples uphill transport of 1 I^- ion to the downhill transport of 2 Na^+ ions down to its electrochemical gradient (**Figure 1.4**). The energy for the active transport is provided from the sodium potassium pump. In addition to its presence in thyroid, the protein is also present in other tissues such as salivary glands, stomach, lactating breast, and small intestine. However the functional importance of the protein is mainly known in thyroid where the iodide uptaken is used in the biosynthesis of the thyroid hormones. These hormones play a major role in the development of brain and lungs throughout the life span as reduced amount of

iodide in diet results in reduced mental ability, lower school and work performance, and loss of an estimated 13.5 intelligence quotient (IQ)[69]. Iodide transport by NIS can be blocked by perchlorate.

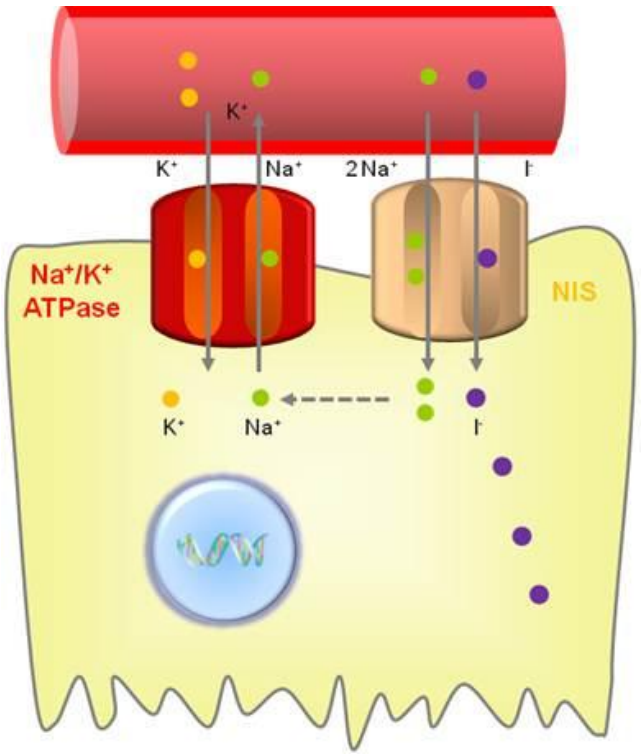

Figure 1.4 *The image showing presence of NIS at basolateral membrane of a thyrocyte. NIS uptakes Na^+ and I^- in 2:1 ratio. The energy for this transport is obtained from Na^+/K^+ ATPase pump*[70].

1.11. 1 Historical perspective of NIS

The direct effect of iodide deficiency, namely endemic goitre and cretinism are known throughout the human history. Courtois et al. reported use of iodine to treat goitre as early as 1812[71]. Thyroid's ability to concentrate I^- was also demonstrated in 1896 [71]. In Switzerland iodide supplementation was introduced for humans and animals as early as in 1922 due to high incidence rate of cretinism [72]. The direct link between iodide

deficiency and cretinism was established in 1966, when a trial was carried out in which half the families received iodized oil and rest half received saline. The trial showed dramatic reduction in the incidence of cretinism and goitre in the treated group as compared to the group that received saline[73]. These studies formed the basis for diagnosis and treatment of thyroid disease that lead to the treatment of thyroid cancer with radioiodide after thyroidectomy[74]. The nature of I^- channel was not known since many decades and phospholipids were also proposed to act as I^- carriers[75]. Ultimately NIS was identified as the molecule required for active I^- transport in thyroid[76]. However, till date, the pathway for I^- uptaken from basolateral surface across the apical surface into the thyroid lumen is not very well known. Many molecules including pendrin, chloride channel and cystic fibrosis transmembrane conductance regulator (CFTR) have been proposed, but the channel responsible for translocation of I^- across apical surface of thyrocyte is still uncertain.

1.11. 2 Iodide organification in thyroid

Once I^- is translocated into thyroid lumen it is oxidized to I_2 and then it gets incorporated into tyrosyl residues. Iodinated tyrosyl residues are coupled to thyroglubulin (Tg) molecule, which is stored in the follicular lumen in colloidal form (**Figure 1.5**). On Tg molecule, 3-4 tyrosyl residues are covalently bonded to iodine. This process is catalyzed by thyroid peroxidase, an apical monotopic membrane protein with a heme catalytic domain which faces the follicular lumen. The colloidal solution includes insoluble microglobules of protein highly cross linked with disulfide, dityrosine and glutamyl-lysine bonds[77]. When the thyroid stimulating hormone (TSH) level in the serum increases, thyroid hormone biosynthesis and release are stimulated. Immediately after TSH stimulation, pseudopod formation and Tg macropinicytosis occurs, internalized Tg

undergoes proteolytic cleavage in lysosomes and T3 and T4 are released into the bloodstream.

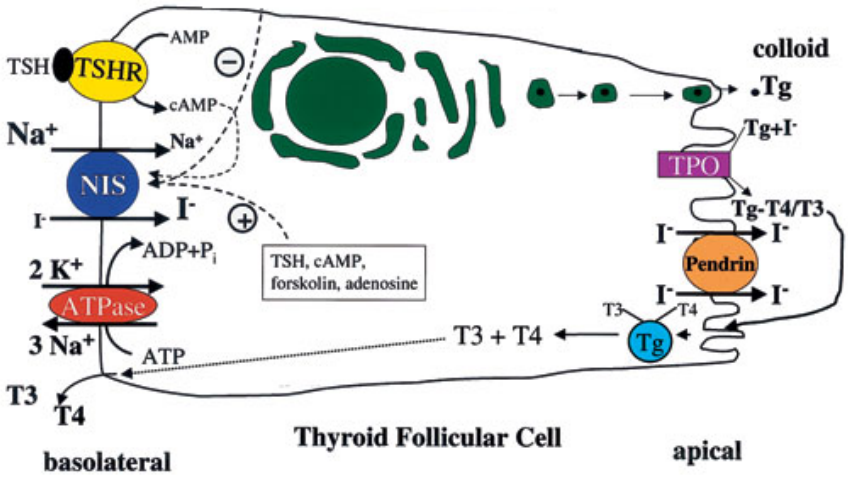

Figure 1.5 *Ilustration of a thyroid follicular cell showing iodide transport by NIS. The transported iodide is further organified in multiple steps with the aid of pendrin and thyroid peroxidise (TPO) molecule*[78].

TSHR = TSH - receptor, NIS = sodium iodide symporter, TPO = thyroid peroxidase, TG = thyroglobulin, T3 = triiodothyronine, T4 = thyroxine.

1.11. 3 Molecular characteristics of NIS

NIS was cloned for the first time in 1996 from rat thyroid cell line FRTL-5 cells and functionally expressed in *Xenopus laevis* oocytes[76]. Since then, NIS protein has been extensively characterized and NIS specific antibodies have been generated[1,79-83]. NIS has the excellent ability to concentrate I^-, 30 to 60 fold in the thyroidal cells[84,85].

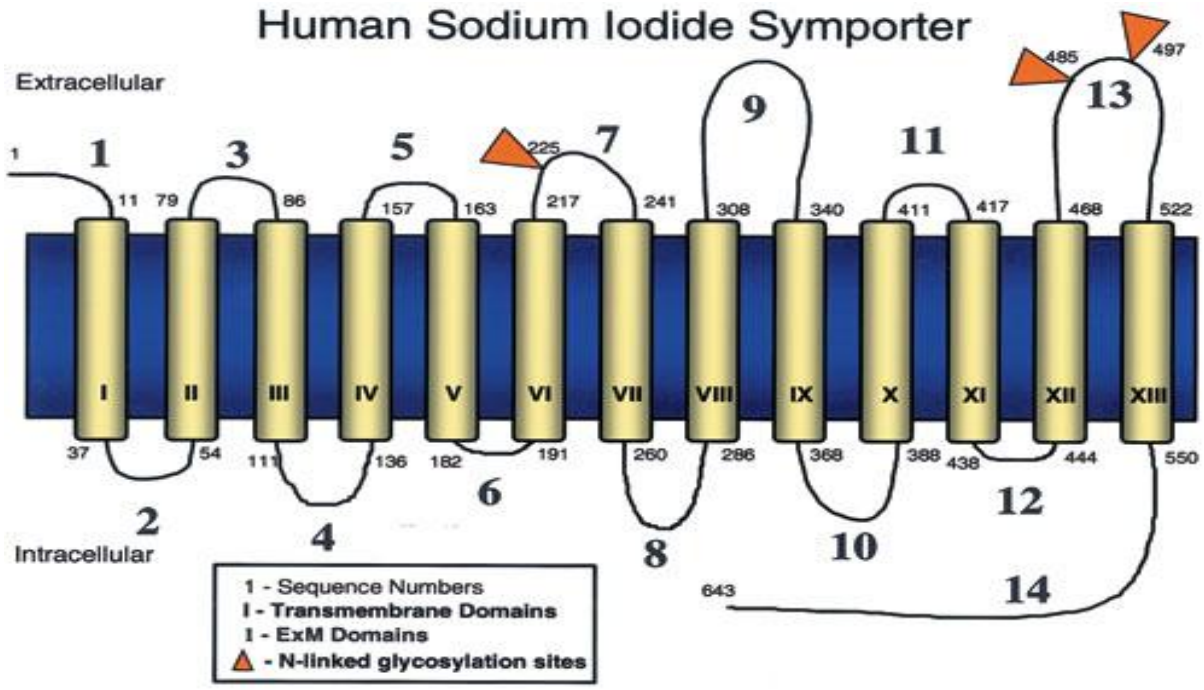

Figure 1.6 *The schematic representing proposed model of NIS with 13 trans membrane helices*[78]**.**

The secondary structure model of NIS shows that it is a hydrophobic protein of 618 amino acids with 13 transmembrane helices (**Figure 1.6**). It has an extra cellular amino terminus and an intra cellular carboxyl terminus[81]. NIS protein is phosphorylated mostly at its carboxyl terminus. Previous reports suggest that the carboxyl terminus is also important for correct trafficking and localization of NIS at the plasma membrane[82]. There are also 3 N-linked glycosylation sites for NIS. These 3 glycosylation sites are present at amino acid position 225, 485 and 497[81]. However whether glycosylation plays any important role in its function and localization is still controversial.

NIS sequence from patients and structural homology modelling suggests that the trans membrane segment III, VII and IX play important role in substrate coupling, coordination, stoichiometry and translocation. Shortly after rat NIS cloning, human NIS was cloned by Smanick et al. in 1996[86]. Human NIS shares 84% identity with rat NIS. The major difference lies in the 5 amino acid insertion between the last 2 trans membrane

segment and a 2 amino acid insertion at the carboxyl terminus of human NIS. Human NIS gene is located on chromosome 19p12-13.2. It belongs to the family of solute carrier protein, which also include the Na^+/glucose transporters (SGLT-1 and 2), the Na^+/monocarboxylate transporters (SMCT-1 and -2), the Na^+/multivitamin transporter (SMVT), and the Na^+/myoinositol transporter (SMIT)[87]. All these transporters show great homology with NIS protein, which is annotated as SLC5A5. In addition to the efficient transport of I^-, NIS can also mediate transport of many other anions including selenium cyanate ($SeCN^-$), thiocyanate (SCN^-) and nitrate (NO_3^-). Pertechnate (TcO_4^-), which exists as $^{99m}TcO_4$ is also transported by NIS and widely used for nuclear medicine applications. NIS also aids transport of perrhenate (ReO_4^-), which is also available in radioactive form and has clinical application, and ClO_4^-, which is a well known inhibitor of NIS[88,89]. In case of Na^+ dependent transporters, Na^+ can be substituted by other cations like H^+/Li^+ but NIS shows very limited activity with Li^+ and does not show any activity with H^+. The location of Na^+ binding site is known to be conserved in all Na^+ dependent as well as Na^+ independent ion channels, by virtue of their available crystal structure.

1.11. 4 NIS expression in extra thyroidal tissues

In addition to thyroid, NIS mediated I^- accumulation has been reported in salivary gland, gastric mucosa, small intestine, lactating mammary gland, choroid plexus and ciliary body of eye[88,90]. NIS expression at the transcript level has also been detected in colon, ovary, uterus and spleen, but functional NIS in these tissues has not been reported[91].

NIS expression in normal breast is observed only during pregnancy and lactating phase. Tazebay et al. reported that in pregnant mice, NIS protein is detected at mid gestation period which is around day 10/11 of pregnancy in a full gestation period of 19 days and the intensity of its expression is maximum at the end of gestation period[1,92]. In lactating mammary gland, NIS is localized in the basolateral membrane of alveolar epithelial cells.

These cells have been shown to uptake I^- from bloodstream and secrete it in the milk for the development of the newborn[93,94]. Other than thyroid, lactating mammary gland is the only organ where I^- is known to be organified by lactoperoxidases in the alveolar cells[95]. Since NIS expression in mammary gland is observed during pregnancy and lactation, many groups have investigated the role of ovarian and pituitary lactogenic hormones in mammary gland NIS regulation. These studies have reported that steroid hormones estrogen and progesterone, and two pituitary lactogenic hormones, prolactin and oxytocin, either individually or in combination, upregulate NIS expression[1,92]. It has also been shown that ERα physically interacts with an estrogen responsive element (ERE) in NIS gene promoter and activates NIS expression. The ERE sequence is localized only 9 base pairs away from NIS gene TATA box element and this position is conserved in rodent and human genomes[96]. NIS expression after child birth is regulated by suckling of nipples. It has been shown experimentally that NIS expression drops on separation of pups from mother for 48 hours [1,92]. Thus, this excellent regulatory mechanism prevents unnecessary iodine transport to mother's milk once pups are grown up.

1.11. 5 NIS expression in thyroid malignancy

Thyroid neoplastic tissues show abnormality in iodine metabolism. In thyroid carcinoma, peroxidase activity is reduced or absent resulting in low iodine organification. As a result, there is low degree of thyroglobulin iodination and a low rate of thyroid hormone synthesis. In normal thyroid tissue, iodine uptake is about 1%/g of the administered activity, whereas it ranges from 0.1%-0.001% in thyroid cancer tissues. Further, the biological half life of iodine in normal thyroid tissues is 6-8 days, whereas in case of neoplastic transformations, the half life is 3-5 days[97]. Activation of a specific oncogenic pathway may be responsible for altered iodide trapping ability of the transformed cells resulting from altered NIS gene expression[98]. Immunohistochemistry (IHC) study to

evaluate NIS expression in human thyroid tumourigenesis demonstrates heterogenous expression as it is detected only in a few malignant papillary or follicular thyroid cells[99]. These studies suggest that, before administration of ^{131}I in thyroid cancer patients, intensive TSH stimulation should be performed to enhance NIS expression levels and iodine uptake in these tissue[100].

1.11. 6 Clinical application of NIS in thyroid cancer

NIS has diagnostic as well as therapeutic value in the treatment of thyroid cancer. In patients suffering with differentiated thyroid cancer, total thyroidectomy is followed by gamma camera imaging with $^{131}I/^{123}I$, as the remaining lesions show efficient absorption of iodide due to NIS expression[101] . Since positron emission tomography (PET) imaging provides better resolution than gamma camera imaging, ^{124}I based PET imaging is more sensitive for detection of the residual lesions compared to ^{131}I mediated whole body scintigraphy. NIS mediated radioiodine therapy of differentiated thyroid cancer patients has been a great example of successful targeted radiotherapy to reduce recurrence and mortality for almost past 70 years[102]. In case of de-differentiated thyroid cancers, NIS expression is downregulated and therefore ^{131}I therapy is not effective in case of anaplastic and medullary thyroid carcinoma. One of the possible ways to enhance NIS expression in de differentiated thyroid cancers is by induction of re differentiation with differentiating agents such as retinoic acid and thiazolidinedione[103]. Additionally, anaplastic and medullary thyroid cancer patients can be treated with ^{131}I after NIS gene delivery to the tumours, however clinical trials are required in this line.

1.11. 7 NIS expression in breast cancer

Radioactive iodine uptake in malignant breast was detected 40 years ago suggesting possible role of NIS mediated diagnosis and therapy of BC patients[104]. However, in absence of the cloning sequence, NIS expression was not detected until 2000, when in a

pioneering study by Tazebay et al., NIS expression was demonstrated in 80% BC cases in a cohort of 23 samples. It was also shown that 20% of extra tumoural adjacent tissues and none of the normal breast tissue showed NIS expression. In subsequent studies, NIS expression was analyzed in larger cohorts by variety of molecular techniques in BC tissue samples and similar results were obtained. Till date, NIS expression in BC has been detected by real time polymerase chain reaction (RT-PCR), RNase protection assay, western blot, scintigraphy and IHC[3,9,13]. The details of these reports are explained in **Chapter 2 & 3**.

At present our knowledge regarding role of NIS in BC and factors that lead to NIS expression during mammary gland tumourigenesis is limited. According to a report, NIS expression leads to enhanced cell migration and invasion without involving ion transport[105]. It was also observed that these functions are mediated by binding of NIS to the leukemia associated RhoA guanine exchange factor that activates small GTPase RhoA. A further increase in cell migration and invasiveness was observed in case of cells showing intra cellular localization of NIS.

1.11. 8 NIS as a therapeutic gene

NIS can be used as a therapeutic gene by virtue of its radioiodide concentrating ability in the target cell[106]. For therapeutic application of radioiodine in non-thyroidal cancers without NIS gene expression, NIS gene transfer is a prerequisite. Cloning of human NIS in 1996 by Carrasco et al. led to the use of this gene in therapeutic applications with ^{131}I by various groups[76]. Some of the other radionuclides like ^{188}Re and ^{211}At, which are also substrates of NIS, have been used for NIS gene mediated therapeutics in non-thyroidal tumours. Use of NIS as a therapeutic gene in BC is explained in **Chapter 4.** Here we have briefly mentioned about the utility of this therapeutic gene for the treatment of various other cancers.

NIS gene transfer in a hepatocarcinoma animal model by adenoviral vector has shown strong tumour growth inhibition and prolonged survival[107]. In this study, inherent tropism of adenoviral vector to the liver and intra portal route of injection resulted in targeted delivery of the NIS gene. Success of gene therapy resides in efficient and targeted delivery of the gene of interest to the desired tissue. For targeted delivery of the gene selectively to malignant tissue, tissue specific promoters play an important role. Tissue specific expression of NIS was demonstrated for the first time in an androgen sensitive prostate cancer cell line (LnCaP cells) using prostate specific promoter, prostate specific antigen (PSA) [108,109] and NIS mediated iodide uptake was observed. Self inactivating lentiviral vector has also been used for NIS gene expression under immunoglobulin promoter, to selectively target multiple myeloma cells and showed efficacious results in mice xenograft model with a tumour free survival in 5 month follow up time[110].

Many studies were followed, further using various tissue specific promoters. One of the important studies was use of telomerase promoter to drive NIS gene expression. Aberrant telomerase expression is well known in cancer[111] and using such a promoter to drive expression of a therapeutic gene allows its use in any kind of tumour cell. Transcriptional targeting of NIS in colon and melanoma xenograft model has been achieved by using promoters of 2 subunits of telomerase, the RNA subunit (hTR) and the reverse transcriptase subunit (hTERT). Using these promoters, delayed tumour progression was observed in xenograft models after a therapeutic dose of 1mCi ^{131}I[112]. NIS gene transfers have also been made by using oncolytic measles virus (MV). MV-NIS has been approved for a phase I clinical trial in patients with advanced or refractory multiple myeloma[113].

In a study, tumouricidal effect of ^{131}I therapy was evaluated in conjunction with canstatin in MDA MB231 metastatic BC xenograft model and transgenic retinal pigmented epithelium spontaneous tumour model[114]. Canstatin is a human basement membrane

derived fragment of human collagen that is known to inhibit angiogenesis and tumour growth. In this study, single dose of ^{131}I as low as 300μCi in combination with canstatin showed tumour growth regression which was sustained throughout the follow up time of 30 days in MDA MB231 xenograft model.

At present several synthetic vectors for efficient delivery of NIS have also been developed. Few of the examples include development of synthetic polyamine vector, polyplexes and biodegradable nanoparticles[115,116]. These synthetic delivery systems definitely offer novel, efficient and promising approach to NIS gene transfer.

One of the important measures that should be taken prior to NIS gene mediated radioiodine therapy in extra thyroidal tissue, is prevention of radioiodine uptake in the healthy thyroid cells. Since thyroid organifies iodine efficiently, it acts like a sink which results in destruction of the thyroidal cells and less availability of the radioiodine to NIS expressing tumour cells that are incapable of iodide organification.

1.11. 9 NIS as a reporter gene

In vivo non- invasive imaging of NIS gene was performed for the first time by Shimura et al.[117] by transfecting rat NIS cDNA into malignantly transformed rat thyroid cells (FRTL). Over the years, importance of NIS gene as a reporter was realized. Unlike receptor proteins used as reporter, which binds the ligand in 1:1 stoichiometry, NIS accumulates its ligands which are in form of radiolabelled substrates, concentrates them and gives signal well above the background. This attribute of NIS makes it a promising reporter gene. NIS has also been used for monitoring the expression and effect of various genes on tumour size by performing diagnostic scintigraphic imaging[92,108,118].

NIS has been used as a reporter for pulmonary gene therapy when in 2005, Niu et al. used adenoviral NIS vector for intranasal delivery in the lungs of Cotton rats and observed signal from ^{124}I PET imaging upto 17 days post vector administration[119]. NIS gene based

cardiac imaging has also been demonstrated by various groups[120]. Since reporter genes can be used for tracing the localization of transplanted cells, Terrovitis et al. introduced lentiviral vector expressing NIS in rat cardiac derived stem cells. Transplantation of these cells back to rats enabled ^{125}I mediated single photon emission computed tomography (SPECT) imaging[121]. NIS has also been used as a reporter for studying the recruitment of macrophages to the site of inflammation.

Thus, as a reporter gene NIS can be used for monitoring gene expression, vector biodistribution and for cell trafficking[122]. Overall, studies suggest that gamma camera and PET based non- invasive imaging of NIS in extra thyroidal cells is feasible.

Recently, it was reported that ^{131}I and ^{124}I have sufficient energy to emit Cerenkov radiation and can be visualized with highly sensitive optical imaging instruments. Using this imaging modality, NIS gene transfected cells have been successfully imaged by optical imaging instrument in an *in vivo* animal model[123].

1.12 Molecular imaging

As mentioned above, there are large numbers of substrates that can be transported by NIS and this allows *in vivo* visualization of NIS expressing cells by various molecular functional imaging modalities. Molecular imaging (MI) aids in characterization and quantitation of biological processes in living subjects. Another advantage of non- invasive animal imaging is that, repetitive study can be performed in the same animal using identical or different imaging modalities at various time points. Such study provides clear picture of the progressive changes *in vivo* and also provides temporal assessment of the therapeutic responses in the same animal without the need to sacrifice it. MI assays also provide the benefit of quantifying the image providing meaningful numerical measures of the biological phenomena. Such advantages suggest that MI plays an important role in

preclinical trials that are conducted to test therapeutic efficacy of certain agents for their biodistribution, pharmacokinetics and tumour growth monitoring non-invasively.

There are two major imaging strategies that are being employed in biomedical research: direct and indirect imaging, of which the latter is predominant in biological studies using pre-clinical animal models. The direct imaging strategy is based on imaging the target molecule directly, usually with a target-specific probe. In nuclear medicine, radioactive-labelled tracers are used for imaging and NIS based radioiodine imaging comes under this category. Whereas indirect MI is based on reporter gene imaging, which involves single or multiple reporter genes and their specific reporter probe partners. The advantage of reporter gene imaging is the ability to develop and validate imaging strategies more rapidly and at considerably lower cost than direct imaging strategies.

1.12. 1 Radionuclide imaging

Radionuclide imaging techniques allow probing a protein with specific radiopharmaceuticals. In PET imaging, high-energy rays emitted from within the subject are recorded. Positron emitting isotopes emit one positron from its nucleus which gets annihilated by a nearby electron to produce two 511Kev γ rays at < 180° apart. Frequently used PET isotopes are ^{13}N, ^{11}C, ^{64}Cu and ^{18}F. Among radioisotopes of iodine ^{124}I is used for PET imaging.

γ emitting isotopes of radioiodine ^{123}I and ^{131}I as well as ^{99m}Tc, which is a substrate for NIS, can be used for NIS based imaging of living subject by applying gamma camera based instruments, including SPECT. The main difference in PET and SPECT is the requirement of lead collimeters in SPECT to define the angle of incidence as compared to electronic collimation in PET imaging. The sensitivity of PET is at least a log order higher than the SPECT. The primary advantage of NIS is that no substrate labelling is

required and the imaging parameters are ideal and well standardized in both small animal and human instruments. A disadvantage of NIS as compared to other commonly used reporter genes is that ^{124}I is the only approved PET isotope for NIS imaging. One of the limitations of ^{124}I decay is that the high energy positrons released have a long range in tissue prior to annihilation, which limits the resolution as well as total yield of positrons from $^{124}I^{124}$.

In our study we have linked NIS with an optical imaging fusion reporter gene, i.e. Turbofp. Fluc2 in which Turbofp represents the fluorescent partner and Fluc2 represents the firefly luciferase gene. Linking a therapeutic gene such as NIS with reporter gene aids in monitoring the expression of the therapeutic gene and at the same time, allows following the effect of therapeutic gene in tumour xenograft model non-invasively by optical imaging.

1.12. 2 Optical imaging

Optical imaging allows non-invasive *in vivo* imaging by capturing light photons for extracting relevant biological information from within the subject. Optical imaging allows relatively low cost alternative to studying reporter gene expression in small animal models. It involves bioluminescence as well as fluorescence imaging, but since we have not used *in vivo* fluorescence imaging in our study, a brief introduction of bioluminescence imaging (BLI) is provided below.

The main advantage with BLI is that it can be used to capture very low levels of visible light as the background signal is almost null. To increase the efficiency of light detection emitted from the animals, highly sensitive detectors have been developed. The imaging system generates a bioluminescence image which is generally represented as a planer colour image and it is superimposed on a gray scale photographic image of the small

animal subject using overlay option of the image analysis software. After imaging, a region of interest (ROI) is selected manually or by automated tool on the area of signal intensity, and the maximum or average intensity is recorded as photons/sec/cm^2/steradian. Optical imaging instruments are easy to operate, have fast acquisition time and allow imaging from 5-6 animals at the same time. These attributes of optical imaging makes it suitable for experimental imaging research.

The mainstay of BLI is the variety of available luciferase enzymes such as firefly luciferase, *Renilla* luciferase, *Gaussia* luciferase, *Metridia* luciferase, *Vargula* luciferase or bacterial luciferase[125-130]. However the most popular enzymes for optical imaging are firefly, *Renilla* and bacterial luciferase. The most commonly used luciferase is firefly luciferase which is obtained from the firefly, *Photonis pyloris*, a member of the beetle family that also includes railroad worms and click beetles which are some of the other luciferase producing insects. The luciferase produced from these organisms is a single polypeptide related to the CoA ligase family of proteins[131]. The substrates for firefly luciferase include a benzothiazole luciferin, ATP and oxygen and they emit photons in the range of 560-614 nm light depending on luciferase and the physiological conditions. Since these enzymes require ATP as well as oxygen, the luciferase expressing cells give maximum signal in a highly metabolic state and aerobic environment. Although optical imaging methods are excellent tools in pre clinical settings, their use in the clinics is limited, as many of these genes and their substrates are immunogenic and tissue depth in the human subjects may result in very low signal intensity.

In recent years, a new source of photon signal has been exploited for MI studies. It is based on the emission of visible light produced by Cerenkov radiation emitted by the biomolecules labelled with β-emitting radionuclides. This allows imaging of many

commonly available and clinically relevant radiotracers in widely available *in vivo* optical imaging systems.

1.12. 3 Cerenkov bioluminescence imaging

The Cerenkov optical phenomenon is known since 1940's however its application for luminescence imaging is known recently since 2009. The principle of Cerenkov imaging is that when radionuclide molecules travel through a dielectric media, they lose energy through interactions with the surrounding matter (**Figure 1.7**). The molecules of dielectric media are randomly oriented, but get polarized when radionucleotide passes through. When the particle travels at a speed higher than the speed of light, these polarized molecules relax by releasing energy in form of visible radiation luminescence.

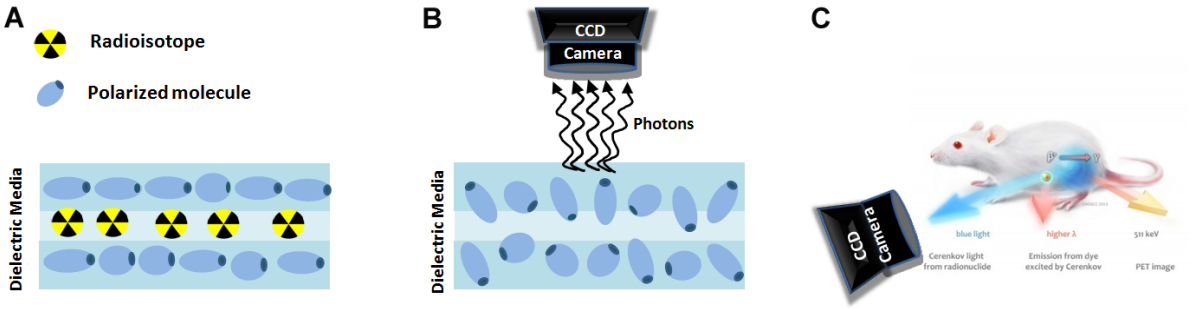

Figure 1.7 *The schematic showing principle of Cerenkov luminescence imaging.* ***A.*** *Polarization of the molecules in dielectric media when a radionuclide travels.* ***B.*** *Once the radionuclide is passed by at a speed higher than the speed of light, the molecules come back to their random state and emit energy in terms of photons* ***C.*** *Cerenkov luminescence emitted from the animals, injected with radionuclide can also be captured through a highly sensitive CCD camera.*

Through several studies, the ability of various radioisotopes for the production of Cerenkov radiation has been evaluated[132-134]. Cerenkov imaging bridges the gap between preclinical optical imaging and clinical nuclear imaging by using the approved tracers and therapeutic agents for optical imaging. Visualizing radiotracer molecule by optical

imaging system has advantages as well as challenges. In small animal PET imaging systems, one animal at a time can be scanned and each scan require 10-15 minutes or more; where as in Cerenkov luminescence imaging (CLI), as many as 5 animals can be scanned simultaneously. Another advantage is that optical imaging units are considerably cheaper than most of the animal PET imaging systems. The procedure of CLI is similar to the BLI, except radionuclide is injected instead of a bioluminescent substrate. Various reports suggest good correlation between PET and CLI using multiple radiotracer molecules[135]. The ability of ^{131}I to produce Cerenkov luminescence has been demonstrated by various groups, but only few reports have shown *in vivo* CLI with ^{131}I[123,133]. It has been demonstrated in a report that CLI enables higher throughput in the identification process of ^{131}I accumulation, specifically in NIS transduced implanted cells[123].

One of the challenges with CLI is the decay of the radioactive material that results in reduction of active material for production of Cerenkov radiation. However, this challenge can be overcome by using Cerenkov generating radionuclides which have a longer half- life. Another issue is the production of low signals generated by CLI as compared to those produced by standard bioluminescence and fluorescence imaging and signal attenuation of Cerenkov spectra that peaks at the blue region by animal tissues. For subcutaneous tumours, this does not pose any problem. But for deep tissue imaging, this causes considerable loss of the luminescence[136].

1.13 Rationale of the study

At present BC disease management is based on adjuvant systemic therapies that are administered before or after surgery to ablate the remaining micro-metastatic cells thereby improving the disease free survival of the patients. Adjuvant therapies have shown success in clinical trials and they reduce the recurrence by nearly 50%[137]. However

side effects of such cytotoxic drugs in BC is well known which includes loss of healthy blood cells, hair loss, tiredness, sore mouth, sore eyes and diarrhea. All over the world there is constant search for development of alternative therapeutic strategies that can specifically target BC cells without harming the normal healthy cells of the body.

Sodium iodide symporter is one such therapeutic protein which offers target specific radioiodine treatment with lesser side effects to healthy tissues as compared to currently available chemotherapeutic drugs. Decades of basic and clinical research work in diagnosis and treatment of thyroid cancers by various radioisotope substrate of NIS has enhanced our learning in the field of NIS biology. However the field of NIS research in BC is relatively at its young state and constant research efforts are being made to develop it to a matured state.

At present NIS expression in BC is well known but knowledge regarding its BC subtype specific variation is limited. A few groups evaluated NIS expression in BC epithelial subtypes but these studies were performed using small cohort of patient samples (n=28-32) and mostly had focussed on selected subtype of BC[2,138]. For these obvious reasons these groups could not observe association of NIS with any specific subtype. In a recent study by Ryan et al. NIS expression was evaluated at the transcript level from 75 BC patient samples including all major subtypes and they observed significantly high NIS expression in ER, PR-ve, HER2 +ve subtypes[13]. However the status of NIS at protein level was not reported. As an ion transporter, the NIS protein expression as well as localization is important. Therefore, IHC for NIS in BC subtypes may provide important information relevant for addressing functional use of NIS based therapy to the clinic.

NIS expression in BC suggests the potential of targeted radioiodine treatment in these cells. To validate this it is important to evaluate the pattern and time course of tumour

response in preclinical model as it may help to guide future applications of NIS based therapy in BC in clinic. Previous literature demonstrates that although ^{131}I alone results in tumour growth inhibition but tumour recurs back after 10-21 days[139,140]. Such observations suggest requirement of further improvement in radioiodine therapy of NIS expressing BC cells. A strategy that can be used, but still unexplored, is addition of radio sensitizers to enhance ^{131}I mediated damage to NIS expressing cells. Exploring the combination of radio sensitizers with radioiodine may show improved therapeutic efficacy in NIS expressing BC cells.

1.14 Aims & Objectives

Based on the above rationale, following are the objectives of the thesis:

1. Understanding of NIS expression in BC patient samples

2. Understanding the efficacy of NIS based radioiodine therapy in an experimental model using engineered cells and imaging method

Aim 1 is covered in chapter 2 & 3 and Aim 2 is covered in chapter 4 & 5.

Evaluation of NIS expression in primary breast tumour tissues and it's correlation with various prognostic markers of breast cancer

2.1 Introduction

The role of sodium iodide symporter (NIS) expression in thyroid malignancies is well known since past many decades; however its expression in BC (BC) was reported only a decade ago and is still under active research investigation. Since NIS mediated radioiodine therapy has been successful and established in case of thyroid cancer; with the dose and timing having been optimized, the strategy can be adopted for the treatment of NIS expressing BC patients.

NIS expression in BC was reported for the first time by Tazebay et al. It was shown that, out of the 8 normal breast tissue sample analyzed by IHC, none of the samples show positive staining for NIS, whereas 83% DCIS and 87% invasive cancer samples show positive NIS expression[1]. 23% of tumour adjacent tissues also showed NIS positivity but the intensity of staining was always less than the malignant tissue. Further it was reported that, in a transgenic female mice model with active *ras* or *neu* oncogene under MMTV promoter, NIS mediated uptake of $^{99m}TcO4^-$ occurs only in the tumour bearing mammary gland and not in the non-tumour bearing mammary gland[1]. Following this study Wapnir et al. evaluated NIS expression from 40 normal breast tissues, 17 DCIS and 91 invasive carcinoma tissues[5]. Majority (87%) of normal breast tissues were found to be negative for NIS expression, while 76% invasive and 88% of non- invasive cancers were positive for NIS expression[5]. NIS staining was intense in these cases and localization was predominantly cytoplasmic. In another report, NIS expression was shown to be upregulated at transcript as well as translational level in BC[3]. Additionally, NIS mediated $^{99m}TcO4^-$ uptake in breast tumour was also observed by gamma scintigraphy in a patient with BC. These observations suggest potential of NIS based radioiodine therapy in BC patients; however few important questions are to investigate if NIS expressing BC tissues

can uptake iodide as efficiently as thyroid cancer tissues and whether NIS mediated radioiodine therapy are effective in these cases despite absence of iodide organification.

From previous literature it is well known that the regulation of NIS expression is different in thyroid and breast[141,142]. In thyroid it is mainly mediated by TSH, whereas TSH is not expected to show any effect on NIS function in mammary gland. This differential regulation gives the advantage of modulating the thyroidal NIS without effecting the status of NIS in BC tissues. Exploiting this differential mechanism of NIS regulation Wapnir et al. made an important measurement in 2004[4]. They blocked the thyroidal NIS with T3 in 13 patients and observed that thyroidal uptake of ^{123}I was significantly less (0.9-2.8%) than the patients where thyroid was not blocked (20-22%). Further addition of methimazole, which inhibits iodine organification decreased thyroidal iodine uptake by 90%.

Few groups have focussed on NIS expression in TNBC (triple negative breast cancer) –a subtype of BC associated with poor prognosis and aggressive tumors, owing to lack of available targeted therapies for the same[6,143]. In a study, 23 TNBC cases were analyzed for NIS expression by IHC, wherein 15 samples (65.2%) showed positive NIS expression[6]. Out of these 15 cases, 11 (47.8%) showed intense NIS expression. Although the localization of NIS was predominantly cytoplasmic, membrane specific NIS staining in 4 tissue samples was evident. One of these patients, exhibiting a striking membrane NIS expression, was subjected to 1.9 mCi dose of $Na^{123}I$ followed by scintigraphic imaging. Higher uptake was observed in the breast with the tumour than the contra-lateral breast without tumour. Although the concentration of radioiodine accumulated in the tumour was not sufficient to elicit a therapeutic effect, consistent increase in iodine uptake was observed in the tumour tissue at different time points. Few groups have also investigated NIS expression with respect to BC epithelial subtypes. Recently Tandon et

al. evaluated NIS protein expression in 32 BC tissue samples, which included 26 cases of ER, PR+ve subtype and 6 cases of ER, PR-ve subtype[144]. NIS expression was positive in 90% samples and it was irrespective of ER and PR status. In another report NIS expression was evaluated in 44 BC patient samples and only 34% samples showed positivity for NIS[145]. This study involved 15 ER+ve and 29 ER-ve tumours. Among the 44 samples, 11 were PR+ve and 33 were PR-ve but association of NIS with these receptors was not observed.

NIS expression in BC metastasis has also been reported by Wapnir et al.[4] and it was shown that the iodine uptake in the metastasized tissue correlates well with the IHC data for NIS expression. NIS transcript level has also been assessed by various groups and expression was observed in 50-70% cases[9,13,146,147]. In a report 75 BC tissue samples were evaluated for NIS expression at the transcript level across various BC subtypes and NIS expression was found to be upregulated as compared to normal breast[13]. Further it was observed that NIS expression in ER, PR-ve, HER2+ve group is significantly higher as compared to any other subtype. NIS mRNA expression was also analyzed in 10 fibroadenoma tissues and expression level was found significantly higher than malignant type.

Many of the previous reports provide information on NIS expression status only in TNBC subtype. In a few studies where comparative analysis of NIS expression in various subtypes was performed, the sample size is very small and each subtype is not well represented. Ryan et al. compared NIS expression in major subtypes of BC with similar number of representative from each subtype; however the report provides NIS expression at transcript level only. Since for a symporter molecule, expression of the protein plays an important role, understanding NIS protein expression in various BC subtypes may

provide some information that may help in the clinical translation of NIS based radioiodine therapy for BC patients.

In order to analyze NIS expression in various BC subtypes we performed IHC in 181 breast tumour tissue samples. We also analyzed NIS expression with respect to the prognostic factors like ER, PR, HER2, age group and menopausal status. NIS mRNA expression in these subtypes was also assessed by quantitative real time PCR and correlation between NIS expression at RNA and protein levels was evaluated. Further, NIS expression in few fibroadenoma tissue samples was also analyzed by IHC.

2.2 Materials and Methods

2.2. 1 Study population

Project approval was obtained from institutional review board and Ethics committee of Tata Memorial Hospital. The paraffin embedded breast tumour tissue blocks were collected from ACTREC tumour tissue repository and used for NIS immunostaining. A total of 181 tumour tissue samples were randomly collected from patients between the age group of 24–73 years. All tumour samples were confirmed as infiltrating ductal carcinoma (IDC), grade III and were classified as 55 ER, PR +ve, HER2–ve, 26 ER, PR+ve, HER2+ve, 41 ER, PR–ve, HER2+ve, and 59 ER, PR-ve, HER2-ve samples on the basis of available standard IHC report. Of all cases, 60 patients were premenopausal, 11 cases were perimenopausal and 87 cases were postmenopausal. For rest of the cases menopausal status was not reported.

For real time PCR analysis, 59 fresh tumour tissue samples were collected randomly in RNAlater solution from ACTREC tumour tissue repository. The samples collected in RNAlater were immediately stored in -80^{o}. All samples were IDC, grade III and were from patients between the age group of 29-73 years. Among these samples, 20 samples

were ER, PR+ve, HER2-ve, 15 were ER, PR+ve, HER2 +ve, 12 were ER, PR-ve, HER2 +ve and 12 were ER, PR-ve, HER2-ve subtype. According to available Electronic Medical Record (EMR), 18 samples were premenopausal and 23 were postmenopausal. For rest of the samples, menopausal status was not marked as per the medical history record.

2.2. 2 Immunohistochemitry

Standard IHC protocol was followed to stain the tumour tissue samples using the mouse monoclonal antibody against NIS (Abcam, ab17795). In brief, 5 µm sized paraffin embedded tissue sections were de-paraffinized with xylene and dehydrated through graded alcohol. Endogenous peroxidase activity was quenched with 3% H_2O_2 in methanol for 30 minutes in dark and subjected to antigen retrieval using 10 mM sodium citrate. For antigen retrieval sections were heated in sodium citrate solution serially at 850, 650 and 340 mega watts, each for 3 minutes. Since fibroadenoma tissues contain large portions of fats, heating these tissues at high temperature results in detachment of the tissue section from slide, therefore in case of fibroadenoma tissues heating was reduced to 350 mega watts for 10 minutes. After the antigen retrieval, sections were washed with 0.01% Tris borate saline-tween20 (TBST) and then blocked with 5% Bovine serum albumin (BSA) for one hour. Slides were incubated at 4^{o} overnight with the mouse monoclonal antibody against NIS diluted with TBS in 1:50 ratio. Slides were washed for 5 minutes in TBST, 3 times and incubated for 1 hour with Horse raddish peroxidise (HRP) conjugated anti mouse antibody diluted with TBS in 1:200 ratios. After washing, slides were incubated with 3, 3'-diaminobenzidine tetrahydrochloride (DAB) till the appearance of brown staining and immediately washed under tap water. Slides not incubated with anti NIS antibody were used as secondary control. Sections were further rehydrated with graded alcohol. For each batch of sample staining, a papillary thyroid carcinoma case was kept as

positive control for NIS expression. A normal salivary gland section was also used as positive control. For analyzing NIS expression in normal breast tissue, tumour adjacent breast normal tissue was used. All the slides were counter stained with haematoxylin. Slides were DPX mounted and observed under light microscope (Carl Zeiss).

2.2. 3 Pathological scoring

Antibody stained permanent slides were examined under light microscope and sections showing less than 10% of stained area were considered as negative where as sections showing 10–20% of stained area were considered as focal, 20–70% of stained area were considered as patchy and more than 70–80% of stained area were considered as diffused. Intensity variation of the staining was visibly examined and scored by pathologist as 0, 1+, 2+ and 3+.

2.2. 4 Digital image analysis

IHC digital images were used for developing semi-automated analysis protocol. As a first step, we used a colour de-convolution technique to un-mix the pure DAB, haematoxylin stained areas leaving a complimentary image. The pixel intensities of separated DAB or haematoxylin images range from 0 to 255. Value 0 represents the darkest shade of the colour while 255 represent the lightest shade of the colour in the image. In-order to assign an automated score by judging the pure DAB staining pattern, histogram profile of every image i.e. the number of pixels of a specific intensity value vs. their respective intensity was raised using imageJ standard program feature. In the histogram profile, we categorized pixel intensity ranges from 0–60 for a score value of 3+, 61–120 for 2+, 121–170 for 1+ and 171–230 for 0. We excluded the pixel intensity values above 230 as the abundant fatty tissues in breast tumour tissue sections were found to contribute in the range of 230–255. A macro was developed and plugged in the ImageJ program to receive automated counting of numbers of pixels in the four different intensity zones. After

determining these numbers, we applied them to a simple algebraic formula as shown below to determine the score of the image.

$$Score = \frac{(Number\ of\ pixels\ in\ a\ zone) \times (Score\ of\ the\ zone)}{Total\ number\ of\ pixels\ in\ the\ image}$$

Any image that has more than 66% of pixels in one zone is directly graded without the need to apply the formula. In line with the standard grading procedure, we assigned a 4 tire scoring system i.e. high positive (3+), positive (2+), low positive (1+) and negative (0).

2.2. 5 Immunofluorescence

For the purpose of immunofluorescence study, tissue sections were treated in the same way as for IHC. After blocking with BSA, sections were incubated with NIS (1:50) and HER2 (1:20) (Abcam, ab8054) antibodies one by one and then stained with respective fluorescent dye labelled secondary antibodies. For NIS staining Alexafluor 488 labelled rabbit secondary antibody (Abcam, ab6737) was used where as HER2 was counter-stained with Dylight633 labelled goat secondary antibody (Thermo Scientific, 35562). Antibody stained sections were washed with TBST and then mounted with vecta-shield (Vector Laboratories) and images were captured using a confocal microscope (Zeiss). The detailed method is mentioned in section 7.47.

2.2. 6 Quantitative real time PCR

Breast tumour tissues were collected in RNase Later and stored in -80^{o}. For RNA extraction, tissues were cut into small pieces and RNA was extracted using RNA extraction kit from Qiagen (74106). Quality of RNA was checked in denaturing gel and integrity of the 2 bands (18s and 28s rRNA) is confirmed. After quality control check c-DNA was synthesized with 1µg of RNA using c-DNA synthesis kit from Invitrogen (18080-051). A standard curve was plotted using 1-100ng of cDNA and their respective

CT (threshold cycle) values. It was observed that 10ng of cDNA is optimum to evaluate NIS and glyceraldehydes 3-phosphate dehydrogenase (GAPDH) expression, the later was used as an endogenous control. Total normal breast RNA from Ambion (AM6952) was used for understanding NIS expression in normal breast tissue. Real time amplification was performed using the TaqMan master mix and (Life technologies, 4304437) primer probe mix from applied biosciences for NIS (Hs00166567_m1) and GAPDH (Hs02758991_g1). The real time reaction was run in Quantstudio 12k flex model from Life technologies. NIS expression level in breast tumour tissue as compared to normal breast tissue was analyzed by $2^{-\Delta\Delta CT}$ method and plotted as fold change in all the graphs. The detailed method is mentioned in section 7.48.

2.2. 7 Statistical analysis

In order to understand the significant difference in NIS protein expression among various subtypes Fisher's exact test was performed. For multivariate analysis logarithmic regression was performed. Further, to analyze significance of difference at the transcript level paired t-test was performed. In order to understand correlation of NIS at RNA and protein level, Spearman's correlation test was performed. All the statistical tests were performed with a confidence interval of 95%.

2.3 Results

2.3. 1 NIS protein expression in primary breast tumour tissue

In order to understand NIS expression level in BC we have performed IHC in 181 primary breast tumour tissue formalin fixed paraffin embedded (FFPE) samples including all major BC subtypes. Demographic details of the samples used are mentioned in the **Table 2.1**.

Table 2.1 *Characteristics of patient cohort from which primary breast tumour tissue samples was procured to evaluate NIS expression by immunohistochemistry*

Total Patient Number	**181**
Age	24-73
Stage	III
Histology	Infiltrating Ductal Carcinoma
Estrogen Receptor	
Positive	81
Negative	100
HER2 Receptor	
Positive	67
Negative	114
Menopausal Status	
Pre	60
Peri	11
Post	87

As appeared in DAB stained tissue sections, the NIS staining is mainly diffused cytoplasmic, however in a limited number of tissue samples (n=4) membrane NIS expression is observed using the same protocol and antibody. Tumour adjacent normal breast tissues are stained negative (**Figure 2.1A**) and membrane specific staining is evident in salivary gland (**Figure 2.1D**).

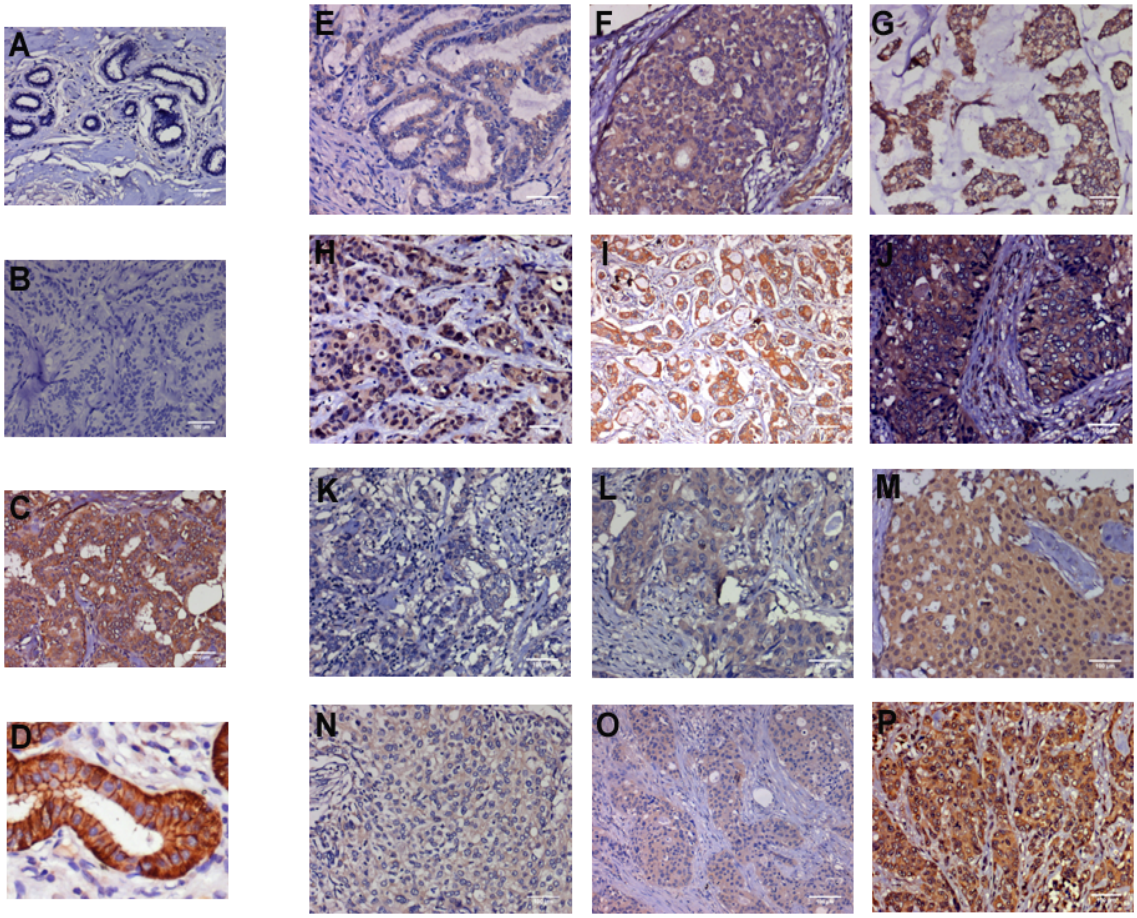

Figure 2.1 *Images of NIS staining pattern in major subtypes of BC.* ***A.*** *Tumour adjacent normal breast tissue showing negative expression of NIS.* ***B.*** *Secondary control for NIS showing absence of any staining.* ***C.*** *Thyroid papillary carcinoma tissue section used as positive control.* ***D.*** *Salivary gland tissue section showing membrane staining for NIS. Image is acquired at 40X.* ***E-G.*** *NIS expression in ER, PR+ve, HER2-ve subtype representing 0, 1+ and 2+ score respectively.* ***H-J.*** *NIS expression in ER, PR+ve, HER2+ve subtype with 0, 1+ and 2+ score respectively* ***K-M.*** *NIS expression in ER, PR-ve, HER2+ve subtype with 0, 1+ and 2+ score respectively.* ***N-P*** *NIS expression in ER, PR-ve, HER2-ve subtype with 0, 1+ and 2+ scores respectively. Scale bar represents 100µm.*

Further NIS staining intensity comparison is done keeping one thyroid papillary carcinoma tissue sample as a positive reference for NIS staining (**Figure 2.1C**). Tumour tissue samples show equivalent or lesser staining intensity as compared to the thyroid

carcinoma reference used and therefore are categorized as 3+, 2+, 1+ and negative (0) scores (**Figure 2.1E-P**) by pathological as well as digital IHC analysis methods[148]. The samples showing 1+ to 3+ score for NIS expression are considered as positive for NIS expression. Of the total number of samples analyzed, 78% BC cases are positively stained for NIS (**Figure 2.2A**). Receptor subtype specific classification shows that 90% samples of ER, PR+ve, HER2-ve and 92% of ER, PR +ve, HER2+ve subtype are positive for NIS expression whereas only 74% HER2 enriched (ER, PR –ve, HER2 +ve) and 62% of TNBC (ER, PR –ve, HER2 -ve) samples are positive for NIS expression (**Figure 2.2B**). Thus we observe significant difference among the subtypes in terms of NIS expression.

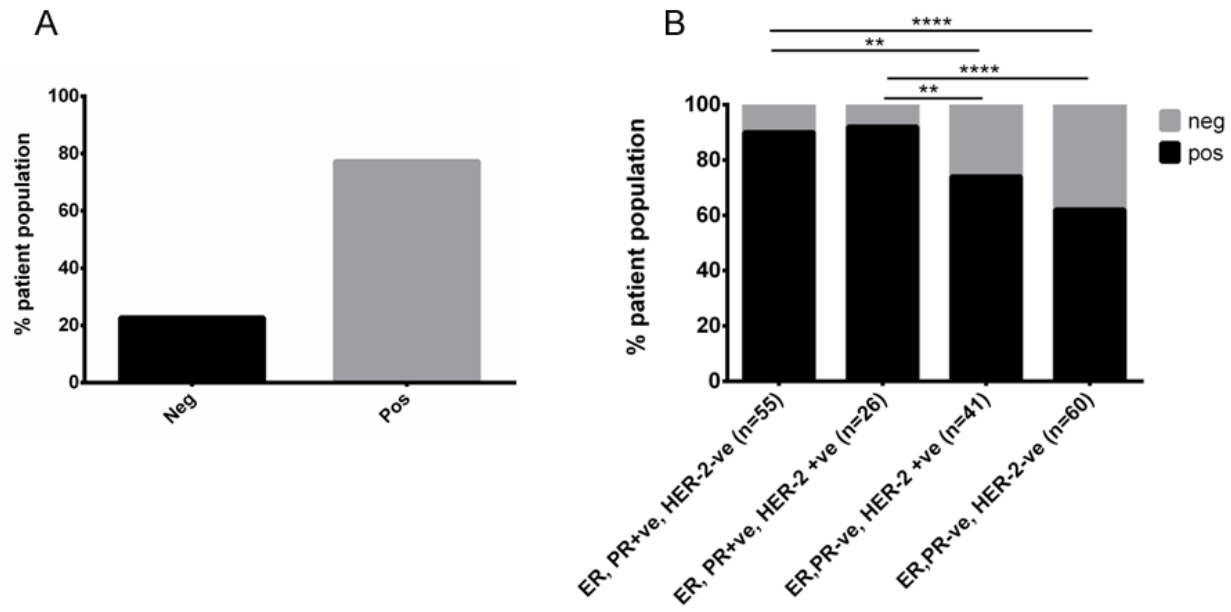

Figure 2.2 *NIS expression in primary breast tumour tissue* ***A.*** *Graph representing positive NIS expression in 78% primary breast tumour tissue samples (n=181)* ***B.*** *NIS positive patient samples in major BC subtypes. Significant difference is observed in various subtypes with increased frequency of NIS expression in ER, PR+ve HER2-ve and ER, PR+ve, HER2+ve subtypes.*

Further classification on the basis of staining intensity shows (**Figure 2.3**) that frequency and intensity of NIS expression is significantly high in ER, PR+ve, HER2-ve and ER,

PR+ve, HER2+ve subtypes as compared to ER, PR-ve, HER2+ve (p=0.0052 and 0.0011 respectively) and ER,PR-ve, HER2-ve subtypes (p=<0.0001).

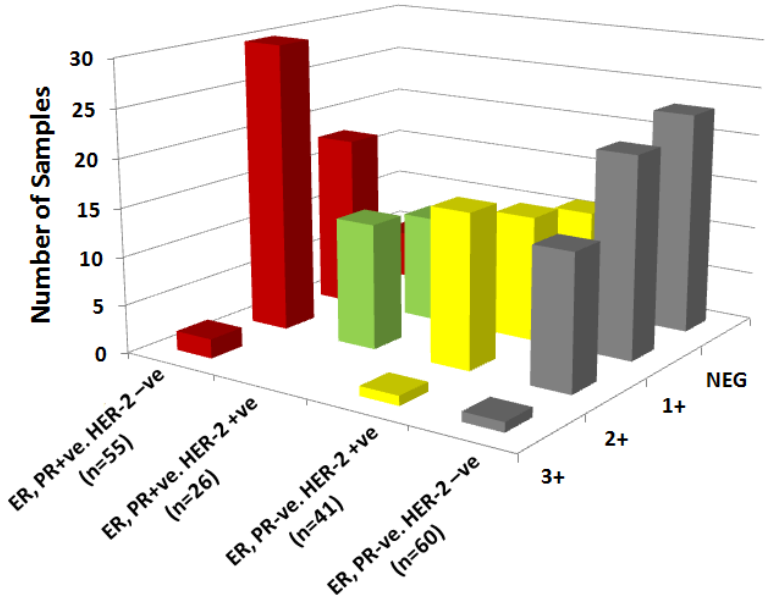

Figure 2.3 *Chart representing IHC scoring intensity in various BC subtypes. It is to be noted that a major number of samples in ER, PR+ve, HER2-ve subtype show 2+ score for NIS where as in TNBC a major number of samples show negative NIS expression.*

2.3. 2 Comparison of digital image analysis with pathological scoring

Images of all 181 BC cases were also analyzed by the software. The IHC images were first colour de-convoluted by modifying the technique described by Ruifrok et al.[149], followed by pixel intensity profiling of deconvoluted DAB stained image using ImageJ program. Comparing the scores assigned by pathological analysis with that obtained by the software based process, a 74% match is observed. Out of the 181 cases, 134 cases show similar score by both the methods (**Table 2.2**).

Table 2.2 *Table showing comparison of digital IHC analysis and pathological scoring. Highlighted boxes are showing number of samples with same score by both the methods.*

Automated scoring	Pathological scoring: 3+ (n=4)	2+ (n=73)	1+ (n=63)	NEG (n=41)
3+ (n=4)	3	5		
2+ (n=71)	1	56	18	2
1+ (n=64)		12	45	9
NEG (n=30)				30

Further, we also found that often software analysis designate lower score in cases where the analyzed image represents low tumour to stroma ratio, requiring physical examination of the whole section **(Figure 2.4)**. Importantly, it is also observed that 77% cases with 2+ score matched by both methods, indicating such digital analysis method can benefit patient stratification for NIS expression across the laboratories.

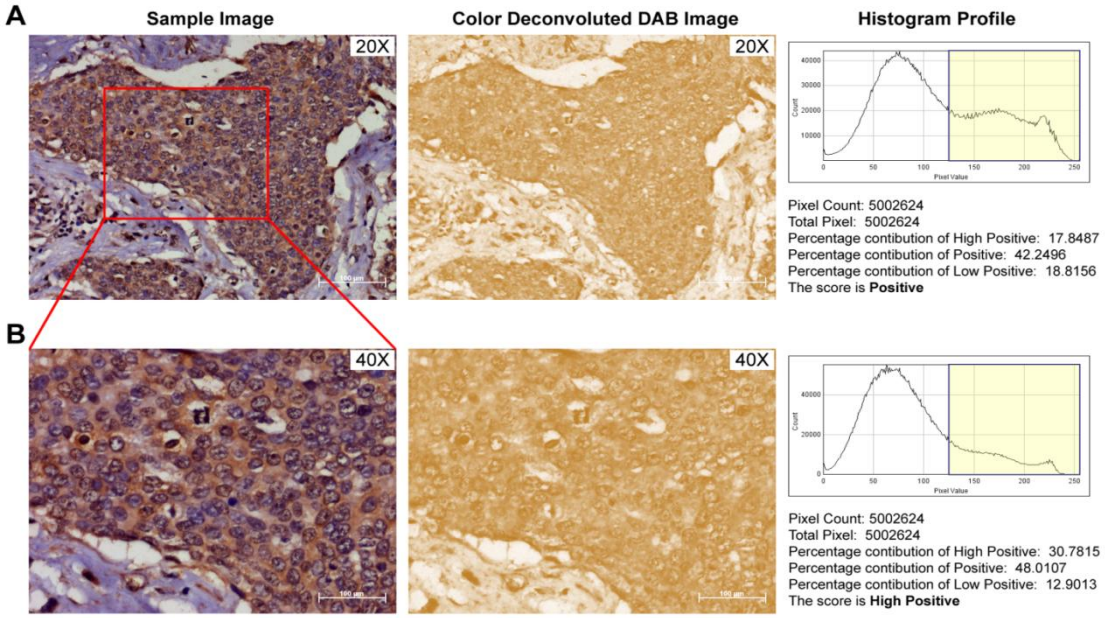

Figure 2.4 *Images captured using higher magnification can assign correct scoring by reducing the averaging effect contributed from the stromal areas.* ***A)*** *Analysis of image score using a 20X image of a case where low tumour cells were present. After colour deconvolution, the macro was used on the DAB image to plot a histogram profile and the score was determined as positive.* ***B)***

When an image is captured using a 40X objective focusing on the marked area of the previous image, score was found to be high positive.

2.3. 3 Localization of NIS in breast cancer tissue

As NIS is a transporter protein; its localization plays a very important role in its function. Except for a few reports which have shown distinct membrane staining[5,147] mostly it appears as an intracellular protein in breast tumour tissue sections. During this study except for salivary gland section and a small number of cases, NIS staining majorly appeared as diffused intracellular by DAB stained tumour tissue sections. This being an important judgment in estimating the utility of NIS mediated radioiodine uptake, we have attempted to verify that if HER2 (membrane receptor) and NIS co-localize in the HER2 receptor positive samples. To achieve this, dual IF staining was performed using NIS and HER2 primary antibodies which are detected by using dual colour fluorescent dye labelled secondary antibodies. As represented in **Figure 2.5**, in a few cases merged confocal microscopic images clearly show marked co-localization of the two molecules at the cell membrane of tissue section which is not apparent in the image of the same case stained with DAB colourimetric staining method (upper panel). However, as represented in the lower panel, in most other cases it is found that similar membrane aggregation of NIS protein is absent and the whole cytoplasmic area shows uniform staining in NIS positive cases by both IF and DAB.

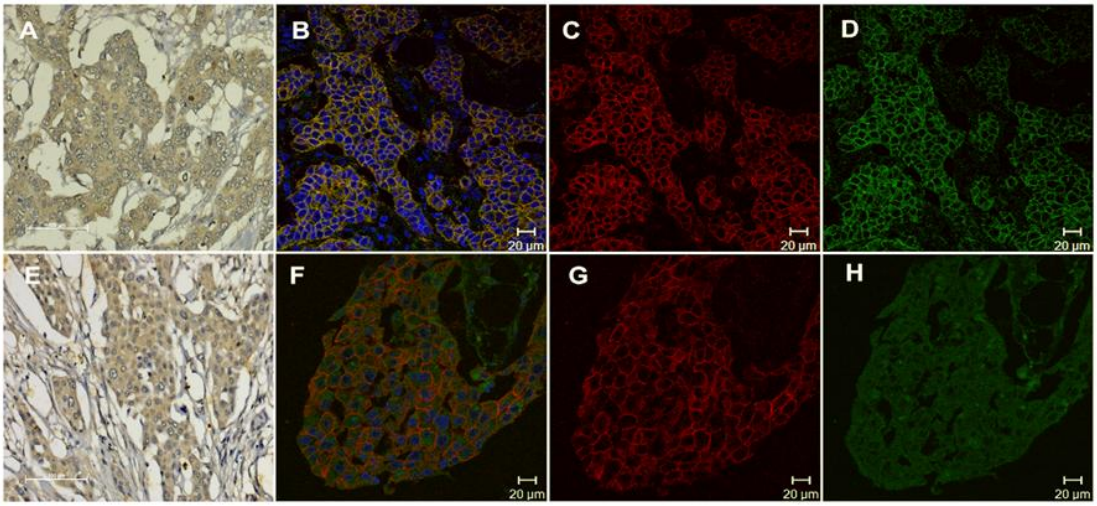

Figure 2.5 *Immunofluorescence staining reveals NIS and HER2 receptor overlaps at the tumour cell membrane in few cases. Human patient tissue samples stained with NIS and HER2 specific antibody followed by detection with Alexafluor488 (green) and Dylight633 (red) labelled secondary antibodies respectively.* ***A, E.*** *DAB stained tissue sections from two representative patient samples showing similar intracellular expression of NIS. Scale bar represents 100µm.* ***B, F.*** *Dual IF stained confocal overlay images of the same patient samples as in A and E respectively. Upper panel clearly showed good overlapping membrane expression of HER2 and NIS staining.* ***C, G.*** *Corresponding images of HER2 staining in red channel and* ***D, H.*** *images of NIS staining in green channel. Scale bar represents 20µm.*

2.3. 4 NIS transcript levels in primary breast tumour tissue

At present aberrant expression of NIS protein is well known in BC, however not much is known about its regulation. To evaluate if NIS expression is deregulated at transcript or translational level in breast malignancies, we analyzed its expression in 59 primary breast tumour tissue samples including major subtypes of BC. The characteristics of the patient samples used are mentioned in the **Table 2.3**.

Table 2.3 *Characteristics of the patient cohort for which tumour tissue was procured to evaluate NIS expression at the transcript level*

Total Patient Number	**59**
Age	28-72
Stage	III
Histology	Infiltrating Ductal Carcinoma
Estrogen Receptor	
Positive	35
Negative	24
HER2 Receptor	
Positive	27
Negative	32
Menopausal Status	
Pre	18
Peri	0
Post	23

Our real time results suggest that NIS expression in BC is upregulated in the range of 1.1 to 8.1 fold as compared to normal breast. Further classification on the basis of BC subtypes suggests that NIS transcript levels in the ER, PR+ve, HER2-ve group is significantly high as compared to TNBC group, which is concordant with our IHC data (**Figure 2.6**). We observe that in case of TNBC, only 2 samples show 2 fold upregulation, whereas all other samples show 1.1 to 1.5 fold increase in NIS transcript levels. Instead in ER, PR+ve, HER2 –ve subgroup, majority of the samples show more than 2 fold increase in NIS transcript. At transcript level we have not observed significant difference among other subtypes in terms of NIS expression.

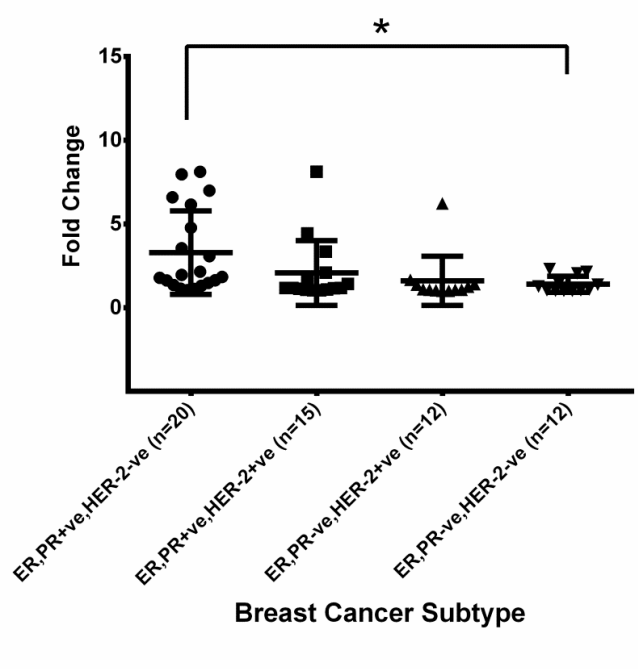

Figure 2.6 *Intensity of NIS expression at transcript level in different subtypes of BC. Data is represented as fold change as compared to normal breast. NIS expression level is significantly high in ER, PR+ve, HER2-ve group as compared to TNBC group*

2.3. 5 NIS protein expression with respect to prognostic markers

BC is a highly heterogenous disease and the treatment plan for BC patient is based on the expression of few of the prognostic markers like ER, PR and HER2 levels, BRCA mutations etc. Since testing the levels of these markers for correct judgment of the treatment plan is part of the routine clinical practice, it is important to understand if NIS has association with any of these markers. Analysis of such association may help in better understanding of the patient subtype, which in turn may ensure maximum benefit from NIS mediated targeted radioiodine therapy in BC. In order to evaluate association of these factors with NIS expression, we have first classified the samples on the basis of ER expression and observed that the frequency of samples showing positive NIS protein expression is significantly high in ER+ve cases as compared to ER-ve cases ($p=<0.0001$) (**Figure 2.7A, B**). We have also classified the samples on the basis of HER2 expression

status (**Figure 2.8A**), but do not find any significant difference in NIS expression levels with respect to HER2 (p=0.3936). Further, we have analyzed NIS expression with respect to age. To do that, all the samples are classified into 2 groups based on patient age i.e. below and above 50 years of age. We have observed that the frequency and intensity of the samples showing positive NIS expression is significantly high in the cases with age group below 50 (**Figure 2.7C, D**).

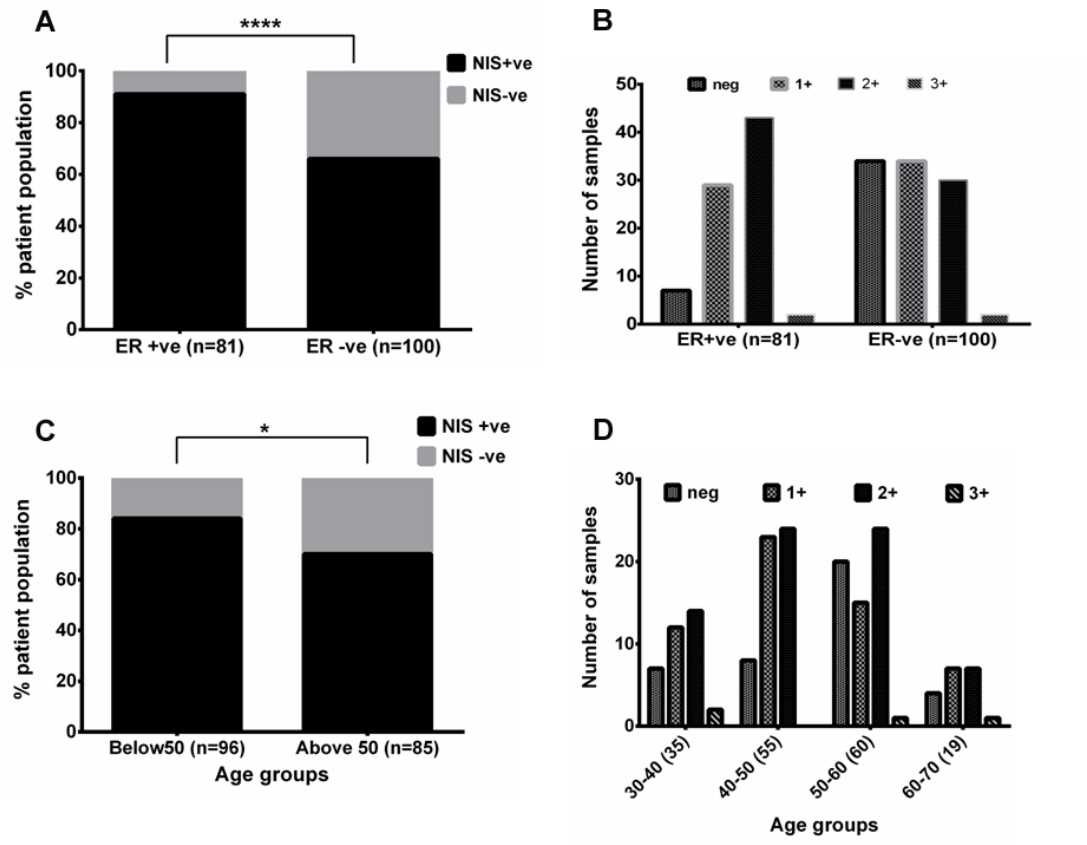

Figure 2.7 *NIS expression in association with ER expression and age group* ***A.*** *Comparison of NIS expression between ER+ve and ER-ve groups shows high association of NIS positivity in ER+ve group.* ***B.*** *Intensity (scores) of NIS expression in ER+ve versus ER-ve patient tissues. It is observed that majority of ER+ve samples show 2+score where as in case of ER-ve samples majority of the samples either show negative or 1+ score for NIS expression.* ***C.*** *Graph showing increased frequency of NIS in the patients with less than 50 yrs of age, where as frequency of NIS decreased in the patients with age group above 50 yrs.* ***D.*** *Intensity (scores) of NIS expression in patients with different age groups.*

Further classification on the basis of menopausal status does not show any significant difference in terms of NIS expression (**Figure 2.8B**).

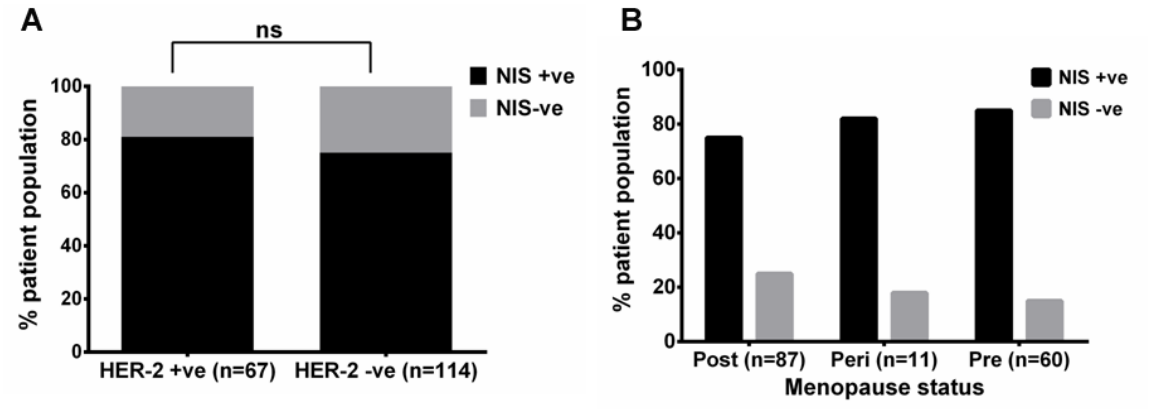

Figure 2.8 *Association of NIS with HER2 and menopausal status* ***A.*** *Comparison of NIS expression between HER2+ve and HER2-ve groups do not show any significant difference in NIS expression.* ***B.*** *Comparison of NIS expression between pre-, post- and perimenopausal groups do not show any significant difference in NIS expression.*

2.3. 6 NIS transcript levels with respect to prognostic markers

As classified previously for IHC studies, the breast tumour tissues are classified on the basis of ER expression and NIS transcript level evaluated (**Figure 2.9A**). We observe that NIS expression is significantly high in ER+ve cases as compared to ER-ve cases (p=0.0194), which is concordant with our IHC data. We have also classified the data on the basis of HER2, age and menopausal status and NIS transcript expression is evaluated with respect to these factors (**Figure 2.9B, C & D**). Our analysis shows that NIS expression is not associated with these factors at the transcript level.

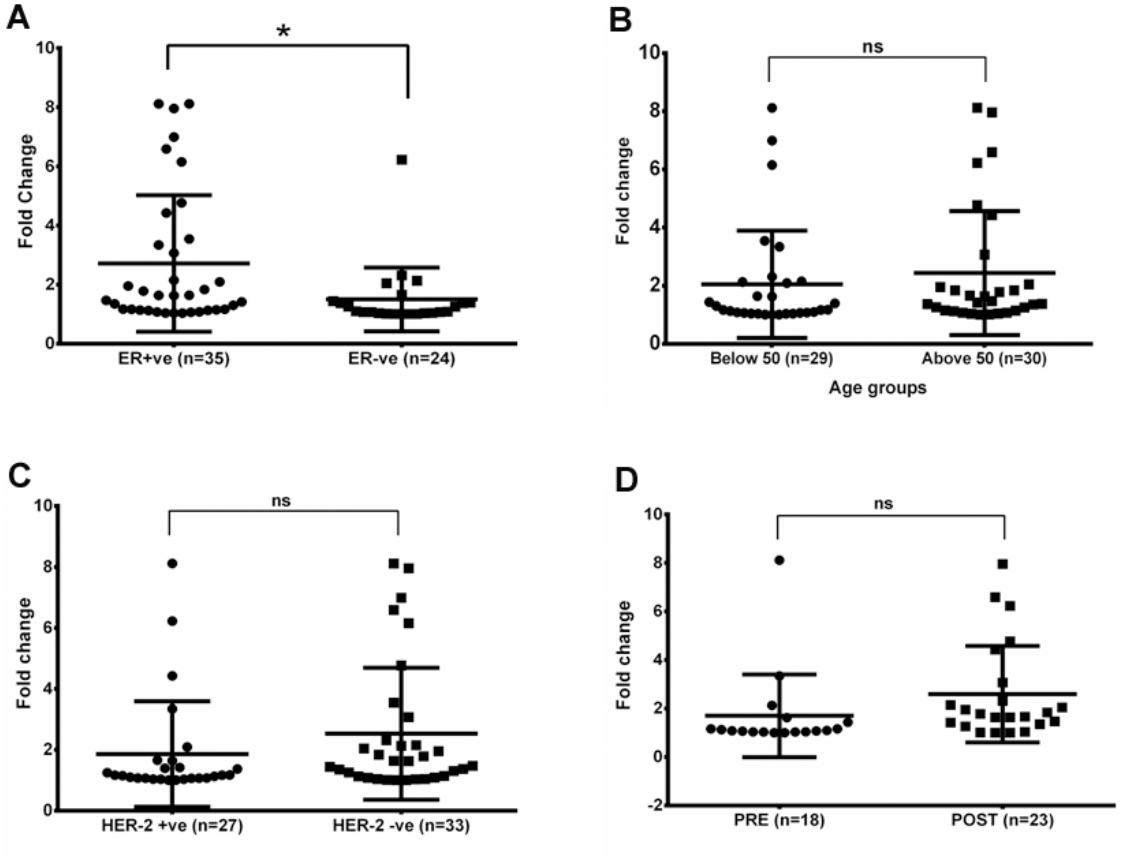

Figure 2.9 *Association of NIS transcript levels with various prognostic factors of BC* ***A.****Comparison of NIS expression between ER+ve and ER-ve groups shows high association of NIS positivity in ER+ve group at the transcript level* ***B.*** *Intensity of NIS expression in patients with different age groups. Intensity of NIS expression is not significantly different among the groups* ***C.*** *Comparison of NIS expression between HER2+ve and HER2-ve groups do not show any significant difference in terms of NIS expression at the transcript level* ***D.*** *Frequency of NIS expression do not show any significant difference between pre and post menopausal patient samples at the transcript level*

2.3. 7 Correlation of NIS expression at RNA and protein level in breast cancer

Since, published data so far poorly depicts correlation between NIS expression at the transcript and translational level, we have thoroughly analyzed the NIS transcript and protein levels in 20 primary breast tumour tissue samples. To investigate the correlation of NIS expression at the transcript and translational level, we procured samples simultaneously in formalin (for IHC) as well as RNAlater (for real time PCR) and

evaluated NIS expression. Except for 2 samples, all other samples show correlated expression of NIS (**Table 2.4**). However for negative and 1+ scoring intensity of NIS at IHC, the difference in NIS expression at RNA level is not significant.

Table 2.4*: Table representing RQ scores for NIS with their respective IHC score. RQ scores are mentioned in the decreasing order and IHC scores drops with the decreasing RQ score.*

S. Number	Case Number	RQ for NIS	IHC Score
1	CL15832	78.73199	3+
2	CL17813	6.5899	3+
3	CL10251	6.225981	2+
4	CL1171	2.311269	2+
5	CL50163	2.1723	2+
6	CL18398	1.953159	2+
7	CL17290	1.659439	2+
8	CL19468	1.640071	2+
9	CL50291	1.302989	2+
10	CL15175	1.174791	1+
11	CL23752	1.165807	1+
12	CL50205	1.125067	1+
13	CL21057	1.075504	NEG
14	CL50313	1.04202	NEG
15	CL12717	1.038494	NEG
16	CL471	1.006287	NEG
17	CL10651	1.042324	ALL FAT
18	CL22743	1.014297	NEGGILGIBLE TISSUE
19	CL25518	1.117672	3+
20	CK31287	1.013249	2+

We also observe that the samples with negative and 1+ score of NIS at IHC show a very narrow range of fold change at transcript level, whereas this range is wider in case of samples with 2+ or 3+ scores of NIS at IHC (**Figure 2.10**). Our data analysis suggests that NIS expression is well correlated at RNA and protein level (R^2=0.6964)

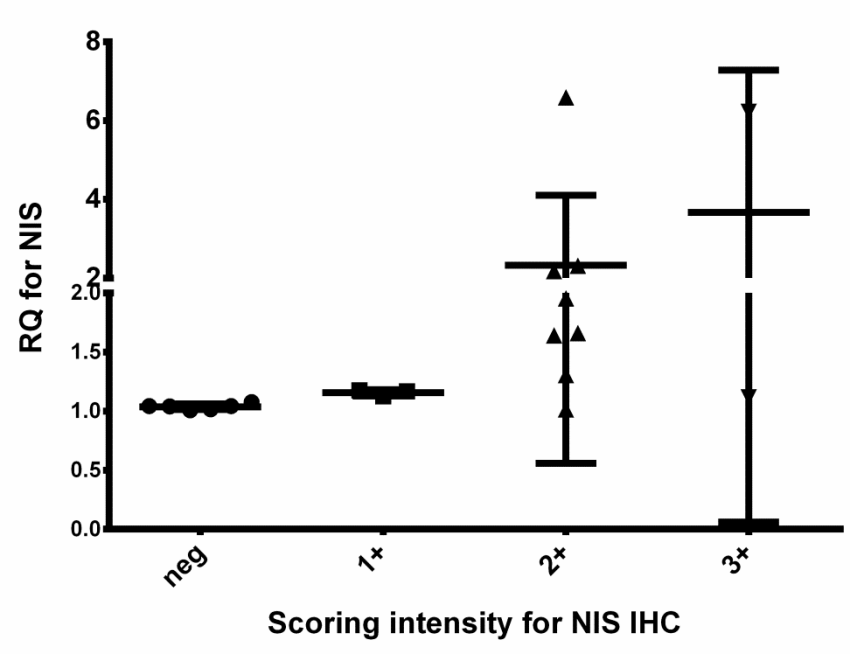

Figure 2.10 *BC tissue samples with their respective transcript and protein level of NIS expression showing correlated NIS expression (R^2=0.6964)*

2.3. 8 NIS expression in breast fibroadenoma

Various isotopes of iodine are used for PET, SPECT and scintigraphy imaging. Since NIS can uptake these radioisotopes, it has been used as reporter gene for the diagnostic purpose. NIS expression in fibroadenoma of breast was an important finding, as its expression undermines the possibility of using this gene expression as a diagnostic marker for BC. Since there are limited reports on NIS expression in fibroadenoma tissues[13,150,151], we evaluated NIS expression in 20 fibroadenoma tissue samples and observed that all the samples show positive NIS expression. The localization of the protein is diffused cytoplasmic. Further classification of the samples on the basis of staining intensity suggests that out of 20 samples, 6 show 3+, 13 show 2+ and only 1 sample shows 1+ score for NIS expression (**Figure 2.11A**). NIS expression in fibroadenoma samples is also compared with that of the BC.

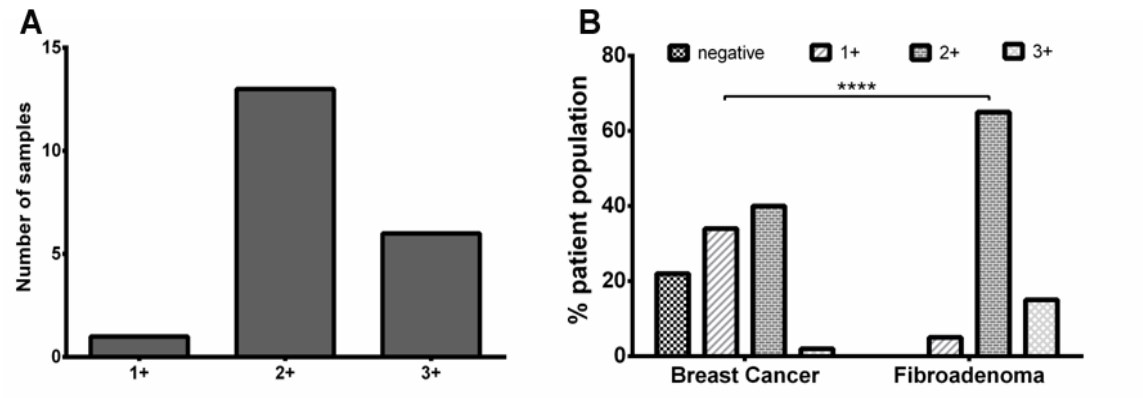

Figure 2.11 *NIS expression in fibroadenoma of breast and its comparison with BC* ***A.*** *Intensity of NIS expression in fibroadenoma tissue samples* ***B.*** *Comparative analysis of NIS expression in fibroadenoma vs. breast tissue samples showing increased frequency as well as intensity of NIS in fibroadenoma tissue samples*

We observe that in fibroadenoma cases, 15% samples show 3+ score as compare to only 2% samples in BC and 65% fibroadenoma tissue samples show 2+ score as compared to 40% samples in BC (**Figure 2.11B**). Thus, the frequency as well as intensity of NIS expression in fibroadenoma samples is significantly high as compared to BC cases ($p=<0.0001$).

2.4 Discussion

Over expression of NIS gene in BC is now well established, as reported by several groups across the world. However, the available reports on NIS expression are often focused on selective groups of patients such as TNBC. Due to paucity of knowledge in literatures available on NIS expression across various BC subtypes, we wanted to conduct a thorough subtype specific analysis using unbiased breast tumour tissue samples. To the best of our knowledge, our study for the first time reported the comparative IHC assessment of NIS protein expression in different subtypes of BC, which indicates that significant difference lies among various subtypes. Analyzing over 181 samples, our result suggests that on an average NIS protein over-express in 78% of BC cases.

Interestingly, our data also shows that ER positive cases have much higher incidence of NIS co-expression i.e. 90% of ER, PR+ve, HER2 -ve samples and 92% of ER, PR+ve, HER2+ve samples are found positive for NIS staining. As opposed to this, only 62% cases of ER, PR-ve, HER2-ve subtype are found positive. Without analyzing cases across the world, it is difficult to estimate at this point if a geographical variation persists in terms of NIS expression.

NIS does not show any significant relationship with the HER2 or menopausal status of the patient. Overall, the study indicates that targeted radioiodine therapy will provide an alternative option for tumour specific and less toxic treatment in cases where the tumours become resistant to tamoxifen and other chemotherapeutic drugs. Next, we envisioned that in order to play its functional role as a transporter, NIS proteins should be localized at the plasma membrane. But in majority of the cases, a diffused intracellular staining pattern is observed. Though a few studies in the past have shown membrane specific staining in breast tumour tissues[5,147], clinical studies using $^{99m}TcO_4^-$ showed visible tumour by scintigraphic imaging only in 17% of BC patients[9]. This being an important aspect to judge the localization of functional NIS molecule, reliable determination of immune-reactivity at plasma membrane required further evaluation. Our immunofluorescence results using HER2 positive cases confirm that in breast tumour tissues, differences lie in terms of NIS membrane staining. In certain cases, NIS staining dominantly overlaps with HER2 receptor staining at the cell surface, whereas in other cases NIS shows uniform distribution throughout the cytoplasm. Further, DAB based IHC staining may not be necessarily sensitive enough to determine sub-cellular localization of NIS protein in FFPE tissue samples.

Prior to the translation of NIS gene based radioiodine therapy, it will be necessary to perform nuclear medicine studies using ^{123}I scintigraphic or ^{124}I PET imaging in BC patients to determine sufficient radioisotope uptake by NIS expressing BC tissues.

Coming to the ER and NIS coexistence in breast tumour tissues, NIS expression is evident in a significantly high percentage (91%) of ER+ve tumours as oppose to only 66% in ER-ve tumours. Close association of NIS with ER, PR+ve tumours indicate that these subtypes will possibly have good response for NIS based targeted radioiodine therapy or radioiodine probe based PET or SPECT diagnosis. Further, it is evident from our quantitative real time PCR data that NIS expression is also upregulated at the transcript levels in malignant tissue as compared to normal breast tissue. It is interesting to note that subtype specific variation in terms of NIS expression is observed at the transcript level as well and maximum intensity of NIS expression is observed in ER, PR+ve, HER2-ve subtype. Further classification of the transcript data on the basis of ER expression shows significantly higher NIS expression in ER+ve patient samples as compared to ER-ve samples ($p=0.0194$), which is concordant with our IHC data. In a recent study by Ryan et al., correlation between NIS gene expression and that of several proven or putative NIS gene regulators were assessed by quantitative molecular techniques and a significant positive correlation was observed between NIS and ERα gene[13]. Our observation is also supported by a finding that the NIS expression is upregulated by ER ligand (E2) and ERα expression in MDA MB231 cells[96]. It is also reported that RNAi mediated downregulation of endogenous ERα in MCF-7 cells suppress trans retinoic acid (tRA) induced NIS expression, indicating that ERα plays an important role in regulation of NIS gene. A novel ERE sequence near TATA element has also been identified in NIS gene promoter and physical interaction between the ERE site at NIS promoter and ERα has been shown by CHIP assay[96]. Various studies also suggest

retinoic acid receptor (RAR) induced increase in NIS expression in ER+ve cell lines where as ER-ve BC cell line such as MDA MB231 do not show iodine uptake and NIS protein expression after tRA treatment [152].

Altogether, these reports suggest that higher incidence of NIS positive cases in ER+ve patient samples may be due to the positive regulation of NIS by ERα, however 60% positive NIS expression in ER-ve samples indicate that there are other factors which also play role for upregulated NIS expression in the malignant breast tissue. Classification of the NIS transcript data on the basis of age did not show any difference in terms of NIS expression, which is not concordant with the IHC data. At the transcript level, loss in association of NIS expression with lower age group may be due to the fact that in this cohort majority of the samples were from TNBC subtype.

For understanding the regulation of NIS in BC, it is important to investigate if NIS gene is up regulated at the transcript or translational level and whether the NIS protein levels are well represented by its expression at the transcript level as well. To do that, we evaluated correlation of NIS RNA and protein. Our study demonstrates that NIS transcript levels are well in coordination with NIS protein status in 18 out of 20 breast tissue samples (R^2=0.6964). In a previous report by Moon et al., discrepancy in NIS mRNA expression and its functionality was observed[9]. Since NIS protein is upregulated in BC tissues but mainly localized in the cytoplasm, the discrepancy observed by Moon et al. may be conferred due to disparity of correct protein targeting to the membrane.

Taking the study forward, we evaluated NIS expression in fibroadenoma samples and observe that all of the fibroadenoma tissues show positive NIS expression. As shown by previous reports, we also observed significantly high NIS frequency as well as intensity in fibroadenoma samples as compared to BC tissue samples. However the localization was diffused cytoplasmic, which is similar to majority of BC tissues. Presence of NIS in

fibroadenoma as discerned by us as well as other reports suggests that NIS expression can't be used as a specific indicator of breast malignancies. At present NIS regulation in fibroadenoma is not understood clearly. Previous literature suggests higher fibroadenoma incidence during pregnancy, when the estrogen levels are high[153,154]. Various reports also suggest role of estrogen in the occurrence of fibroadenoma[153]. Thus higher level of estrogen during fibroadenoma may be responsible for upregulated NIS expression in these tissues. However, factors responsible for NIS expression in fibroadenoma tissues has not been investigated thoroughly by any groups as of yet.

In summary, our data indicates upregulation of NIS at transcript as well as translational level in BC. For the first time, our report shows subtype specific variation in NIS protein expression in a large cohort of unbiased patient group. Association of NIS with ER suggests possible use of NIS mediated radioiodine therapeutic response in BC patients with positive ER status. Since the localization of NIS in BC is predominantly cytoplasmic as observed by our and various other groups, future directions are required to investigate the factors that can drive protein targeting to the membrane for efficient radioiodine uptake in these cells.

Understanding of NIS expression in breast cancer patients with primary and metastatic tumour

3.1 Introduction

As discussed in the 1st chapter, metastasis is a matter of concern because it is the main cause of death in BC. Approximately 10–15% of patients diagnosed with BC develop distant metastases within 3 years[45]. The common sites for BC metastasis are lungs, bone, brain and liver [155]. Despite years of research, BC metastasis remains incomprehensible. One of the major hurdles is that, once the tumour cells spread from the original site, they become comparatively undetectable and can stay in a dormant state for years even after the removal of primary tumour. Thus at present, many research groups are focussed on understanding the molecular mechanisms of metastasis, to find ways of early detection and device therapeutics for metastatic BC. Previous literature suggests that BC subtypes show differences in their metastatic spread[156-158]. In a study, it was reported that TNBC subtype shows higher tropism for lung with an OS of 4.3 years whereas ER, PR-ve, HER2+ve subtype is associated with higher rate of liver metastasis with an OS of 3.61 years[156].

Standard therapy for BC metastasis is chemotherapy and targeted therapy. At present chemotherapy includes anthracycline, taxane and 5-fluorouracil as 1st, 2nd and 3rd line of therapy respectively[159]. In younger women with BC, chemotherapy increases the 15 year survival rate by 10% where as for older women this increase is only 3%. As with majority of the cytotoxic drugs, side effects of these agents are still a burden, for example, anthracyclines are known to cause cardiac dysfunction[160].

Targeted therapy for BC includes hormonal, immunological and antiangiogenic therapy. High dose tamoxifen has shown extremely positive result in bone metastasis in patients with BC[161]. Treatment of metastatic BC with trastuzumab in addition to chemotherapy is known to improve OS rate, response rate and time to progression[162].

Despite the advancements in the therapeutic strategies, metastatic BC is still considered as incurable disease[64,159,63]. Various studies suggest poor response rate to trastuzumab therapy in metastatic settings, and many patients develop resistance eventually[163-167]. In the same way, although most patients with ER+ve metastatic disease benefit from aromatase inhibitors (AIs) as first-line endocrine therapy, approximately 30% patients do not respond to this treatment[168,169].

Thus, there is constant search of new therapeutic targets to treat these patients. In 2004, Wapnir et al. reported NIS expression and I^- accumulation in metastatic BC[4]. In this report, 35% BC tissue samples showed significant NIS expression at the primary site and of these, I^- transport and accumulation in the metastatic site was observed in 25% samples. In 2 cases, NIS expression was lost in the metastatic tissue whereas the primary tissue showed weak staining for NIS. There were 5 cases where NIS was detected but I^- accumulation was not observed by scintigraphic scan. Since NIS mediated ^{131}I therapy has been used successfully for past 70 years to ablate thyroid cancer metastasis, the same approach may be applied to NIS expressing breast metastatic cancer.

Before clinical trials of NIS based therapy to metastatic BC patients, it is important to evaluate NIS expression levels in the metastasized tissue. Most of the current treatment regimens are based on the biomarker characteristics of the primary tumour tissue, but literature suggests alteration in the expression levels during tumour progression from primary to metastatic state. Several reports suggest significant discordance in ER, PR and HER2 status between primary and metastatic tissue and its association with worser prognosis and poor overall survival[170-178]. Thus, evaluation of these biomarkers at the recurrent or metastatic carcinoma may improve treatment efficacy of targeted therapy and overall survival.

Although NIS mediated iodide uptake has been detected in BC metastasis by scintigraphy as well as NIS expression in BC brain metastasis has been demonstrated by IHC[2,4], none of the previous studies have reported comparison between NIS protein expression in the metastatic tissue and primary breast tumour tissue. If a significant proportion of BC patients show similar level of NIS expression in the primary and metastatic tumour tissue, the level of NIS expression in the primary tissue can be considered as its measure in the metastatic tissue. At the same time, ^{131}I therapy could potentially be considered and tested as an alternative approach for selective targeting of BC metastatic cells. To answer these questions, in the present study we evaluated NIS expression in lymph node metastatic tissue and compared its expression with their respective primary tumour tissue.

3.2 Methods

3.2. 1 Study population

Project approval was obtained from institutional review board and Ethics committee of Tata Memorial Hospital. The paraffin embedded lymph node metastatic tumour tissue and their respective primary breast tumour tissue blocks were collected from ACTREC tumour tissue repository and used for NIS immunostaining. A total of 45 tumour tissue samples were randomly collected from patients between the age group of 28–73 years. All tumour samples were confirmed as IDC, grade III and were classified as 18 ER, PR +ve, HER2-ve, 5 ER, PR+ve, HER2+ve, 13 ER, PR-ve, HER2+ve, and 9 ER, PR-ve, HER2-ve samples on the basis of available standard IHC report. Of all cases, 16 patients were premenopausal and 22 cases were postmenopausal. For rest of the cases menopausal status was not reported.

3.2. 2 Statistical analysis

In order to understand the significant difference in NIS protein expression in primary and metastatic tissues representing various subtypes, Fisher's exact test was performed. For multivariate analysis logarithmic regression was performed. All the statistical tests were performed with a confidence interval of 95%.

3.3 Results

3.3. 1 NIS expression in breast cancer lymph node metastatic tissue

NIS expression is evaluated in 45 lymph node metastatic tissues by IHC. **Table 3.1** shows the clinical details of the samples used in the study.

Table 3.1 *Characteristics of patient cohort from which primary as well as lymph node meastatic breast tumour tissue was procured to evaluate NIS expression by immunohistovhemistry*

Total Patient Number	**45**
Age	28-73
Stage	III
Histology	Infiltrating Ductal Carcinoma
Estrogen Receptor	
Positive	23
Negative	22
HER2	
Positive	18
Negative	27
Menopausal Status	
Pre	16
Peri	0
Post	22

We observe NIS positivity in 94% cases. As mentioned in the previous chapter, samples are scored on the basis of intensity of NIS keeping one thyroid papillary carcinoma as a positive control. The pattern of expression is mainly diffused cytoplasmic, however one of the metastatic tissues shows faint membrane staining for NIS (**Figure 3.1**). Interestingly in the primary BC tissue of the same sample, NIS expression is diffused

cytoplasmic. We also observe an opposite case, where primary BC tissue displays membranous NIS expression, whereas the respective lymph node metastatic tissue shows diffused cytoplasmic localization for NIS (**Figure 3.1**). These findings suggest differential localization of NIS in primary breast tumour and its lymph node metastatic tissue. Further analysis of all the samples on the basis of staining intensity suggests that, among the metastatic cases, only 1 (2%) sample shows 3+ score, 30 (67%) samples show 2+ score, 11 (24%) samples show 1+ score and 3 samples are negative for NIS expression.

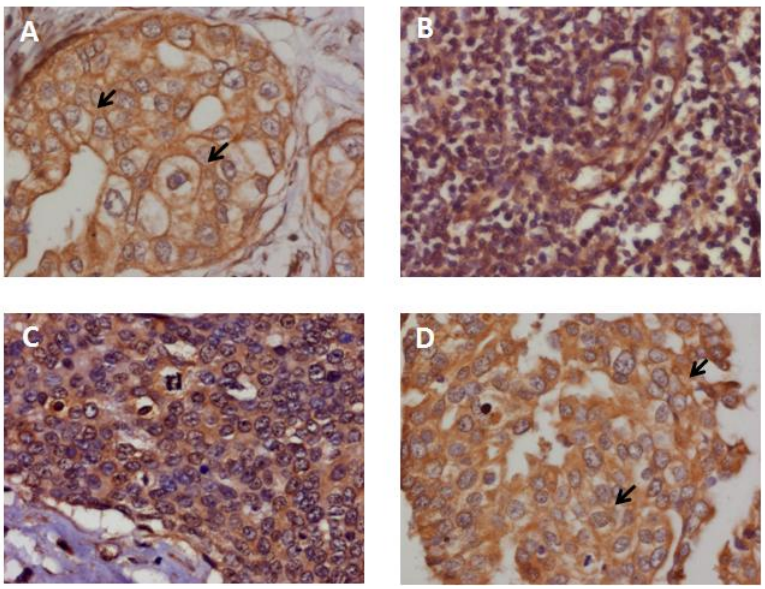

Figure 3.1 *Representative immunohistochemistry images for NIS in primary breast tissue and their respective lymph node metastatic tissue showing variation in subcellular localization.* ***A.*** *Membranous localization of NIS in a primary breast tissue sample* ***B.*** *Cytoplasmic localization of NIS in the respective lymph node.* ***C.*** *Cytoplasmic NIS in a primary breast tumour tissue where as* ***D.*** *its respective lymph node tissue shows faint membrane staining together with the cytoplasmic staining. Images are acquired at 40X.*

Further classification on the basis of subtypes (**Figure 3.2**) as well as prognostic markers such as ER, HER2, age and menopause does not show association of NIS with any of these factors (**Figure 3.3**).

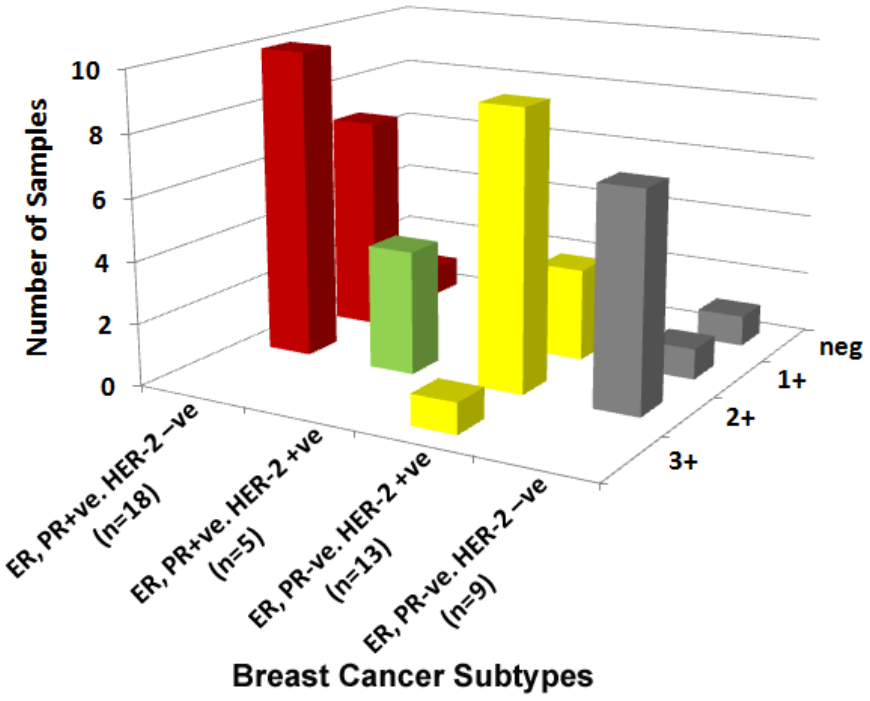

Figure 3.2 *Intensity of NIS expression in lymph node metastatic tissues. Any significant difference was not observed among various subtypes on the basis of NIS expression.*

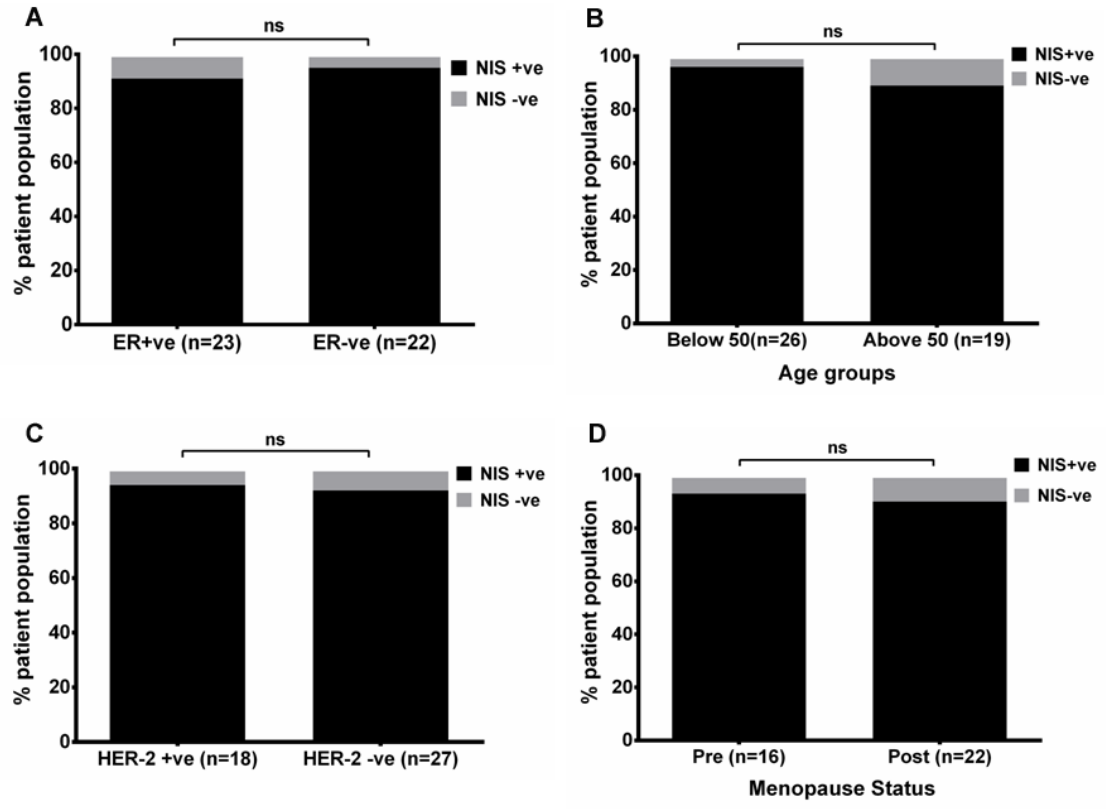

Figure 3.3 *NIS expression in lymph node metastatic tissue with respect to* ***A.*** *ER status* ***B.*** *Age* ***C.*** *HER2 and* ***D.*** *Menopause status*

3.3. 2 NIS expression in metastatic lymph node tissue as compared to primary BC tissue

Previous literature suggests altered expression of many molecules during metastasis. At present, alteration in NIS expression from primary to metastatic tissue is not known. In order to evaluate changes in NIS expression, we have performed IHC in 45 paired (primary and lymph node metastatic tumours from the same patients) paraffin embedded BC tissue samples. NIS expression in metastatic tumour tissue samples is compared with their respective primary tumour tissue samples.

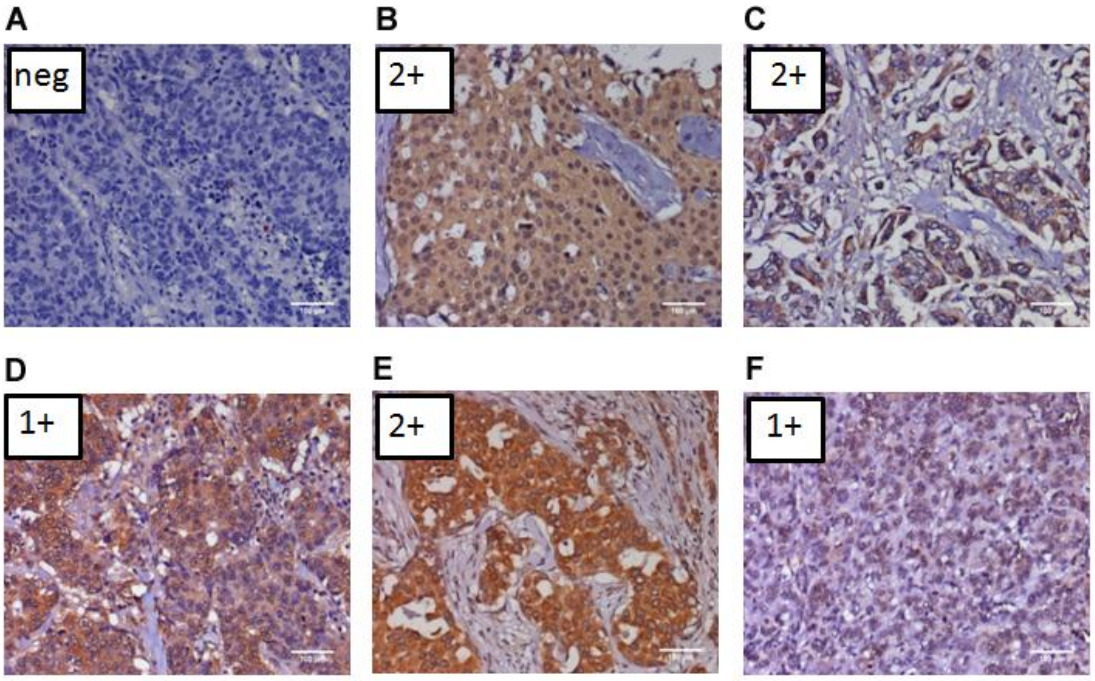

Figure 3.4 *IHC images of representative primary breast tumour tissues and their respective lymph node metastatic tissues.* ***A, B and C*** *NIS expression in primary breast tumour tissues.* ***D-F.*** *NIS expression in respective paired lymph node metastatic tissue showing higher* ***(D)*** *equal* ***(E)*** *and lower* ***(F)*** *expression of NIS as compared to respective primary tumour as in A, B and C respectively. Scale bar represents 100µm.*

The comparative results suggest that intensity of NIS expression in lymph node metastatic tissue is same as the primary tumour in many cases (over 50%); however in a small subset of metastatic tissues NIS expression can be found with either lower or higher intensity than their respective primary tumour tissue (**Figure 3.4**).

More importantly, classification on the basis of subtypes suggest that none of the ER, PR+ve, HER2-ve subtype samples and 33% ER, PR-ve, HER2-ve samples show higher NIS expression in the metastatic tissue as compared to primary tumour tissue (**Figure 3.5**). We do not observe significant difference in NIS expression among other subtypes.

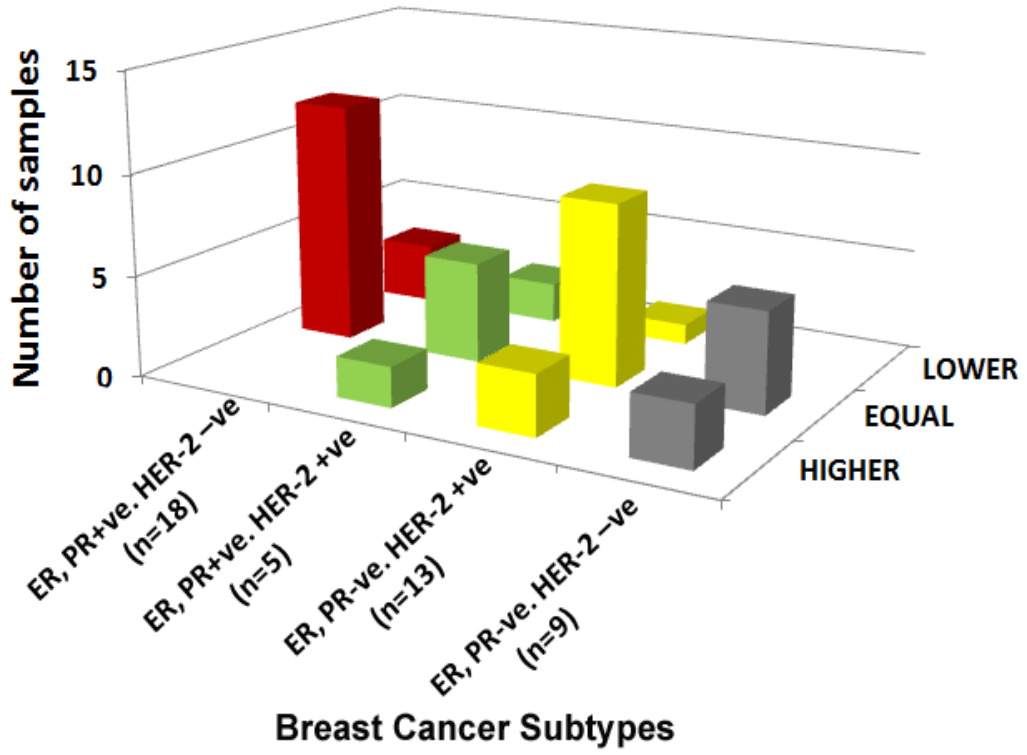

Figure 3.5 *Comparison of NIS expression variation between primary and lymph node metastatic tumour tissue in various BC subtypes. The graph suggests that majority of the samples show equal or higher expression in lymph node metastatic tissue as compared to their respective primary tumour tissue and a very small subset of population shows lower NIS expression in the lymph node than their primary counterpart.*

3.4 Discussion

In the present study, we have evaluated how NIS expression in lymph node metastatic breast tissue varies from primary breast tumour tissue by IHC analysis. To the best of our knowledge, this is the first study on comparison of NIS expression between primary and lymph node metastatic breast tissue. NIS expression in the distant metastatic tissue could not be analyzed as it is difficult to procure such metastatic tissue samples.

NIS expression levels and localization are different in primary and respective metastasis cases for few cases, although these parameters are similar for majority of samples. However in majority of the cases NIS levels are maintained in the metastasized tissue. Association of NIS with ER in primary breast tumour tissue shown in chapter 2 is not

evident in the metastatic lymph node tissues and we do not observe significant differences among various subtypes in terms of NIS expression. Lack of association between NIS and ER in metastatic tissues suggests possibility of distinct factors regulating NIS expression in primary and metastatic tissues. Alternately, change in ER status of the metastatic tissue may be responsible for the disparity. Overall, NIS expression in majority of lymph node metastatic tissues observed in our study, indicates potential of NIS mediated targeted radioiodine therapy in the metastatic BC.

One of the major obstacles in radioiodine therapy of extra thyroidal tissues is efficient uptake and organification of iodide by thyroid gland, increasing its exposure to high dose of radiation and resulting in regional inflammation and hypothyroidism. For example, when ^{131}I tagged monoclonal antibody is given to the lymphoma patients, cleaved ^{131}I from ^{131}I-Abs is concentrated in thyroid and causes hypothyroidism[179,180]. However in a recent study, significant blocking of thyroidal iodine uptake was demonstrated by thyroidal hormones T3 and T4 in combination with methimazole, which blocks the organification of iodide in the thyroid gland; thus lowering the exposure amount and time of radioactive iodine to the thyroid gland[4]. The advantage of targeted therapy with ^{131}I is that it is well tolerated and inexpensive, as observed in thyroid cancer treatment. Side effects are also usually very less and may include nausea, light pain, swelling of salivary gland, gastritis and cystitis. In very rare cases leukemia or myelodysplasia has been reported.

For translation of the radioiodine therapy to the BC patients, two of the limitations are its lack of membrane localization and iodide organification. Inspite of these limitations, several preclinical studies suggest tumour ablation by radioiodine in extra thyroidal tissues. In addition, there is constant search of the factors that govern upregulation and membrane targeting of NIS in BC. Our data on NIS expression from lymph node

metastatic tissues suggests that IHC should be performed on primary as well as axillary lymph node tissue sections to evaluate NIS expression for better therapeutic targeting of radioiodine therapy in BC patients. Since NIS mediated uptake of various radioisotopes also allows diagnostic imaging, a diagnostic scan may enable *in vivo* evaluation of uptake in these tissues.

Future studies will require evaluating *in vivo* dynamics of iodide in NIS expressing metastatic BC and the underlying molecular mechanisms of radioiodine therapy in BC cells. Such studies will help to understand the therapeutic potential of targeting metastatic BC with ^{131}I in absence of iodide organification.

Development of a NIS over-expressing breast cancer cell model & Evaluation of radioiodide mediated therapeutic effect in the model by molecular imaging techniques

4.1 Introduction

As mentioned in the previous chapter, various groups including us have observed NIS expression in 70-80% BC patients; however attempts to evaluate functional relevance of NIS expression in BC patients show radioiodide uptake in a very small subset (25%)[1,2,4,6,181]. It appears from these literatures that the major hurdles in the translation of NIS-based radioiodide therapy to BC patients is the lack of NIS protein localization on the cancer cell membrane. A second issue that has been hypothesized is insufficient radioiodide accumulation due to lack of proper iodide organification in BC tissues, promoting fast efflux of radioiodine[146]. Therefore, prior to clinical trials of radioiodide therapy in NIS positive BC patients, it would be important to evaluate the therapeutic benefit of this modality in pre clinical xenograft models using NIS over-expressing BC cells. Cloning of rat NIS gene in 1996 allowed the transfer of this therapeutically important gene to several non-thyroidal tumour tissues for radioiodide based imaging and therapy[86]. Since then various preclinical studies have been performed to evaluate the efficacy and feasibility of NIS gene therapy. Many of the early studies on NIS gene therapy did not show significant iodide uptake due to insufficient expression of NIS resulting in less delivery of iodide[182]. However over the years, using improved gene delivery vectors it has been demonstrated that NIS gene can be successfully delivered and expressed in non-thyroidal cells. As a result significant reduction in tumour volume in various experimental cancer models were reported[113,183-186]. Previous reports suggest that in case of optimum gene expression, NIS mediated radioiodide therapy shows success in various extra thyroidal cancers including liver, prostate, colon, ovarian, pancreatic, cervical carcinoma, melanoma, glioma and multiple myeloma by *in vitro* as well as *in vivo* studies[110,184,187-200].

Although endogenous NIS expression is well known in BC, very limited numbers of studies have actually focused on evaluation of radioiodide therapy in NIS over-expressing preclinical BC models. Biodistribution of radioiodide in MCF-7 BC xenograft model has been reported earlier detailing the efflux, biological half-life and tissue distribution of radioiodide[201]. In a study conditionally replicating adenoviral vector was developed which express E1A gene under the tumour specific promoter cell surface associated mucin (MUC-1) for transcriptional regulation[11,202]. In addition, NIS gene was inserted under the non-specific Rous Sarcoma virus (RSV) promoter. Since MUC1 gene is over expressed by more than 90% human BCs, using this approach viral replication and consequently NIS expression can be targeted to a wide range of BC patients. Although effective targeting and NIS mediated iodide uptake has been observed but ^{131}I mediated toxicity was not evaluated. In another study replication deficient adenoviral vectors were developed to target ER+ve BC cells by using estrogen response promoter for driving NIS gene expression[12]. Using this adenoviral vector ZR-75-1 xenograft model was developed and PET scanning post 48 hours of intra-tumoural adenoviral injection showed iodide accumulation in the treated tumour. Further the mice that received intra-tumoural injection of adenovirus were treated with a single dose of 2mCi ^{131}I and slight reduction in tumour volume was observed after day 10 by BLI. However, in this study thyroid was not significantly blocked by 3 days of T3 treatment and also the follow up time after tumour regression has not been reported. In a recent study a replication competent, recombinant vaccinia virus was developed for NIS gene delivery in TNBC cell line MDA MB231[10]. In the virus infected cells and tumour xenografts high radioiodide uptake was observed; still a single dose of as high as 5mCi ^{131}I did not show significant decrease in the tumour volume.

In gene therapy trials with preclinical models one of the limitations is detection of gene expression. The ideal detection method should be non- invasive to study the localization, intensity and dynamics of gene expression[203]. Since most of the therapeutic genes do not have substrates or ligands for functional imaging, several strategies for correlated reporter genes expression have been developed which allows monitoring the therapeutic gene in action using non- invasive imaging. The advantage of NIS based therapeutics is that it can also be used for reporter imaging by uptake of various radioisotopes that are useful for various imaging modalities. Plethora of studies has shown NIS based functional imaging in various tissues[92,108,119,120,204-208]. Various imaging substrates that can be transported by NIS include I^-, Br^-, TcO_4^- and ReO_4. These radionucleotides are highly cost effective and widely available. In addition to these imaging modalities, a recent development in the field of radionuclide imaging is the ability to visualize a decay signal from a radioactive molecule with a highly sensitive CCD camera and the phenomenon is known as Cerenkov imaging[135]. *In vivo* optical images can be obtained for several radioactive probes such as 2-deoxy-2-[^{18}F]fluoro-D-glucose (^{18}FFDG), Na^{18}F, Na^{131}I, $^{90}YCl_3$ and a ^{90}Y labelled peptide that specifically target tumours[133]. Since Na^{131}I can also be used for Cerenkov imaging, it aids in evaluation of NIS based radioiodide therapy and to study the biodistribution and retention of radioactive molecule in whole animal by optical imaging.

Herein, we have developed experimental NIS over-expressing BC model using MCF-7 and ZR-75-1 BC cell lines. To follow the effect of radioiodide *in vivo*, a bifusion reporter expressing a fluorescent and a luminescence gene has also been over expressed. The plasmid vector system we used has an attB site which undergoes homologous recombination with the pseudo attP site present in the human chromosome and helps in stable and robust expression of the gene of interest in the mammalian system. Further we thoroughly evaluated correlated NIS and luciferase expression in the experimental model.

The model was characterized for NIS specific radioiodide uptake and retention time of iodide. After basic caracterization of gene expression and functions, therapeutic efficacy of ^{131}I was evaluated *in vitro* and *in vivo*. For *in vivo* studies Cerenkov imaging was performed to evaluate iodide uptake in tumour and its retention and effect on tumour size was followed by BLI.

4.2 Methods

4.2. 1 Plasmids used

pTA attB plasmid (Plasmid #18937) was obtained from Addgene. From this vector attB segment was isolated and introduced into the pcDNA3.1+ vector (Addgene, V790-20) upstream to the CAG promoter previously made in lab. The pcDNA3.1+attB-CAG-FTT (Fluc2-tdtomato-thymidine kinase) vector generated was used as a backbone for the present study. We also used pIRES vector (Clonetech, 631605) for introducing IRES upstream to fusion reporter gene. The vector map of both the plasmids is displayed in **Figure 4.1**.

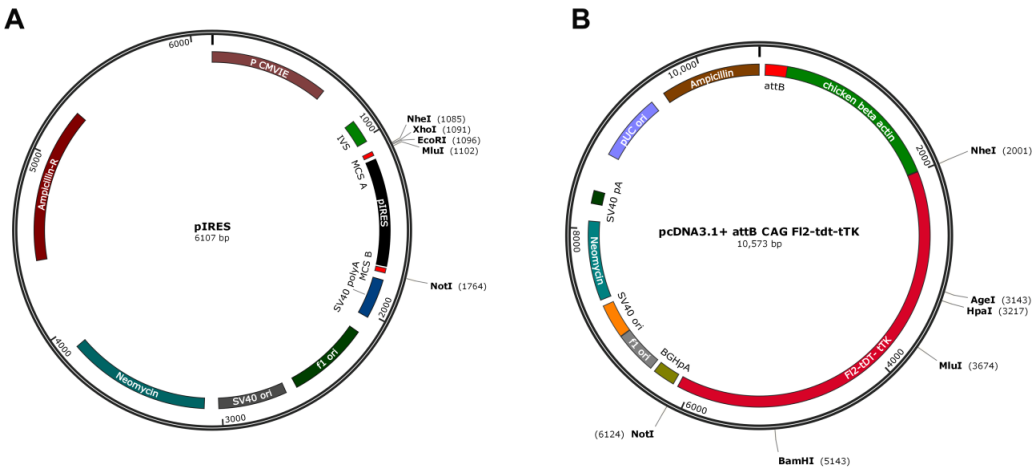

Figure 4.1 *Vector map of the plasmid backbones used in the study **A**. pIRES vector used for integration of NIS cDNA upstream to IRES **B.** pcDNA3.1+ attB-CAG vector used as backbone for expression of the therapeutic and reporter gene in mammalian cell.*

4.2. 2 Preparation of NIS over-expression plasmid

NIS gene flanked by a NheI 5'end and EcoRI 3' end was isolated from a lentiviral vector backbone and cloned into pIRES vector resulting in pNIS-IRES (**Figure 4.2A**). The positive clone was validated by sequencing and restriction digestion and used for further experiments (**Figure 4.2D**). Next, NIS-IRES sequence from pNIS-IRES vector was isolated by NheI and NotI enzymes and cloned into pcDNA3.1+attB-CAG-FTT vector to yield pcDNA3.1+attB-CAG-NIS-IRES (**Figure 4.2B & E**). Next step was insertion of the fusion reporter gene which is Turbofp. Fluc2. For this Turbofp. Fluc2 gene was PCR amplified with forward primer GGGGATCCGCCACCATGGTGGGT and reverse primer GCGCGGCCGCTTACACGGCGATCTTG and cloned downstream to NIS IRES in pcDNA3.1+attB-CAG-NIS-IRES vector using NotI and BamHI enzymes (**Figure 4.2C**). Thus the clone obtained (pcDNA3.1+ attB CAG-NIS IRES TurbofP. Fluc2/ACNITFl2) is validated by sequencing and restriction enzyme digestion and used for all the experiments (**Figure 4.2F**).

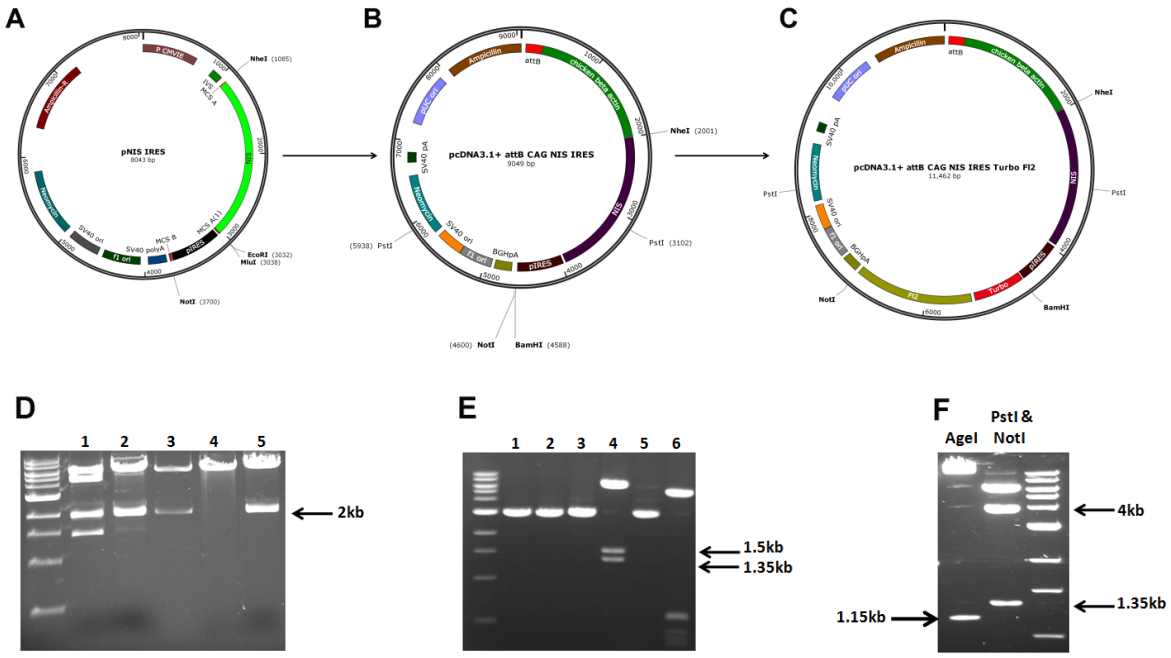

Figure 4.2 *Cloning strategy for construction of pcDNA3.1+ attB-CAG-NIS-IRES-Turbofp. Fluc2.* ***A.*** *Vector map of pNIS IRES plasmid generated by insertion of NIS between 5'Nhe and 3'EcoRI* ***B.*** *Vector map of pcDNA3.1+attB-CAG-NIS-IRES generated by insertion of NIS between 5'Nhe and 3'Not I* ***C.*** *Vector map of pcDNA3.1+attB-CAG-NIS-IRES-Turbofp. Fluc2 by insertion of the PCR amplified reporter gene between 5'BamHI and 3'NotI* ***D.*** *Confirmation of pNIS IRES vector construct by digestion with NheI and EcoRI showing release of a 2kb NIS fragment in clones 2, 3 and 5* ***E.*** *Confirmation of pcDNA3.1+attB-CAG-NIS-IRES vector construct by digestion with PstI and NotI showing release of a 1.5kb fragment which corresponds to the sequence between PstI at 3100 and NotI 4613 position and the other fragment of 1.35 kb which corresponds to the DNA sequence between NotI at 4613 and PstI at 5948. Only clone 4 showed release of both fragments and thus used for further subcloning.* ***F.*** *Confirmation of pcDNA3.1+attB-CAG-NIS-IRES-Turbofp. Fluc2 vector construct by digestion with AgeI and another digestion with PstI and NotI. Digestion with AgeI shows release of a 1.15kb turbo fragment and digestion with PstI and NotI shows release of a 4 kb fragment which corresponds to the sequence between PstI at 3100 and NotI at 7015 position and a 1.35 kb fragment that corresponds to a sequence between NotI at 7015 and PstI at 8350. The vector constructed was sequenced and used for further experiments.*

4.2. 3 Cells and culture conditions

The different BC cell lines used and their respective media are mentioned in the following table:

Table4.1 *Characteristics of the cell lines used in the study*

Cell line	Origin	Pathology	ER	PR	HER2	Medium
MCF-7	Pleural effusion	Invasive ductal carcinoma	+	+	+	RPMI
ZR-75-1	Ascites	Invasive ductal carcinoma	+	-	+	RPMI
MDA MB231	Pleural effusion	Adenocarcinoma	-	-	-	L-15

All the media were supplemented with 10% FBS (Gibco) and 1% penicillin- streptomycin (Gibco). Cultures were maintained in 5% CO_2 and humidified chamber in a 37°C incubator.

4.2. 4 Preparation of NIS expressing breast cancer cell line

MCF-7 and ZR-75-1 cells were co-transfected with ACNITFl2 and integrase vector [209]. As the plasmid contained neomycin gene, positive clones were selected out using 500µg G418. The isolated cell colonies were first screened for luciferase expression and the clones with positive luciferase activity were further screened for NIS expression by immunofluorescence and functional iodide uptake assay. Cell clones with optimum luciferase activity and NIS expression were used for the experiments.

4.2. 5 Luciferase assay

Cells were cultured in 24 well flat bottom plate at an equal density. The lysates were collected and the firefly luciferase activity was measured using LAR2 from Promega. Luciferase activity was measured in a Berthold luminometer for 1 second. The data is plotted as relative light unit per second (RLU/sec) normalised with protein estimated by Bradford method.

4.2. 6 Immunofluorescence for NIS and γH2A.X foci assay

Cells were seeded on cover slip in 35 mm plate and after transfection/ ^{131}I treatment washed with 1X PBS for three times and fixed with 4% PFA in PBS at 37°C. An additional permeabilization step with 0.2% TritonX 100 in 4% PFA was carried out for foci staining. Non-specific sites were blocked using 2% BSA in PBS. Cells were then incubated with γH2A.X/ NIS antibody in 1:400/ 1:50 dilutions respectively for overnight at 4°C in a humid chamber. After incubation with primary antibody cells were washed with 1XPBS and incubated with anti rabbit/anti mouse Dylight 633 antibody (1:200) for 1 hour at room temperature in dark humid chamber. Cells were washed with 1X PBS and nucleus was stained with DAPI (4',6-diamidino-2-phenylindole). Cells were mounted with Vecta Shield and images were captured under confocal microscope (LSM510, Zeiss). Foci assay was performed within 1 hour of ^{131}I treatment.

4.2. 7 Iodide uptake assay

50,000 MCF-7 NIS expressing cells were seeded in 24 well plate in duplicates and incubated with 2μCi ^{125}I/ml for 1 hour in uptake buffer (10mM HEPES in HBSS) in absence or presence of 30μM $KClO_4$ blocking. Next, media was removed; cells were washed once with cold uptake buffer, trypsinized and collected. The iodide uptake in the cells is measured by beta counter. For colorimetric method of radioiodide uptake, the same protocol was followed as published in previous literature[210].

4.2. 8 Iodide efflux assay

50,000 cells were seeded in 24 well plate in duplicate and incubated with ^{125}I for 1 hour. At the end of 1 hour ^{125}I containing media was removed and replaced with plain media. Cells were collected at the mentioned time points and remaining ^{125}I activity was measured by beta counter.

4.2. 9 Real time PCR

For RNA isolation $2*10^6$ cells were collected and RNA was isolated by RNA extraction kit from Qiagen (74106) and quality was checked on the denaturing RNA gel. 1µg RNA was used for the preparation of cDNA by cDNA synthesis kit from invitrogen (18080-051). Real time amplification was performed using the TaqMan master mix and (Life technologies, 4304437) primer probe mix from applied biosciences for NIS (Hs00166567_m1) and GAPDH (Hs02758991_g1). The real time reaction was run in Quantstudio12k flex from life technologies. NIS expression level in NIS over-expressing cell clones was evaluated as compared to control cells and data was analyzed by $2^{-\Delta\Delta CT}$ method and plotted as fold change in all the graphs.

4.2. 10 Western blotting

MCF-7 NIS expressing cells were gently scraped from the plate, lysed in RIPA lysis buffer and collected in ice chilled microcentrifuge tube. Cells were vortexed vigorously for 30 seconds and incubated on ice for 2 hours. Lysed cells were sonicated and centrifuged at 14,000rpm, 4°C for 45 minutes. The supernatant was collected, and protein concentration was determined by using Bradford assay. Required amount of protein was mixed with gel loading buffer and heated at 37°C for 30 minutes. Protein samples were electrophoresed on a 7.5% SDS-PAGE and subsequently transferred to nitro cellulose membrane. The membrane was incubated in fresh blocking buffer (0.1% tween 20 in Tris-buffered saline, pH 7.4, containing 5% nonfat dried milk) at room temperature for 1 hour and then probed with the monoclonal NIS antibody (1:1000) in blocking buffer at 4°C overnight. After washing the membrane with TBST (TBS and 0.1% tween 20) three times for 10 min each, it was incubated in the anti mouse HRP-conjugated secondary antibody (1:10000) at room temperature for another 1hour and washed again three times in TBST buffer. The transferred proteins were incubated with ECL substrate solution and

visualized with autoradiography Xray-film. All blots were stripped and reprobed with α-tubullin antibody (1:10000) to ascertain equal loading of protein.

4.2. 11 Glycosylation PCR array

The Glycosylation PCR Array supplied by Qiagen (PAHS46Z) is based on SYBR green based real time PCR array. It profiles the expression of 84 key genes encoding enzymes that post- translationally add or remove sugar residues to and from proteoglycans and glycoproteins. **Figure 4.3A** depicts a representative array plate, which contains primers for various control genes in addition to primers for glycosylation enzyme's genes.

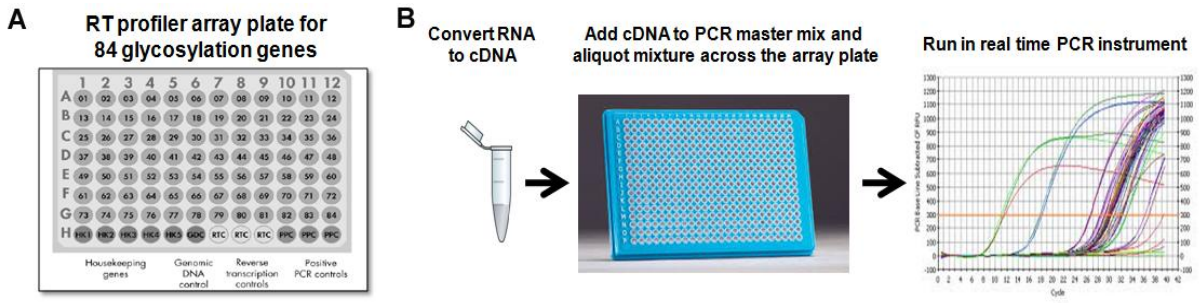

Figure 4.3 *Schematic of the workflow for glycosylation PCR array* ***A.*** *Overlay of an array plate showing wells for 84 genes involved in the process of glycosylation, 5 housekeeping genes, 1 genomic DNA control, 3 Reverse transcription control and 3 Positive PCR control* ***B.*** *Workflow of the array involves cDNA synthesis, addition of the cDNA and PCR master mix to different wells of the array plate containing primers for respective genes. Real time PCR is performed which is followed by the data analysis to evaluate glycosylation enzyme's gene expression level.*

The work flow (**Figure 4.3B**) of the array involves isolation of RNA, digestion of residual DNA, preparation of cDNA and loading the SYBR green together with the cDNA and PCR mix in individual wells, which already contain the primer for the reaction. After setting the reaction real time PCR is run (Quantstudio 12K flex) and the data obtained is analyzed by the software available from Qiagen (http://www.sabiosciences.com/dataanalysis.php).

4.2. 12 Clonogenic assay

$2x10^6$ cells were seeded in 25mm flask and either treated with radiation or incubated with 50µCi ^{131}I /ml in HBSS for 5-6 hours. After treatment ^{131}I containing media was removed and cells were washed with cold HBSS. Cells were trypsinized and 1000 cells were seeded in 6 well plates in triplicate. Media was changed at regular intervals and after 14 days cells were fixed with 10% chilled formaldehyde and stained with 4% crystal violet in methanol. Stained colonies were counted under stereomicroscope and survival fraction was calculated according to the protocol mentioned in previous publication[211].

4.2. 13 Cell cycle analysis and apoptosis assay

At the mentioned time points $1*10^6$ cells were trypsinized, collected and washed with 1X PBS. For cell cycle analysis cells were fixed with 70% ethanol and incubated overnight at -20°C. Next day cells were pallet down and washed with 1X PBS. Washed cells were treated with 1µg/ml RNase A for 10 minutes at 37°C. 300µl of 50µg/ml propidium iodide was added in each tube, incubated for 30 minutes at 37°C and acquired in FACS calibre.

For apoptotic cell count, Annexin V apoptosis detection kit (Abcam, 14085) was used and protocol mentioned in the kit was followed.

4.2. 14 Tumour xenografts and ^{131}I therapy

Stably transfected NIS-IRES-TurbofP. Fluc2 ZR-75-1 cells (clone 1) were cultured until 75% confluent. Cells were trypsinized, washed in PBS, counted and resuspended in PBS. $6*10^6$ cells were implanted subcutaneously at right dorsal flanks of six to seven week old female nude mice. Mice were divided into two groups of three mice each. Before starting the ^{131}I therapy all the mice in both the groups were treated with T4 (2µg) and methimazole (10µg) everyday for 10 days to block the thyroid and this blocking was continued for next 3 weeks. The experimental group was injected with a weekly dose of 1

mCi of ^{131}I for 3 weeks. Serial bioluminescent monitoring began on the day before the 1st dose of ^{131}I therapy, designated as Day 0, and continued for the next 35 days. 1 of the treated mice died after 3 weeks of treatment.

4.2. 15 *In vivo* bioluminescence imaging

Bioluminescence was measured after an intraperitoneal injection of mice (n= 3 in each group) with 100 µL of 30 mg/mL of D-luciferin (Biosynth International). Imaging was carried out on IVIS Spectrum imaging platform equipped with a highly sensitive CCD camera and viewed in real time on a computer screen using a color scale expressed as total flux (photons per second per square centimeter per steradian [photons/sec/cm^2/ sr]). Mice were anesthetized with isofluorane and placed in the 37^{o}C warmed platform chamber with continuous 2% isofluorane administration via a nasal cone. Acquisition times of 10 seconds were used and signal was measured in the ROI overlying the tumour. Serial readings were taken after each injection and maximum values obtained from each mouse at individual time points were averaged for each set and the mean values were compared over time. Baseline readings were taken in all mice before the 1st dose ^{131}I treatment. Serial bioluminescence was monitored every time prior to ^{131}I therapy on Days 1, 7, 14, 21, 28 and 35. Data were analyzed using Living image (4.4) software. Optical signal was normalized to photons per second per square centimeter per steradian [photons/sec/cm^2/ sr].

4.2. 16 Cerenkov luminescence imaging

CLI was performed with the same IVIS spectrum system as used for BLI. For *in vitro* studies, radioiodine (^{131}I) was diluted in phosphate-buffered saline and different amounts were placed in each well of flat bottom 96 wells black plates. The signal is acquired for 10 seconds using open filter.

For *in vivo* Cerenkov imaging animals (n=3) were injected with 1mCi of ^{131}I intraperitoneally. Cerenkov imaging was performed after 24 and 72 hours of ^{131}I injection. Animals were placed in a light-tight chamber under isofluorane anesthesia. For Cerenkov imaging signal was acquired for 3 minutes each and dorsal as well as ventral scans were acquired.

4.2. 17 Statistics

Data is presented as mean +/- standard error. Student's t-test was used to judge the significance of difference. All tests were two sided and $p < 0.05$ was considered as significant. Graph pad Prizm software was used for all the statistical analysis. To calculate the correlation of 2 proteins, Pearson's correlation test was applied.

4.3 Results

4.3. 1 Preparation of NIS over-expressing MCF-7 cells

For validation of the vector construct (ACNITFl2), a BC cell line MDA MB231 and an ovarian cancer cell line A2780 is co-transfected with the bicistronic vector containing NIS and bifusion reporter gene (**Figure 4.4A**) and integrase vector. Both the cell lines show expression of the luciferase and fluorescent reporter gene (**Figure 4.4B & C**). pTFl2 plasmid was used as a positive control, which shows expression of the fusion reporter gene under Cytomegalovirus (CMV) promoter. Further, transient transfection of these vectors in MCF-7 cells shows over expression of NIS as evident from **Figure 4.4D**.

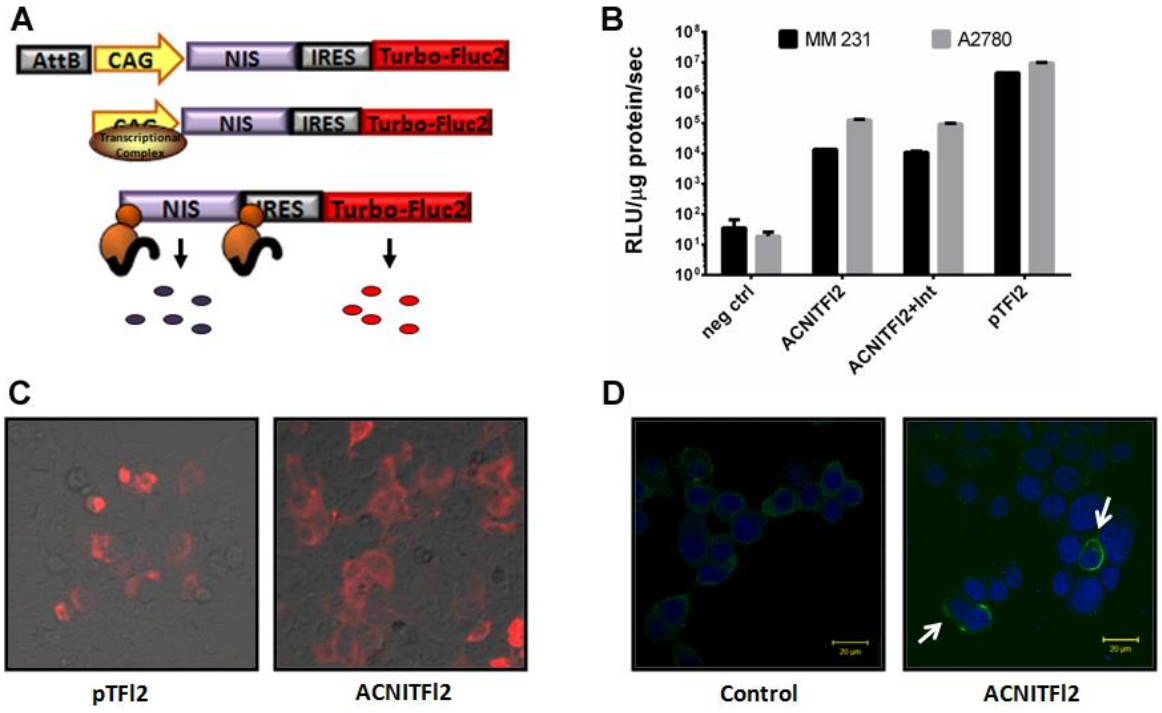

Figure 4.4 *Validation of the vector construct developed to evaluate expression of various genes* ***A.*** *Cartoon depicting the bicistronic vector used in the study. The therapeutic gene (NIS) and the reporter gene (Turbofp. Fluc2) are linked by IRES sequence. Use of IRES sequence allows transcription of both the genes under same promoter. Further protein synthesis of the first gene in the sequence takes place by CAP dependent and of the second gene by CAP independent translation* ***B.*** *Transient transfection with the bicistronic vector shows luciferase activity in 2 cell lines, MDA MB231 and A2780 in presence or absence of integrase vector (Int). pTFl2 was used as a positive control which expresses fusion reporter gene (Turbofp. Fluc2) under CMV promoter.* ***C.*** *Expression of the fluorescent gene expression (Turbofp) in MCF-7 cells transiently transfected with ACNITFl2.* ***D.*** *Immunofluorescence assay shows NIS expression in transiently transfected MCF-7 cells. Scale bar represents 20µm.*

Once the plasmid vector mediated gene expression is evaluated in multiple cell lines we analyzed the basal level of NIS expression in a panel of BC cell lines. It is observed that all the BC cells show very faint NIS expression which is predominantly cytoplasmic (**Figure 4.5**).

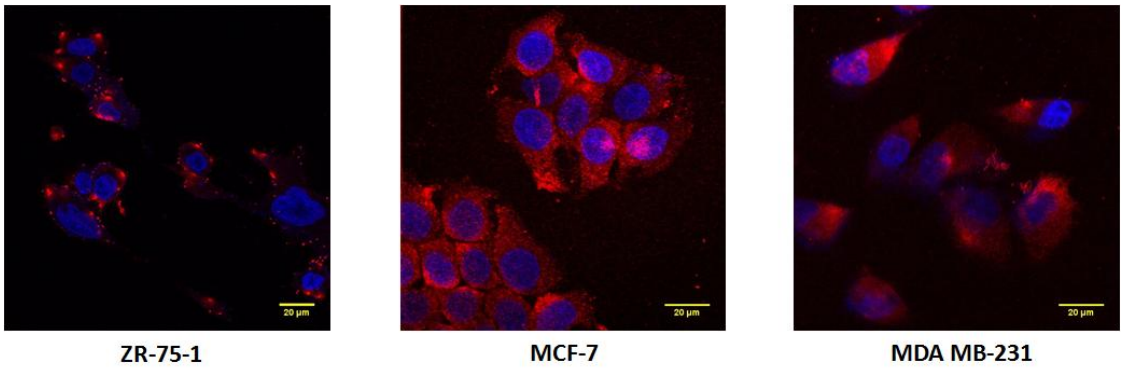

Figure 4.5 *Endogenous NIS expression in a panel of BC cell lines showing weak cytoplasmic staining. Scale bar represents 20µm.*

Since our patient sample data suggests that receptor positive patients may get maximum benefit by NIS mediated radioiodide therapy, an ER/PR+ve cell line MCF-7 is used as a model for NIS over expression in the present study. MCF-7 stable cell clones are generated by co transfection of the bifusion vector and the integrase vector. As evident from the **Figure 4.6A** we observe a wide range of luciferase expression from various cell clones. Interestingly further screening for NIS expression analysis reveals that in majority of the clones NIS expression is predominantly cytoplasmic where as in very few cell clones membranous NIS expression is evident (**Figure 4.6B**). We do not observe any significant difference in terms of luciferase expression between cells expressing NIS in cytoplasm versus membrane.

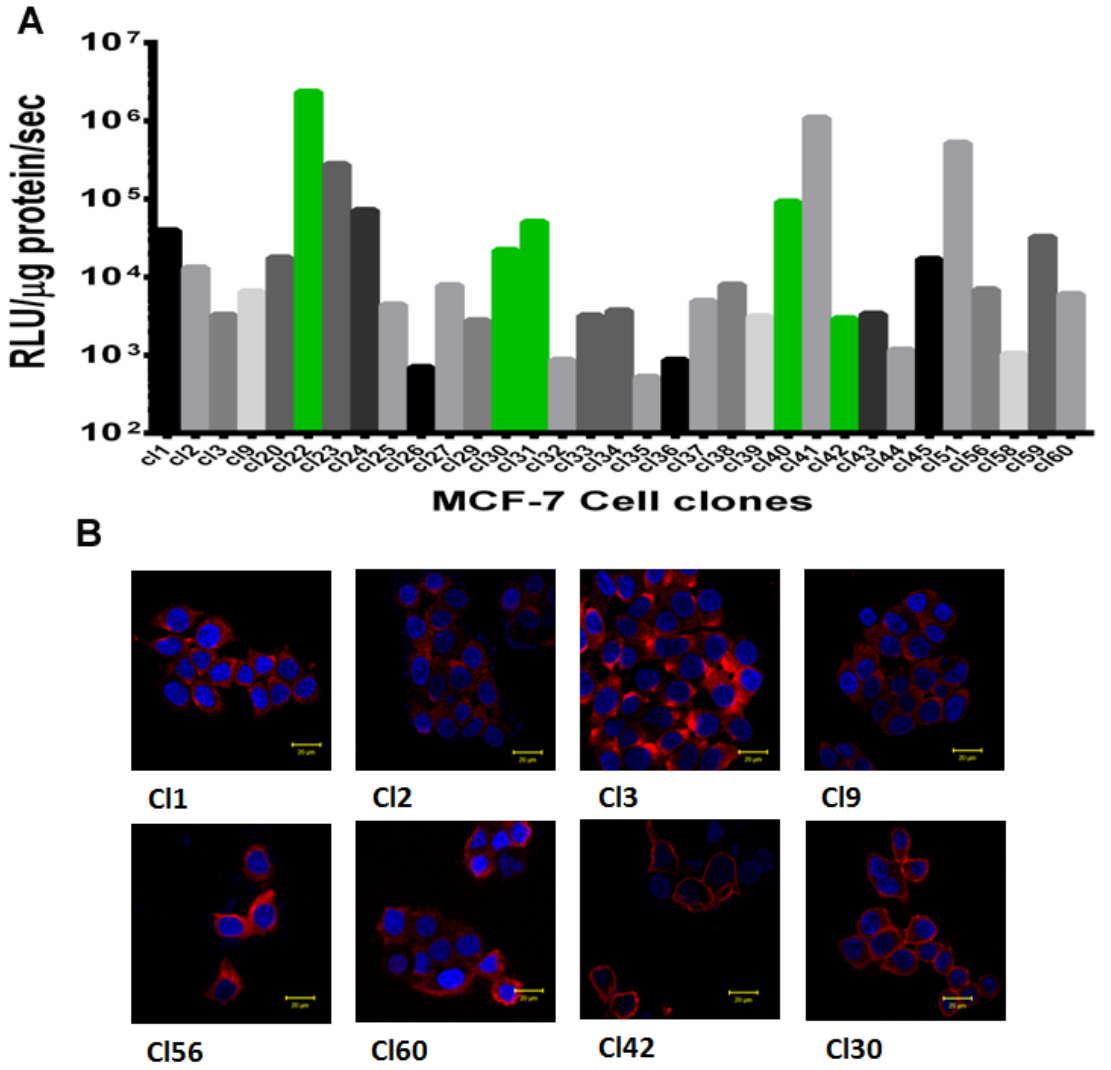

Figure 4.6 *Screening of MCF-7 cells transfected with the bicistronic vector for co-expression of the therapeutic and a reporter gene* ***A.*** *Luciferase expression in various MCF-7 clone. The bars highlighted in green represent the cell clones with membranous NIS expression* ***B.*** *NIS expression in various MCF-7 cell clones showing difference in localization of NIS. Scale bar represents 20µm.*

Since this observation was striking, so to validate these cells were maintained in culture over multiple passages and as shown in **Figure 4.7 A-D** we observe that luciferase expression as well as differential NIS localization is maintained over long passages in various clones. To avoid confusion we named cytoplasmic NIS expressing clones used in

the study as A3, A4, A5, A6 and membrane NIS expressing clones are numbered as clone 22, 30, 31, 40, and 42.

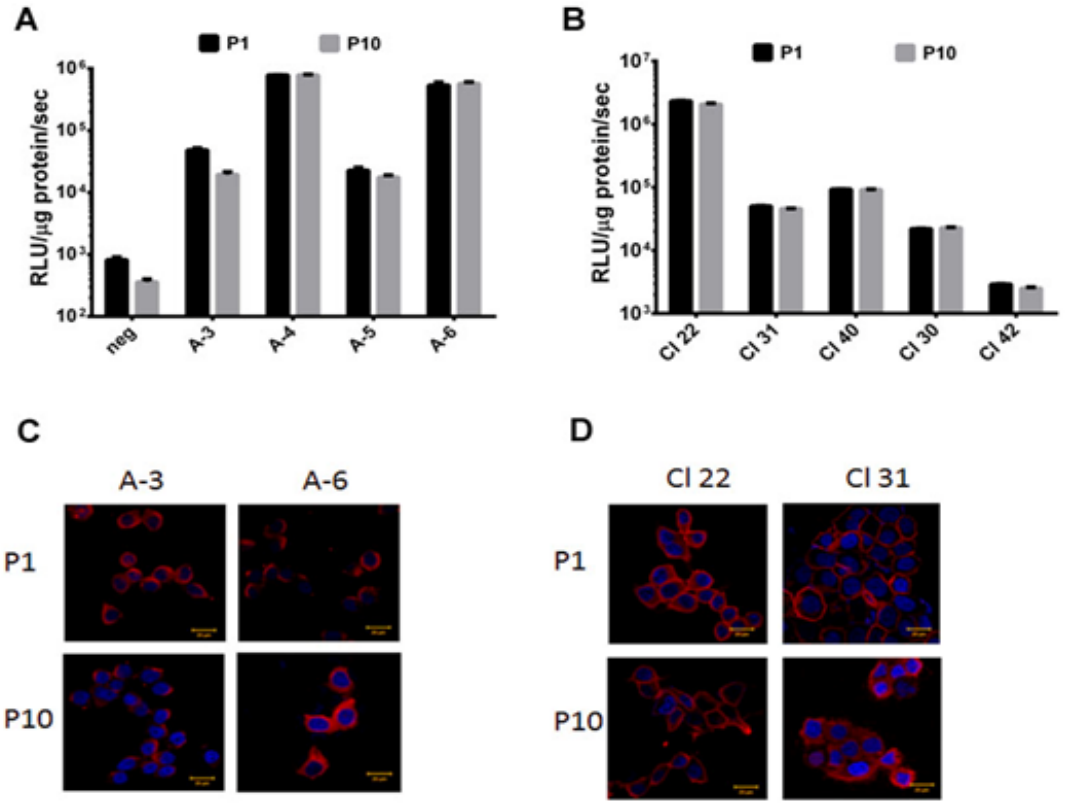

Figure 4.7 *Maintenance of the NIS and reporter gene expression over various passages* ***A.*** *Luciferase expression in various cytoplasmic NIS expressing clones showing well maintained luciferase activity* ***B.*** *Consistent lucifearse expression in membrane NIS expressing clones* ***C.*** *Immunofluorescence images for NIS showing that the localization of NIS in cytoplasm is maintained over various passages in cytoplasmic clones* ***D.*** *Immunofluorescence images for NIS showing that the localization of NIS in membrane is maintained over various passages in membrane NIS expressing clones. Scale bar represents 20µm.*

4.3. 2 Glycosylation gene expression profile of the cells expressing NIS in membrane versus cytoplasm

As we observed distinct differences in the localization pattern of NIS among various MCF-7 cell clones, it was of great interest to understand the factors responsible for its

membrane targeting. To evaluate if glycosylation of NIS plays any role in differential localization of NIS, western blot analysis is performed to check the glycosylated forms of NIS in the two different clonal populations. As evident from the western blot image in **Figure 4.8A** in clone 22 (membranous NIS) we observe higher intensity of the completely glycosylated form of NIS (97 kd) where as the intensity of this band is lower in A4 which shows cytoplasmic localization of NIS but we do not observe significant difference in the band intensity of partially and incompletely glycosylated forms of NIS between the 2 clonal populations (50-67kd).

We further investigated if the key players of glycosylation enzyme machinery have any important role in its localization. To clarify that, a real time PCR based array is performed for evaluating the expression profile of 84 genes involved in the process of glycosylation. To do this cDNA samples from 2 of the cytoplasmic NIS expressing MCF-7 cell clones (A4 and A6) and 1 membrane NIS expressing MCF-7 cell clones (clone31) are run in this array platform, together with the plain MCF-7 cells. Data analysis from the array shows that there is distinct up- or down-regulation of specific classes of glycosylation enzymes in the two established cell populations (**Figure 4.8B**). The experiment was further repeated with 2 other membrane NIS expressing clones namely clone 2 and 22.

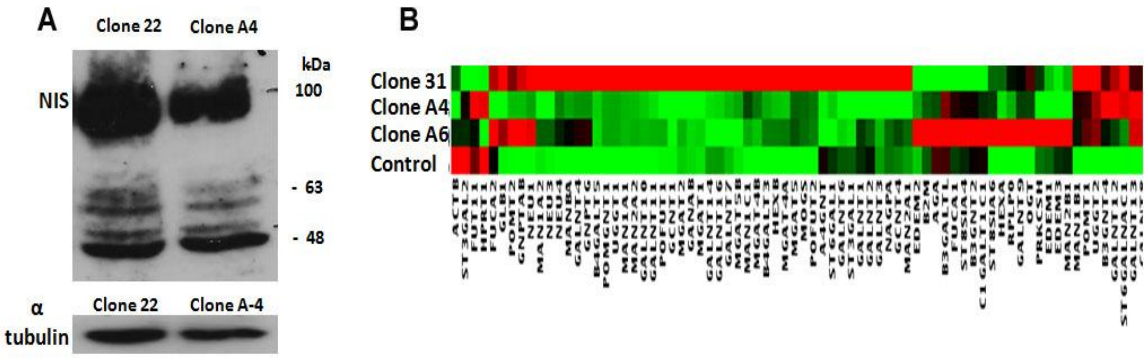

Figure 4.8 *Role of glycosylation in differential localization of NIS* **A.** *Western blot image showing high intensity of completely glycosylated form of NIS (97kd) in clone 22 which shows*

membranous NIS expression where as the band intensity is lesser in A4 clone which shows predominantly cytoplasmic NIS ***B.*** *Data analysis from the glycosylation PCR array shows distinct differences in the expression level of glycosylation genes****.*** *It is evident from figure that many of the glycosylation genes are upregulated in clone 31 (membrane NIS expressing clone) as compared to A4, A6 and MCF-7 plain cells.*

Further clustering analysis through MEV software classifies all the samples in to 2 groups, 1 of the groups includes A4 and A6 (Cytoplasmic clones) together with the MCF-7 plain cells and another group includes all the cell clones with membranous NIS expression, namely clone 2, 22 and 31 (**Figure 4.9**). Thus the glycosylation array data analysis suggests that the glycosylation gene expression profile of the membrane NIS and cytoplasmic NIS expressing clones are distinctly different and cytoplasmic NIS expressing clones show a glycosylation gene expression profile which is similar to MCF-7 plain cells. Specifically, the expression level of mannosidases, sialidases, mannosyltranferases and sialyltransferases are significantly high in NIS membrane clones as compared to cytoplasmic NIS clones and MCF-7 plain cells (**Figure 4.10A-D**). Among mannosidases the maximum difference is observed in case of MAN1A1 and MAN1B1 enzymes (**Figure 4.10A**) and among mannosyl transferases the maximum difference is observed in MGAT4B and MGAT5 (**Figure 4.10B**). Previous literature suggests that NIS is rich in mannose residues and significant difference in mannose related glycosylation enzyme's expression suggests its possible role in NIS membrane targeting.

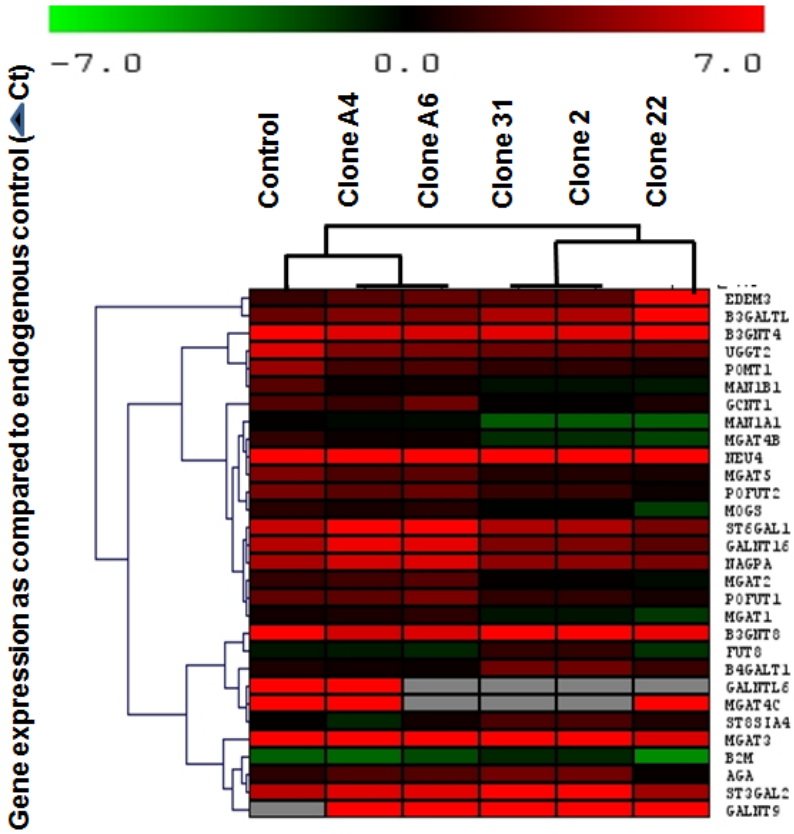

Figure 4.9 *Clustering analysis of the glycosylation PCR array data by MEV software showing 2 distinct clusters of MCF-7 clones based on the expression of genes involved in the process of glycosylation.*

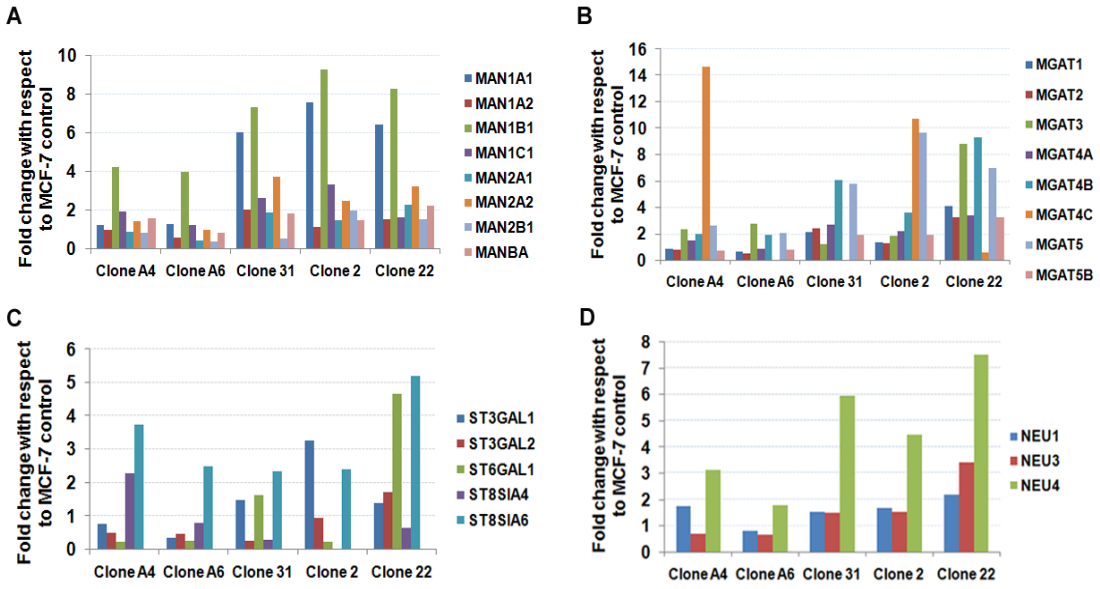

Figure 4.10 *Graphs depicting the levels of glycosylation genes in membrane vs. cytoplsmic NIS expressing clones.* ***A.*** *Expression level of mannosidases in various MCF-7 NIS expressing clones. It is evident that expression level of MAN1A1 and MAN1B1 is high in membrane NIS expressing*

clones as compared to cytoplasmic NIS expressing clones ***B.*** *Expression level of mannosyl transferases in various MCF-7 NIS expressing clones. MGAT4B and MGAT5 shows increased expression in membrane NIS expressing clones as compared to cytoplasmic NIS expressing clones* ***C.*** *Expression level of sialyl transferases in various MCF-7 NIS expressing clones. ST3GAL1 is consistently high in all membrane NIS expressing clones where as ST6GAL1 is high only in clone 31 and 22* ***D.*** *Expression level of sialidases in various MCF-7 NIS expressing clones. A slight increase in Neu4 gene is observed in membrane NIS expressing clones. Alltogether the data suggests distinct upregulation of many important glycosylation enzyme genes in membrane NIS expressing clones which may play an important role in proper NIS targeting*

4.3. 3 Characterization of the experimental model with correlated expression of the therapeutic and reporter gene

As mentioned previously we have used bicistronic vector to monitor the expression of the therapeutic gene through the reporter gene. For such bicistronic vector models close association of both the genes is obligatory. Since earlier reports suggest that for effective iodide accumulation inside cells, presence of NIS transporter protein at membrane is crucial, so keeping this fact in mind we have verified correlated activity of NIS and luciferase in membrane NIS expressing clones only. Overall we observe membranous NIS expression in 5 MCF-7 cell clones, which show variable intensity of NIS as well as luciferase expression (**Figure 4.11A - D**). Except one clone (clone 30), all the other cell clones show very good correlated expression of NIS with luciferase (R^2=0.0908) (**Figure 4.11E**). NIS transcript level is also evaluated in these clones and we observe difference in the intensity which is concordant with the NIS protein expression observed by immunofluorescence assay (**Figure 4.11B & C**).

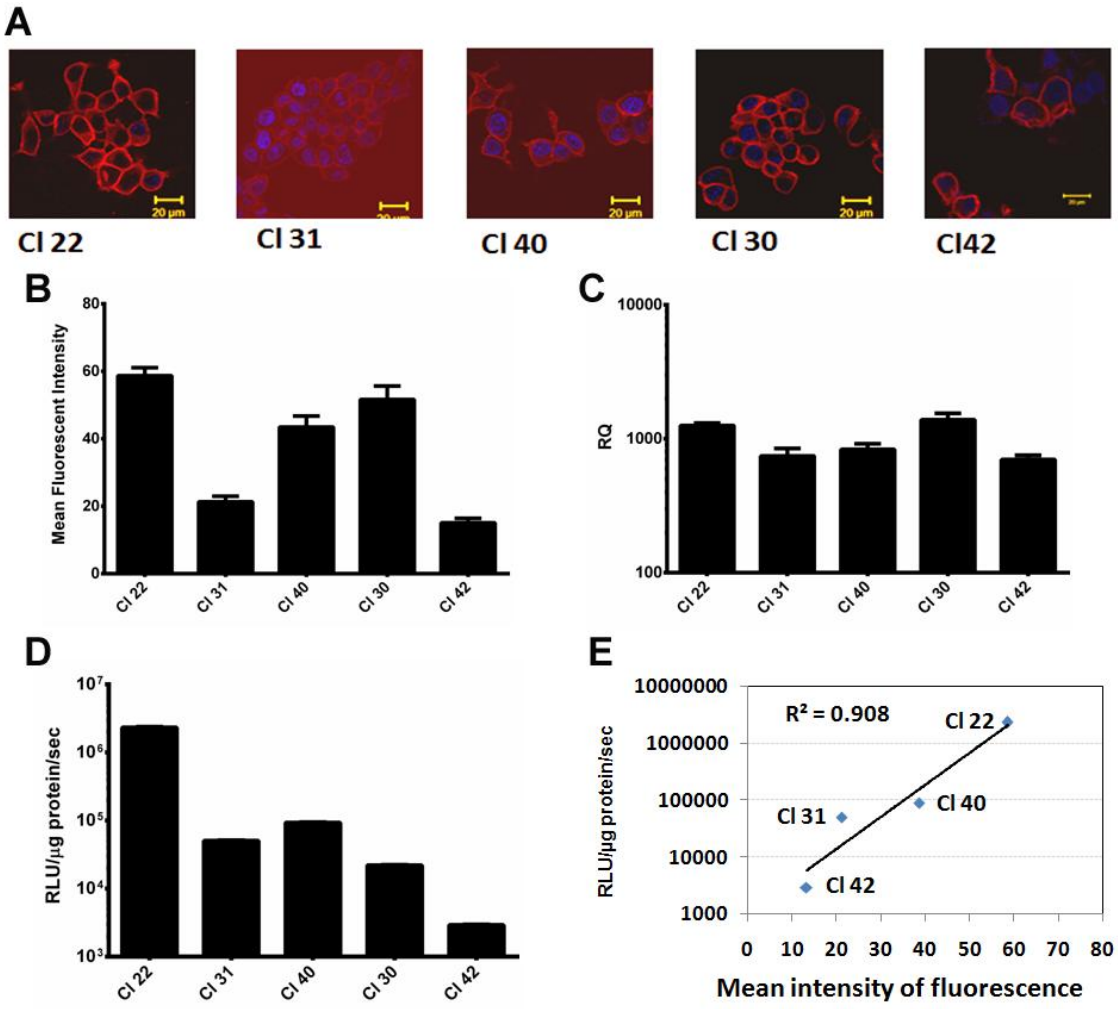

Figure 4.11 *Development of the experimental MCF-7 BC model with correlated expression of the therapeutic and reporter gene.* ***A.*** *Different levels of membrane NIS expression in various clones detected by immunofluorescence using human NIS monoclonal antibody. Scale bar represents 20µm.* ***B.*** *Quantitation of the NIS immunofluorescence staining* ***C****. NIS transcript levels in various clones which is concordant with immunofluorescence data* ***D.*** *Quantitaion of luciferase activity in these clones shows different levels of luciferase expression* ***E.*** *Graph showing correlated expression of NIS with the luciferase activity in these clones. Except clone 30 all the clones show close association of both the genes.*

Further to validate the functionality of the molecule in these clones iodide uptake assay is performed with radioactive iodide (^{125}I). Data from iodide uptake assay suggests that MCF-7 NIS clones with decreasing level of NIS expression show decrease in amount of iodide uptake (**Figure 4.12A**). Further to show NIS specific uptake of iodide in these

cells, cells are treated with a NIS blocker, $KClO_4^-$ and we observe significant reduction in iodide uptake indicating that iodide accumulation in these cells specifically takes place through NIS (**Figure 4.12A**). We also observe increase in total iodide uptake with increasing number of clone 22 cells (**Figure 4.12C**). It is observed that iodide uptake ability of cells with NIS localized at membrane is significantly high as compared to plain MCF-7 cells or cytoplasmic NIS over-expressing MCF-7 cells. All together these data indicate that for efficient delivery of iodide inside the BC cells localization of the symporter molecule at the membrane is essential.

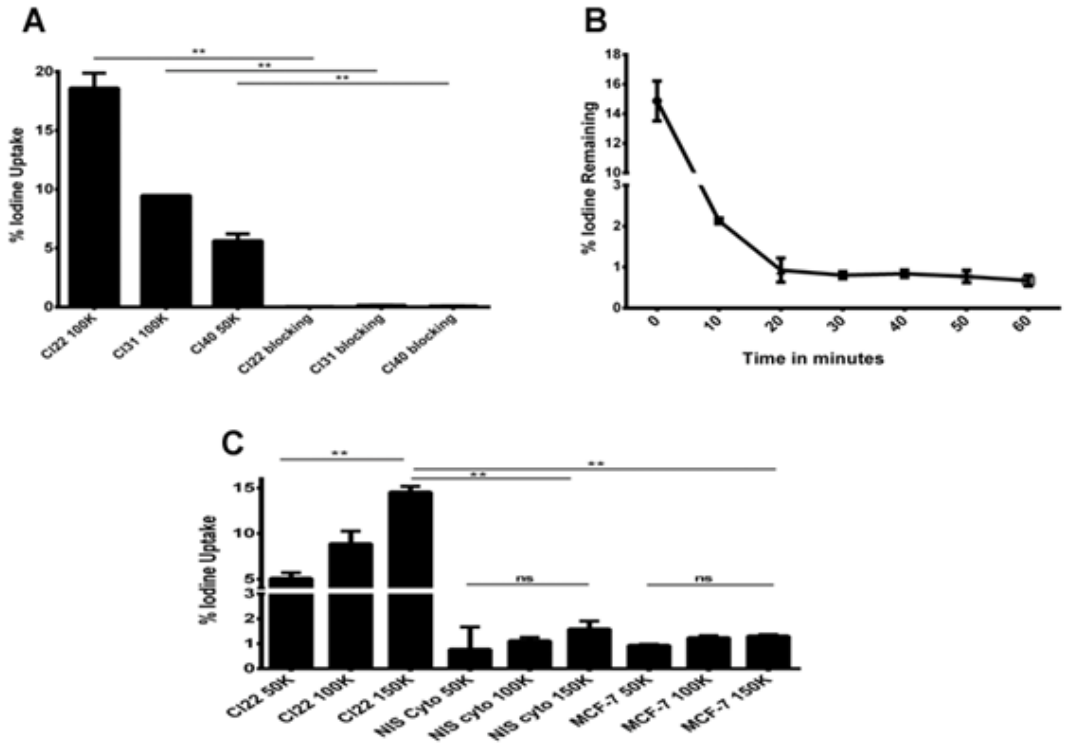

Figure 4.12 *Radioactive iodide (^{125}I) uptake assay in MCF-7 NIS expressing clones* ***A.*** *Uptake assay with three of the membrane clones suggest difference in the amount of iodide uptaken which is according to the level of NIS expression in these clones. Blocking of NIS with perchlorate shows significant decrease in iodide uptake indicating NIS specific uptake of iodide* ***B.*** *Efflux assay with radioactive iodide suggests major efflux of iodide within 15 minutes of incubation. Retention of iodide for such a short time window in these cells is due to lack of iodide orgaification system in BC cells* ***C.*** *The graph shows concomitant increase in iodide uptake with*

increase in cell number. It is also evident that the amount of iodide uptaken by control MCF-7 cells or cytoplasmic NIS (clone A4) expressing cells is significantly lower than the membrane NIS (clone 22) expressing cells.

For better therapeutic efficacy of radioiodide treatment in BC cells retention time of the iodide molecule may play an important role, as longer period of radioiodide retention in the cells will result in more damage. To evaluate the retention time of radioactive iodide inside NIS over-expressing cells iodide efflux assay is performed and we observe that 90% of radioiodide is effluxed out within 15 minutes of incubation in iodide free medium (**Figure 4.12B**).

4.3. 4 Therapeutic efficacy of radioiodide in NIS over-expressing MCF-7 cells

After validating the iodide uptake ability in NIS expressing clones, we evaluated the therapeutic efficacy of ^{131}I on MCF-7-NIS membrane expressing cell line (clone 22) by measuring the survival fraction by clonogenic assay. A brief exposure of these cells to 50μCi ^{131}I is found to cause significant decrease in cell survival ($p < 0.0001$, CI=95%) than the untreated cells **(Figure 4.13A)**. Radiation injury resulting cellular apoptosis is assessed by annexin V staining protocol, which shows only 46.5% live cells in case of ^{131}I treatment as compared to 86% in control **(Figure 4.13B)**. To confirm that such brief and low-dose exposure of MCF-7-NIS cell still cause DNA double strand break, γH2A.X foci formation assay is performed at different time intervals after ^{131}I treatment. Formation of a significantly large numbers of foci in treated cells is noted as compared to the untreated cells **(Figure 4.13C)**. Further cell cycle analysis post ^{131}I treatment shows G2-M arrest which is relieved after 48 hours of treatment (**Figure 4.13D**). Thus, together our results confirm that although major amount of iodide is effluxed out by these cells within a short duration, still sufficient radio-ablative effects on MCF-7-NIS cell are evident.

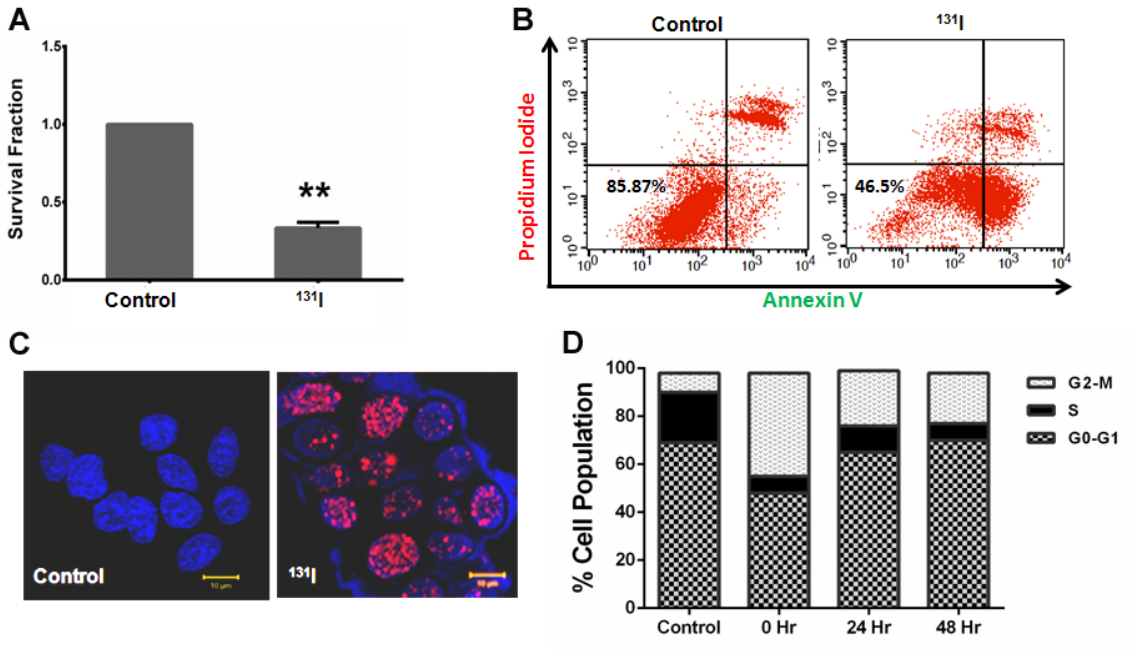

Figure 4.13 *Evaluation of in vitro therapeutic efficacy of radioiodide (^{131}I) in MCF-7 membrane NIS over-expressing clone (clone 22)* ***A.*** *Clonogenic assay showing significant decrease in survival fraction post ^{131}I treatment* ***B.*** *Apoptotic assay showing decrease in live cell population after ^{131}I treatment* ***C.*** *Immunofluorescence staining for γH2A.X foci shows increased numbers of foci formation in ^{131}I treated cells than untreated controls. Scale bar represents 10µm.* ***D.*** *Cell cycle analysis is performed at immediate end of 7 hours ^{131}I treatment which is considered as 0 hour time point. It is also analyzed at 24 and 48 hours of treatment. Data shows G2-M arrest at 0 hour time point however this arrest is relieved after 24-48 hours of radioiodide treatment.*

4.3. 5 Development of ZR-75-1 NIS over-expressing cells

Although we observe significant cytotoxic effects of ^{131}I in membrane NIS expressing MCF-7 cells but these cells failed to form tumour in available immunocompromised mice and therefore we developed another NIS expressing experimental cell model using ZR-75-1 cell line, which is also a receptor positive BC cell line and shows tumour formation in available immunocompromised mice. ZR-75-1 cells are transfected with the same bifusion integrase plasmid vector (**Figure 4.14A**) and live cell screening of positive clones with G418 selection shows very few cell clones with luciferase activity in the culture plate (**Figure 4.14B**). The positive cell clones are further amplified and

quantitation of luciferase activity is performed. Luciferase activity is observed in 2 clones (clone 1 & 3) (**Figure 4.14C**). Immunofluorescence and colorimetric iodide uptake assay results show NIS over expression and iodide uptake in both the clones however clone 1 shows higher NIS expression and iodide uptake as compared to clone 3 (**Figure 4.14D&E**). As opposed to MCF-7 cells, NIS localization is predominantly cytoplasmic in both the ZR-75-1 NIS over-expressing cell clones.

The firefly luciferase component of the bi-fusion reporter is used in this study to monitor the expression of the NIS therapeutic gene and radioiodide mediated abrogation as an indirect measure in the present study. Prior to *in vivo* BLI the signal intensity of the luciferase reporter in live cells is evaluated and we observe that 40,000 cells of ZR-75-1 clone1 generate sufficient photon signal which is significantly above the background level (**Figure 4.14F&G**).

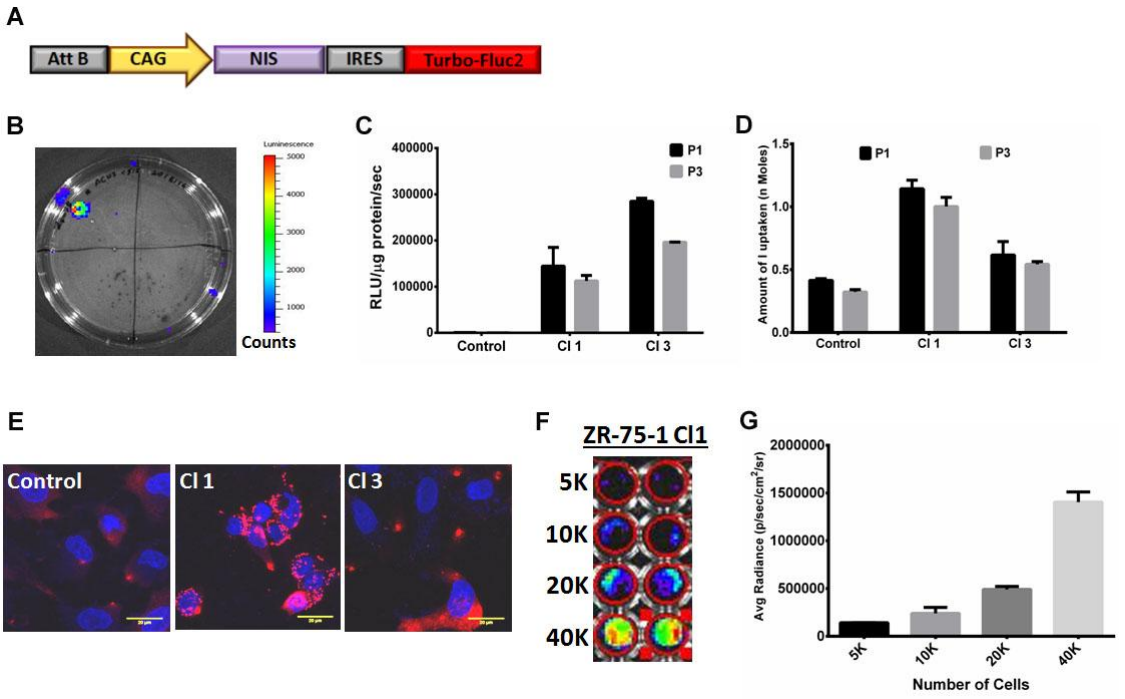

Figure 4.14 *Development of NIS expressing ZR-75-1 BC cells* ***A.*** *Diagrammatic representation of attB-CAG-NIS-IRES-Turbofp.Fluc2 plasmid DNA vector used for establishing NIS expressing cell*

lines ***B.*** *Screening of luciferase positive cell clones in 10cm plate using IVIS imaging system* ***C.*** *Quantitation of luciferase activity in positive clones shows luciferase activity in clone1 and clone3* ***D.*** *Colorimetric iodide uptake assay of luciferase positive clones showing high iodide uptake in clone1 as compared to clone3* ***E.*** *Immunofluorescence assay for NIS expression shows increased NIS expression in the stable cells generated as compared to plain ZR-75-1 cells. The localization pattern of NIS is however mainly found as cytoplasmic. Scale bar represents 20µm.* ***F.*** *Live cell luciferase imaging using D-Luciferin substrate with different numbers of ZR-75-1 clone1 cells in 96 well plate* ***G.*** *Quantitative data of luciferase signal obtained from live cell imaging showing incremental luciferase signal intensity.*

Prior to *in vivo* ^{131}I toxicity experiments, *in vitro* ^{131}I toxicity is evaluated in ZR-75-1 NIS expressing cells and treatment with 50µCi ^{131}I shows significant decrease in the survival fraction as observed with clonogenic assay (**Figure 4.15 A**). Radioactive molecule mediated DNA damage is also measured by γH2A.X assay and we observe high frequency and intensity of foci in ^{131}I treated cells as compared to control cells (**Figure 4.15B)**.

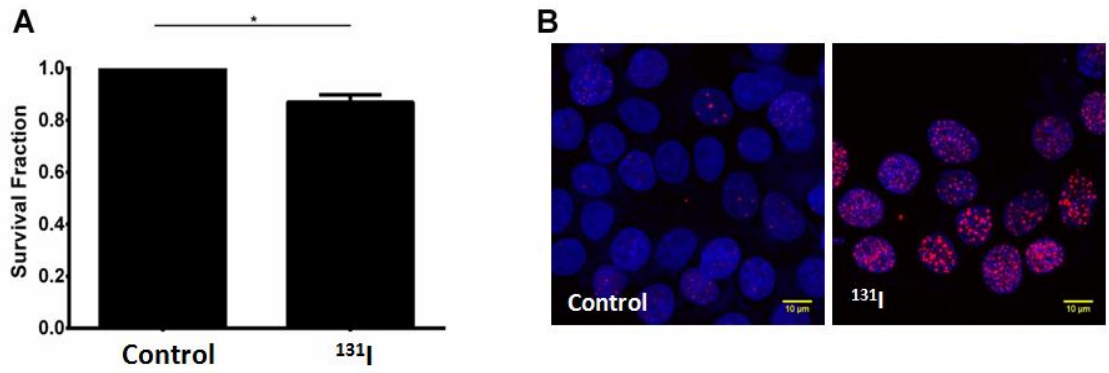

Figure 4.15 *^{131}I toxicity assay in ZR-75-1 clone1 cells* ***A.*** *Clonogenic assay shows significant decrease in survival fraction post ^{131}I therapy* ***B.*** *γH2A.X assay to detect DNA damage shows higher number of foci in the ^{131}I treated cells as compared to untreated cells. Scale bar represents 10µm.*

4.3. 6 Evaluation of radioiodide mediated therapeutic effect in NIS expressing tumour cell model by molecular imaging techniques

Before evaluation of radioiodide mediated toxicity in the BC xenograft model, it is important to understand the distribution of ^{131}I in the animal model. To do this we performed CLI to image the radiation emitted from the radioisotope molecule. As a process of standardization different doses of ^{131}I is added in 96 black well plate and CLI is performed using IVIS *in vivo* imaging system. We observe dose dependent increase in the signal intensity (**Figure 4.16A & B**). Further emission spectra was recorded from 200 and 100µCi ^{131}I and maximum average radiance was observed at 500 nanometre (**Figure 4.16 C**).

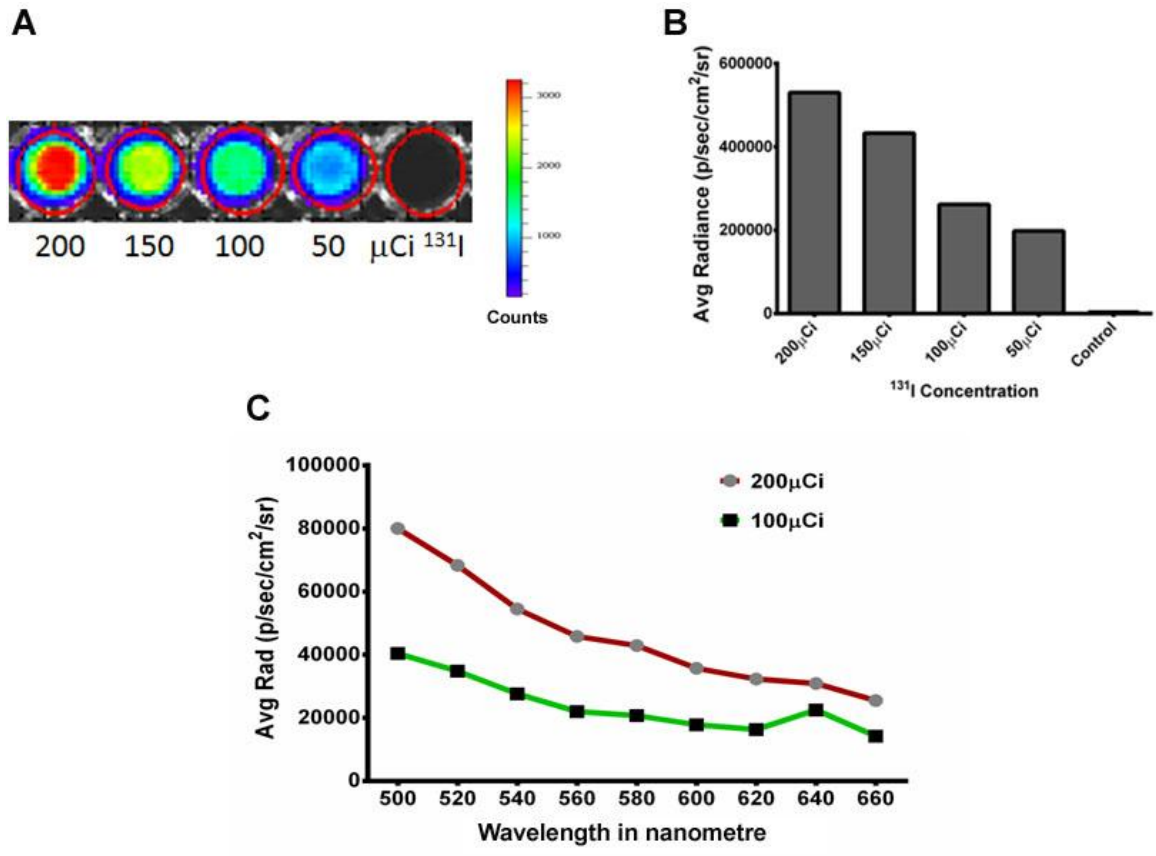

Figure 4.16 *Cerenkov luminescence imaging with ^{131}I* ***A.*** *Qualitative data showing Cerenkov luminescence signal obtained from ^{131}I. No signal is obtained from the control well in which ^{131}I was not added.* ***B.*** *Quantitation of signal intensity showing dose dependent decrease in Cerenkov*

*signal **C.** Spectral profile measured from various concentration of ^{131}I indicating peak at around 500 nanometre.*

Further to perform *in vivo* CLI, ZR-75-1 xenografted nude mice are injected with 1mCi of ^{131}I. Image acquisition after 24 hours of intra peritoneal injection with ^{131}I shows signal in the thyroid in the ventral scan (**Figure 4.17A**) and tumour in the dorsal scan suggesting possibility of using CLI in *in vivo* mice xenograft model. Signal is also obtained from stomach, which is due to NIS expression in gastric mucosa.

For *in vivo* evaluation of therapeutic potential of radioiodide treatment, $6x10^6$ NIS over-expressing ZR-75-1 cells (clone 1) are implanted for subcutaneous tumour growth in nude mice and when the tumour volume reached to a measurable size, we initiated ^{131}I therapy. Before starting ^{131}I therapy, thyroid of the control as well as treated group mice is blocked with T4 and methimazole and is continued further throughout the experiment. We observe that 6 days of thyroidal blocking do not show much effect in thyroidal iodine uptake but 14 days of blocking significantly reduces iodine uptake in thyroid (**Figure 4.17B & C**). Tumour bearing mice were randomized into 2 groups, control and ^{131}I treated. Based on the previous literature reports we treated tumour bearing mice with weekly dose of 1mCi ^{131}I for 3 weeks. Further CLI imaging after 24 hours of 1mCi ^{131}I injection (intra peritoneal) shows tumour specific accumulation where as thyroid is significantly blocked as no signal is detected from thyroid where as signal is obtained from stomach (**Figure 4.17 D**). We also performed CLI to check the retention of iodide in these tissues after 72 hours and observed that majority of iodide is effluxed from the tumour tissue but a faint signal is obtained from stomach (**Figure 4.17D**).

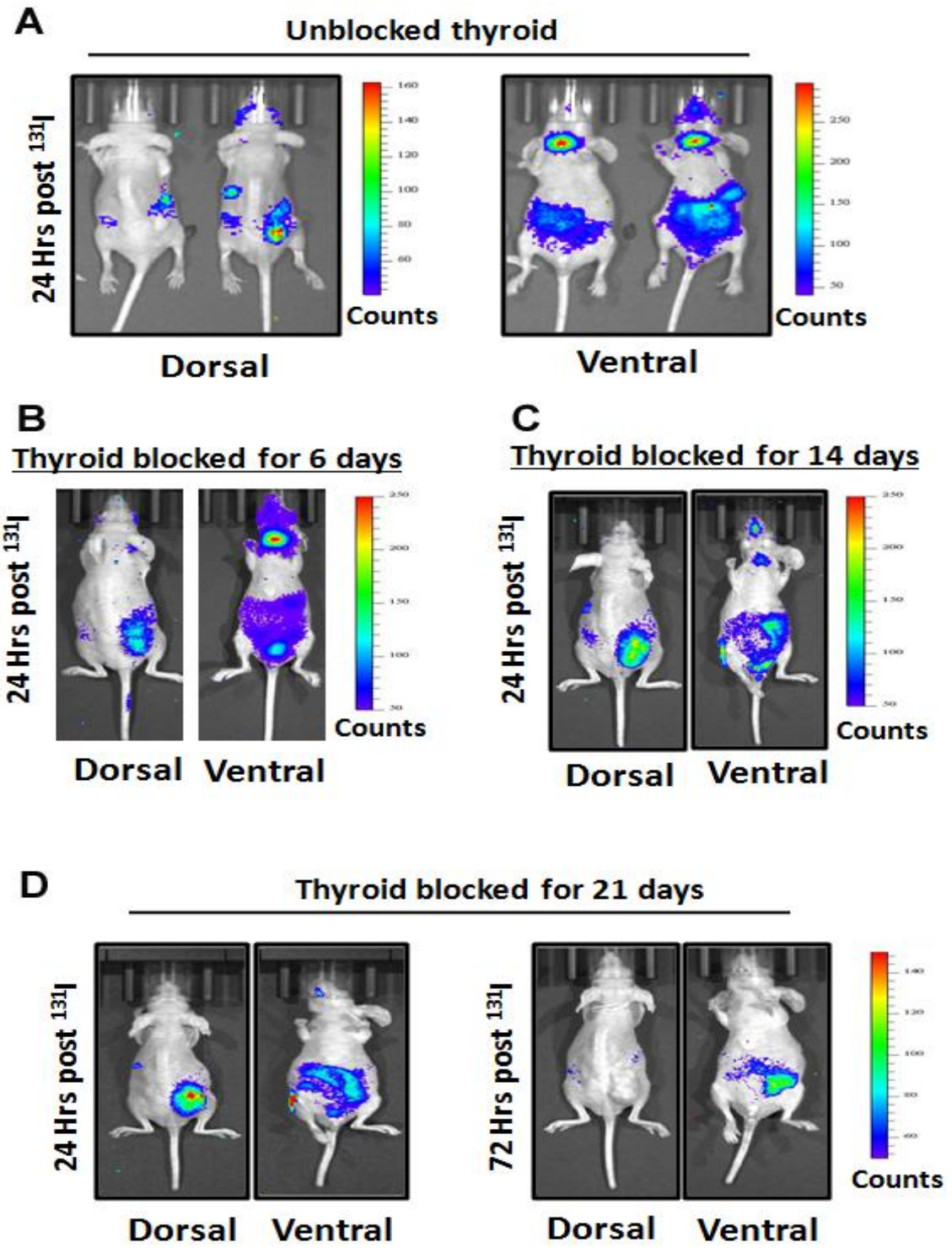

Figure 4.17 *In vivo Cerenkov luminescence imaging with ^{131}I in NIS expressing ZR-75-1 tumour bearing mice. Mice undergoing methimazole and T4 treatment were non-invasively monitored for ^{131}I distribution in tumour and thyroid. Mice were imaged after 24 and 72 hours of 1mCi ^{131}I intraperitoneal injection.* ***A.*** *Dorsal scan showing Cerenkov signal obtained from tumour. Ventral scan showing major signal from unblocked thyroid. Signal is also obtained from stomach*

and a very faint signal is noted in bladder. ***B.*** *CLI after 6 days of thyroid blocking shows signal in tumour as well as thyroid indicating insufficient blocking of thyroidal NIS.* ***C.*** *CLI after 14 days of blocking shows significant reduction in iodine uptake by thyroidal NIS.* ***D.****CLI after 21 days of continuous blocking of thyroidal NIS by T4 and methimazole. Imaging after 24 hours of* ^{131}*Itherapy shows major signal in tumour in dorsal scan. The ventral scan shows signal from stomach. No signal is obtained from thyroid showing significant blocking of thyroidal NIS by T4 and methimazole. Imaging procedure repeated after 72 hours of* ^{131}*I therapy shows absence of iodide from tumour tissue however a faint signal is obtained from stomach.*

To monitor the efficacy of radioiodide therapy BLI is performed and quantification of the luminescence signal shows that in the control group there is continuous increase in the signal intensity over 3 weeks, which remains constant till 5 weeks (**Figure 4.18A**). However in the treated group luminescence signal intensity was decreased after 2 weeks of therapy and it reduced further after 3 weeks, indicating tumour regression by radioiodide treatment. After 3 weeks of treatment mice are followed for 2 more weeks and it is observed that the tumour size remains the same in 4th week but a slight increase in the luminescence intensity was observed at the end of 5th week in the treated group (**Figure 4.18B**).

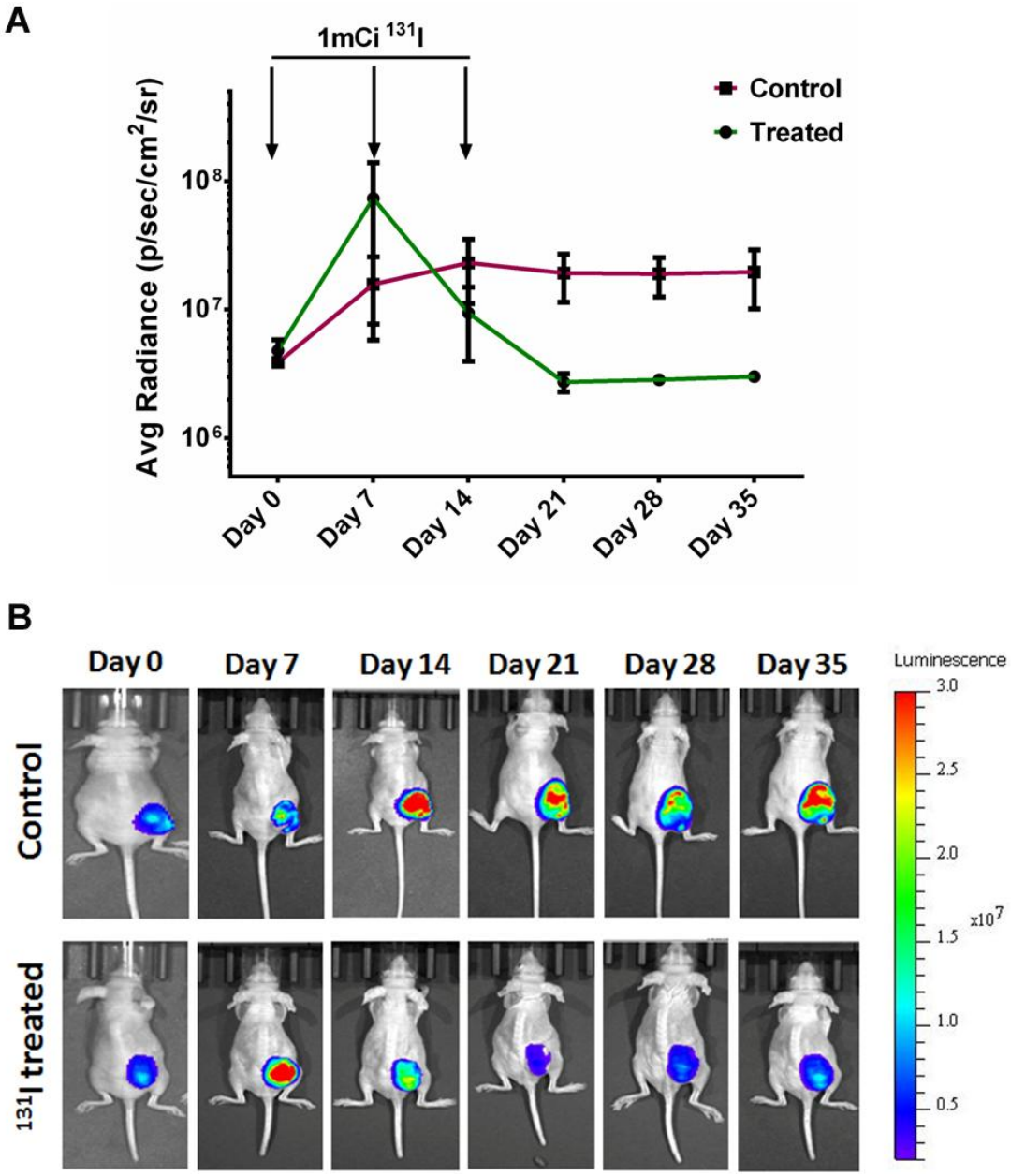

Figure 4.18 *In vivo BLI with ^{131}I in ZR-75-1 NIS over-expressing tumour bearing mice to evaluate therapeutic efficacy of radioiodide. The mice in the treated group (n=3) were injected with weekly dose of 1mCi ^{131}I for 3 weeks. BLI was performed weekly prior to the therapy.* ***A.*** *Quantitation of the bioluminescence signal to evaluate the effect of radioiodide on tumour size. The graph shows regression in the tumour volume after 2 doses of ^{131}I therapy in the treated group. In the control group constant increase in the size of the tumour is noted.* ***B.*** *BLI images of tumour bearing mice showing increased signal in the tumour tissue of control mice over different weeks where as the signal obtained from the treated tumour is reduced after ^{131}I therapy.*

4.4 Discussion

In the present study we have developed NIS over-expressing BC cell model. We have thoroughly validated NIS gene expression and its function in terms of cellular iodide uptake and toxicity by *in vitro* assays. Further, we have also evaluated the therapeutic efficacy of ^{131}I using ZR-75-1 NIS over-expressing mice tumour xenograft by non-invasive imaging methods.

We used attB based plasmid vector system for stable integration of NIS gene in BC cell lines. This integration system is significantly more efficient and specific than the other available alternatives[212]. Co-transfection of the attB containing plasmid vector together with the integrase vector also ensures site specific integration of the gene of interest instead of random integration observed with retro/lentiviral vectors. Our study for the first time used attB based plasmid vector system for NIS gene expression and we observe high and stable gene expression in long term culture.

We used a dual expressing plasmid vector that expresses both the therapeutic gene (human NIS) and a bifusion reporter gene Turbofp. Fluc2. At present there are several strategies available to link a therapeutic gene with a reporter gene expression. Few of these strategies include bidirectional promoter, same vector with independent promoter, peptide 2A based linking and bicistronic transcripts with IRES sequence expressed from the same promoter[213-219]. Each method has its own advantages and disadvantages. The major concern for successful non-invasive monitoring of the therapeutic gene through reporter gene is the close association of therapeutic gene expression with the quantitative measurement of the reporter gene[140]. In the present study we used EMCV-IRES (encephalomyocarditis virus IRES) for linking both the genes, which showed a good correlation of luciferase expression with the intensity of NIS expression in MCF-7 BC cell clones established.

An interesting observation during development of the stable cell clones using MCF-7 was that transfection with the customized expression plasmid (pattBCAG-NIS-IRES-Turbofp Fluc2) lead to generation of two different clonal variant where the populations of cells either represents NIS in the cytoplasm or in the plasma membrane. Over long term culture where cells undergo several passages, NIS protein expression was found to maintain respective cellular location in clone specific manner. The frequency of cells showing distinct membrane expression was very low which is also observed in patient tumour samples as discussed in Chapter 2. Such observation heightened our curiosity to investigate the cellular factors that may play important role in NIS localization, where we hypothesized that perhaps heterogeneous cellular glycosylation processes are responsible for this differential behavior in NIS protein localization. Western blot analysis data suggested that there is difference in the intensity of completely glycosylated form of NIS between membrane and cytoplasmic NIS expressing clones. This observation is further supported by glycosylation array data which shows that many of the enzymes involved in the process of glycosylation are upregulated in the membrane NIS expressing clones. Taken together our data suggests that glycosylation appears to play an important role in membrane targeting of NIS; however further studies will be required to validate this observation, which is out of scope for the current study objectivities. Previous literature suggests that NIS is glycosylated at 3 amino acids located on the extracellular domains near carboxy terminus, but there are contradicting reports indicating NIS membrane targeting may or may not be glycosylation dependent[81,141,220].

Staying focused on our study to prove that iodine transporter expressed is functional or not, we performed uptake assay and observed that even when NIS is localized in cytoplasm there is iodide uptake at a very low scale. The reason for iodide pumping in cytoplasmic NIS expressing clones may be due to weak NIS expression at the membrane

which is beyond the detection limit by immunofluorescence assays or possibly due to abundant cytoplasmic NIS staining, membrane staining is difficult to judge. However when NIS is expressed at the membrane, significant amount of iodide is concentrated inside these cells, which can be specifically inhibited by potassium perchlorate treatment showing specificity of NIS for transport of iodide inside the cells. Since BC cells lack the ability to organify iodide we observe that majority of iodide is effluxed out within 15 minutes of incubation. Further to validate if the iodide concentrated for such a short time window is sufficient to cause cytotoxicity in these cells or not, we performed toxicity assays. Our data from clonogenic as well as apoptosis in MCF-7 cells suggests significant cell death in ^{131}I treated cells as compared to untreated cells.

Since MCF-7 NIS expressing cells did not show tumour formation in the nude or SCID mice available to us, we developed NIS over-expressing BC model using ZR-75-1 cells, which shows tumourigenic ability. All the NIS transfected ZR-75-1 cells however showed cytoplasmic localization of NIS with low iodide uptake capacity suggesting weak NIS expression at the membrane which was not resolved by immunofluorescence microscopy. Further, *in vitro* cytotoxicity data suggests low but significant cell death after ^{131}I therapy. We therefore developed mouse xenograft model using NIS over-expressing ZR-75-1 cells in which we tested the ability of NIS mediated radioiodide therapy for tumour regression.

Recent advances in the field of non-invasive MI allows optical imaging instruments to be used for imaging of visible range photons (luminescence) produced by radioactive materials[132,133,136]. We performed CLI to visualize the tissue distribution of ^{131}I after 24 hours of intra-peritoneal injection and observed accumulation of radioiodide in the tumour. The major signal was observed in the thyroid and in addition to thyroid, signals were also obtained from stomach and bladder. Blocking the thyroidal NIS with T4 and methimazole for 14 days showed significant decrease in thyroidal radioiodide uptake.

Thyroid blocking is an important aspect to achieve in case of radioiodide therapy to the extra thyroidal tissue as it helps in minimizing exposure of thyroid to the radioactive compound and at the same time increases the probability of better uptake in the non-thyroidal NIS expressing tissues. For evaluation of tumour inhibition after ^{131}I administration, we co-expressed the luciferase reporter gene with NIS and performed BLI. BLI provides a relative measure of the tumour volume and is a very useful tool for non-invasive, serial monitoring of the same animals over long duration of treatment period. We observe decrease in the bioluminescence signal in the treated mice after 2 doses of 1mCi ^{131}I, which decreased further after the 3rd dose of ^{131}I as compared to untreated mice.

Previously reported clinical trials with NIS based radioiodide imaging in BC patients has shown positive uptake in a very few cases and it has been suggested that mere presence of NIS in BC would not be sufficient to produce a therapeutic effect, since these tissues lack the ability to organify iodide and therefore the biological half life of the radioisotope in breast tissue is short. Herein, use of dual imaging modalities demonstrated distribution of radioiodide by CLI and radioiodide mediated tumour regression by BLI. These observations provide insights into the pattern of radiotracer distribution non- invasively and also provide information on time course of radiation effects in human BC xenograft treated with ^{131}I. In our study with the NIS expressing BC xenograft model, we do observe significant regression in the tumour growth in animals treated with ^{131}I. We performed *in vivo* experiments with ZR-75-1 NIS expressing cells, which shows localization of NIS predominantly in the cytoplasm. At this point, we do expect that NIS based radioiodide therapy may prove to be more effective where the protein is predominantly represented on the cell membrane, resulting in abundant intake of the radioactive molecule and thereby higher toxicity. It is also evident from our *in vitro*

toxicity data which shows higher toxicity in MCF-7 NIS expressing cells as compared to ZR-75-1 NIS expressing cells after ^{131}I therapy. It is quite possible that this difference in the toxicity profile is due to the distinct difference in the localization of the transporter molecule. Thus there is a need to explore the strategies that can direct membrane targeting of NIS molecule. Various compounds including retinoic acid and HDAC inhibitors have been shown to induce NIS expression in breast cancer cells resulting in increased iodine uptake[152,221]. In addition to this, June et al. reported membrane targeting of NIS by EGF treatment in BC cells, which is through activation of MAPK pathway[222]. However, EGF treatment in breast cancer patients is not suitable as it may activate plethora of signalling pathways. Therefore it is important to investigate the compounds and strategies that can target NIS to the membrane in BC cells and also have potential to be translated in the clinic. The present study provides an excellent experimental cell model that can be applied to test the compounds which modulates localization of NIS.

Nevertheless some additional consideration can be taken into account for improvement of this therapy. One of the factors that can be considered is use of other radioisotopes with higher energy emissions that are also transported by NIS, could potentially boost the efficacy of the regime. Both ^{188}Re and ^{211}At have been shown to deliver approximately five times the dose of radiation delivered by ^{131}I to NIS expressing tumours. The other approach could be use of radio sensitizer molecules to enhance local radiation effect in the BC cells, which has been experimented in the following chapter.

Effect of 2-DG and metformin as radio sensitizers for increased radioiodine mediated DNA damage in NIS expressing breast cancer cells

5.1 Introduction

The unique function of NIS to transport iodide into thyroid cells and its success in clinic for radioiodine mediated thyroid cancer ablation has lead to the proposal and testing of exogenously induced NIS expression in non-thyroidal cells for radioiodine ablation treatment[196,223-225]. Such studies in BC are promising but still clinical application's result prompted requirement of more studies to improve radioiodine based therapeutic efficacy, specificity and safety. In the earlier chapters we have delineated NIS expression in BC tissues and its potential as a target for radioiodine therapy in experimental BC model[1,5,226,227]. The major reason for insufficient iodide uptake observed in these tissues is believed to be due to intracellular localization of NIS protein and lack of proper iodide organification system in these cells[1,5,4,6,9]. These discrepancies widen the scope of multiple studies which have focussed on modulating the expression level of NIS with agents such as retinoic acids and HDACs before ^{131}I therapy[142,228,229]. Another strategy that is still unexplored is to enhance the ^{131}I treatment efficacy itself by using radio sensitizer drugs. Use of radio sensitizers may enhance cytotoxicity of ^{131}I therapy in case of a very low iodine uptake when NIS expression is low. At the same time with the use of radio sensitizers a lower concentration of ^{131}I can be used when NIS expression is high, which may benefit by minimizing the side effects of radiation in other NIS expressing tissues where entry of radioiodine can't be avoided. Further, without the presence of a defined iodide organification mechanism in BC cells, radio sensitizers may enhance radio-ablative effect even during the short presence of ^{131}I inside these cells enhancing DNA damage and cell death. Since radiation therapy is known to show cytotoxicity via free radical mediated oxidative damage, it has been proposed that combining radiation therapy with agents that cause oxidative stress induced injury may sensitize cells to the cytotoxic effect of radiation [230,231].

One of the radio sensitizer that causes oxidative stress and used during this study is 2-deoxy glucose (2-DG). 2-DG is a glucose analog that competes with glucose for entry in to glycolytic pathway. It is converted to phosphorylated 2-DG by hexokinase, which gets trapped inside the cell and inhibits hexokinase [232]. Thus 2-DG treatment causes a glucose deprived state preferentially in the cancer cells resulting reduced output from glycolysis and pentose phosphate pathway. Selective effect of 2-DG in cancer cells is due to several metabolic alterations in these cells including increased expression of GLUT transporters[233]. Recently 2-DG has been shown to function as a radio sensitizer in many reports[234-247]. The possible mechanism is that 2-DG mediated glucose deprivation results in increased pro-oxidant production and profound disruption in thiol metabolism, inducing an oxidative stressed state [248-250].

The other radio sensitizer used in the present study is metformin, which is a biguanide drug, well known for its use in the treatment of hyperglycemia and type 2 diabetes. Recent reports suggest association of metformin to low risk of BC in diabetic patients[251-256]. Various studies suggest that metformin inhibits proliferation of a great range of cancer cells[257-264]. It induces apoptosis in certain cancer cell lines and has also been reported recently to target cancer initiating cells[265]. Mice model studies using metformin has also been shown to reduce tumor growth in breast, colon and prostate cancer[228,257,266,267]. The mechanism of metformin action involves lowering the level of insulin and LKB1 mediated activation of AMPK and reduction in mTOR signalling [268,269]. Since radiation activates AMPK , metformin enhances radiation induced AMPK activation and cancer cell death [270-272]. Recently in a report metformin has been successfully used as a radio sensitizer for BC cells and showed eradication of radioresistant cancer stem cells by activating AMPK and suppressing mTOR[273].

To date, this is the first study to show the combination of 2-DG and metformin as radio sensitizers for enhancement of Cobalt60 or ^{131}I radio-ablative effect on the cancer cells. We focus on combining the two radio sensitizer drugs against the two different radiation exposure methods and measure the benefit using BC cells. We show that a combination of metformin and 2-DG along with Cobalt60 radiation or NIS mediated ^{131}I radiation shows significantly enhanced cytotoxicity.

5.2 Materials and Methods

5.2. 1 MTT assay

5000 cells/well were seeded in 96 well plate. Cells were allowed to adhere overnight before they were treated with mentioned drug doses of metformin or 2-DG. After 48 hours of treatment, cell viability was measured by MTT assay and data is represented as percentage cell viability as compared to the untreated cells.

5.2. 2 Drug treatment

All the drug treatments were given 12 hours before the ^{131}I treatment/radiation therapy and were replaced by plain medium after 12 hours of ^{131}I treatment, and assay was performed after 24 hours of the treatment.

5.2. 3 ATP measurement

Total cellular ATP was determined by using manufactured recommended protocol of Luciferase based ATP detection kit (FF2000, Promega). Total ATP was measured after 24 hours of radiation or ^{131}I therapy.

5.2. 4 Statistics

Data is presented as mean +/- standard error. Student's t-test was used to judge the significance of difference. All tests were two sided and $p < 0.05$ was considered as significant. Graph pad Prizm software was used for all the statistical analysis.

5.3 Results

5.3. 1 Effect of 2-DG and metformin combination on tumor cell ablation upon Cobalt60 radiation treatment

To determine the cytotoxic effect of 2-DG and metformin, BC cell lines are first exposed to various concentrations of these two drugs ranging between 0.1-100 mM and viable cell count was measured by MTT assay (**Figure 5.1**).

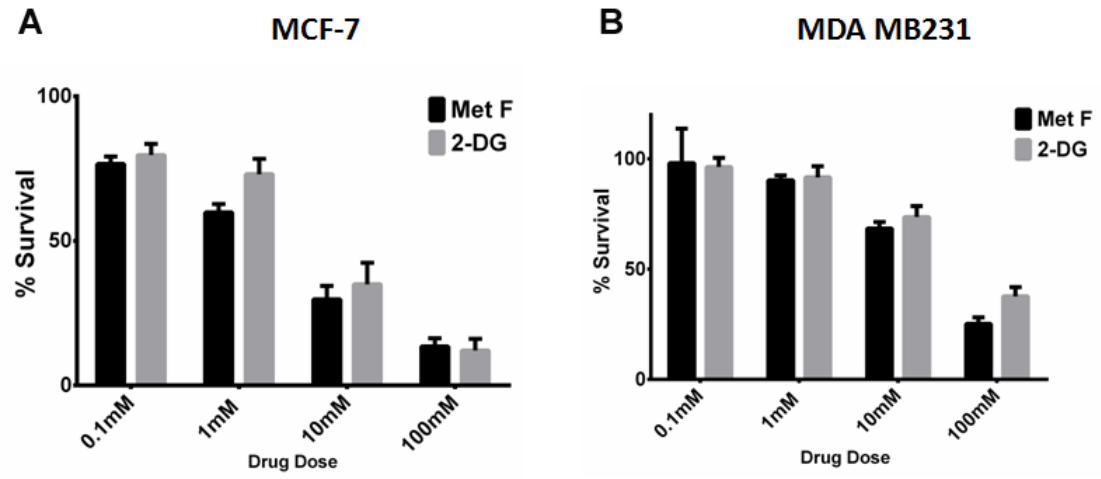

Figure 5.1 *Cytotoxic effect of 2-DG and metformin in **A**. MCF-7 and **B**. MDA MB 231 BC cell lines*

Further, based on the MTT data 10-50 mM dose of 2-DG and 2-10 mM dose of metformin is combined with 1 or 2 Gy Cobalt60 radiation to determine the minimal optimum drug dose required for maximum radiosensitization and cell survival analysis is performed by clonogenic assay in MCF-7 cells. We observe a combination of 20mM 2-DG with 1 Gy reduces 2 fold cell survival as compared to 1 Gy radiation alone, while it's combination with 2 Gy radiation shows 1.6 fold decrease in cell survival than radiation alone (**Figure 5.2A**). Further increment in 2-DG dose does not show any significant enhancement in radiosensitization effect. Similarly, treatment of cells with metformin shows dose dependent radiosensitization effect (**Figure 5.2B**). Combination of 2mM metformin with 1 Gy radiation dose shows 1.5 fold decrease in cell survival as

compared to 1 Gy radiation alone while the combination of 2 mM metformin with 2 Gy radiation results in 1.9 fold decrease in cell survival as compared to 2 Gy radiation alone.

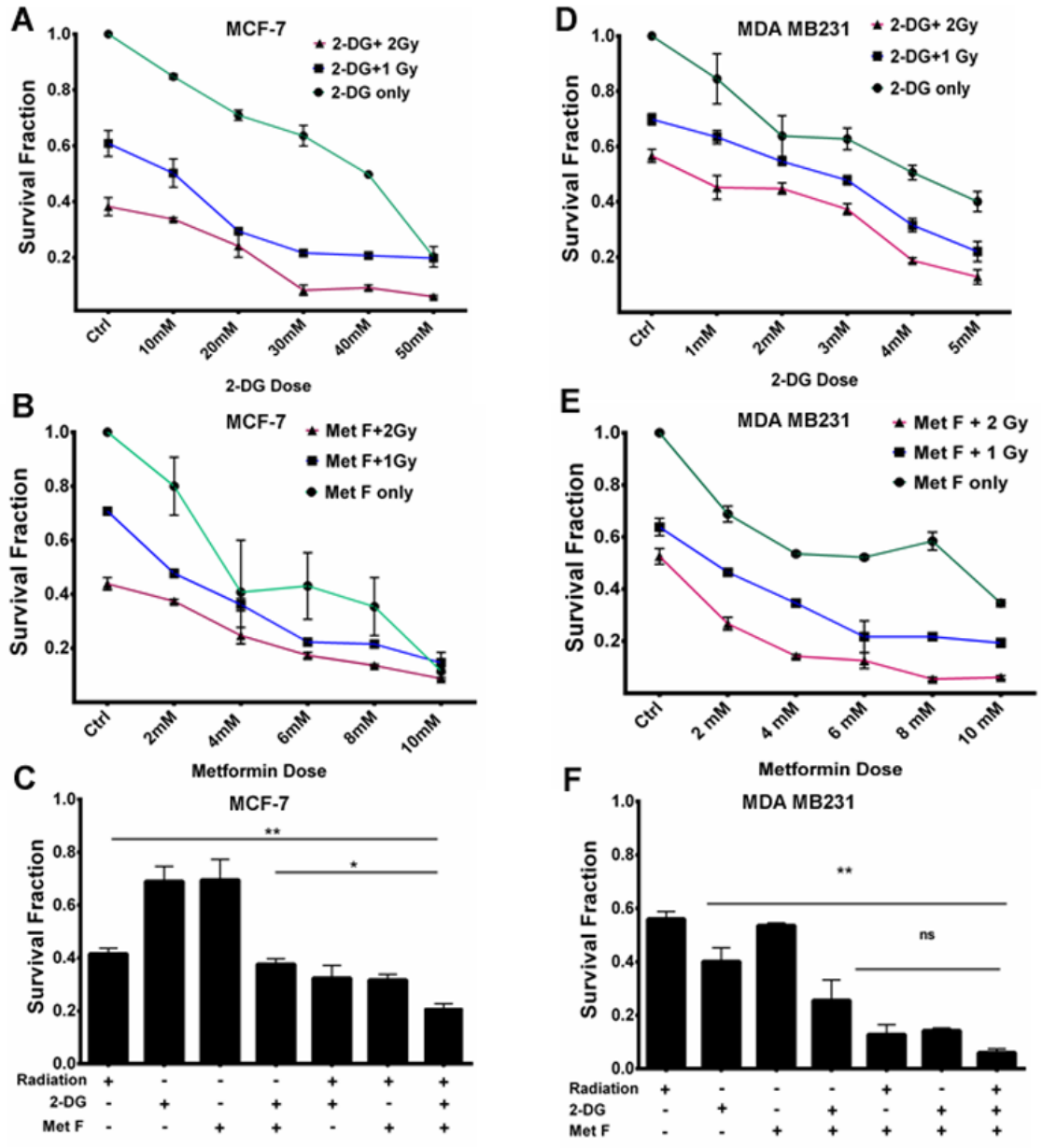

Figure 5.2 *Effect of 2-DG, metformin and their combination with Cobalt60 radiation on MCF-7 and MDA MB231 cells.* ***A*** *Graph showing survival fraction of MCF-7 cells treated with different doses of 2-DG in presence or absence of radiation* ***B.*** *Survival fraction of MCF-7 cells treated with different doses of metformin with or without radiation exposure* ***C.*** *Combination of 20mM 2-DG and 2mM metformin with 2 Gy radiation dose showing further decrease in survival fraction* ***D & E.*** *Survival fraction of MDA MB231 cells treated with different dose of 2-DG or metformin*

respectively with or without radiation exposure for 24 hours ***F.*** *Combination of 5mM 2-DG and 4mM metformin with 2 Gy radiation dose showing further decrease in survival fraction.*

Upon deciding the effective minimal drug doses, we also combined both the drugs and tested in combination with 2 Gy Cobalt60 radiation. Cell survival shows significant drop in cells treated with dual drug radiosensitization to that of cells treated with radiation alone (p=0.0094, CI=95%) (**Figure 5.2C**). In addition to MCF-7 cells, the effect of radio sensitizers on Cobalt60 radiotherapy in MDA MB231 cells has also been evaluated. In MDA MB231 cells 4mM metformin and 5mM 2-DG dose shows radiosensitization with 1Gy as well as 2 Gy radiation dose (**Figure 5.2D & E**). Further combination of both the drugs with 2 Gy radiation shows significant decrease in cell survival as compared to 2 Gy radiation alone (p=0.0020, CI=95%) (**Figure 5.2F**).

5.3. 2 Effect of radio sensitizers on different prospects of irradiated cells

Further, γH2A.X foci assay is performed to ensure increased cell death is associated to increased DNA double strand break (**Figure 5.3A**) and quantification of the immunofluorescence images indicates increase in foci intensity in cells treated with drug for 12 hours followed by the measured radiation exposure as compared to cells treated with similar radiation dose alone (**Figure 5.3B**). In case of untreated cells or cells treated with drugs alone, foci formation is recorded as negligible. Since metformin and 2-DG therapy are known to reduce ATP content of the cell, we have also analyzed ATP content with or without drug treatment and observe a significant drop in cells treated with metformin (p=0.0058, CI=95%) where as this drop is not significant when cells are treated with 2-DG alone (**Figure 5.3C**). Further decrease in ATP content is noted when both the drugs are combined.

Cell cycle analysis is also performed at different time points after the combination therapy which reveals S phase arrest after 12 hours of treatment in combination as well

as in case of only radiation therapy **(Figure 5.4)**. It is also observed that after 24 and 48 hours of combination therapy cells remain arrested in S phase whereas in case of only radiation therapy this arrest is relieved at these time points indicating prolonged cytotoxic effect of combination therapy.

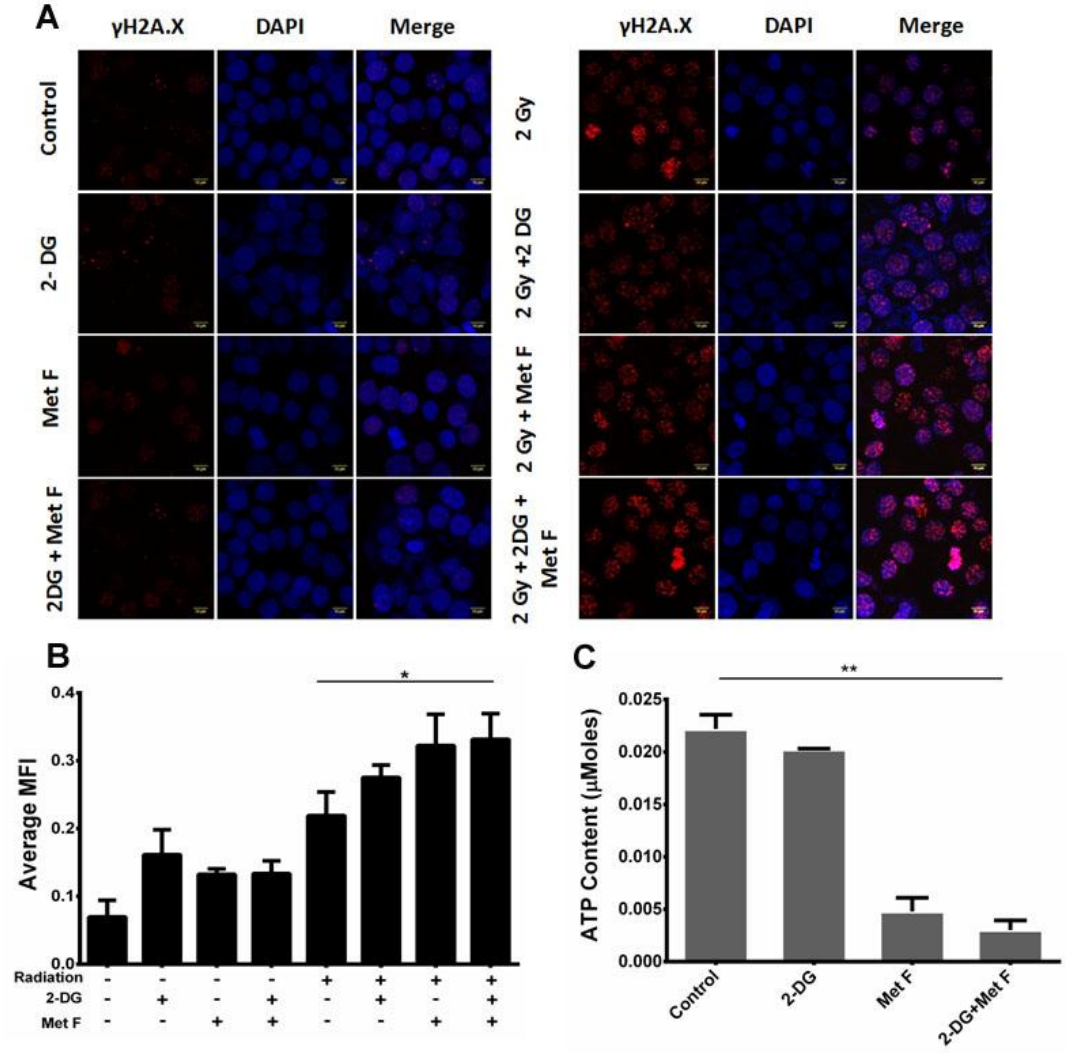

Figure 5.3 *Effect of cobalt 60 radiation in combination with radio sensitizers on DNA damage of MCF-7 cells* ***A.*** *Foci assay in cells treated with cobalt 60 radiation and combination with radio sensitizers showing foci staining with Dylight 633 secondary antibody in red channel, Nucleus stained with DAPI in blue channel and merged image showing co-localization of foci with nucleus. Scale bar represents 10µm* ***B****. Quantification of foci from the immunofluorescence images. In each sample 50 cells are quantified for intensity of staining from various fields of the cover slip.* ***C.*** *Metformin, but not 2-DG, treatment shows significant decrease in ATP content of the cells.*

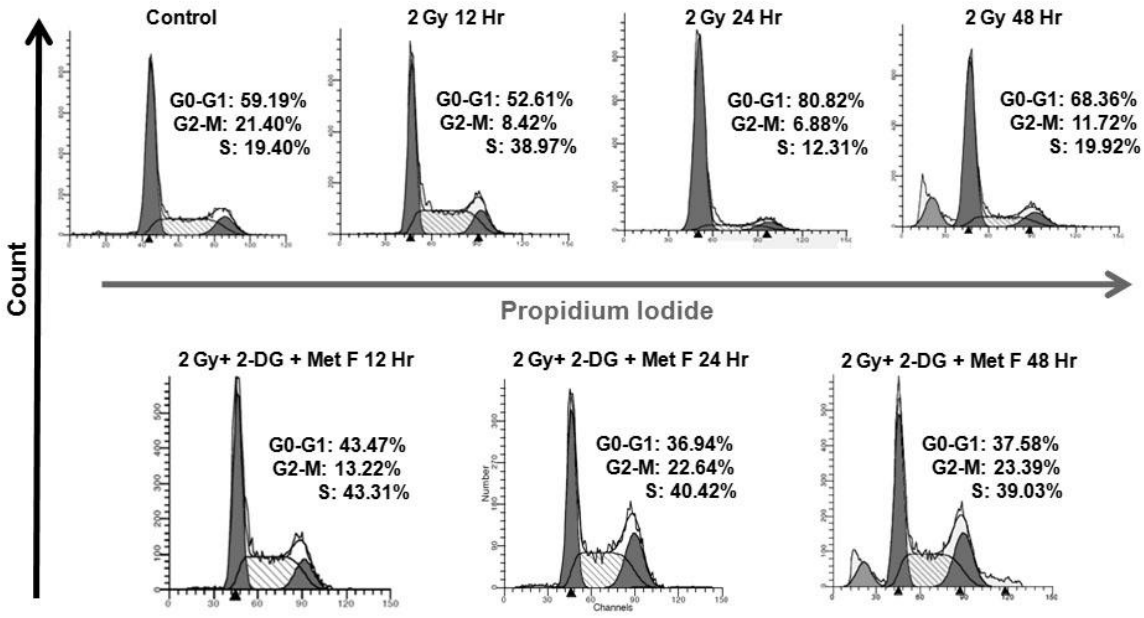

Figure 5.4 *Cell cycle status at different time points of treatment of MCF-7 cell. Data showing elongation of S phase in combination therapy after 48 hours of treatment. However, S phase elongation is not maintained till 48 hours when cells are treated with radiation alone.*

5.3. 3 Effect of 2-DG and metformin combination on treatment efficacy of radioiodine (^{131}I) in NIS expressing cells

The effective 2-DG and metformin dose of 20mM and 2mM respectively was tested prior with Cobalt60 radiation treatment. The similar treatment is applied in combination with ^{131}I radioisotope in NIS expressing cells (clone22 mentioned in the previous chapter). Treatment of cells with 100µCi of ^{131}I alone results in high number of cell death (data not shown) making radiosensitization effects obscure, a lowered concentration (50µCi) of ^{131}I is used for all the experiments. Combination of dual drugs with 50µCi ^{131}I shows 9.5 fold decrease in survival fraction when compared to the cells treated with ^{131}I alone (p=0.0019) and 4 fold decrease when compared with cells treated with the two drugs alone (p=0.0036) **(Figure 5.5A)**. The change in cell survival is further confirmed by Annexin-V staining to measure apoptosis in parallel **(Figure 5.5B)**. Cells are analysed for apoptosis after 48 hours of treatment and it is observed that live cell population is 37.37%

in case of ^{131}I therapy where as it is only 11% for the combination therapy. When cells are treated with both the drugs together in absence of ^{131}I 55.54% cells are live. Thus the combination of both the drugs with ^{131}I therapy in NIS expressing cells results in a significant drop in live cell population.

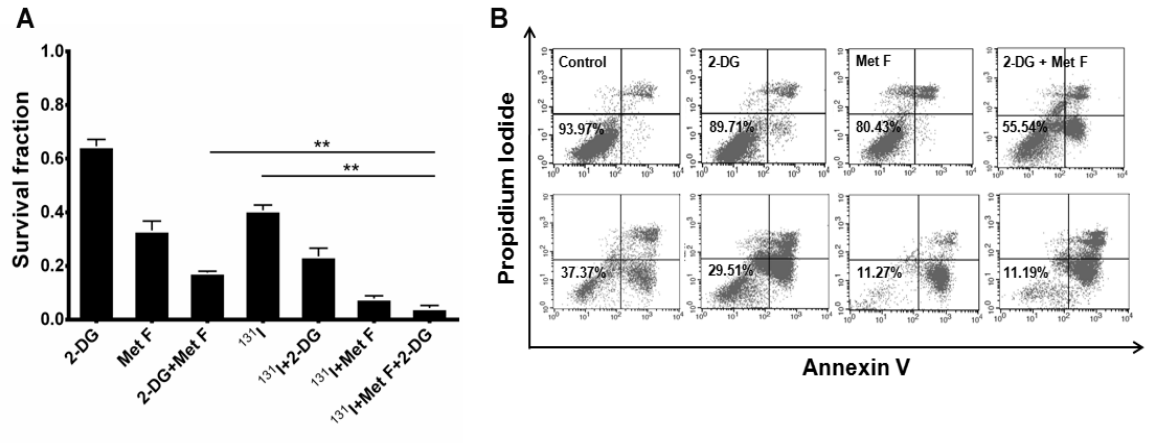

Figure 5.5 *Effect of 2-DG, metformin and their combination with ^{131}I treatment on MCF-7-NIS cell survival and apoptosis.* ***A.*** *Clonogenic assay in MCF-7-NIS cell population treated with 20mM 2-DG and 4mM metformin with or without ^{131}I (50µCi) for 24 hours. Graph showing significant decrease in survival fraction in case of combination therapy as compared to control or only ^{131}I treated cells* ***B.*** *Apoptotic assay showing significant decrease in live cell population in combination therapy than other treatment controls.*

5.3. 4 Effect of radio sensitizers in combination with radioiodine (^{131}I) on foci formation

Further γH2A.X foci immunofluorescence staining shows increase in number and intensity variation of foci in case of combined treatment, while in case of ^{131}I treatment alone the number and size of foci are much lower **(Figure 5.6)**. This result confirms that the combination of 2-DG and metformin can effectively radiosensitize BC cell and thus can be combined with either Cobalt60 radiation or NIS targeted radioiodine therapy.

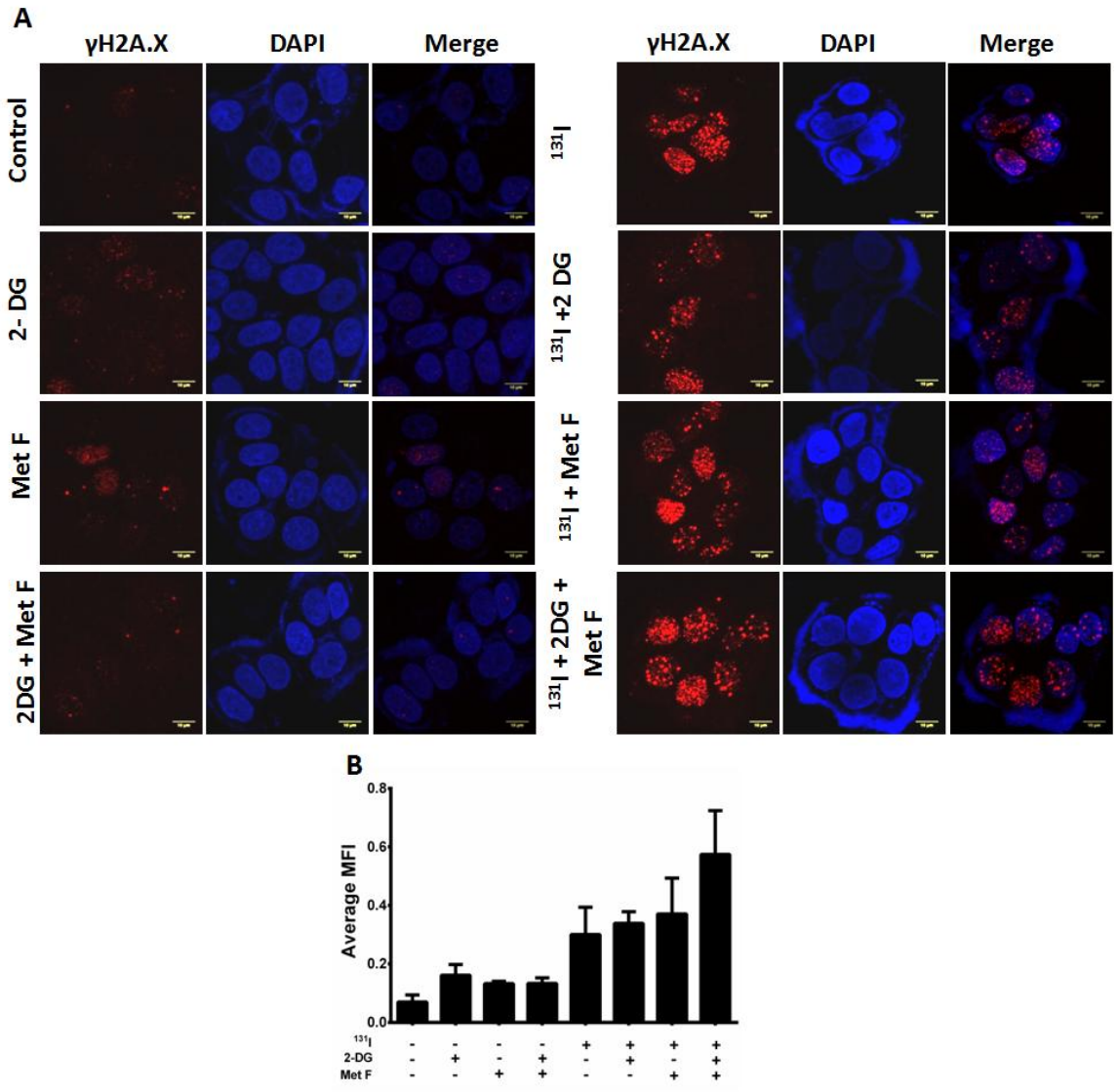

Figure 5.6 *Effect of ^{131}I in combination with radio sensitizers on DNA damage of MCF-7 NIS expressing cells* ***A.*** *Foci assay images of MCF-7 NIS cells treated with ^{131}I and its combination with radio sensitizers showing foci staining with Dylight 633 secondary antibody in red channel, Nucleus stained with DAPI in blue channel and merged image showing co-localization of foci with nucleus. Scale bar represents 10µm.* ***B****. Quantification of foci from the immunofluorescence images. In each sample 50 cells were quantified for intensity of staining from various fields of the cover slip.*

5.3. 5 Toxicity effect of radio sensitizers in combination with ^{131}I on plain MCF-7 cells with cytoplasmic NIS localization

Since in majority of the BC patients NIS expression is localized in the cytoplasm, it is important to evaluate the effect of radio sensitizers combined with ^{131}I in plain MCF-7 cells. Our data suggests that treatment with 50µCi ^{131}I results in 30% cell death (**Figure 5.7A**) as opposed to 60% death in case of MCF-7 NIS over-expressing cells. However addition of radio sensitizers to the ^{131}I therapy results in significant increase in cell death (70%) as compared to ^{131}I alone (p=0.0110, CI=95%). Thus combination therapy of ^{131}I with radio sensitizers in MCF-7 cells is as effective as ^{131}I therapy alone in MCF-7 NIS cells, where NIS is localized at membrane.

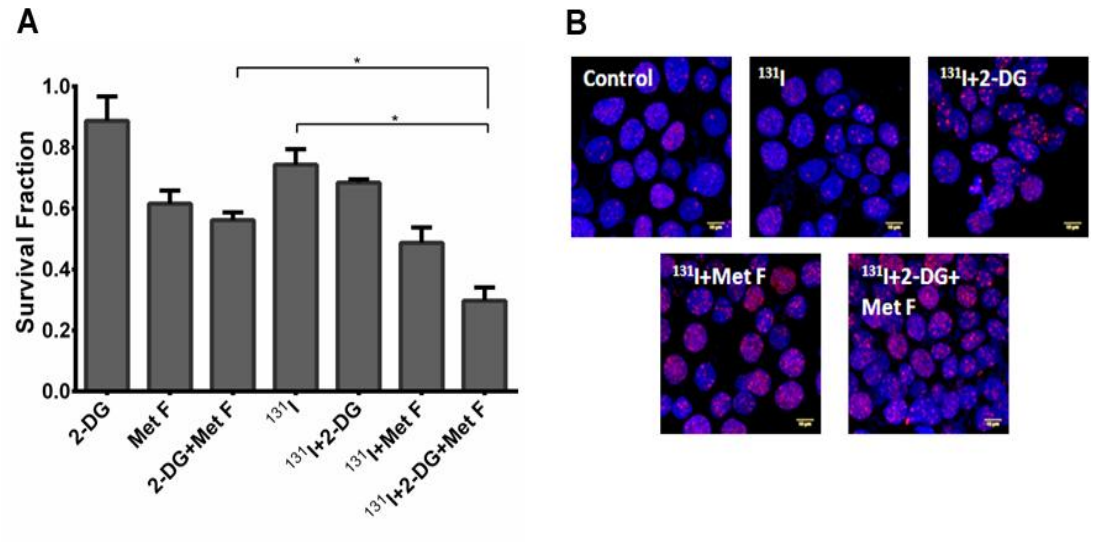

Figure 5.7 *Effect of 2-DG, metformin and their combination with ^{131}I treatment on survival of plain MCF-7 cells.* ***A.*** *Survival fraction of MCF-7 cells treated with 20mM 2-DG and 4mM metformin with or without ^{131}I (50µCi) for 24 hours. Treatment with ^{131}I alone shows only 30% decrease in cell survival, however its combination with 2-DG and metformin results in significant loss in live cell.* ***B.*** *Immunofluorescence analysis of γH2A.X foci showing increased expression in combination therapy than various treatment controls as marked. Scale bar represents 10µm. It is to be noted that the intensity and frequency of foci is lesser in MCF-7 plain cells as compared to MCF-7 NIS clonal population.*

We also performed γH2A.X assay to evaluate DNA damage response in plain MCF-7 cells in presence or absence of radio sensitizers (**Figure 5.7B**). Our data shows foci formation post ^{131}I therapy in plain MCF-7 cells. As expected the intensity of foci in MCF-7 plain cells (**Figure 5.7B**) is much less than the intensity in MCF-7 NIS cells (**Figure 5.6A**) undergoing the same treatment.

5.4 Discussion

In the present study we have tested 2-DG and metformin or a comination of the two to sensitize radio-ablative effect in BC cell and tested the cytotoxic efficacy in combination with different sources of radiation, i.e. Cobalt60 radiation or ^{131}I in NIS expressing MCF-7 cells. 2-DG treatment creates a glucose deprived state preferentially in cancer cells and output from glycolysis and pentose phosphate pathway is reduced. Metformin is a bi-guanide and anti-diabetic drug, which inhibits gluconeogenesis in liver and thus helps to control the sugar levels in diabetic patients. Previously, metformin was also known to inhibit proliferation of a large range of cancer cells by inducing apoptosis [257,258,260,263]. It has also been shown recently to target cancer initiating cells [265]. Individually the use of 2-DG and metformin has been reported as radio sensitizer [249,273,274], whereas the use of both in combination with low dose radiation (either from Cobalt60 source or NIS gene targeted ^{131}I) shown for first time during this study indicating much enhanced radio-ablative effect than either of the drugs alone. To avoid drug toxicity at higher doses we used very low dose of these drugs as radio sensitizers, as evident from MTT assay. We observe nearly 2-fold decrease in survival fraction upon 2mM metformin treatment in combination with 2Gy radiation as compared to radiation alone which corroborates with the earlier study by Song *et al.* where 5mM metformin showed radiosensitization effect in MCF-7 cells [273]. When 20mM 2-DG was combined with 2 Gy radiation dose we observed 1.6 fold decrease in cell survival as compared to radiation alone as was reported in a study by Lin

et al. [228]. The minor variation in our results may be due to differences in accurate drug dosing, timing of 2-DG and radiation dose. However, when we combine both 2-DG and metformin with 2 Gy radiation dose we observe a dramatic difference in cell survival, a nearly 3 fold decrease (p=0.0094, CI=95%) as compared to 2 Gy radiation alone. Combined drug treatment mediated cell death proved to be by significantly enhanced radiosensitization effect than any of the treatment.

Further, our study on γ-H2A.X foci formation suggests increase in the intensity of foci in case of dual-drug combined treatment than radiation alone, confirming radiosensitization by these agents. It is noteworthy here that cellular heterogeneity for foci formation encountered can possibly be explained by the presence of cells at different stages of cell cycle. Previous reports suggest the action of metformin and 2-DG is due to lowered ATP content of the cell. Metformin alters mitochondrial oxidative phosphorylation and 2-DG inhibits ATP synthesis through glycolysis. Therefore, we have also evidenced lowered ATP content of the cell in case of metformin or dual drug treatment, but not the 2-DG treatment. Further we looked into cell cycle status under different drug treatment conditions and observed that combined treatment results in elongation of S phase, this S phase elongation was also observed in case of radiation but was relieved after 48 hours of treatment whereas it remained nearly constant in case of combination therapy even at 48 hours.

Since 20mM 2-DG and 2mM metformin shows effective radiosensitization with Cobalt60 radiation, we maintained the similar dose and time points in experiments combining 2-DG and metformin with ^{131}I treatment in MCF7-NIS and plain MCF-7 cells. The use of 100µCi ^{131}I treatment alone resulted in complete cell death. Therefore, 50% lower dose of ^{131}I (i.e. 50µCi) was attempted which shows 1.5 fold decrease in survival fraction in MCF-7 NIS cells as compared to untreated cells. Thus for all the radioiodine therapy

experiments only 50µCi of ^{131}I was used. Even at this low radiation dose, the dual drug use for radiosensitization showed significant decrease in cell survival which is near-equivalent to the 2 fold higher dose (i.e. 100µCi alone) of ^{131}I. Apoptosis data corroborates with the result of clonogenic assay showing significant increase in apoptotic population with the addition of dual drug radio sensitizers. Since localization of NIS is crucial for ^{131}I therapy and various reports suggest cytoplasmic localization of NIS in breast tumor tissues, it is important to evaluate the potential of radio sensitizers with ^{131}I therapy in plain MCF-7 cells[275]. Our results indicate that although ^{131}I therapy alone shows minimal effect on cell survival, combination of radioiodine with radio sensitizers results in significant loss of live cell population in plain MCF-7cells. Thus the present study demonstrates the potential of metformin and 2-DG combination treatment as radio sensitizer in combination with Cobalt60 or ^{131}I radiation in NIS expressing cells. The combination can deliver better therapeutic efficacy than either of these drugs as a single agent. In addition to their drug toxicity, such radiosensitization effect may further boost mass reduction in cancer cases. To note, at present there are ongoing clinical trial with both these drugs either in combination with chemotherapy or radiation[276,277]. Thus combination of 2-DG and metformin with Cobalt60 radiation might play even more important role in sensitizing radioresistant population as was observed previously with combination of metformin and radiation [273]. Previous report suggests that combination of metformin and 2-DG induces p53 dependent apoptosis in prostate cancer cells through AMPK pathway and metformin inhibits 2-DG induced autophagy in these cells [278]. In future, it will be interesting to understand how these mechanistic pathways are regulated when Cobalt 60 radiation or ^{131}I is combined with these two drug combination. Further it would also be important to understand the effect of these drugs *in vivo* in combination with ^{131}I in NIS expressing breast tumour in preclinical and clinical settings.

In the present study we have shown the use of a combination of two radio sensitizers, 2-DG and metformin, to enhance the radio-ablative effect in combination with either cobalt60 radiation or targeted sodium iodide symporter mediated radioiodine therapy. The combination of the radio sensitizers improves therapeutic efficacy effectively in BC cell lines than any one of the radio sensitizer. Thus, in addition to the drug cytotoxicity, the radiosensitization effect may further boost effective mass reduction in pre-surgical cancer cases.

Summary

BC is a challenge to the currently available treatment regimes. Constant research efforts are hence being directed towards development of novel and efficacious targeted therapies for BC patients. One of the several targets under investigation is NIS. NIS is a membrane glycoprotein that mediates active transport of Na^+ and I^- in the thyroid follicular cells for synthesis of thyroid hormones, and is a major target for radioiodine therapy in thyroid cancer patients. NIS expression in malignant breast tissues, and lack of the same in normal breast; opens up exiting avenues for NIS mediated specific targeting of radioiodine to BC cells. Several studies have demonstrated NIS expression by IHC in 70-80% of BC patients[1,4]. However analysis of NIS expression with respect to breast epithelial subtypes may provide better insight of NIS biology in BC.

Therefore, we evaluated NIS expression in 181 randomly collected BC tissues and analyzed it's correlation with prognostic markers such as ER, PR and HER2, and risk factors like age and menopausal status. We observed upregulated NIS expression in 78% cases as compared to adjacent breast normal tissue used as control. A significant positive correlation of NIS with ER is observed, although association with other factors was not evident. The intensity of NIS expression in BC was equivalent to its expression in thyroid papillary carcinoma used as a positive control. Being a transporter molecule we anticipated its expression on the membrane but in majority of the BC tissues its expression is predominantly in the cytoplasm. Questioning the reliability of IHC technique to determine localization of NIS, we performed immunofluorescence in few tissue sections and observed that there are certain cases where NIS expression is evident at membrane by IF which also shows overlap with HER2 membrane staining whereas IHC with DAB staining in the same tissues showed intra cellular localization of NIS protein. This is a very important observation as it also explains the disparity between high

percentage of NIS positive BC cases but very few cases showing positive uptake of iodine in several earlier reports[2,4].

Additionally we analyzed NIS expression in 59 primary breast tumour tissues by quantitative real time PCR using TaqMan assays. Our results suggest upregulated NIS expression and positive correlation between NIS and ER at the transcript level. At present our knowledge regarding correlation between NIS protein and RNA level, that may enhance our understanding of its regulation, is limited. More investigation may help in establishing an appropriate technique for analyzing NIS expression in BC pathology before the translation of this therapeutic modality to clinic. In a small sample cohort (n=20) we observe a significant positive correlation of NIS RNA and protein levels (R^2=0.6964). We have also evaluated NIS expression in 20 fibroadenoma samples by IHC and our data corroborates with previous smaller studies which show increased NIS expression in fibroadenoma samples as compared to malignant breast tissue[3,146]. Presence of NIS in fibroadenoma tissues makes it clear that endogenous NIS expression in BC can not serve as a useful marker of breast malignancy.

Taking the study forward we developed a mammalian expressing plasmid vector for correlated expression of NIS and a reporter gene Turbofp. Fluc 2 through EMCV IRES mediated translation of the 2nd gene which is the fusion reporter gene. By transfection of this plasmid vector stably expressing MCF-7 and ZR-75-1 cells were established. Thorough analysis of the established cells showed consistent and correlated expression of the therapeutic and reporter gene over multiple passages. Extensive in detailed analysis of NIS expression in various clones showed 2 distinct clonal population of MCF-7 NIS expressing cells, 1 with evident membranous NIS staining and the another with predominantly cytoplasmic NIS staining. Interestingly the 2 distinct populations were developed by transfection of the same plasmid under identical condition. To find out the

factors responsible for difference in localization of NIS molecule, we first investigated the glycosylation status of NIS molecule from cells expressing it at membrane and cytoplasm. The western blot analysis suggested increased level of completely glycosylated form of NIS in the NIS membrane expressing cells. Further analysis of the glycosylation enzyme's status in the two clonal populations by quantitative real time PCR array suggested elevated expression of many glycosylation genes in the membrane NIS expressing clone, compared to cytoplasmic NIS expressing clone, indicating possible role of glycosylation in the efficient targeting of NIS protein.

NIS over-expressing MCF-7 and ZR-75-1 cell lines were characterized for *in vitro* iodine uptake and cytotoxicity assay. Significant loss in live cell population and radioiodine mediated DNA damage was observed with both the cell lines. To further evaluate the therapeutic efficacy of ^{131}I, subcutaneous human xenograft ZR-75-1 tumour was developed in nude mice. The bio-distribution of radioiodine was analyzed by performing *in vivo* CLI. Site specific localization of ^{131}I was observed in thyroid as well as in NIS expressing xenografted tumour. A significant reduction in thyroidal iodine uptake is seen after blocking thyroid with T4 and methimazole. This prevents damage to normal thyroid and increases radioiodine availability to the tumour tissue. Despite complete efflux of radioiodine from tumour tissue within 72 hours of ^{131}I therapy due to lack of iodine organification in breast cancer cells, we observe radioiodine mediated damage to the NIS expressing tumour cells, as evident from reduced bioluminescence signal obtained from the tumour of treated group of animals as compared to untreated group. Results of the BLI studies show that even the short retention time of radioiodine in BC cells result in significant abrogation of these cells.

As therapeutic potential of NIS in BC is often limited due to low uptake and fast efflux rate of iodine, the scope of using two radio sensitizers i.e. 2-DG and metformin to further

improve NIS mediated ^{131}I therapeutic efficacy was explored. Treatment of NIS expressing cells with ^{131}I showed further reduction in cell viability by the application of these radio sensitizers in combination.

Taken together, the aim of the study was to investigate NIS expression in various subtypes of BC and to evaluate its therapeutic efficacy in pre clinical experimental model. Our study suggests potential of targeted radioiodine therapy in BC patients. Results of the study, wherein ^{131}I and radio sensitizer were used in combination, opens up new possibilities of enhanced radioiodine treatment efficacy in BC cells over-expressing NIS protein. We believe that our study brings us one step closer towards understanding of NIS expression and its therapeutic application in BC.

Bibliography

1. Tazebay UH, Wapnir IL, Levy O, et al. The mammary gland iodide transporter is expressed during lactation and in breast cancer. *Nature medicine.* Aug 2000;6(8):871-878.

2. Renier C, Vogel H, Offor O, Yao C, Wapnir I. Breast cancer brain metastases express the sodium iodide symporter. *Journal of neuro-oncology.* Feb 2010;96(3):331-336.

3. Upadhyay G, Singh R, Agarwal G, et al. Functional expression of sodium iodide symporter (NIS) in human breast cancer tissue. *Breast cancer research and treatment.* Jan 2003;77(2):157-165.

4. Wapnir IL, Goris M, Yudd A, et al. The Na+/I- symporter mediates iodide uptake in breast cancer metastases and can be selectively down-regulated in the thyroid. *Clinical cancer research : an official journal of the American Association for Cancer Research.* Jul 1 2004;10(13):4294-4302.

5. Wapnir IL, van de Rijn M, Nowels K, et al. Immunohistochemical profile of the sodium/iodide symporter in thyroid, breast, and other carcinomas using high density tissue microarrays and conventional sections. *The Journal of clinical endocrinology and metabolism.* Apr 2003;88(4):1880-1888.

6. Renier C, Yao C, Goris M, et al. Endogenous NIS expression in triple-negative breast cancers. *Annals of surgical oncology.* Apr 2009;16(4):962-968.

7. Ryan J, Curran CE, Hennessy E, et al. The sodium iodide symporter (NIS) and potential regulators in normal, benign and malignant human breast tissue. *PloS one.* 2011;6(1):e16023.

8. Tandon A. Sodium iodide symporter, estrogen receptor, and progesterone receptor expression in carcinoma breast- An immunohistochemical analysis *Indian journal of pathology and microbiology.* 2011;54(4):745-751.

9. Moon DH, Lee SJ, Park KY, et al. Correlation between 99mTc-pertechnetate uptakes and expressions of human sodium iodide symporter gene in breast tumor tissues. *Nuclear medicine and biology.* Oct 2001;28(7):829-834.

10. Gholami S, Chen CH, Lou E, et al. Vaccinia virus GLV-1h153 in combination with 131I shows increased efficiency in treating triple-negative breast cancer. *FASEB journal : official publication of the Federation of American Societies for Experimental Biology.* Feb 2014;28(2):676-682.

11. Trujillo MA, Oneal MJ, Davydova J, Bergert E, Yamamoto M, Morris JC, 3rd. Construction of an MUC-1 promoter driven, conditionally replicating adenovirus that expresses the sodium iodide symporter for gene therapy of breast cancer. *Breast cancer research : BCR.* 2009;11(4):R53.

12. Montiel-Equihua CA, Martin-Duque P, de la Vieja A, et al. Targeting sodium/iodide symporter gene expression for estrogen-regulated imaging and therapy in breast cancer. *Cancer Gene Ther.* Jul 2008;15(7):465-473.

13. Ryan J, Curran CE, Hennessy E, et al. The Sodium Iodide Symporter (NIS) and Potential Regulators in Normal, Benign and Malignant Human Breast Tissue. *PloS one.* Jan 2011;6(1).

14. DeSantis C, Siegel R, Bandi P, Jemal A. Breast cancer statistics, 2011. *CA: a cancer journal for clinicians.* Nov-Dec 2011;61(6):409-418.

15. Ferlay J, Shin HR, Bray F, Forman D, Mathers C, Parkin DM. Estimates of worldwide burden of cancer in 2008: GLOBOCAN 2008. *International journal of cancer. Journal international du cancer.* Dec 15 2010;127(12):2893-2917.

16. Murthy NS, Chaudhry K, Nadayil D, Agarwal UK, Saxena S. Changing trends in incidence of breast cancer: Indian scenario. *Indian journal of cancer.* Jan-Mar 2009;46(1):73-74.

17. Anders CK, Johnson R, Litton J, Phillips M, Bleyer A. Breast cancer before age 40 years. *Seminars in oncology.* Jun 2009;36(3):237-249.

18. Fredholm H, Eaker S, Frisell J, Holmberg L, Fredriksson I, Lindman H. Breast cancer in young women: poor survival despite intensive treatment. *PloS one.* 2009;4(11):e7695.

19. Agarwal G, Pradeep PV, Aggarwal V, Yip CH, Cheung PS. Spectrum of breast cancer in Asian women. *World journal of surgery.* May 2007;31(5):1031-1040.

20. Dinshaw KA, Sarin R, Budrukkar AN, et al. Safety and feasibility of breast conserving therapy in Indian women: two decades of experience at Tata Memorial Hospital. *Journal of surgical oncology.* Aug 1 2006;94(2):105-113.

21. Mathew A, Pandey M, Rajan B. Do younger women with non-metastatic and non-inflammatory breast carcinoma have poor prognosis? *World journal of surgical oncology.* 2004;2:2.

22. Shavers VL, Harlan LC, Stevens JL. Racial/ethnic variation in clinical presentation, treatment, and survival among breast cancer patients under age 35. *Cancer.* Jan 1 2003;97(1):134-147.

23. Jemal A, Siegel R, Ward E, et al. Cancer statistics, 2008. *CA: a cancer journal for clinicians.* Mar-Apr 2008;58(2):71-96.

24. Mani SA, Guo W, Liao MJ, et al. The epithelial-mesenchymal transition generates cells with properties of stem cells. *Cell.* May 16 2008;133(4):704-715.

25. Onder TT, Gupta PB, Mani SA, Yang J, Lander ES, Weinberg RA. Loss of E-cadherin promotes metastasis via multiple downstream transcriptional pathways. *Cancer research.* May 15 2008;68(10):3645-3654.

26. Peinado H, Olmeda D, Cano A. Snail, Zeb and bHLH factors in tumour progression: an alliance against the epithelial phenotype? *Nature reviews. Cancer.* Jun 2007;7(6):415-428.

27. Zeleniuch-Jacquotte A, Afanasyeva Y, Kaaks R, et al. Premenopausal serum androgens and breast cancer risk: a nested case-control study. *Breast cancer research : BCR.* 2012;14(1):R32.

28. Bottom K OLM, Sheaffer BA, et al. Chapter 9: Breast Cancer2007.

29. Henson DE, Ries L, Freedman LS, Carriaga M. Relationship among outcome, stage of disease, and histologic grade for 22,616 cases of breast cancer. The basis for a prognostic index. *Cancer.* Nov 15 1991;68(10):2142-2149.

30. Bloom HJ, Richardson WW. Histological grading and prognosis in breast cancer; a study of 1409 cases of which 359 have been followed for 15 years. *British journal of cancer.* Sep 1957;11(3):359-377.

31. Elston CW, Ellis IO. Pathological prognostic factors in breast cancer. I. The value of histological grade in breast cancer: experience from a large study with long-term follow-up. *Histopathology.* Nov 1991;19(5):403-410.

32. Frkovic-Grazio S, Bracko M. Long term prognostic value of Nottingham histological grade and its components in early (pT1N0M0) breast carcinoma. *Journal of clinical pathology.* Feb 2002;55(2):88-92.

33. Reed W, Hannisdal E, Boehler PJ, Gundersen S, Host H, Marthin J. The prognostic value of p53 and c-erb B-2 immunostaining is overrated for patients with lymph node negative breast carcinoma: a multivariate analysis of prognostic factors in 613 patients with a follow-up of 14-30 years. *Cancer.* Feb 15 2000;88(4):804-813.

34. Dimri G, Band H, Band V. Mammary epithelial cell transformation: insights from cell culture and mouse models. *Breast cancer research : BCR.* 2005;7(4):171-179.

35. Parl FF, Schmidt BP, Dupont WD, Wagner RK. Prognostic significance of estrogen receptor status in breast cancer in relation to tumor stage, axillary node metastasis, and histopathologic grading. *Cancer.* Nov 15 1984;54(10):2237-2242.

36. Anderson WF, Chu KC, Chatterjee N, Brawley O, Brinton LA. Tumor variants by hormone receptor expression in white patients with node-negative breast cancer from the surveillance, epidemiology, and end results database. *Journal of clinical oncology : official journal of the American Society of Clinical Oncology.* Jan 1 2001;19(1):18-27.

37. Hilsenbeck SG, Ravdin PM, de Moor CA, Chamness GC, Osborne CK, Clark GM. Time-dependence of hazard ratios for prognostic factors in primary breast cancer. *Breast cancer research and treatment.* 1998;52(1-3):227-237.

38. Slamon DJ, Clark GM, Wong SG, Levin WJ, Ullrich A, McGuire WL. Human breast cancer: correlation of relapse and survival with amplification of the HER-2/neu oncogene. *Science.* Jan 9 1987;235(4785):177-182.

39. Slamon DJ, Godolphin W, Jones LA, et al. Studies of the HER-2/neu proto-oncogene in human breast and ovarian cancer. *Science.* May 12 1989;244(4905):707-712.

40. Seshadri R, Firgaira FA, Horsfall DJ, McCaul K, Setlur V, Kitchen P. Clinical significance of HER-2/neu oncogene amplification in primary breast cancer. The South Australian Breast Cancer Study Group. *Journal of clinical oncology : official journal of the American Society of Clinical Oncology.* Oct 1993;11(10):1936-1942.

41. Vogel CL, Cobleigh MA, Tripathy D, et al. Efficacy and safety of trastuzumab as a single agent in first-line treatment of HER2-overexpressing metastatic breast cancer. *Journal of clinical oncology : official journal of the American Society of Clinical Oncology.* Feb 1 2002;20(3):719-726.

42. Sorlie T, Perou CM, Tibshirani R, et al. Gene expression patterns of breast carcinomas distinguish tumor subclasses with clinical implications. *Proceedings of the National Academy of Sciences of the United States of America.* Sep 11 2001;98(19):10869-10874.

43. Perou CM, Sorlie T, Eisen MB, et al. Molecular portraits of human breast tumours. *Nature.* Aug 17 2000;406(6797):747-752.

44. Curtis C, Shah SP, Chin SF, et al. The genomic and transcriptomic architecture of 2,000 breast tumours reveals novel subgroups. *Nature.* Jun 21 2012;486(7403):346-352.

45. Weigelt B, Peterse JL, van 't Veer LJ. Breast cancer metastasis: markers and models. *Nature reviews. Cancer.* Aug 2005;5(8):591-602.

46. Page DL. Prognosis and breast cancer. Recognition of lethal and favorable prognostic types. *The American journal of surgical pathology.* Apr 1991;15(4):334-349.

47. Koscielny S, Tubiana M, Le MG, et al. Breast cancer: relationship between the size of the primary tumour and the probability of metastatic dissemination. *British journal of cancer.* Jun 1984;49(6):709-715.

48. Ross JS, Fletcher JA, Linette GP, et al. The Her-2/neu gene and protein in breast cancer 2003: biomarker and target of therapy. *The oncologist.* 2003;8(4):307-325.

49. Stathopoulou A, Vlachonikolis I, Mavroudis D, et al. Molecular detection of cytokeratin-19-positive cells in the peripheral blood of patients with operable breast cancer: evaluation of their prognostic significance. *Journal of clinical oncology : official journal of the American Society of Clinical Oncology.* Aug 15 2002;20(16):3404-3412.

50. Pierga JY, Bonneton C, Vincent-Salomon A, et al. Clinical significance of immunocytochemical detection of tumor cells using digital microscopy in peripheral blood and bone marrow of breast cancer patients. *Clinical cancer research : an official journal of the American Association for Cancer Research.* Feb 15 2004;10(4):1392-1400.

51. Braun S, Pantel K, Muller P, et al. Cytokeratin-positive cells in the bone marrow and survival of patients with stage I, II, or III breast cancer. *The New England journal of medicine.* Feb 24 2000;342(8):525-533.

52. Wiedswang G, Borgen E, Karesen R, et al. Detection of isolated tumor cells in bone marrow is an independent prognostic factor in breast cancer. *Journal of clinical oncology : official journal of the American Society of Clinical Oncology.* Sep 15 2003;21(18):3469-3478.

53. William Stewart Halsted (1852-1922). *CA: a cancer journal for clinicians.* Mar-Apr 1973;23(2):94-95.

54. Davies C, Godwin J, Gray R, et al. Relevance of breast cancer hormone receptors and other factors to the efficacy of adjuvant tamoxifen: patient-level meta-analysis of randomised trials. *Lancet.* Aug 27 2011;378(9793):771-784.

55. Greenspan EM, Fieber M, Lesnick G, Edelman S. Response of advanced breast carcinoma to the combination of the antimetabolite, Methotrexate, and the alkylating agent, thio-TEPA. *Journal of the Mount Sinai Hospital, New York.* May-Jun 1963;30:246-267.

56. Bonadonna G, Veronesi U, Brambilla C, et al. Primary chemotherapy to avoid mastectomy in tumors with diameters of three centimeters or more. *Journal of the National Cancer Institute.* Oct 3 1990;82(19):1539-1545.

57. Smalley RV, Carpenter J, Bartolucci A, Vogel C, Krauss S. A comparison of cyclophosphamide, adriamycin, 5-fluorouracil (CAF) and cyclophosphamide, methotrexate, 5-fluorouracil, vincristine, prednisone (CMFVP) in patients with metastatic breast cancer: a Southeastern Cancer Study Group project. *Cancer.* Aug 1977;40(2):625-632.

58. Ghersi D, Wilcken N, Simes J, Donoghue E. Taxane containing regimens for metastatic breast cancer. *The Cochrane database of systematic reviews.* 2005(2):CD003366.

59. Gregory RK, Smith IE. Vinorelbine--a clinical review. *Br J Cancer.* Jun 2000;82(12):1907-1913.

60. O'Shaughnessy JA, Kaufmann M, Siedentopf F, et al. Capecitabine monotherapy: review of studies in first-line HER-2-negative metastatic breast cancer. *The oncologist.* 2012;17(4):476-484.

61. Yardley DA. Activity of ixabepilone in patients with metastatic breast cancer with primary resistance to taxanes. *Clinical breast cancer.* Dec 2008;8(6):487-492.

62. Pean E, Klaar S, Berglund EG, et al. The European medicines agency review of eribulin for the treatment of patients with locally advanced or metastatic breast cancer: summary of the scientific assessment of the committee for medicinal products for human use. *Clinical cancer research : an official journal of the American Association for Cancer Research.* Sep 1 2012;18(17):4491-4497.

63. Chia SK, Speers CH, D'Yachkova Y, et al. The impact of new chemotherapeutic and hormone agents on survival in a population-based cohort of women with metastatic breast cancer. *Cancer.* Sep 1 2007;110(5):973-979.

64. Luu T, Chung C, Somlo G. Combining emerging agents in advanced breast cancer. *The oncologist.* 2011;16(6):760-771.

65. Jensen EV, Jordan VC. The estrogen receptor: a model for molecular medicine. *Clinical cancer research : an official journal of the American Association for Cancer Research.* Jun 2003;9(6):1980-1989.

66. Effects of chemotherapy and hormonal therapy for early breast cancer on recurrence and 15-year survival: an overview of the randomised trials. *Lancet.* May 14-20 2005;365(9472):1687-1717.

67. Carter P, Presta L, Gorman CM, et al. Humanization of an anti-p185HER2 antibody for human cancer therapy. *Proceedings of the National Academy of Sciences of the United States of America.* May 15 1992;89(10):4285-4289.

68. Diaby V, Tawk R, Sanogo V, Xiao H, Montero AJ. A review of systematic reviews of the cost-effectiveness of hormone therapy, chemotherapy, and targeted therapy for breast cancer. *Breast cancer research and treatment.* May 2015;151(1):27-40.

69. Santiago-Fernandez P, Torres-Barahona R, Muela-Martinez JA, et al. Intelligence quotient and iodine intake: a cross-sectional study in children. *The Journal of clinical endocrinology and metabolism.* Aug 2004;89(8):3851-3857.

70. Ahn BC. Sodium iodide symporter for nuclear molecular imaging and gene therapy: from bedside to bench and back. *Theranostics.* 2012;2(4):392-402.

71. Towery BT. The physiology of iodine. *Bulletin of the World Health Organization.* 1953;9(2):175-182.

72. Delange F, Burgi H, Chen ZP, Dunn JT. World status of monitoring iodine deficiency disorders control programs. *Thyroid.* Oct 2002;12(10):915-924.

73. Pharoah PO, Buttfield IH, Hetzel BS. Neurological damage to the fetus resulting from severe iodine deficiency during pregnancy. *Lancet.* Feb 13 1971;1(7694):308-310.

74. Mazzaferri EL. Long-term outcome of patients with differentiated thyroid carcinoma: effect of therapy. *Endocrine practice : official journal of the American College of Endocrinology and the American Association of Clinical Endocrinologists.* Nov-Dec 2000;6(6):469-476.

75. Vilkki P. An iodide-complexing phospholipid. *Archives of biochemistry and biophysics.* May 1962;97:425-427.

76. Dai G, Levy O, Carrasco N. Cloning and characterization of the thyroid iodide transporter. *Nature.* Feb 1 1996;379(6564):458-460.

77. Saber-Lichtenberg Y, Brix K, Schmitz A, et al. Covalent cross-linking of secreted bovine thyroglobulin by transglutaminase. *FASEB journal : official publication of the Federation of American Societies for Experimental Biology.* May 2000;14(7):1005-1014.

78. Spitzweg C, Morris JC. Sodium iodide symporter (NIS) and thyroid. *Hormones (Athens).* Jan-Mar 2002;1(1):22-34.

79. Eskandari S, Loo DD, Dai G, Levy O, Wright EM, Carrasco N. Thyroid Na+/I- symporter. Mechanism, stoichiometry, and specificity. *The Journal of biological chemistry.* Oct 24 1997;272(43):27230-27238.

80. Levy O, Dai G, Riedel C, et al. Characterization of the thyroid Na+/I- symporter with an anti-COOH terminus antibody. *Proceedings of the National Academy of Sciences of the United States of America.* May 27 1997;94(11):5568-5573.

81. Levy O, De la Vieja A, Ginter CS, Riedel C, Dai G, Carrasco N. N-linked glycosylation of the thyroid Na+/I- symporter (NIS). Implications for its secondary structure model. *The Journal of biological chemistry.* Aug 28 1998;273(35):22657-22663.

82. Dohan O, De la Vieja A, Carrasco N. Molecular study of the sodium-iodide symporter (NIS): a new field in thyroidology. *Trends in endocrinology and metabolism: TEM.* Apr 2000;11(3):99-105.

83. Dohan O, Baloch Z, Banrevi Z, Livolsi V, Carrasco N. Rapid communication: predominant intracellular overexpression of the Na(+)/I(-) symporter (NIS) in a large sampling of thyroid cancer cases. *The Journal of clinical endocrinology and metabolism.* Jun 2001;86(6):2697-2700.

84. Kaminsky SM, Levy O, Salvador C, Dai G, Carrasco N. Na(+)-I- symport activity is present in membrane vesicles from thyrotropin-deprived non-I(-)-transporting cultured thyroid cells. *Proceedings of the National Academy of Sciences of the United States of America.* Apr 26 1994;91(9):3789-3793.

85. Rhoden KJ, Cianchetta S, Duchi S, Romeo G. Fluorescence quantitation of thyrocyte iodide accumulation with the yellow fluorescent protein variant YFP-H148Q/I152L. *Anal Biochem.* Feb 15 2008;373(2):239-246.

86. Smanik PA, Liu Q, Furminger TL, et al. Cloning of the human sodium lodide symporter. *Biochemical and biophysical research communications.* Sep 13 1996;226(2):339-345.

87. Wright EM, Turk E. The sodium/glucose cotransport family SLC5. *Pflugers Archiv : European journal of physiology.* Feb 2004;447(5):510-518.

88. Wolff J. Transport of Iodide and Other Anions in the Thyroid Gland. *Physiological reviews.* Jan 1964;44:45-90.

89. Dohan O, Portulano C, Basquin C, Reyna-Neyra A, Amzel LM, Carrasco N. The Na+/I symporter (NIS) mediates electroneutral active transport of the environmental pollutant perchlorate. *Proceedings of the National Academy of Sciences of the United States of America.* Dec 18 2007;104(51):20250-20255.

90. Wright EM. Active transport of iodide and other anions across the choroid plexus. *The Journal of physiology.* Aug 1974;240(3):535-566.

91. Spitzweg C, Joba W, Eisenmenger W, Heufelder AE. Analysis of human sodium iodide symporter gene expression in extrathyroidal tissues and cloning of its complementary deoxyribonucleic acids from salivary gland, mammary gland, and gastric mucosa. *The Journal of clinical endocrinology and metabolism.* May 1998;83(5):1746-1751.

92. Cho JY, Xing S, Liu X, et al. Expression and activity of human Na+/I- symporter in human glioma cells by adenovirus-mediated gene delivery. *Gene Ther.* May 2000;7(9):740-749.

93. Nurnberger CE, Lipscomb A. Transmission of radioiodine (I131) to infants through human maternal milk. *Journal of the American Medical Association.* Dec 6 1952;150(14):1398-1400.

94. Thorpe SM. Increased uptake of iodide by hormone-responsive compared to hormone-independent mammary tumors in GR mice. *International journal of cancer. Journal international du cancer.* Sep 15 1976;18(3):345-350.

95. Patrick L. Iodine: deficiency and therapeutic considerations. *Alternative medicine review : a journal of clinical therapeutic.* Jun 2008;13(2):116-127.

96. Alotaibi H, Yaman EC, Demirpence E, Tazebay UH. Unliganded estrogen receptor-alpha activates transcription of the mammary gland Na+/I- symporter gene. *Biochemical and biophysical research communications.* Jul 14 2006;345(4):1487-1496.

97. Filetti S, Bidart JM, Arturi F, Caillou B, Russo D, Schlumberger M. Sodium/iodide symporter: a key transport system in thyroid cancer cell metabolism. *European journal of endocrinology / European Federation of Endocrine Societies.* Nov 1999;141(5):443-457.

98. Trapasso F, Iuliano R, Chiefari E, et al. Iodide symporter gene expression in normal and transformed rat thyroid cells. *European journal of endocrinology / European Federation of Endocrine Societies.* May 1999;140(5):447-451.

99. Caillou B, Troalen F, Baudin E, et al. Na+/I- symporter distribution in human thyroid tissues: an immunohistochemical study. *The Journal of clinical endocrinology and metabolism.* Nov 1998;83(11):4102-4106.

100. Thomas-Morvan C, Carayon P, Schlumberger M, Vignal A, Tubiana M. Thyrotrophin stimulation of adenylate cyclase and iodine uptake in human differentiated thyroid cancer. *Acta endocrinologica.* Sep 1982;101(1):25-31.

101. Ahn BC, Lee SW, Lee J, Kim C. Pulmonary aspergilloma mimicking metastasis from papillary thyroid cancer. *Thyroid.* May 2011;21(5):555-558.

102. Mazzaferri EL, Kloos RT. Clinical review 128: Current approaches to primary therapy for papillary and follicular thyroid cancer. *The Journal of clinical endocrinology and metabolism.* Apr 2001;86(4):1447-1463.

103. Oh SW, Moon SH, Park do J, et al. Combined therapy with 131I and retinoic acid in Korean patients with radioiodine-refractory papillary thyroid cancer. *Eur J Nucl Med Mol Imaging.* Oct 2011;38(10):1798-1805.

104. Eskin BA, Parker JA, Bassett JG, George DL. Human breast uptake of radioactive iodine. *Obstetrics and gynecology.* Sep 1974;44(3):398-402.

105. Lacoste C, Herve J, Bou Nader M, et al. Iodide transporter NIS regulates cancer cell motility and invasiveness by interacting with the Rho guanine nucleotide exchange factor LARG. *Cancer research.* Nov 1 2012;72(21):5505-5515.

106. Baril P, Martin-Duque P, Vassaux G. Visualization of gene expression in the live subject using the Na/I symporter as a reporter gene: applications in biotherapy. *British journal of pharmacology.* Feb 2010;159(4):761-771.

107. Herve J, Cunha AS, Liu B, et al. Internal radiotherapy of liver cancer with rat hepatocarcinoma-intestine-pancreas gene as a liver tumor-specific promoter. *Hum Gene Ther.* Sep 2008;19(9):915-926.

108. Spitzweg C, Zhang S, Bergert ER, et al. Prostate-specific antigen (PSA) promoter-driven androgen-inducible expression of sodium iodide symporter in prostate cancer cell lines. *Cancer research.* May 1 1999;59(9):2136-2141.

109. Spitzweg C, Dietz AB, O'Connor MK, et al. In vivo sodium iodide symporter gene therapy of prostate cancer. *Gene Ther.* Oct 2001;8(20):1524-1531.

110. Dingli D, Diaz RM, Bergert ER, O'Connor MK, Morris JC, Russell SJ. Genetically targeted radiotherapy for multiple myeloma. *Blood.* Jul 15 2003;102(2):489-496.

111. Ouellette MM, Wright WE, Shay JW. Targeting telomerase-expressing cancer cells. *Journal of cellular and molecular medicine.* Jul 2011;15(7):1433-1442.

112. Riesco-Eizaguirre G, De la Vieja A, Rodriguez I, et al. Telomerase-driven expression of the sodium iodide symporter (NIS) for in vivo radioiodide treatment of cancer: a new broad-spectrum NIS-mediated antitumor approach. *The Journal of clinical endocrinology and metabolism.* Sep 2011;96(9):E1435-1443.

113. Dingli D, Peng KW, Harvey ME, et al. Image-guided radiovirotherapy for multiple myeloma using a recombinant measles virus expressing the thyroidal sodium iodide symporter. *Blood.* Mar 1 2004;103(5):1641-1646.

114. Magnon C, Opolon P, Ricard M, et al. Radiation and inhibition of angiogenesis by canstatin synergize to induce HIF-1alpha-mediated tumor apoptotic switch. *The Journal of clinical investigation.* Jul 2007;117(7):1844-1855.

115. Klutz K, Russ V, Willhauck MJ, et al. Targeted radioiodine therapy of neuroblastoma tumors following systemic nonviral delivery of the sodium iodide symporter gene. *Clinical cancer research : an official journal of the American Association for Cancer Research.* Oct 1 2009;15(19):6079-6086.

116. Chisholm EJ, Vassaux G, Martin-Duque P, et al. Cancer-specific transgene expression mediated by systemic injection of nanoparticles. *Cancer research.* Mar 15 2009;69(6):2655-2662.

117. Shimura H, Haraguchi K, Miyazaki A, Endo T, Onaya T. Iodide uptake and experimental 131I therapy in transplanted undifferentiated thyroid cancer cells expressing the Na+/I- symporter gene. *Endocrinology.* Oct 1997;138(10):4493-4496.

118. Portulano C, Paroder-Belenitsky M, Carrasco N. The Na+/I- symporter (NIS): mechanism and medical impact. *Endocr Rev.* Feb 2014;35(1):106-149.

119. Niu G, Krager KJ, Graham MM, Hichwa RD, Domann FE. Noninvasive radiological imaging of pulmonary gene transfer and expression using the human sodium iodide symporter. *Eur J Nucl Med Mol Imaging.* May 2005;32(5):534-540.

120. Miyagawa M, Beyer M, Wagner B, et al. Cardiac reporter gene imaging using the human sodium/iodide symporter gene. *Cardiovascular research.* Jan 1 2005;65(1):195-202.

121. Terrovitis J, Kwok KF, Lautamaki R, et al. Ectopic expression of the sodium-iodide symporter enables imaging of transplanted cardiac stem cells in vivo by single-photon emission computed tomography or positron emission tomography. *J Am Coll Cardiol.* Nov 11 2008;52(20):1652-1660.

122. Barton KN, Stricker H, Brown SL, et al. Phase I study of noninvasive imaging of adenovirus-mediated gene expression in the human prostate. *Molecular therapy : the journal of the American Society of Gene Therapy.* Oct 2008;16(10):1761-1769.

123. Jeong SY, Hwang MH, Kim JE, et al. Combined Cerenkov luminescence and nuclear imaging of radioiodine in the thyroid gland and thyroid cancer cells expressing sodium iodide symporter: initial feasibility study. *Endocr J.* 2011;58(7):575-583.

124. Kemerink GJ, Visser MG, Franssen R, et al. Effect of the positron range of 18F, 68Ga and 124I on PET/CT in lung-equivalent materials. *Eur J Nucl Med Mol Imaging.* May 2011;38(5):940-948.

125. Wood KV, Lam YA, Seliger HH, McElroy WD. Complementary DNA coding click beetle luciferases can elicit bioluminescence of different colors. *Science.* May 12 1989;244(4905):700-702.

126. Lorenz WW, McCann RO, Longiaru M, Cormier MJ. Isolation and expression of a cDNA encoding Renilla reniformis luciferase. *Proceedings of the National Academy of Sciences of the United States of America.* May 15 1991;88(10):4438-4442.

127. Verhaegent M, Christopoulos TK. Recombinant Gaussia luciferase. Overexpression, purification, and analytical application of a bioluminescent reporter for DNA hybridization. *Analytical chemistry.* Sep 1 2002;74(17):4378-4385.

128. Markova SV, Golz S, Frank LA, Kalthof B, Vysotski ES. Cloning and expression of cDNA for a luciferase from the marine copepod Metridia longa. A novel secreted bioluminescent reporter enzyme. *The Journal of biological chemistry.* Jan 30 2004;279(5):3212-3217.

129. Thompson EM, Nagata S, Tsuji FI. Cloning and expression of cDNA for the luciferase from the marine ostracod Vargula hilgendorfii. *Proceedings of the National Academy of Sciences of the United States of America.* Sep 1989;86(17):6567-6571.

130. Meighen EA. Molecular biology of bacterial bioluminescence. *Microbiological reviews.* Mar 1991;55(1):123-142.

131. Schroder J. Protein sequence homology between plant 4-coumarate:CoA ligase and firefly luciferase. *Nucleic acids research.* Jan 11 1989;17(1):460.

132. Ruggiero A, Holland JP, Lewis JS, Grimm J. Cerenkov luminescence imaging of medical isotopes. *Journal of nuclear medicine : official publication, Society of Nuclear Medicine.* Jul 2010;51(7):1123-1130.

133. Liu H, Ren G, Miao Z, et al. Molecular optical imaging with radioactive probes. *PloS one.* 2010;5(3):e9470.

134. Beattie BJ, Thorek DL, Schmidtlein CR, Pentlow KS, Humm JL, Hielscher AH. Quantitative modeling of Cerenkov light production efficiency from medical radionuclides. *PloS one.* 2012;7(2):e31402.

135. Thorek D, Robertson R, Bacchus WA, et al. Cerenkov imaging - a new modality for molecular imaging. *American journal of nuclear medicine and molecular imaging.* 2012;2(2):163-173.

136. Mitchell GS, Gill RK, Boucher DL, Li C, Cherry SR. In vivo Cerenkov luminescence imaging: a new tool for molecular imaging. *Philosophical transactions. Series A, Mathematical, physical, and engineering sciences.* Nov 28 2011;369(1955):4605-4619.

137. Polychemotherapy for early breast cancer: an overview of the randomised trials. Early Breast Cancer Trialists' Collaborative Group. *Lancet.* Sep 19 1998;352(9132):930-942.

138. Tandon A, Shrivastava A, Kumar A, Prayaga AK, Sundaram C, Godbole MM. Sodium iodide symporter, estrogen receptor, and progesterone receptor expression in carcinoma breast - An immunohistochemical analysis. *Indian Journal of Pathology and Microbiology.* Oct-Dec 2011;54(4):745-751.

139. Montiel-Equihua CA, Martin-Duque P, de la Vieja A, et al. Targeting sodium/iodide symporter gene expression for estrogen-regulated imaging and therapy in breast cancer. *Cancer Gene Therapy.* Jul 2008;15(7):465-473.

140. Ghosh M, Gambhir SS, De A, Nowels K, Goris M, Wapnir I. Bioluminescent monitoring of NIS-mediated (131)I ablative effects in MCF-7 xenografts. *Mol Imaging.* Apr-Jun 2006;5(2):76-84.

141. Beyer S, Lakshmanan A, Liu YY, et al. KT5823 differentially modulates sodium iodide symporter expression, activity, and glycosylation between thyroid and breast cancer cells. *Endocrinology.* Mar 2011;152(3):782-792.

142. Kogai T, Taki K, Brent GA. Enhancement of sodium/iodide symporter expression in thyroid and breast cancer. *Endocrine-related cancer.* Sep 2006;13(3):797-826.

143. Yao C, Pan Y, Li Y, et al. Effect of sodium/iodide symporter (NIS)-mediated radioiodine therapy on estrogen receptor-negative breast cancer. *Oncol Rep.* Jul 2015;34(1):59-66.

144. Tandon A, Shrivastava A, Kumar A, Prayaga AK, Sundaram C, Godbole MM. Sodium iodide symporter, estrogen receptor, and progesterone receptor expression in carcinoma breast--an immunohistochemical analysis. *Indian journal of pathology & microbiology.* Oct-Dec 2011;54(4):745-751.

145. Oh HJ, Chung JK, Kang JH, et al. The relationship between expression of the sodium/iodide symporter gene and the status of hormonal receptors in human breast cancer tissue. *Cancer research and treatment : official journal of Korean Cancer Association.* Aug 2005;37(4):247-250.

146. Kilbane MT, Ajjan RA, Weetman AP, et al. Tissue iodine content and serum-mediated 125I uptake-blocking activity in breast cancer. *The Journal of clinical endocrinology and metabolism.* Mar 2000;85(3):1245-1250.

147. Damle AA, Narkar AA, Badwe RA. Radioiodide uptake and sodium iodide symporter expression in breast carcinoma. *Indian Journal of Experimental Biology.* Jun 2011;49(6):416-422.

148. Varghese F, Bukhari AB, Malhotra R, De A. IHC Profiler: an open source plugin for the quantitative evaluation and automated scoring of immunohistochemistry images of human tissue samples. *PloS one.* 2014;9(5):e96801.

149. Ruifrok AC, Katz RL, Johnston DA. Comparison of quantification of histochemical staining by hue-saturation-intensity (HSI) transformation and color-deconvolution. *Applied immunohistochemistry & molecular morphology : AIMM / official publication of the Society for Applied Immunohistochemistry.* Mar 2003;11(1):85-91.

150. Rai R, Shrivastava A, Tandon A, et al. Human sodium iodide symporter (hNIS) in fibroadenoma breast-A mmunohistochemical study. *Indian Journal of Experimental Biology.* Feb 2011;49(2):113-117.

151. Berger F, Unterholzner S, Diebold J, Knesewitsch P, Hahn K, Spitzweg C. Mammary radioiodine accumulation due to functional sodium iodide symporter expression in a benign fibroadenoma. *Biochemical and biophysical research communications.* Nov 2006;349(4):1258-1263.

152. Kogai T, Kanamoto Y, Che LH, et al. Systemic retinoic acid treatment induces sodium/iodide symporter expression and radioiodide uptake in mouse breast cancer models. *Cancer research.* Jan 1 2004;64(1):415-422.

153. Santen RJ. Benign Breast Disease in Women. In: De Groot LJ, Beck-Peccoz P, Chrousos G, et al., eds. *Endotext*. South Dartmouth (MA)2000.

154. Bidgoli SA, Eftekhari T. Role of exogenous and endogenous sources of estrogen on the incidence of breast fibroadenoma: case-control study in Iran. *Asian Pacific journal of cancer prevention : APJCP.* 2011;12(5):1289-1293.

155. Brockton NT, Gill SJ, Laborge SL, et al. The Breast Cancer to Bone (B2B) Metastases Research Program: a multi-disciplinary investigation of bone metastases from breast cancer. *BMC cancer.* 2015;15:512.

156. Gerratana L, Fanotto V, Bonotto M, et al. Pattern of metastasis and outcome in patients with breast cancer. *Clinical & experimental metastasis.* Feb 2015;32(2):125-133.

157. Chambers AF, Groom AC, MacDonald IC. Dissemination and growth of cancer cells in metastatic sites. *Nature reviews. Cancer.* Aug 2002;2(8):563-572.

158. Fidler IJ. Critical determinants of metastasis. *Seminars in cancer biology.* Apr 2002;12(2):89-96.

159. Nicolini A, Giardino R, Carpi A, et al. Metastatic breast cancer: an updating. *Biomedicine & pharmacotherapy = Biomedecine & pharmacotherapie.* Nov 2006;60(9):548-556.

160. Von Hoff DD, Layard MW, Basa P, et al. Risk factors for doxorubicin-induced congestive heart failure. *Annals of internal medicine.* Nov 1979;91(5):710-717.

161. Stathopoulos GP, Trafalis D. High-dose tamoxifen in breast cancer bone metastasis. *Journal of B.U.ON. : official journal of the Balkan Union of Oncology.* Apr-Jun 2013;18(2):532-534.

162. Slamon DJ, Leyland-Jones B, Shak S, et al. Use of chemotherapy plus a monoclonal antibody against HER2 for metastatic breast cancer that overexpresses HER2. *The New England journal of medicine.* Mar 15 2001;344(11):783-792.

163. Larson JS, Goodman LJ, Tan Y, et al. Analytical Validation of a Highly Quantitative, Sensitive, Accurate, and Reproducible Assay (HERmark) for the Measurement of HER2 Total Protein and HER2 Homodimers in FFPE Breast Cancer Tumor Specimens. *Pathology research international.* 2010;2010:814176.

164. de Alava E, Ocana A, Abad M, et al. Neuregulin expression modulates clinical response to trastuzumab in patients with metastatic breast cancer. *Journal of clinical oncology : official journal of the American Society of Clinical Oncology.* Jul 1 2007;25(19):2656-2663.

165. Piccart M, Lohrisch C, Di Leo A, Larsimont D. The predictive value of HER2 in breast cancer. *Oncology.* 2001;61 Suppl 2:73-82.

166. Wolff AC, Hammond ME, Schwartz JN, et al. American Society of Clinical Oncology/College of American Pathologists guideline recommendations for human epidermal growth factor receptor 2 testing in breast cancer. *Archives of pathology & laboratory medicine.* 2007;131(1):18-43.

167. Paik S, Bryant J, Tan-Chiu E, et al. Real-world performance of HER2 testing--National Surgical Adjuvant Breast and Bowel Project experience. *Journal of the National Cancer Institute.* Jun 5 2002;94(11):852-854.

168. Dodwell D, Wardley A, Johnston S. Postmenopausal advanced breast cancer: options for therapy after tamoxifen and aromatase inhibitors. *Breast.* Oct 2006;15(5):584-594.

169. Chia S, Gradishar W, Mauriac L, et al. Double-blind, randomized placebo controlled trial of fulvestrant compared with exemestane after prior nonsteroidal aromatase inhibitor therapy in postmenopausal women with hormone receptor-positive, advanced breast cancer: results from EFECT. *Journal of clinical oncology : official journal of the American Society of Clinical Oncology.* Apr 1 2008;26(10):1664-1670.

170. Lindstrom LS, Karlsson E, Wilking UM, et al. Clinically used breast cancer markers such as estrogen receptor, progesterone receptor, and human epidermal growth factor receptor 2 are unstable throughout tumor progression. *Journal of clinical oncology : official journal of the American Society of Clinical Oncology.* Jul 20 2012;30(21):2601-2608.

171. Dieci MV, Barbieri E, Piacentini F, et al. Discordance in receptor status between primary and recurrent breast cancer has a prognostic impact: a single-institution analysis. *Annals of oncology : official journal of the European Society for Medical Oncology / ESMO.* Jan 2013;24(1):101-108.

172. Niikura N, Liu J, Hayashi N, et al. Loss of human epidermal growth factor receptor 2 (HER2) expression in metastatic sites of HER2-overexpressing primary breast tumors. *Journal of clinical oncology : official journal of the American Society of Clinical Oncology.* Feb 20 2012;30(6):593-599.

173. Lower EE, Glass E, Blau R, Harman S. HER-2/neu expression in primary and metastatic breast cancer. *Breast cancer research and treatment.* Jan 2009;113(2):301-306.

174. Amir E, Miller N, Geddie W, et al. Prospective study evaluating the impact of tissue confirmation of metastatic disease in patients with breast cancer. *Journal of clinical*

oncology : official journal of the American Society of Clinical Oncology. Feb 20 2012;30(6):587-592.

175. Thompson AM, Jordan LB, Quinlan P, et al. Prospective comparison of switches in biomarker status between primary and recurrent breast cancer: the Breast Recurrence In Tissues Study (BRITS). *Breast cancer research : BCR.* 2010;12(6):R92.

176. Amir E, Clemons M, Purdie CA, et al. Tissue confirmation of disease recurrence in breast cancer patients: pooled analysis of multi-centre, multi-disciplinary prospective studies. *Cancer treatment reviews.* Oct 2012;38(6):708-714.

177. Santinelli A, Pisa E, Stramazzotti D, Fabris G. HER-2 status discrepancy between primary breast cancer and metastatic sites. Impact on target therapy. *International journal of cancer. Journal international du cancer.* Mar 1 2008;122(5):999-1004.

178. Simmons C, Miller N, Geddie W, et al. Does confirmatory tumor biopsy alter the management of breast cancer patients with distant metastases? *Annals of oncology : official journal of the European Society for Medical Oncology / ESMO.* Sep 2009;20(9):1499-1504.

179. Press OW, Eary JF, Appelbaum FR, et al. Phase II trial of 131I-B1 (anti-CD20) antibody therapy with autologous stem cell transplantation for relapsed B cell lymphomas. *Lancet.* Aug 5 1995;346(8971):336-340.

180. van Santen HM, de Kraker J, van Eck BL, de Vijlder JJ, Vulsma T. High incidence of thyroid dysfunction despite prophylaxis with potassium iodide during (131)I-meta-iodobenzylguanidine treatment in children with neuroblastoma. *Cancer.* Apr 1 2002;94(7):2081-2089.

181. Chatterjee S, Malhotra R, Varghese F, et al. Quantitative immunohistochemical analysis reveals association between sodium iodide symporter and estrogen receptor expression in breast cancer. *PloS one.* 2013;8(1):e54055.

182. Riesco-Eizaguirre G, Santisteban P. A perspective view of sodium iodide symporter research and its clinical implications. *European journal of endocrinology / European Federation of Endocrine Societies.* Oct 2006;155(4):495-512.

183. Kogai T, Brent GA. The sodium iodide symporter (NIS): regulation and approaches to targeting for cancer therapeutics. *Pharmacol Ther.* Sep 2012;135(3):355-370.

184. Faivre J, Clerc J, Gerolami R, et al. Long-term radioiodine retention and regression of liver cancer after sodium iodide symporter gene transfer in wistar rats. *Cancer research.* Nov 1 2004;64(21):8045-8051.

185. Spitzweg C, O'Connor MK, Bergert ER, Tindall DJ, Young CY, Morris JC. Treatment of prostate cancer by radioiodine therapy after tissue-specific expression of the sodium iodide symporter. *Cancer research.* Nov 15 2000;60(22):6526-6530.

186. Dwyer RM, Schatz SM, Bergert ER, et al. A preclinical large animal model of adenovirus-mediated expression of the sodium-iodide symporter for radioiodide imaging and therapy of locally recurrent prostate cancer. *Molecular therapy : the journal of the American Society of Gene Therapy.* Nov 2005;12(5):835-841.

187. Shen DH, Marsee DK, Schaap J, et al. Effects of dose, intervention time, and radionuclide on sodium iodide symporter (NIS)-targeted radionuclide therapy. *Gene Ther.* Jan 2004;11(2):161-169.

188. Boland A, Ricard M, Opolon P, et al. Adenovirus-mediated transfer of the thyroid sodium/iodide symporter gene into tumors for a targeted radiotherapy. *Cancer research.* Jul 1 2000;60(13):3484-3492.

189. Mandell RB, Mandell LZ, Link CJ, Jr. Radioisotope concentrator gene therapy using the sodium/iodide symporter gene. *Cancer research.* Feb 1 1999;59(3):661-668.

190. Chen RF, Li ZH, Pan QH, et al. In vivo radioiodide imaging and treatment of pancreatic cancer xenografts after MUC1 promoter-driven expression of the human sodium-iodide symporter. *Pancreatology.* 2007;7(5-6):505-513.

191. Dwyer RM, Bergert ER, O'Connor MK, Gendler SJ, Morris JC. Adenovirus-mediated and targeted expression of the sodium-iodide symporter permits in vivo radioiodide imaging and therapy of pancreatic tumors. *Hum Gene Ther.* Jun 2006;17(6):661-668.

192. Dwyer RM, Bergert ER, O'Connor MK, Gendler SJ, Morris JC. Sodium iodide symporter-mediated radioiodide imaging and therapy of ovarian tumor xenografts in mice. *Gene Ther.* Jan 2006;13(1):60-66.

193. Scholz IV, Cengic N, Baker CH, et al. Radioiodine therapy of colon cancer following tissue-specific sodium iodide symporter gene transfer. *Gene Ther.* Feb 2005;12(3):272-280.

194. Spitzweg C, Baker CH, Bergert ER, O'Connor MK, Morris JC. Image-guided radioiodide therapy of medullary thyroid cancer after carcinoembryonic antigen promoter-targeted sodium iodide symporter gene expression. *Hum Gene Ther.* Oct 2007;18(10):916-924.

195. Riedel C, Dohan O, De la Vieja A, Ginter CS, Carrasco N. Journey of the iodide transporter NIS: from its molecular identification to its clinical role in cancer. *Trends in biochemical sciences.* Aug 2001;26(8):490-496.

196. Spitzweg C, Morris JC. The sodium iodide symporter: its pathophysiological and therapeutic implications. *Clin Endocrinol (Oxf).* Nov 2002;57(5):559-574.

197. Chung JK, Kang JH. Translational research using the sodium/iodide symporter in imaging and therapy. *Eur J Nucl Med Mol Imaging.* Jun 2004;31(6):799-802.

198. Kakinuma H, Bergert ER, Spitzweg C, Cheville JC, Lieber MM, Morris JC. Probasin promoter (ARR(2)PB)-driven, prostate-specific expression of the human sodium iodide symporter (h-NIS) for targeted radioiodine therapy of prostate cancer. *Cancer research.* Nov 15 2003;63(22):7840-7844.

199. Willhauck MJ, Sharif Samani BR, Klutz K, et al. Alpha-fetoprotein promoter-targeted sodium iodide symporter gene therapy of hepatocellular carcinoma. *Gene Ther.* Feb 2008;15(3):214-223.

200. Kim SH, Chung HK, Kang JH, et al. Tumor-targeted radionuclide imaging and therapy based on human sodium iodide symporter gene driven by a modified telomerase reverse transcriptase promoter. *Hum Gene Ther.* Sep 2008;19(9):951-957.

201. Nakamoto Y, Saga T, Misaki T, et al. Establishment and characterization of a breast cancer cell line expressing Na+/I- symporters for radioiodide concentrator gene therapy. *Journal of nuclear medicine : official publication, Society of Nuclear Medicine.* Nov 2000;41(11):1898-1904.

202. Dwyer RM, Bergert ER, O'Connor M K, Gendler SJ, Morris JC. In vivo radioiodide imaging and treatment of breast cancer xenografts after MUC1-driven expression of the sodium iodide symporter. *Clinical cancer research : an official journal of the American Association for Cancer Research.* Feb 15 2005;11(4):1483-1489.

203. Tjuvajev JG, Stockhammer G, Desai R, et al. Imaging the expression of transfected genes in vivo. *Cancer research.* Dec 15 1995;55(24):6126-6132.

204. Penheiter AR, Russell SJ, Carlson SK. The sodium iodide symporter (NIS) as an imaging reporter for gene, viral, and cell-based therapies. *Curr Gene Ther.* Feb 1 2012;12(1):33-47.

205. Miyagawa M, Anton M, Wagner B, et al. Non-invasive imaging of cardiac transgene expression with PET: comparison of the human sodium/iodide symporter gene and HSV1-tk as the reporter gene. *Eur J Nucl Med Mol Imaging.* Sep 2005;32(9):1108-1114.

206. Lee KH, Kim HK, Paik JY, et al. Accuracy of myocardial sodium/iodide symporter gene expression imaging with radioiodide: evaluation with a dual-gene adenovirus vector. *Journal of nuclear medicine : official publication, Society of Nuclear Medicine.* Apr 2005;46(4):652-657.

207. Rao VP, Miyagi N, Ricci D, et al. Sodium iodide symporter (hNIS) permits molecular imaging of gene transduction in cardiac transplantation. *Transplantation.* Dec 27 2007;84(12):1662-1666.

208. Seo JH, Jeon YH, Lee YJ, et al. Trafficking macrophage migration using reporter gene imaging with human sodium iodide symporter in animal models of inflammation. *Journal of nuclear medicine : official publication, Society of Nuclear Medicine.* Oct 2010;51(10):1637-1643.

209. Groth AC, Olivares EC, Thyagarajan B, Calos MP. A phage integrase directs efficient site-specific integration in human cells. *Proceedings of the National Academy of Sciences of the United States of America.* May 23 2000;97(11):5995-6000.

210. Waltz F, Pillette L, Ambroise Y. A nonradioactive iodide uptake assay for sodium iodide symporter function. *Anal Biochem.* Jan 1 2010;396(1):91-95.

211. Franken NA, Rodermond HM, Stap J, Haveman J, van Bree C. Clonogenic assay of cells in vitro. *Nature protocols.* 2006;1(5):2315-2319.

212. Vega MA. Prospects for homologous recombination in human gene therapy. *Human genetics.* Jul 1991;87(3):245-253.

213. De A, Lewis XZ, Gambhir SS. Noninvasive imaging of lentiviral-mediated reporter gene expression in living mice. *Molecular therapy : the journal of the American Society of Gene Therapy.* May 2003;7(5 Pt 1):681-691.

214. Ray P, De A, Min JJ, Tsien RY, Gambhir SS. Imaging tri-fusion multimodality reporter gene expression in living subjects. *Cancer research.* Feb 15 2004;64(4):1323-1330.

215. Ray P, Wu AM, Gambhir SS. Optical bioluminescence and positron emission tomography imaging of a novel fusion reporter gene in tumor xenografts of living mice. *Cancer research.* Mar 15 2003;63(6):1160-1165.

216. Yu X, Zhan X, D'Costa J, et al. Lentiviral vectors with two independent internal promoters transfer high-level expression of multiple transgenes to human hematopoietic stem-progenitor cells. *Molecular therapy : the journal of the American Society of Gene Therapy.* Jun 2003;7(6):827-838.

217. Licursi M, Christian SL, Pongnopparat T, Hirasawa K. In vitro and in vivo comparison of viral and cellular internal ribosome entry sites for bicistronic vector expression. *Gene Ther.* Jun 2011;18(6):631-636.

218. Szymczak AL, Workman CJ, Wang Y, et al. Correction of multi-gene deficiency in vivo using a single 'self-cleaving' 2A peptide-based retroviral vector. *Nature biotechnology.* May 2004;22(5):589-594.

219. Ibrahimi A, Vande Velde G, Reumers V, et al. Highly efficient multicistronic lentiviral vectors with peptide 2A sequences. *Hum Gene Ther.* Aug 2009;20(8):845-860.

220. Paire A, Bernier-Valentin F, Selmi-Ruby S, Rousset B. Characterization of the rat thyroid iodide transporter using anti-peptide antibodies. Relationship between its expression and activity. *The Journal of biological chemistry.* Jul 18 1997;272(29):18245-18249.

221. Kogai T, Brent GA. The sodium iodide symporter (NIS): Regulation and approaches to targeting for cancer therapeutics. *Pharmacology & Therapeutics.* Sep 2012;135(3):355-370.

222. Jung KH, Paik JY, Ko BH, Lee KH. Mitogen-activated protein kinase signaling enhances sodium iodide symporter function and efficacy of radioiodide therapy in nonthyroidal cancer cells. *Journal of nuclear medicine : official publication, Society of Nuclear Medicine.* Dec 2008;49(12):1966-1972.

223. Baker CH, Morris JC. The sodium-iodide symporter. *Current drug targets. Immune, endocrine and metabolic disorders.* Sep 2004;4(3):167-174.

224. Hingorani M, Spitzweg C, Vassaux G, et al. The biology of the sodium iodide symporter and its potential for targeted gene delivery. *Curr Cancer Drug Targets.* Mar 2010;10(2):242-267.

225. Cho JY. A transporter gene (sodium iodide symporter) for dual purposes in gene therapy: imaging and therapy. *Curr Gene Ther.* Dec 2002;2(4):393-402.

226. Welcsh PL, Mankoff DA. Taking up iodide in breast tissue. *Nature.* Aug 17 2000;406(6797):688-689.

227. Boelaert K, Franklyn JA. Sodium iodide symporter: a novel strategy to target breast, prostate, and other cancers? *Lancet.* Mar 8 2003;361(9360):796-797.

228. Liu Z, Xing M. Induction of sodium/iodide symporter (NIS) expression and radioiodine uptake in non-thyroid cancer cells. *PloS one.* 2012;7(2):e31729.

229. Kogai T, Schultz JJ, Johnson LS, Huang M, Brent GA. Retinoic acid induces sodium/iodide symporter gene expression and radioiodide uptake in the MCF-7 breast cancer cell line. *Proceedings of the National Academy of Sciences of the United States of America.* Jul 18 2000;97(15):8519-8524.

230. Biaglow JE, Clark EP, Epp ER, Morse-Guadio M, Varnes ME, Mitchell JB. Nonprotein thiols and the radiation response of A549 human lung carcinoma cells. *International journal of radiation biology and related studies in physics, chemistry, and medicine.* Nov 1983;44(5):489-495.

231. Mitchell JB, Russo A. The role of glutathione in radiation and drug induced cytotoxicity. *The British journal of cancer. Supplement.* Jun 1987;8:96-104.

232. Parniak M, Kalant N. Incorporation of glucose into glycogen in primary cultures of rat hepatocytes. *Canadian journal of biochemistry and cell biology = Revue canadienne de biochimie et biologie cellulaire.* May 1985;63(5):333-340.

233. Farooque A, Afrin F, Adhikari JS, Dwarakanath BS. Protection of normal cells and tissues during radio- and chemosensitization of tumors by 2-deoxy-D-glucose. *Journal of cancer research and therapeutics.* Sep 2009;5 Suppl 1:S32-35.

234. Farooque A, Singh N, Adhikari JS, Afrin F, Dwarakanath BS. Enhanced antitumor immunity contributes to the radio-sensitization of ehrlich ascites tumor by the glycolytic inhibitor 2-deoxy-D-glucose in mice. *PloS one.* 2014;9(9):e108131.

235. Sharma PK, Varshney R. 2-Deoxy-D-glucose and 6-aminonicotinamide-mediated Nrf2 down regulation leads to radiosensitization of malignant cells via abrogation of GSH-mediated defense. *Free radical research.* Dec 2012;46(12):1446-1457.

236. Sharma PK, Dwarakanath BS, Varshney R. Radiosensitization by 2-deoxy-D-glucose and 6-aminonicotinamide involves activation of redox sensitive ASK1-JNK/p38MAPK signaling in head and neck cancer cells. *Free radical biology & medicine.* Oct 1 2012;53(7):1500-1513.

237. Aghaee F, Pirayesh Islamian J, Baradaran B. Enhanced radiosensitivity and chemosensitivity of breast cancer cells by 2-deoxy-d-glucose in combination therapy. *Journal of breast cancer.* Jun 2012;15(2):141-147.

238. Sandulache VC, Skinner HD, Wang Y, et al. Glycolytic inhibition alters anaplastic thyroid carcinoma tumor metabolism and improves response to conventional chemotherapy and radiation. *Mol Cancer Ther.* Jun 2012;11(6):1373-1380.

239. Bhardwaj R, Sharma PK, Jadon SP, Varshney R. A combination of 2-deoxy-D-glucose and 6-aminonicotinamide induces cell cycle arrest and apoptosis selectively in irradiated human malignant cells. *Tumour biology : the journal of the International Society for Oncodevelopmental Biology and Medicine.* Aug 2012;33(4):1021-1030.

240. Kalia VK, Prabhakara S, Narayanan V. Modulation of cellular radiation responses by 2-deoxy-D-glucose and other glycolytic inhibitors: implications for cancer therapy. *Journal of cancer research and therapeutics.* Sep 2009;5 Suppl 1:S57-60.

241. Perumal V, Solomon PF, Jayanth VR. Modification of 2-deoxy-D-glucose on radiation-and chemotherapeutic drug-induced chromosomal aberrations. *Journal of cancer research and therapeutics.* Sep 2009;5 Suppl 1:S48-52.

242. Gupta S, Farooque A, Adhikari JS, Singh S, Dwarakanath BS. Enhancement of radiation and chemotherapeutic drug responses by 2-deoxy-D-glucose in animal tumors. *Journal of cancer research and therapeutics.* Sep 2009;5 Suppl 1:S16-20.

243. Khaitan D, Chandna S, Arya MB, Dwarakanath BS. Differential mechanisms of radiosensitization by 2-deoxy-D-glucose in the monolayers and multicellular spheroids of a human glioma cell line. *Cancer Biol Ther.* Sep 2006;5(9):1142-1151.

244. Varshney R, Dwarakanath B, Jain V. Radiosensitization by 6-aminonicotinamide and 2-deoxy-D-glucose in human cancer cells. *Int J Radiat Biol.* May 2005;81(5):397-408.

245. Singh D, Banerji AK, Dwarakanath BS, et al. Optimizing cancer radiotherapy with 2-deoxy-d-glucose dose escalation studies in patients with glioblastoma multiforme. *Strahlentherapie und Onkologie : Organ der Deutschen Rontgengesellschaft ... [et al].* Aug 2005;181(8):507-514.

246. Aft RL, Lewis JS, Zhang F, Kim J, Welch MJ. Enhancing targeted radiotherapy by copper(II)diacetyl- bis(N4-methylthiosemicarbazone) using 2-deoxy-D-glucose. *Cancer research.* Sep 1 2003;63(17):5496-5504.

247. Latz D, Thonke A, Juling-Pohlit L, Pohlit W. Tumor response to ionizing radiation and combined 2-deoxy-D-glucose application in EATC tumor bearing mice: monitoring of tumor size and microscopic observations. *Strahlentherapie und Onkologie : Organ der Deutschen Rontgengesellschaft ... [et al].* Jul 1993;169(7):405-411.

248. Blackburn RV, Spitz DR, Liu X, et al. Metabolic oxidative stress activates signal transduction and gene expression during glucose deprivation in human tumor cells. *Free radical biology & medicine.* Feb 1999;26(3-4):419-430.

249. Lin X, Zhang F, Bradbury CM, et al. 2-Deoxy-D-glucose-induced cytotoxicity and radiosensitization in tumor cells is mediated via disruptions in thiol metabolism. *Cancer research.* Jun 15 2003;63(12):3413-3417.

250. Spitz DR, Sim JE, Ridnour LA, Galoforo SS, Lee YJ. Glucose deprivation-induced oxidative stress in human tumor cells. A fundamental defect in metabolism? *Annals of the New York Academy of Sciences.* 2000;899:349-362.

251. Bowker SL, Majumdar SR, Veugelers P, Johnson JA. Increased cancer-related mortality for patients with type 2 diabetes who use sulfonylureas or insulin. *Diabetes care.* Feb 2006;29(2):254-258.

252. Decensi A, Puntoni M, Goodwin P, et al. Metformin and cancer risk in diabetic patients: a systematic review and meta-analysis. *Cancer Prev Res (Phila).* Nov 2010;3(11):1451-1461.

253. Landman GW, Kleefstra N, van Hateren KJ, Groenier KH, Gans RO, Bilo HJ. Metformin associated with lower cancer mortality in type 2 diabetes: ZODIAC-16. *Diabetes care.* Feb 2010;33(2):322-326.

254. Libby G, Donnelly LA, Donnan PT, Alessi DR, Morris AD, Evans JM. New users of metformin are at low risk of incident cancer: a cohort study among people with type 2 diabetes. *Diabetes care.* Sep 2009;32(9):1620-1625.

255. Monami M, Lamanna C, Balzi D, Marchionni N, Mannucci E. Sulphonylureas and cancer: a case-control study. *Acta diabetologica.* Dec 2009;46(4):279-284.

256. Kim HJ, Kwon H, Lee JW, et al. Metformin increases survival in hormone receptor-positive, HER2-positive breast cancer patients with diabetes. *Breast cancer research : BCR.* 2015;17:64.

257. Ben Sahra I, Laurent K, Loubat A, et al. The antidiabetic drug metformin exerts an antitumoral effect in vitro and in vivo through a decrease of cyclin D1 level. *Oncogene.* Jun 5 2008;27(25):3576-3586.

258. Buzzai M, Jones RG, Amaravadi RK, et al. Systemic treatment with the antidiabetic drug metformin selectively impairs p53-deficient tumor cell growth. *Cancer research.* Jul 15 2007;67(14):6745-6752.

259. Cantrell LA, Zhou C, Mendivil A, Malloy KM, Gehrig PA, Bae-Jump VL. Metformin is a potent inhibitor of endometrial cancer cell proliferation--implications for a novel treatment strategy. *Gynecologic oncology.* Jan 2010;116(1):92-98.

260. Dowling RJ, Goodwin PJ, Stambolic V. Understanding the benefit of metformin use in cancer treatment. *BMC medicine.* 2011;9:33.

261. Gotlieb WH, Saumet J, Beauchamp MC, et al. In vitro metformin anti-neoplastic activity in epithelial ovarian cancer. *Gynecologic oncology.* Aug 2008;110(2):246-250.

262. Isakovic A, Harhaji L, Stevanovic D, et al. Dual antiglioma action of metformin: cell cycle arrest and mitochondria-dependent apoptosis. *Cellular and molecular life sciences : CMLS.* May 2007;64(10):1290-1302.

263. Zakikhani M, Dowling R, Fantus IG, Sonenberg N, Pollak M. Metformin is an AMP kinase-dependent growth inhibitor for breast cancer cells. *Cancer research.* Nov 1 2006;66(21):10269-10273.

264. Camacho L, Dasgupta A, Jiralerspong S. Metformin in breast cancer - an evolving mystery. *Breast cancer research : BCR.* 2015;17:88.

265. Hirsch HA, Iliopoulos D, Tsichlis PN, Struhl K. Metformin selectively targets cancer stem cells, and acts together with chemotherapy to block tumor growth and prolong remission. *Cancer research.* Oct 1 2009;69(19):7507-7511.

266. Anisimov VN, Berstein LM, Egormin PA, et al. Effect of metformin on life span and on the development of spontaneous mammary tumors in HER-2/neu transgenic mice. *Experimental gerontology.* Aug-Sep 2005;40(8-9):685-693.

267. Tomimoto A, Endo H, Sugiyama M, et al. Metformin suppresses intestinal polyp growth in ApcMin/+ mice. *Cancer science.* Nov 2008;99(11):2136-2141.

268. Cusi K, Consoli A, DeFronzo RA. Metabolic effects of metformin on glucose and lactate metabolism in noninsulin-dependent diabetes mellitus. *The Journal of clinical endocrinology and metabolism.* Nov 1996;81(11):4059-4067.

269. Dowling RJ, Zakikhani M, Fantus IG, Pollak M, Sonenberg N. Metformin inhibits mammalian target of rapamycin-dependent translation initiation in breast cancer cells. *Cancer research.* Nov 15 2007;67(22):10804-10812.

270. Rashid A, Liu C, Sanli T, et al. Resveratrol enhances prostate cancer cell response to ionizing radiation. Modulation of the AMPK, Akt and mTOR pathways. *Radiat Oncol.* 2011;6:144.

271. Sanli T, Rashid A, Liu C, et al. Ionizing radiation activates AMP-activated kinase (AMPK): a target for radiosensitization of human cancer cells. *International journal of radiation oncology, biology, physics.* Sep 1 2010;78(1):221-229.

272. Zannella VE, Cojocari D, Hilgendorf S, et al. AMPK regulates metabolism and survival in response to ionizing radiation. *Radiotherapy and oncology : journal of the European Society for Therapeutic Radiology and Oncology.* Jun 2011;99(3):293-299.

273. Song CW, Lee H, Dings RP, et al. Metformin kills and radiosensitizes cancer cells and preferentially kills cancer stem cells. *Scientific reports.* 2012;2:362.

274. Dwarkanath BS, Zolzer F, Chandana S, et al. Heterogeneity in 2-deoxy-D-glucose-induced modifications in energetics and radiation responses of human tumor cell lines. *International journal of radiation oncology, biology, physics.* Jul 15 2001;50(4):1051-1061.

275. Beyer SJ, Jimenez RE, Shapiro CL, Cho JY, Jhiang SM. Do cell surface trafficking impairments account for variable cell surface sodium iodide symporter levels in breast cancer? *Breast cancer research and treatment.* May 2009;115(1):205-212.

276. Cazzaniga M, Bonanni B, Guerrieri-Gonzaga A, Decensi A. Is it time to test metformin in breast cancer clinical trials? *Cancer epidemiology, biomarkers & prevention : a publication of the American Association for Cancer Research, cosponsored by the American Society of Preventive Oncology.* Mar 2009;18(3):701-705.

277. Mohanti BK, Rath GK, Anantha N, et al. Improving cancer radiotherapy with 2-deoxy-D-glucose: phase I/II clinical trials on human cerebral gliomas. *International journal of radiation oncology, biology, physics.* Apr 1 1996;35(1):103-111.

278. Ben Sahra I, Tanti JF, Bost F. The combination of metformin and 2-deoxyglucose inhibits autophagy and induces AMPK-dependent apoptosis in prostate cancer cells. *Autophagy.* Jul 2010;6(5):670-671.

Materials & Methods

Materials:

The following chemicals were obtained from **Applied Biosystems:**

Agarose powder (15510-027), DNA loading dye (Blue juice, 10816-015), RPMI (31800-02), Heat inactivated FBS (10082-147), Antibiotic-Antimicotic (15240-062), 0.25% Trpsin-EDTA (25200-072), Lipofectamine (11668-027), HBSS (24020-117), 2X TaqMan master mix (Part No. 4384266), primer probe mix for human NIS (Hs00166567_m1), GAPDH (Hs02758991_g1), MicroAmp optical 384-well reaction plate with Barcode (4309849) and MicroAmp optical adhesive film kit (4313663), MTT (M6494), Superscript first strand cDNA synthesis kit (18080-051), First choice human breast total RNA (AM6952).

The following chemicals were obtained from **Sigma Chemicals:**

Poly L-Lysine (P8920), TRIS (T1378), Tween-20 (P9416), BSA (A7030), DAPI (D8417), β mercaptoethanol (M3148), PIPES (P2949), $CaCl_2$ (C7902), $MnCl_2$ (M8054), $MgCl_2$ (M4880), NaCl (71736), Ampicillin salt (A9518), G418 (A1720) DEPC (D5758), DMSO (D8418), EDTA, Ethidium bromide (E8751), L-15 (L4386), Propidium iodide (P4170), Para formaldehyde (P6148), Triton X-100 (T8787), HEPES (H4034), Ponceau (P7170), Bradford reagent (B6916), Potassium perchlorate (241830), Sodium iodide (), DEPC, Formamide (F9037), DAB enhanced liquid substrate system (D3939), monoclonal antibody for α tubulin (T5168), 2-DG (D6134), Metformin (1396309), L-Thyroxine (T2376), Methimazole (M8506), Ammonium Cerium (31173), Arsenic oxide (A1010), Sodium citrate (W302600), oligonucleotide primers

The following chemicals were obtained from **Qiagen:**

RNA extraction kit (74106), plasmid mini prep DNA extraction kit (27106), Gel extraction kit (28706), Glycosylation PCR array kit (PAHS-046), Superfect transfection kit (301305)

The following chemicals were obtained from **Thermo Fisher Scientific:**

Hydrogen peroxide (18755), Xylene (32297), Fusion polymerase (F-530S), dNTPs (R0191), monoclonal ntibody for γH2A.X (MA5-15130), Goat anti rabit secondary antibody labelled with Dylight633 (35562)

The following chemicals were obtained from **Merck, SRL or SD fine chemicals:**

Methanol (Merck 106009), Glacial Acetic Acid (Merck 100063), Sodium borohydrate (SRL 1948108), Ethanol (SD fine chemical 58051), Boric acid (Merck 194810), Formaldehyde (CB4F640180), Protease inhibitor cocktail (Merck 535140)

The following chemicals were obtained from **Abcam:**
Monoclonal antibody for NIS (ab17795), Annexin V FITC kit (14085), Prism ultra protein ladder (ab116028), Rabit polyclonal secondary antibody to mouse IgG(HRP) (ab6728)
The following chemicals were obtained from **Promega:**
Enliten ATP assay kit (FF2000), Luciferase assay system (E4030)

Vecta shield was obtained from **Vector laboratories** (H1000), Luria broth and agar was obtained from **HiMedia** (M557 &M575), restriction enzymes, T4 DNA ligase, molecular biology buffers and DNA gel ladder were obtained from **NEB**, Phusion high fidelity DNA polymerase was obtained from **Finzymes** (F-530S), MOPS was obtained from **Amresco**, Cell lysis buffer was obtained from **Cell signalling.**

The water used for the preparation of all solutions and reagents was Ultrapure water (Resistivity = 18 MΩ cm) obtained from a Milli-Q water plant (**Millipore,** Billerica, MA, USA).
Disposable plastic ware (certified DNase, RNase, and protease-free) was obtained from **Axygen**. Disposable sterile plastic ware for tissue culture was obtained from **Nunc**.

Methods:

i. Immunohistochemistry

Composition of TBS

500mM Tris base, 1500mM NaCl. Dissolve in 800ml autoclaved water. Adjust the pH 7.5 with HCl. Make up the volume to 1L. (10X buffer stock was made and diluted to 1X for use) (10X buffer stock was made and diluted to 1X for use)

Protocol

1. 5µm sized tissue sections were obtained in poly L-lysine coated slides.
2. Slides containing tissue sections were incubated at 60°C for overnight.
3. Next day tissue sections were deparaffinizaed by 3 washes of xylene for 10 minutes each at room temperature.

4. Tissue sections were air dried to remove remaining xylene and rehydrated with subsequent washes of alcohol from 100% to 90% and then to 75%.
5. Slides were washed under tap water for 15 minutes.
6. Next endogenous peroxidase was quenched with 3% H_2O_2 in methanol for 30 minutes in dark at room temperature.
7. Tissues were then subjected to antigen retrieval using 10 mM sodium citrate. For antigen retrieval sections were heated in sodium citrate solution serially at 850, 650 and 340 mega watts, each for 3 minutes. Tissues were kept for cooling till they come to room temperature.

   *Since fibroadenoma tissues contain large portions of fats, heating these tissues at high temperature results in detachment of the tissue section from slide, therefore in case of fibroadenoma tissues heating was reduced to 350 mega watts for 10 minutes.
8. After the antigen retrieval, sections were washed with TBST (0.01% Tween 20) twice each for 5 minutes at room temperature.
9. Tissues were then blocked with 5% BSA for one hour at room temperature.
10. Slides were then incubated at $4^{\circ}C$ overnight with the mouse monoclonal antibody against NIS diluted with TBS in 1:50 ratio.

    *For secondary control a tissue section was incubated with TBS instead of NIS antibody.
11. Slides were then washed for 5 minutes in TBST, 3 times and incubated for 1 hour with HRP conjugated anti mouse antibody diluted with TBS in 1:200 ratios.
12. Tissue sections were washed with TBST for 3 times, 5 minutes each.
13. After washing, tissues were incubated with DAB (1:30) (3, 3'-diaminobenzidine tetrahydrochloride) till the appearance of brown staining
14. Tissues were immediately washed under tap water.
15. Sections were further dehydrated with graded alcohol and xylene. For each batch of sample staining, a papillary thyroid carcinoma case was kept as positive control for NIS expression.
16. All the slides were counter stained with haematoxylin.
17. Slides were DPX mounted and observed under light microscope (Carl Zeiss).

ii. Immunofluorescence on tissue sections

1. Steps 1-8 were followed in the same way as for IHC mentioned in the section i.
2. In the next step autofluorescence was blocked with 1% sodium borohydrate in TBS for 30 minutes at room temperature in dark.

3. Tissue sections were washed twice with TBST (0.01% Tween 20) each for 5 minutes.
4. Tissue sections were blocked then with 1% BSA in TBS for 30 minutes at room temperature.
5. Tissue sections were incubated for overnight at 4°C with NIS primary antibody diluted 1:50 in TBS.
6. Next day tissues were washed with TBST twice, each for 5 minutes.
7. Slides were incubated for 1 hour at room temperature with anti mouse secondary antibody labeled with alexa fluor488 diluted 1:100 in TBS.
8. Unbound antibody was removed by 2 washes of TBST, each for 5 minutes.
9. Tissues were again blocked with 1% BSA in TBS for 30 minutes at room temperature.
10. Tissue sections were incubated with the 2nd primary antibody which is against HER2 diluted in (1:20) TBS and incubated for overnight at 4°C.
11. Next day tissues were washed with TBST twice, each for 5 minutes.
12. Tissues were then incubated for 1 hour in dark at room temperature with goat anti rabbit secondary antibody labeled with dylight 633 diluted (1:100) in TBS.
13. Tissues were washed 2 times with TBST for 5 minutes each.
14. For nucleus staining tissues were incubated for 2 minutes with DAPI (1mg/ml) diluted (1:50) in TBS.
15. Sections were washed twice with TBST, each for 5 minutes.
16. Tissue sections were mounted with vecta shield and images were captured under confocal microscope (LSM 510, Zeiss).

iii. RNA extraction from tissue samples:

Collection of samples:

BC tissues were collected from ACTREC operation theatre in cryo vials containing 1 ml of RNA later solution. Vials were immediately transferred to -80°C refrigerator.

RNA extraction was performed by kit obtained from qiagen. RNA was extracted by following protocol:

1. Before starting 10µl of β mercaptoethanol was added to 1 ml of RLT buffer and 350µl of this solution was added to each tube.
2. Cryovials containing BC tissue was removed from -80°C refrigerator and placed in ice. A small section from tumor tissue obtained was cut by sterile scalpel on a clean surface and dipped in 350µl RLT buffer. Rest of the tissue was immediately placed back in cryovial and kept in -80°C refrigerator.

3. The tissue in RLT buffer was homogenized thoroughly with the help of a handheld homogenizer for 30 seconds to 1 minute.
4. The lysate obtained was centrifuged at full speed for 3 minutes at room temperature.
5. Supernatant was removed carefully by pipetting and transferred to a fresh sterile microcentrifuge tube.
6. 350µl buffer RW1 was added to the RNeasy spin column. The lid was closed gently, and centrifuged for 30 seconds at 14, 000 rpm to wash the spin column membrane. The flow- through was discarded.
7. 500µl buffer RPE was added to the RNeasy spin column. The lid was closed gently, and centrifuged for 30 seconds at 14, 000 rpm to wash the spin column membrane. The flow- through was discarded.
8. 500µl buffer RPE was added to the RNeasy spin column. The lid was closed gently, and centrifuged for 2 minutes at 14, 000 rpm to wash the spin column membrane.
9. The RNeasy spin column was placed in a new 2 ml- collection tube, the lid was closed gently and centrifuged at full speed for 1 minute. This step ensured that any residual buffer RPE or ethanol was eliminated from the column.
10. The RNeasy spin column was placed in a new 1.5 ml- collection tube. 30- 50µl RNase-free water was added directly to the spin column membrane and centrifuged for 1 minute at 14, 000 rpm to elute the RNA.
11. The total RNA extracted was quantified by NanoDrop.

Bacterial cell culture

Luria-Bertani (LB) medium

A minimal growth medium is used for culture and maintenance of different *E. coli* strain DH5α. This strain is further used for harbouring desired plasmids. Powdered Luria broth (20 g) was dissolved in 800 ml deionized 'MilliQ' processed water (D/W) and the volume was adjusted to 1 litre (L) with D/W and sterilized by autoclaving. For making LB-agar plates, 35 g Luria agar powder was dissolved/ L sterilized by autoclaving and poured in 90 mm sterile plates. Specific antibiotic either ampicillin or kanamycin was added in the medium according to the plasmid antibiotic marker.

iv. Preparation of ultra-competent cells

Composition of transformation buffer (TB)

The following components were added to 100 ml of distilled water;

10mM PIPES, 15mM $CaCl_2$, 250 mM KCl, adjusted pH to 6.7 with 5N KOH, 55 mM $MnCl_2$, filter sterilized through 0.2 µ membrane filter.

Composition of super optimal broth (SOB)

Following components were mixed in the required volume of D/W; 2% Bactotryptone, 0.5%Yeast extract, 10 mM NaCl, 2.5 mM KCl, 10 mM $MgCl_2$, and 10 mM $MgSO_4$.

Protocol:

1. E.coli DH5α strain glycerol stock was streaked on a fresh LB agar plates without antibiotics and incubated overnight at 37°C.
2. Single colony was inoculated in 250 ml SOB broth and incubated at 18°C /250 rpm till O.D.600 reached ~0.4 (Approximately 3-4 days of incubation are required).
3. The cells were harvested by pelleting down at 4°C and resuspended in 80 ml of TB followed by incubation on ice for 10 minutes and centrifugation.
4. The cell pellet was resuspended in 18.6 ml TB. 1.4 ml (7%) DMSO was added to the cells and mixed completely.
6. 100µl aliquots of the cells were made in sterile microfuge tubes and snap frozen in liquid nitrogen followed by storage at -80°C.

v. Bacterial transformation

1. Competent cells (100 µl) were thawed on ice and mixed with 1-5ng of plasmid DNA or 20 µl of ligation mixture and incubated on ice for 30 minutes.
2. Heat shock is given to the mixture at 42°C for 60 sec and the sample was snap chilled on ice.
3. LB medium was added to the cells and incubated at 37°C for 60 minutes at 170 rpm.
4. The cells are then plated on an LB agar plate with the appropriate antibiotic.

vi. Plasmid DNA mini-preparation:

The plasmid isolation was performed following the procedure described in the Qiagen mini prep kit. Briefly following steps were performed.

1. Overnight grown, 5 ml of bacterial cultures transformed with plasmids were spun in a micro-centrifuge tube at 3500rpm for 15-20 minutes at 4°C.
2. Bacterial pellet was resuspended in 250µl of Buffer P1 (Re-suspension buffer containing RNase (10mg/ml)).
3. The cells were incubated at room temperature (RT) for 5 minutes and 250µl Buffer P2 (lysis solution) was added followed by invert mixing.
4. The cells were incubated at RT for 5 minutes and 350µl of Buffer N3 (neutralizing solution) was added and incubated at RT for 5 minutes. after complete invert mixing.
5. The above mixture was then centrifuged at 12,000 x g for 10 minutes.
6. The supernatants from step 5 was applied to the QIAprep spin column by decanting or

pipetting.

7. The column was centrifuged for 30–60 seconds and the flow-through was discarded.
8. QIAprep spin column was washed by adding 0.75 ml buffer PE and centrifuging for 30–60 seconds.
9. The flow-through was discarded and centrifuged at full speed for an additional 1 minutes to remove residual wash buffer.
10. The QIAprep column was placed in a clean 1.5 ml micro centrifuge tube. DNA was eluted by addition of 50 µl buffer EB (10 mM Tris HCl, pH 8.5) or water to the centre of each QIAprep spin column and centrifuged for 1 minute.
11. The eluate contains pure DNA which is measured by nanodrop spectrophotometer.

vii. Polymerase Chain Reaction (PCR)

Following contents were mixed in PCR tube and PCR was set in a thermal cycler (Bio-Rad, CA).

Component	Volume
GC buffer (1X)	4µl
dNTP (200µM each)	1µl
Fwd primer (0.5µM)	0.5µl
Rev primer (0.5µM)	0.5µl
Template DNA (20ng)	1µl
DMSO	0.6µl
Fusion polymerase	0.2µl
Milli Q water	12.4µl

The cycling profile was standardized according the target DNA to be amplified. Amplified product is visualised and analysed by agarose gel electrophoresis.

viii. Agarose gel electrophoresis and Gel extraction:

Composition of the tris borate–EDTA buffer (TBE)

0.9 M Tris base, 0.9 M Boric acid, 0.02 M EDTA

(10X buffer stock was made and diluted to 1X for use)

Protocol

1. 0.8% agarose gel was casted on the gel tray. 2µl of EtBr (10mg/ml) was added while casting the gel as an intercalating agent.
2. Solidified gel was transferred to the electrophoresis tank that has electrode fitted to it at the two ends.

3. The required 1X TBE buffer is then poured into the tank over the gel. Before loading the PCR product into the wells, the PCR product is mixed with the loading dye containing glycerol and bromophenol blue which indicate the DNA migration front.
4. Standard DNA markers of known fragment sizes were run in parallel to the samples in order to have standard reference. The gel was run at a constant voltage.
5. EtBr stained DNA bands were visualized and documented on a gel documentation system.

ix. Gel extraction

The PCR amplified product was gel extracted and purified by using Qiagen gel extraction kit. Briefly, the following procedure was followed:

1. The DNA fragment from the agarose gel was excised with a clean, sharp scalpel.
2. The gel slice was weighed in a micro centrifuge tube. 3 volumes Buffer QG was added to 1 volume gel (100 mg ~ 100 µl).
3. Reaction was incubated at 50°C for 10 minutes (or until the gel slice has completely dissolved). Vortex the tube every 2–3 minutes to help dissolve gel.
4. 1 gel volume of isopropanol was added to the sample and mixed. Thereafter, a Qiaquick spin column were placed on a 2 ml collection tube and the above reaction mix was added in the column.
5. The tube was incubated for 1-2 minutes and centrifuged for 1 minute at 13000 rpm.
6. The flow-through was discarded and further washed with 0.5ml of buffer QG by centrifugation for 1minute at 13000rpm.
7. Buffer PE (0.75 ml) was added to QIAquick column and was incubated for 5 minutes before centrifuging for 1 minute at 13000 rpm. The flow-through was discarded and was given another wash with buffer PE.
8. An additional dry spin was given to the column and the column was placed in a clean 1.5 ml micro centrifuge tube.
9. To elute DNA, 50 µl Buffer EB (10 mM Tris·Cl, pH 8.5) or water was added to the centre of the QIAquick membrane and centrifuged at 13000 rpm for 1 minute.

x. Restriction digestion

Both insert and vector were digested with two RE enzymes simultaneously. NEB buffer that results in maximum activity of both the enzymes was chosen using the enzyme activity chart. Before beginning with digestion the recommended buffer was thawed completely on ice and the water bath was set at 37°C. The reaction mixture for digestion was incubated at 37°C water bath, overnight.

xi. Ligation

The ligation reaction was set depending upon the concentration of the insert. Ideally the vector to insert ratio is (1:3) which is essential for carrying out successful ligation reaction.

1. The ligation reaction was carried out at 4°C for overnight using T4 DNA ligase and transformed next day in the DH5α competent cells.
2. After transformation ampicillin containing LB agar plates were placed in the incubator for overnight. After 16-18 hours of incubation, the plates were checked for colonies.
3. Colonies were cultured in LB broth and plasmid was isolated. Screening for the positive clone was performed by restriction digestion.

Positive clone obtained by cloning was further verified by DNA sequencing.

Sequencing was performed using the ABI automated DNA sequencer present in the genomics facility of ACTREC.

Cell culture

Composition of Phosphate Buffered Saline (PBS) (pH 7.4) 10X / 1L:

80g NaCl, 2g KCl, 14.4g Na_2HPO_4, 2.4g KH_2PO_4, Dissolve in 800ml autoclaved water. Adjust the pH 7.4. Make up the volume to 1L.

xii. Cell lines & subculturing

Standard aseptic practice was followed for performing cell culture. All of these adherent cell lines were maintained and sub-cultured in their respective media supplemented with 10% FBS, 100U/ml penicillin and 100 μg/ml streptomycin solutions.

xiii. Procedure of subculturing

1. Spent medium was aspirated off from the culture flask using a 10 ml glass pipette.
2. The cells were given two gentle washes with sterile phosphate buffered saline (PBS) (1X)
3. The cells were treated with 1 ml trypsin (for a 10 cm culture plate) and incubated in a 5% CO_2 incubator for 2- 3 minutes.
4. The trypsin was neutralized by addition of complete RMPI medium (1 part Trypsin: 2 parts complete RPMI).
5. The cells were flushed in and out thoroughly using a micropipette in order to ensure most of the cells had detached from the surface of the culture plate and to obtain a homogenous cell suspension.
6. A suitable cell density was transferred to a new culture plate and provided with fresh complete RPMI for their optimal growth and survival.

xiv. Cryopreservation

1. Adherent cells in culture were trypsinized and a homogenous cell suspension was obtained.
2. The cell suspension was centrifuged at a speed of 1500 rpm at 4 °C for 3-5 minutes in order to obtain a cell pellet.
3. Freezing medium was prepared by adding 90% FBS, 0-5% incomplete medium and 5-10% DMSO.
4. 1-2*10^6 cells were suspended in 1 ml of freezing medium, mixed thoroughly and immediately transferred to the cryopreservation vial.
5. The cryovial was then placed in an isopropanol containing freezing container which allows temperature decrease at the rate of -1°/ hour in a -80°C refrigerator. Finally cells were transferred to liquid nitrogen container maintained at -196°C.

xv. Revival of cryopreserved cells

1. Cryopreserved cells were thawed in a water bath preset at 37°C.
2. The thawed cells were suspended in 1 ml of complete RPMI medium.
3. The contents of the tube were centrifuged at a speed of 1500 rpm at 4°C for 2- 3 minutes to obtain the cell pellet.
4. The cell pellet was resuspended in a suitable volume of complete RPMI medium and transferred to a new culture flask and supplied with fresh complete medium.
5. The culture flask was incubated in a 5% CO_2 incubator for maintenance of the revived culture.

xvi. Transfection

Transfection was done using Lipofectamine/ Superfect transfection reagent as per manufacturer's instructions. In brief, the following procedure was followed for transient/stable transfection of cell lines.

Protocol for lipofectamine based transfection:

1. Prior to the day of transfection cells were seeded in culture vessel at a confluency of 70- 90%.
2. Four amounts of lipofectamine was diluted in opti MEM or incomplete media. The complex was incubated for 5 minutes.
3. In a separate tube required amount of DNA is diluted in opti MEM media. Volume of lipofetamine, DNA and opti MEM media are decided by the culture vessel chosen for

transfection. The complex was incubated for 5 minutes.

4. Diluted DNA was added to diluted lipofectamine in a 1:1 ratio and the complex was incubated for 25 minutes.
5. In the meantime the medium from the culture vessel was aspirated and fresh complete media was added to to the cells.
6. After 25 minutes of incubation, definite amount of complete media was added to the transfection mixture and this was added in the culture vessel. The plate was swirled gently to uniformly distribute the complex and incubated at 37°C, 5% CO_2 incubator.
7. After 6 hours, the transfection media was aspirated, washed with 1X PBS and complete media was added to the cells. For stable transfection, after 48 hours of transfection, the cells are trypsinized and are subcultured in the selection media containing G418.

Protocol for superfect based transfection:

1. Prior to the day of transfection cells were seeded in culture vessel at a confluency of 70- 80%.
2. DNA-Superfect reagent complex were prepared by adding required amount of plasmid/s and transfection reagent in appropriate amounts of incomplete medium with gentle mixing. This mixture was then incubated for 10 minutes at room temperature.
4. In the meantime. The medium was aspirated from the culture vessel and washed twice with 1X PBS.
5. Definite amount of complete media was added to the transfection mixture and this was added in the culture vessel. The plate was swirled gently to uniformly distribute the complex and incubated at 37°C, 5% CO_2 incubator.
6. After 3 hours, the transfection media was aspirated, washed with 1X PBS and complete media was added to the cells.

Note: For transfection with ACNITFL2 and integrase vector both the plasmids were used in a 1:1 ratio.

xvii. MTT Assay

1. The cells were seeded in 96 well plate at a density of 3000 cells per well. The experiment was done in triplicate.
2. Next day cells were treated with various drug concentration of 2-DG or metformin.
3. After 48 hours of treatment 20µl of 5mg/ml MTT was added into each well and incubated for 5 hours.

4. The spent media from each well was removed completely.
6. 200µl DMSO per well was added to solubilise the dye.
7. It was then kept in shaker for 15-20 minutes until the whole dye gets solubilised and then preceded for measuring the absorbance at wavelength 560nm and 670nm.

Note- The absorbance at 560nm is subtracted from the absorbance at 670nm to remove the background caused by the presence of DMSO and % viability is calculated with respect to untreated cells.

xviii. Propidium iodide (PI) staining & cell cycle analysis

1. 1-2*10^6 cells were harvested and washed with 1×PBS after centrifugation at 1200rpm for 5 minutes and supernatant was discarded.
2. Ice cold 70% ethanol was added (1ml/10^6 cells) drop wise with gentle tapping and cell pellet was resuspended.
3. The cells were stored at -20°C for overnight.
4. Fixed cells were collected and pelleted by spinning at 1200 rpm for 5 minutes.
5. The cells were washed twice with 1×PBS, centrifuged and supernatant was discarded.
6. Cells were treated with 30µl of 10µg/µl of RNase A and incubated at 37°C incubator for 10 minutes.
7. For PI staining 500µl of 50µg/ml stock of PI solution was added into each FACS tube in dark and tubes were incubated at 37°C incubator for 30 minutes in dark.
8. The FACS-tubes were tapped every 10 minutes to mix the cell and buffer properly. The cells were passed through a 26 gouge needle followed by PI fluorescence acquisition using FACS Caliber. Data was analyzed using Cell Quest software.

xix. Immunoflurescence assay on breast cancer cells:

1. 1*10^6 cells were seeded on a sterile coverslip in a 35 mm culture plate and incubated in a 5% CO_2 incubator overnight.
2. Next day cells were washed with 1xPBS thrice, each for 5 minutes at 37°C.
3. The cells were fixed using 4% paraformaldehyde (4% PFA prepared in 1X PBS) and incubated for 10 minutes at 37°C.
4. For staining of nuclear proteins, an additional step of permeabilization was performed by treating cells with 0.2% tritonX100 in 4% PFA for 7-10 minutes at room temperature.
5. The fixed cells were given three washes with 1xPBS for 5 minutes each at room temperature.

6. Non- specificity was reduced by incubating the cells in BSA (2% BSA prepared in 1X PBS) for 30 to 45 minutes at room temperature.
7. The cells were then incubated overnight at 4°C with antibody diluted in PBS (1X).
8. Cells were again washed with 1XPBS thrice, for 5 minutes each at room temperature.
9. From this point onwards, all steps of the experiment were performed in dark.
10. Cells on the coverslip were incubated for 30 to 45 minutes at room temperature with secondary antibody diluted in 1XPBS.
11. Cells were given three washes of 1XPBS each for 10 minutes at room temperature for the removal of unbound secondary antibody from cells.
12. Nucleus of the cells was stained with DAPI for 1 minute and cells were again washed with 1XPBS for 5 minutes.
13. The coverslips were mounted onto glass slides using Vecta Shield and images were taken using a Confocal Microscope (Zeiss).

xx. Iodide uptake assay

Non radioactive colorimetric method

The standard assay for NIS function is based on the measurement of radioiodide uptake (^{125}I) in NIS expressing cells. However its applications are limited due to cost and safety issues. Thus we used a simple spectrophotometric assay for the determination of iodide accumulation in NIS expressing cells based on the catalytic effect of iodide on the reduction of yellow cerium (IV) to colorless cerium (III) in the presence of arsenious acid (Sendell- Kolthoff reaction). Assay reliability is tested by using known inhibitors of iodide uptake like ClO_4^- anions.

Composition of ammonium cerium sufate (42mM):

Ammonium cerium (IV) sulfate hydrate (12.53 gm) was dissolved in water (200 ml). Concentrated H_2SO_4 (50 ml) was then added to the solution, which was cooled with an ice bath. After cooling, the solution was diluted to 500 ml with water. This solution was diluted fourfold with water prior to use.

Composition of sodium arsenite solution (96mM):

Arsenic(III) oxide (4.75 gm) and NaCl (24 g) were dissolved in 2 M NaOH (50 ml). The mixture was then diluted to 500 ml with water and centrifuged to remove insoluble material. This solution was diluted fourfold with water prior to use.

Protocol:

1. 30,000 cells were seeded in triplicate in a 96- well plate and incubated overnight in a 5% CO_2 incubator.
2. Media was first decanted only from wells seeded with cells that were to be blocked with $KClO_4$, an inhibitor to iodide uptake by NIS. Upto 90 µl of Uptake Buffer (10mM HEPES in HBSS) was added to each of these wells.
3. These cells were then treated with $KClO_4$ (30µM) and incubated in a 5% CO_2 Incubator for 30 minutes.
4. Media was decanted from the remaining wells of the 96- well plate and was replaced by 90 µl of uptake buffer per well.
5. Next, NaI (100 µM) was added to all the wells and the plate was incubated for 60 minutes in a 5% CO_2 Incubator.
6. The wells were washed with an appropriate volume of chilled uptake buffer following the incubation. This was done to terminate any further uptake of iodide by the cells.
7. Remaining uptake buffer was removed from the wells by inverting over a tissue paper.
8. 100 µl Ammonium Cerium Sulphate (42 mM), followed by 100 µl Sodium Arsenite (96 mM) were added to each well and incubated for 30 minutes in dark at room temperature.
9. The absorbance at 420 nm was recorded in a spectrophotometer.

Radioactive iodide uptake assay:

1. 50,000 cells were seeded in duplicate in 24 well plate and incubated overnight in a 5% CO_2 incubator.
2. Media was first decanted only from wells seeded with cells that were to be blocked with $KClO_4$, an inhibitor to iodide uptake by NIS.
3. These cells were then treated with $KClO_4$ (30 µM) in uptake buffer and incubated in a 5% CO_2 Incubator for 30 minutes.
4. Media was decanted from the remaining wells of the 24 well plate and was replaced by uptake buffer.
5. Next, 500µl $Na^{125}I$ (2 µCi/ml) was added to all the wells and the plate was incubated for 60 minutes in a 5% CO_2 incubator.
6. The wells were washed with an appropriate volume of chilled uptake buffer following the incubation. This was done to terminate any further uptake of iodide by the cells.

7. Cells were collected by trpsinization and remaining $Na^{125}I$ inside the cells was measured by beta counter.

xxi. Iodide effux assay

Efflux assay is performed to evaluate the time for which iodide retains inside NIS expressing cells in absence of any organification system.

Protocol:

1. 50000 cells were seeded in 24 well plate a day prior to the experiment. Cells were seeded in duplicate for each time point.
2. Next day the media was decanted off and 500µl uptake buffer containing $Na^{125}I$ (2µCi/ml) was added in each well.
3. $Na^{125}I$ in uptake buffer was incubated for 1 hour and at the end of time point $Na^{125}I$ containing uptake buffer was removed from each well plate.
4. Wells were washed with chilled uptake buffer.
5. Except for the well representing 0 time point, in all the wells uptake buffer without $Na^{125}I$ was added and plate was incubated at $37^{\circ}C$ CO_2 incubator.
6. From the well representing 0 time point, cells are tripsinized, collected in tube and radioactivity is measured by beta counter.
7. In the same way from all the wells cells are trypsinized and remaining activity is measured at the mentioned time points by beta counter.

xxii. RNA Extraction from cells

RNeasy mini kit (Qiagen) was used for the extraction of total RNA from cells.

Protocol:

1. A 70-80% confluent monolayer of cells in culture was trypsinized and cells were pelleted down by centrifugation at a speed of 1500 rpm for 5 minutes at 4°C.
2. The cells were given two gentle washes with sterile PBS (1X) and taken in a 1.5 ml eppendorf tube.
3. The cells were completely resuspended in 350 µl buffer RLT by pipetting to mix.
4. The cell suspension was then homogenized using a hand held homogenizer for 30 seconds.
5. 350µl of 70% Ethanol, prepared in Diethylpyrocarbonate (DEPC) treated water was added to the homogenized lysate and mixed well by pipetting.
6. Upto 700µl of the sample was transferred to an RNeasy spin column placed in a 2 ml-collection tube. The lid was closed gently and centrifuged for 30 seconds at 14, 000 rpm. The flow- through was discarded.

7. Rest of the steps was same as mentioned in section iii from step 6.

xxiii. Quality control of RNA

Before preparation of cDNA from the RNA obtained, quality of RNA was checked in a denaturing agarose gel. The RNA sample was thus run on a denaturing agarose gel electrophoresis. RNA bands were visualized by ethidium bromide staining.

Composition of 1% denaturing agarose gel:

Agarose (1.08g) was added to 76.5 ml RNase free water and boiled to melt agarose completely. 10X MOPS buffer (9ml) and formaldehyde (4.5ml) and EtBr was added. The gel is poured in the gel casting tray with a comb and allowed to solidify.

Protocol:

1. The denaturing agarose gel was cast and 1µg RNA was loaded onto the gel along with the RNA loading dye. The composition of the RNA loading dye is as follows:

Component	Amount
RNA	2µg
MOPS (10X)	1µl
Formamide	3µl
Formaldehyde	1µl
Blue juice loading dye(10X)	1µl
RNase free water	To 10µl

2. After loading the RNA sample gel was run at 80 V.
3. EtBr staining for visualization of bands was carried out by placing the gel in a chamber immersed in 100 ml DEPC treated water containing 5µl EtBr dye for 30-40 minutes.
4. Destaining was performed by immersing the gel in 100 ml DEPC treated water and kept on slow rocking for 15 – 20 minutes. This step was repeated once more.
5. Visualization of bands was carried out using a UV transilluminator.
6. RNA was considered as of good quality when 2 bands were visualized on gel and the density of upper band was twice the density of the lower band.

xxiv. cDNA synthesis for real time PCR:

cDNA from RNA is prepared by superscript III first strand synthesis system (Invitrogen). This kit allows cDNA synthesis from 1pg to 5µg RNA.

Protocol:

1. All the contents of the kit are thawed and briefly centrifuged before use.

2. Following components are added in a 0.6 ml tube.

Components	Volume
1 µg total RNA	nµl
50µM oligo$(dT)_{20}$	1µl
50ng/µl random hexamer	0.5µl
10mM dNTP mix	1µl
DEPC treated water	to 10µl

3. The mix of the above components were incubated in a dry bath at 65°C for 5 minute and then placed on ice for at least 1 minute.
4. For cDNA syntheses following components were mixed in the same order as indicated.

Component	Volume
10X RT buffer	2µl
25mM $MgCl_2$	4µl
0.1M DTT	2µl
RNase OUT (40U/µl)	1µl
Superscript III RT	1µl

5. 10µl of cDNA synthesis mix was added to 10 µl of RNA and primer mix made previously. Both the mixtures are mixed gently and briefly centrifuged.
6. The mixture is placed in a PCR tube and following cycle is run in a thermal cycler

Temperature	Time
25°C	10 min
50°C	50 min
85°C	5 min

7. Reaction is chilled on ice and collected by brief centrifugation.
8. 1µl RNase H was added in each tube and the reaction is incubated at 37°C for 20 minutes.
9. cDNA made is either used immediately for PCR or stored at -20°C.

xxv. Real- time PCR

Real- time PCR based on TaqMan chemistry was performed to check NIS mRNA expression in NIS expressing clonal variants. The housekeeping gene Glyceraldehyde 3-phosphate dehydrogenase (GAPDH) was used for normalization of results. The PCR plate was run on a real time cycler (Quant Studio 12K Flex, Applied Biosystems)

Protocol:

1. cDNA obtained from reverse transcription reaction was diluted to 10 ng /µl with DEPC-treated Milli-Q water for use in the PCR reaction.
2. In a separate tube TaqMan master mix and TaqMan primer and probe mix for the gene of interest were added in the following concentration:

Component	Volume
2X TaqMan master mis	2.5µl
TaqMan Primer+probe	0.25µl
RNase free water	to 4µl

3. 1µl of diluted cDNA (10ng/µl) was added to the TaqMan master mix and primer + probe mix and this whole mixture was added to a well of 396 well real time PCR plate.
4. In 1 of the sample TaqMan master mix and primer + probe is mixed with RNase free water instead of cDNA. Ct value from this well was used as non template control to detect any contamination or non specificity in the reaction.
5. GAPDH gene was used as an endogenous control.
6. For each sample and gene, reaction was carried out in triplicate and average Ct value was used to determine fold change.
7. After addition of reaction in different wells, PCR plate is sealed.
8. The plate was centrifuged briefly to remove any air bubble and to bring the mixture at the bottom of the well.

9. The real time PCR was performed using following PCR protocol:

PCR step	Temperature	Time
Initial denaturation	95°C	5min
Denaturation	95°C	45sec
Primer annealing	60°C	45sec
Primer extension	72°C	45sec
Final extension	72°C	5min
Hold	72°C	5min

xxvi. Western blot analysis

Preparation of sample

1. Cells were washed with cold 1X PBS (2x) in 6-well plate.
2. 50µl of RIPA buffer was added to cells and plate was incubated on ice for 5 minutes.
3. Cells were gently scraped using cell scraper and collected in an ice cold eppendorf tube.
4. Cells were vortexed vigourlsly for 30 seconds.
5. Cells were incubated on ice for 2 hours on ice with intermediate vortexing.
6. The lysed cells were then sonicated at 10% amplitude for 10 seconds for 3 cycles.
7. Lysed cells were centrifuged at 14000rpm 4°C for 45minutes.
8. The supernatant was collected and stored at 4°C.
9. Protein estimation was done using the above lysate.

Protein estimation by Bradford assay:

Bradford is a colorimetric protein assay based on the absorbance shift of the dye Coomassie Brilliant Blue G-250 in which under acidic conditions the red/brown form of the dye is converted into its bluer form to bind to the protein being assayed. This colour change is estimated by using the formula obtained by plotting the absorbance of standards (1-5 µg/ml) in a linear regression analysis.

Protocol:

1. BSA standards were made by serially diluting 1mg/ml stock in transparent 96 well flat bottom plates.

Concentration	Volume of BSA	Volume of Milli Q water
Blank	0	5µl
1µg	1µl	4µl
2µg	2µl	3µl
3µg	3µl	2µl
4µg	4µl	1µl
5µg	5µl	0

2. Absorbance was measured at 595nm, values were subtracted against the blank and a standard curve was plotted by using the linear regression analysis. The formula derived from the standard curve was used for estimating protein concentration of the cell lysates.
3. Lysates were diluted 5X using 1X PBS.
4. 250µl of Bradford reagent was added in each well of a 96 well plate.
5. 5µl of protein lysate was added per well and mixed thoroughly.
6. Absorbance was measured at 595nm in a spectrophotometer.
7. Protein concentration was calculated using the formula derived from the standard curve.

Appropriate volume of protein lysate for the desired concentration was taken and mixed with gel loading dye. The reaction mix was heated at 37°C for 30minutes in water bath. and a short spin was given. The samples were kept on ice until they were loaded on the gel.

Composition of 30% Acrylamide

(30% acrylamide / 0.8% bisacrylamide) weight/volume in distilled water

Composition of Resolving Buffer

1.5mM Tris base, adjust the pH to 8.8 using 1N-HCl

Composition of Stacking Buffer

0.5mM Tris base, adjust the pH to 6.8 using 1N-HCl

Composition of Running Buffer

25mM Tris-Cl- 3.208g; 200mM Glycine-15.012g;0.1%w/v SDS

Composition of Transfer buffer

25mM Tris base, 190mM Glycine, 0.04% SDS, 20% methanol

Composition of blocking buffer

1X TBS with 5% milk

Composition of Wash buffer (TBSt)

1X TBS with 0.05% Tween 20

Composition of stripping buffer

20%SDS, 100µM β-mercaptoethanol and 50µM Tris, pH6.8

Contents of 7.5% resolving gel (8ml):

Milli Q	**30% acrylamide**	**1.5M Tris-Cl pH-8.8**	**10% SDS buffer (w/v)**
3.8ml	2ml	2ml	80µl

Degassing was carried out with pipette and 80µL of 10% APS and 8µL TEMED was added followed by gentle mixing.

Contents of 4% stacking gel (5ml)

Milli Q	**30% acrylamide**	**0.5M Tris-Cl pH-6.8**	**10% SDS buffer (w/v)**
3ml	0.67ml	1.25ml	50µl

50µL of 10% APS and 5 µL of TEMED was added to the mixture followed by swirling.

Preparation of sample

Appropriate volume of protein lysate for the desired concentration was taken and mixed with gel loading dye. The reaction mix was heated at 100°C on dry bath for 3 minutes and a short spin was given. The samples were kept on ice until they were loaded on the gel.

Composition of blocking buffer

1X TBS with 5% BSA

Composition of Wash buffer (TBSt)

1X TBS with 0.05% Tween 20

Composition of stripping buffer

20%SDS, 100μM β-mercaptoethanol and 50μM Tris, pH6.8

Protocol

1. Glass plates were cleaned thoroughly and were set up carefully in the casting stand.
2. According to the protein of interest, the required percentage of resolving gel was prepared.
3. Immediately the resolving gel solution was loaded between the glass plates using the pipette and the gel was overlaid with 1ml of milliQ.
5. The gel was allowed to polymerize for 35-40 minutes.
6. After the resolving gel was solidified completely, the MilliQ layer was washed thoroughly and the stacking gel was prepared.
7. The wells for loading the samples were formed by placing the 10-well comb. The gel was allowed to polymerize for 15-25 minutes.
8. The solidified gel was placed in the cassette and fitted with electrodes in the tank.
9. The tank was filled with 1X running buffer till (1/4)th of its volume. The comb was then gently removed and the wells were washed with the buffer to remove the traces of any acryl/bisacrylamide deposits.
10. The sample prepared was then loaded into respective wells and 4μL of pre-stained ladder was also loaded in one of the wells.
11. The gel electrophoresis was performed at 60V, 400mA. After the sample entered the resolving gel the voltage was increased to 80V. The run was stopped as soon as the dye reached the bottom of the gel.
12. The gel, blotting paper and nitrocellulose membrane were then soaked in 1X transfer buffer and incubated for 10 minutes.
13. Onto the base of the Trans blot system the two soaked blotting papers were placed one after another, the transfer buffer was poured on top of the membrane and the air bubbles were removed carefully. Then, the nitrocellulose membrane was placed and the gel was placed over it properly.
14. The remaining two blotting papers were placed on the top of the gel and same as before the transfer buffer was poured, ensuring that the bubbles were removed. Then, the system was started and the transfer was set to 13V, 400mA for 1 hour.
15. After complete transfer the membrane was removed carefully and then incubated in 10ml of 5% non-fat milk for 1 hour on a shaker.

16. After blocking, the membrane was probed with NIS primary antibody and incubated overnight at 4^{o}C with gentle shaking.
17. Next day, the membrane was washed thrice with the wash buffer (1X TBST) and then incubated with the secondary antibody for 1 hour.
19. After the secondary Ab incubation the membrane was again washed thrice with the wash buffer.
20. The proteins present on the membrane could be visualized by using the advance chemiluminiscence detection system.

Stripping and reprobing the membrane:

1. In order to reprobe the membrane with another primary antibody stripping protocol is used.
2. For stripping the membrane was incubated with the stripping buffer for 10 minutes at RT.
3. The membrane was then washed thrice with 1X TBST, blocked with the blocking buffer for 1 hour, then incubated with primary antibody overnight at 4^{o}C with gentle shaking.
4. The next day, the membrane was again washed with 1X TBST, incubated with secondary antibody for 1-2 hour at RT with continuous shaking and then washed with wash buffer and developed in dark with the ECL detection system.

xxvii. cDNA synthesis for glycosylation PCR array

cDNA synthesis was performed using the RT^{2} First Strand cDNA synthesis kit (Qiagen).

Protocol:

1. All the contents of the kit were thawed on ice and vortexed briefly to bring the contents to the bottom of the tube
2. The genomic DNA elimination mix was prepared for each RNA sample. It was mixed by gentle pipetting and centrifuged briefly.

Component	Amount
RNA	400ng
Buffer GE	2µl
RNase free water	to 10µl

3. The genomic DNA elimination mix was incubated for exactly 5 minutes in a dry bath preset at 42°C, and then placed immediately on ice for at least 1 minute.
4. The reverse transcription mix was prepared as follows:

Component	Volume
Buffer BC3 (5X)	4µl
Control P2	1µl
RE3 Reverse transcriptase mix	2µl
RNase free water	3µl

5. 10 µl reverse transcriptase mix was added to 10 µl genomic DNA elimination mix and mixed by gentle pipetting.
6. The mix was incubated at 42°C for exactly 15 minutes and the reaction was immediately stopped by incubating at 95°C for 5 minutes.
7. 91µl RNase free water was added to each reaction and mixed by gently pipetting several times.
8. The cDNA synthesized was stored at -20°C until required.

xxviii. Glycosylation PCR array (RT^2 profiler PCR array system, Qiagen)

PCR arrays or microarrays are one of the most reliable and sensitive gene expression profiling technologies for analyzing a panel of genes in signal transduction pathways, biological processes or disease related gene networks.

The Glycosylation PCR Array supplied by Qiagen profiles the expression of 84 key genes encoding enzymes that post translationally add or remove sugar residues to and from proteoglycans and glycoproteins. Running this array on a real time PCR machine lets us analyze the expression of a focused panel of genes involved in protein glycosylation.

The PCR array uses SYBR Green as the fluorescent reporter dye during the real time cycling. SYBR Green detects PCR products by binding to double stranded DNA present in the sample.

The RT^2SYBR Green qPCR Matermix (Qiagen) consists of the following:

- HotStart DNA *Taq* Polymerase
- PCR Buffer
- dNTP mix (dATP, dCTP, dGTP, dTTP)
- SYBR Green dye

Protocol:

1. The contents of the RT^{2}SYBR Green qPCR mastermix were briefly centrifuged to bring the contents to the bottom of the tube.
2. The PCR components mix was prepared in a loading reservoir
   PCR components mix contains the following:

Component	Volume
RT^2 SYBR green qPCR mastermix (2X)	650µl
cDNA synthesis reaction	102µl
RNase free water	548µl

3. The PCR components mix was dispensed as equal aliquots into each well of the RT^2 Profiler PCR Array.
4. The PCR Array plate was run on a real- time cycler (Quant Studio 12K Flex, Applied Biosystems)
5. The PCR reaction cycle was as follows:

Initial Denaturation	95 °C for 5 minutes	
Denaturation	95 °C for 45 seconds	35 times
Primer Annealing	60 °C for 45 seconds	
Primer Extension	72 °C for 45 seconds	
Final Extension	72 °C for 5 minutes	
Hold	4 °C for 5 minutes	

6. The raw data obtained was analyzed using a web- based software (http://www.sabiosciences.com/dataanalysis.php)

xxix. Clonogenic assay

1. After drug/ radiation/ ^{131}I therapy cells were trypsinized, washed with 1X PBS and counted in a cell counter.
2. For MCF-7 cells 500 cells and for MDA MB231 cell line 1000 cells were seeded in each well of 6 well plate. For ZR-75 cells 1000 cells were seeded in 60mm plate.
3. For each treatment cells were seeded in duplicate.
4. Cells were then incubated in 5% CO_2 at 37°C for 14 days.

5. Cells were feeded with fresh media at duration of 3 days.
6. After 14 days, cells were washed thrice with PBS for 5 minutes and fixed in 1ml chilled formalin i.e. 10% formaldehyde in PBS for 20minutes at 4°C.
8. Formalin was removed after 20 minutes and cells were washed with 1XPBS (X3).
9. After washing cells were stained with 1ml of 0.5% crystal violet in 25% methanol for 5 minutes at room temperature.
10. After 5 minutes, crystal violet was removed and excess stain was washed with fresh water.
11. Number of colonies was counted under microscope. Colonies consisting of at least 50 cells were counted.
12. Survival fraction was calculated using the formula mentioned in previous literature.

xxx. Annexin V staining for apoptosis assay

Annexin V staining to detect apoptosis is based on the principle that during apoptosis the membrane phosphatidyl serine in cells gets translocated from inner face to the cell surface of plasma membrane. The translocated phosphatidyl serine can be easily detected by staining with fluorescent dye conjugated annexin V molecule. The staining of the samples with propidium iodide along with annexin V allows differentiation between apoptosis and necrosis. Annexin V staining was performed by apoptosis kit from Abcam. Brief protocol is as follows:

1. 1-5*10^5 cells were seeded in 24 well plates a day prior to experiment.
2. Cells were treated with drug/ ^{131}I/ combination of both.
3. At the end of treatment the media as well as cells were collected by centrifugation.
4. Cells were resuspended in 500µl of 1Xbinding buffer.
5. To this 5µl annexin V-FITC and 5µl of propidium iodide was added.
6. For controls the 2*10^6 untreated cells were collected along with the media. These cells were resuspended in 2ml of 1X binding buffer. In 4 tubes 500µl of this cell suspension was distributed. In 1 tube only 5µl annexin V is added, in 2nd tube only 5µl propidium iodide is added, in 3rd tube both 5µl annexin V and 5µl propidium iodide is added and in the 4th tube none of the stain is added.
7. All the tubes were incubated at room temperature for 5 minutes in the dark.
8. The binding of the dyes were analyzed by flow cytometry using FITC detector (FL1) and phycoerythrin signal detector (FL2). The data was analyzed using cell quest software.

xxxi. Luciferase assay:

The luciferase reporter assay is commonly used as a tool to study gene expression at the transcriptional level. Luciferases make up a class of oxidative enzymes found in several species that enable the organisms that express them to 'bioluminesce' or emit light. The light emitted is a by-product of the oxidative reaction catalyzed by the luciferase enzyme. The protocol is as follows:

1. Transfected cells were collected and lysate was made by passive lysis buffer.
2. 10µl of lysate was added in each well. Lysate from untransfected cells was used as negative control.
3. 50µl of LAR2 was added to each well and photons generated were measured in a berthold luminometer in open filter for 1 second.
4. The relative light unit per second (RLU/sec) obtained was normalised with protein estimated by Bradford method.

Preparation of lysates

1. 1-2*10^6 cells were harvested after trypsinization by centrifugation at 1200 rpm for 5minutes at 4°C.
2. The cell pellet was washed with 1X PBS by centrifugation at 1200 rpm for 5 minutes.
3. Supernatant was discarded and approximately 50µl of 1X passive lysis buffer/1*10^6 cells was added.
4. Thereafter, 1µl of 10X protease inhibitor per 100µl of 1X passive lysis buffer was added in the cell lysate.
5. The reaction was thoroughly mixed by vortexing and incubated at RT for 10-15 minutes.
6. After incubation the reaction mixture was centrifuged at 13,000 rpm for 25 minutes at 4˚C.
7. The supernatant was collected and protein estimation was performed using Bradford reagent.

xxxii. *In Vivo* bioluminescence imaging in living mice

BLI allows a non-invasive and real time analysis of biological processes at the molecular level in living organisms. We measured in vivo bioluminescence by Cooled charge-coupled device (CCD)-based Xenogen IVIS 200 biophotonic imager from Caliper (Alameda, CA.). The system excels at imaging light emitted from small animals such as mice or rats but can also be used to image light emitted directly from cells in 96-well plates. The system is capable of measuring the intensities of BL signals produced by

luciferases and other bioluminescent reporters, as well as fluorescence signals produced by fluorescent proteins (GFP, RFP, etc.) and other fluorescent molecules. The output is generally a superimposed image of photographic and luminescence/fluorescence image captured sequentially.

Cell preparation

The cells are cultured in standard growth conditions and amplified in amount required for implantation in specific number of mice. While amplification cells are always maintained in log phase, which means they were never more than 70-80% confluent. An *in vitro* validation of the bioluminescence activity was performed earlier by *in vitro* luciferase assay.

Animal injection:

1. A 70-80% confluent flask cells were harvested by trypsinisation and counted using trypan blue.
2. $6*10^6$ cells per mouse were used for implantation. Accordingly total number of live cells required were counted and pelleted down. The pelleted cells were then resuspended in PBS in a concentration of $6*10^6$ cells/50µl PBS.
3. Usually, in order to facilitate optimal formation of tumor athymic immunocompromised mice were preferred for implantation. Animal care and euthanasia were performed with the approval from Institutional Animal Ethics Committee of ACTREC. Cells were implanted subcutaneously in the right flank of the mice.

Animal anesthesia:

1. The mice were placed into a clear plexiglass anesthesia box that allows visual monitoring of mice to realize the effect of anesthesia. The release of isofluorane can be adjusted from 1-5% according to the weight and number of mice.
2. The tube that supplies the anesthesia to the box is split so that the same concentration of anesthesia is pumped to the anesthesia manifold located inside the imaging chamber.
3. After the mice were fully anesthetized, they were transferred to the imaging chamber with their snout placed to the nose cones attached inside and close the door.

Preparation and injection of D-luciferin:

1. A fresh stock solution of D-luciferin 30 mg/ml in PBS was prepared.
2. Each mouse was injected with 100 µl of 30 mg/ml of D-luciferin (to deliver 3 mg).

3. D-luciferin solution was injected via an intraperitoneal (i.p.) route and substrate was allowed to distribute in awake animals for about 5–15 minutes.

Image acquisition and data analysis:

1. As per manufacturer's recommendation, the IVIS system was initialized before starting image acquisition.
2. Animals were placed inside the black box imaging chamber and postured with the imaging surface facing the camera. This is important to minimize the path length of the luminescent light through different tissues/organs.
3. Now, on the IVIS software, different parameters were set, such as integration time, bin, FOV, and emission filter. Integration time can range from 10 seconds to 5 minutes depending upon the cellular luciferase expression. Bin is generally set medium, which balances between sensitivity and resolution of the CCD camera. Depending upon number of mice scanned at a time, the FOV can be set at higher or lower range.
4. Images were acquired by clicking the "acquire image" button on the displayed screen. After the acquisition is over, a superimposed image of the photographic view and the pseudo colour luminescence image will appear on the screen.
5. Images were acquired in sequence till increase in the luciferase activity is observed. For data analysis image with the maximum luciferase activity was used to quantitate activity.
6. For data analysis, ROI was drawn by clicking on the "create ROI" button and by clicking on the measure button photon values were measured.

xxxiii. *In vivo* cerenkov imaging in living mice

CLI is an emerging hybrid modality in which light emitted from commonly used medical isotopes is used for generation of signal. Cerenkov radiation has been described before 100 years but its application for biomedical imaging purpose is known since past few years only. The modality is of great interest as it allows use of commonly used BLI equipments for visualization of clinical diagnostic (all PET radioisotopes) and many therapeutic radionuclides. The disadvantage is that the signal intensity generated is significantly lower than that in other optical imaging techniques such as bioluminescence and fluorescence. However, significant advantages include the use of approved radiotracers and lack of an incident light source, resulting in high signal to background ratios.

Cell preparation and implantation in animals:

NIS expressing cells were prepared and implanted in the same way as mentioned in xxxii.

^{131}I injection:

1. 10 days prior to ^{131}I therapy thyroid blocking was initiated by daily dose of T4 and methimazole by intra peritoneal injection.
2. On the day of treatment ^{131}I present in the vial was measured by gamma counter and volume required for 1mCi ^{131}I was calculated.
3. 1mCi ^{131}I was removed from the vial to the syringe. Each animal in the treated group was injected with 1mCi ^{131}I.
4. The radioactivity in the syringe was further measured to ensure the amount of radioactivity injected in mice.
5. Before removing the mice from cage the working area of the hood was covered with spread sheet. This was done to reduce the risk of contamination with radioactivity.
6. All the mice in the treated group were administered with intra peritoneal injection of 1mCi of ^{131}I.

*Note: All the radioactivity experiments were performed with extreme care to avoid any spillage or contamination through radioactivity. While handling radioactivity body was covered with full sleeves apron, mask and double gloves. TLD batch was constantly worn during the radioactivity experiments and to check contamination all the area was inspected with dosimeter after the experiments.

Animal anesthesia:

Animal anesthesia was given in the same way as mentioned in the section xxxii. Except that a sheet was spread to the floor of the anaesthesia chamber to avoid contamination.

Cerenkov image acquisition:

1. Cerenkov imaging was performed after 24 and 72 hours of ^{131}I administration.
2. Imaging was performed in the same way as the BLI. For Cerenkov imaging images were acquired by keeping dorsal as well ventral surface facing the camera to understand the distribution of ^{131}I.

*Note: To avoid radioactivity contamination a black paper is placed at the base of the IVIS chamber to keep the mice and the paper is thrown into the radioactive discard after the experiment.